UNIVERSITY OF SOUTHAMPTON

Bone & Joint Research Group

Faculty of Medicine

Novel approaches towards the successful implementation of tissue engineering strategies in impaction bone grafting

by

Edward Robert Tayton

Thesis for the degree of Doctor of Philosophy

March 2014

UNIVERSITY OF SOUTHAMPTON

ABSTRACT

FACULTY OF MEDICINE, HEALTH & LIFE SCIENCES

Doctor of Philosophy

NOVEL APPROACHES TOWARDS THE SUCCESSFUL IMPLEMENTATION OF TISSUE ENGINEERING STRATEGIES IN IMPACTION BONE GRAFTING

By Edward Robert Tayton

Introduction

Tissue engineering offers exciting potential for the treatment of many orthopaedic conditions that involve loss of bone. Impaction bone grafting (IBG) is a technique for the replacement of lost bone stock during revision hip replacement procedures. It uses donor allograft, which has drawbacks including cost, availability, disease transmission and variation in quality.

Methods

An array of polymer scaffolds were tested for both the mechanical and biocompatibility characteristics to be used as potential alternatives to allograft in IBG. Differences in polymer type and molecular weight were assessed, as well as the effects of porosity, and the addition of hydroxyapatite (HA) particles. The best performing polymers were selected and analysed via an *in vivo* (murine) model, and the optimal polymer scaffold further analysed via a scaled-up ovine femoral condyle critical defect model.

Further experiments examined potential translational issues surrounding tissue engineered constructs for use in IBG. The effects of setting bone cement on skeletal stem cell (SSC) survival was evaluated, along with potential methods of reducing exothermic cellular damage.

Results

High molecular weight Poly(DL-Lactide) ($P_{DL}LA$) and poly(DL-lactide-co-glycolide) ($P_{DL}LGA$)showed enhanced mechanical and biocompatibility characteristics over allograft controls. Porous versions of these scaffolds supported increased cellular growth and the addition of HA promoted further osteoblastic differentiation. $P_{DL}LA$ + 10% HA + SSCs showed increased osteogenicity in the murine model, and was selected for the scaled-up ovine model. After 3 months *in vivo* the ovine femoral condyle defects showed *de novo* bone formation from both the SSC seeded and control scaffolds, although the mechanical integrity and volume of bone in the control scaffolds was enhanced.

Exothermic damage of setting bone cement was shown to occur within 5mm of the cement bone interface, although there was a significant surviving cell population in this region. None of the suggested techniques were shown to enhance cell survival.

Conclusion

This thesis details a stepwise evaluation of polymer and polymer composite scaffolds to produce a potential osteogenic alternative to allograft for use in IBG. High molecular weight $P_{DL}LA$ + 10% HA showed the optimal characteristics from all tested scaffolds, and performed well as an osteoconductive and osteoinductive scaffold *in vivo*. The addition of SSCs ultimately diminished these properties, raising questions as to the cell seeding methodology, as well as the actual need for a cellular component.

TABLE OF CONTENTS PAGE

LIST OF FIGURES

Page

CHAPTER 1

CHAPTER 2

CHAPTER 3

CHAPTER 4

CHAPTER 5

CHAPTER 6

CHAPTER 7

LIST OF TABLES PAGE

CHAPTER 1

CHAPTER 3

CHAPTER 4

CHAPTER 5

CHAPTER 6

Declaration

I hereby declare that this thesis is composed entirely of my own work, as a member of a research group. Contributions from other members of the research group, and collaborations with other institutions, are acknowledged in the appropriate sections where this has occurred. I have not submitted this thesis in candidature for any other degree, diploma or professional qualification.

…..…….....

Mr Edward Robert Tayton MBBS FRCS MSc PGCE

Acknowledgements

I would like to thank the following for advice and support, as well as technical assistance throughout the production of this work. People have been specifically mentioned at relevevant points in the thesis.

Supervisors:

Professor Richard OC Oreffo, Mr Douglas G Dunlop

Bone & Joint Research Group:

Mr James Smith, Mr Alexander Aarvold, Mr Nicholas Evans

Spandan Kalra, Esther Ralph, Carol Roberts, Stefanie Inglis

Dr Stuart Lanham, Dr Janos Kanczler

Bioengineering Science Research Group:

Dr Adam Briscoe, Dr Alex Dickinson, Dr Richard Cook

Biomedical Research Unit:

Jas Barley, Kerry Taylor

Biomedical imaging unit:

Dr David Johnston, Dr Anton Page, Dr Hans Schuppe

MuVis Centre:

Dr Dmitry Grinev, Dr Mark Mavrogordato, Professor Ian Sinclair

Southampton University Hospitals Trust:

Dr Darren Fowler

University of Nottingham:

Matthew Purcell, Sherif Fahmy, Professor Steve Howdle, Professor Kevin Shakesheff

University College London:

Professor Gordon Blunn

Royal Veterinary College, Hertfordshire:

Professor Allen Goodship, Gillian Hughes

Queensland University of Technology, Brisbane, Australia:

Professor Dietmar Hutmacher, Dr Johannes Reichert

University of Adelaide, Australia:

Professor David Findlay, Professor Stan Gronthos, Professor Andrew Zannettino

Flinders University, Adelaide, Australia:

Professor John Field

Family:

My Mother and Father, without whose support (and financial backing!) this work would not have been possible and of course my long term partner Beth, for putting up with everything endlessly.

List of Abbreviations

3D	Three-Dimensional
Abs	Absorbance
ALP	Alkaline Phosphatase
αMEM	Minimum Essential Medium Eagle, alpha modification
ANOVA	Analysis Of Variance
A/S	Alcian blue/ Sirius red
AVN	Avascular Necrosis
β-actin	Beta actin
BMA	Bone Marrow Aspirate
BMP	Bone Morphogenetic Protein
BSA	Bovine Serum Albumin
BSP	Bone Sialoprotein
BV	Bone Volume
C	Celsius
c	*circa*
Ca	Calcium
cDNA	Complementary Deoxyribonucleic Acid
CFU-F	Colony Forming Unit-Fibroblastic
CMFDA	CellTracker™ Green (5-chloromethylfluorescein diacetate)
CO_2	Carbon dioxide
Col-1	Collagen type I
Conc.	Concentration
CT	Computed Tomography
CTG	CellTracker™ Green (5-chloromethylfluorescein diacetate)
DAPI	4’,6-diamidino-2-phenylindole
DBM	Demineralised Bone Matrix
DNA	Deoxyribonucleic acid
DO	Distraction Osteogenesis
ECM	Extracellular Matrix
EDTA	Ethylenediaminetetraacetic acid
EGF	Epidermal Growth Factor
EH-1	Ethidium Homodimer
EMF	A great band from the 90’s
F	Female
FCS	Fetal Calf Serum
FDA	Food and Drug Administration
FGF-1	Fibroblast Growth Factor 1 (acidic)
FITC	Fluorescein isothiocyanate
GMP	Good Manufacturing Practice
H+	Hydrogen ion
H_2O	Water
HA	Hydroxyapatite
HBMSC	Human Bone Marrow Stromal Cell
HCV	Hepatitis C Virus
HIV	Human Immunodeficiency Virus
HLA	Human Leukocyte Antigen
IBG	Impaction Bone Grafting
IGF	Insulin-like Growth Factor

IL	Interleukin
iPSC	induced Pluripotent Stem Cell
ISO	International Organisation for Standardisation
LA	Local anaesthetic
LREC	Local Research Ethics Committee
J	Joule
M	Male
MACI	Matrix induced Autologous Chondrocyte Implantation
M-CSF	Macrophage Colony-Stimulating Factor
MHRA	Medicines and Healthcare products Regulatory Agency
MRI	Magnetic Resonance Imaging
Mwt	Molecular weight
MuVis	Multidisciplinary, Multiscale, Microtomographic Volume Imaging
µCT	Micro Computed Tomography
n	Number
N	Newton
N_2	Nitrogen
NaCl	Sodium Chloride
NHS	National Health Service
ns	No significant difference
OA	Osteoarthritis
OC	Osteocalcin
Pa	Pascal
PBS	Phosphate Buffered Saline
PCL	Polycaprolactone
PDGF	Platelet Derived Growth Factor
$P_{DL}LA$	Poly(DL-lactide)
$P_{DL}LGA$	Poly (DL-lactide-co-glycolide)
PGA	Poly(glycolic) acid
PMMA	Polymethyl methacrylate
PO_4	Phosphate
ppm	Parts per million
pQCT	Peripheral quantitative computed tomography
PRP	Platelet-Rich Plasma
psi	Pounds per square inch
RBC	Red Blood Cell
rh	Recombinant human
RNA	Ribonucleic acid
ROI	Region of Interest
rpm	Revolutions per minute
SCF	Supercritical Foaming
SD	Standard Deviation
SEM	Scanning Electron Microscope/Microscopy
SOX-9	Sex determining region Y, box 9
SPSS	Statistical Package for the Social Sciences
SSC	Skeletal Stem Cell
TCP	Tricalcium Phosphate
TGF-β	Transforming Growth Factor Beta
THR	Total Hip Replacement
TNF-α	Tumour Necrosis Factor-alpha

TRAP	Tartrate-resistant acid phosphatase
Tris	Tris(hydroxymethyl)aminomethane
TV	Total Volume
UK	United Kingdom
USA	United States of America
UV	Ultraviolet
V	Volt
v	Volume
VEGF	Vascular Endothelial Growth Factor
Ver.	Version
Vol.	Volume
WST-1	2-(4-Iodophenyl)-3-(4-nitrophenyl)-5-(2,4-disulfophenyl)-2H-tetrazolium

Publications & Book chapters

Published Papers

1. **A comparison of polymer and polymer-hydroxyapatite composite tissue engineered scaffolds for use in bone regeneration. An in vivo and in vitro study.**
   Tayton E, Purcell M, Aarvold A, Smith JO, Kalra S, Briscoe A, Shakesheff K, Howdle SM, Dunlop DG, Oreffo RO.
   J Biomed Mater Res A. 2013 Aug 21.

2. **The effects of setting bone cement on tissue engineered bone graft: a potential barrier to clinical translation?**
   Tayton E, Smith J, Evans N, Dickinson A, Aarvold A, Purcell M, Howdle S, Dunlop D, Oreffo ROC.
   J Bone Joint Surg Am. 2013;95(8):736-43.

3. **A tissue engineering strategy for the treatment of avascular necrosis of the femoral head.**
   Aarvold A, Smith JO, **Tayton ER**, Jones AM, Dawson JI, Lanham S, Briscoe A, Dunlop DG, Oreffo RO.
   Surgeon. 2013 Mar 26.

4. **The effect of porosity of a biphasic ceramic scaffold on human skeletal stem cell growth and differentiation in vivo.**
   Aarvold A, Smith JO, **Tayton ER**, Lanham SA, Chaudhuri JB, Turner IG, Oreffo RO.
   J Biomed Mater Res A. 2013;101(12):3431-7.

5. **An analysis of polymer type and chain length for use as a biological composite graft extender in impaction bone grafting: A mechanical and biocompatibility study.**
   Tayton E, Fahmy S, Aarvold A, Smith J, Dunlop D, Oreffo ROC.
   J Biomed Mater Res A. 2012;100(12):3211-9.

6. **From bench to clinic and back: skeletal stem cells and impaction bone grafting for regeneration of bone defects.**
   Aarvold A, Smith JO, **Tayton ER**, Jones AM, Dawson JI, Lanham S, Briscoe A, Dunlop DG, Oreffo RO.
   J Tissue Eng Regen Med. 2012 Oct 5.

7. **Translational hurdles to tissue engineering: an analysis of commonly used local anaesthetics on skeletal stem cell survival.**
   Tayton E, Smith J, Aarvold A, Dunlop D, Oreffo ROC.
   J Bone Joint Surg Br. 2012;94(6):848-55.

8. **Supercritical CO2 fluid-foaming of polymers to increase porosity: a method to improve the mechanical and biocompatibility characteristics for use as a potential alternative to allografts in impaction bone grafting?**
   Tayton E, Purcell M, Aarvold A, Smith JO, Kalra S, Briscoe A, Shakesheff K, Howdle SM, Dunlop DG, Oreffo RO.
   Acta Biomater. 2012;8(5):1918-27.

9. **Skeletal Regeneration: application of nanotopography and biomaterials for skeletal stem cell based bone repair.**
   Dawson JI, Kingham E, Evans N, **Tayton E**, Oreffo RO.
   Inflammation and Regeneration 2012;32(3)72-89.

10. **Skeletal Tissue Regeneration: Current Approaches, Challenges, and Novel Reconstructive Strategies for an Aging Population.**
    Smith JO, Aarvold A, **Tayton ER**, Dunlop DG, Oreffo RO.
    Tissue Eng Part B Rev. 2011;17(5):307-20.

11. **Taking tissue engineering principles into theatre: retrieval analysis from a clinically translated case.**
    Aarvold A, Smith JO, **Tayton ER**, Tilley S, Dawson JI, Lanham SA, Briscoe A, Dunlop DG, Oreffo RO.
    Regen Med. 2011;6(4):461-7.

Published Abstracts

1. "An analysis of six polymers for both the mechanical and biocompatibility characteristics required for use as an osteogenic alternative to allograft in impaction bone grafting."
   Tayton ER, Fahmy S, Aarvold A, Smith JO, Dunlop DG, Shakesheff K, Howdle S, Oreffo ROC.
   IMECHE event proceedings 2011;1:87(IMECHE: Engineers and surgeons joined at the hip III 2011).

2. "Tissue engineering strategies to extending the orthopaedic applications of Tantalum trabecular metal - Addition of skeletal stem cells to enhance the bone-implant interface."
   Smith JO, Sengers B, Aarvold A, **Tayton ER**, Dunlop DG, Oreffo ROC.
   IMECHE event proceedings 2011;1:88-92 (IMECHE: Engineers and surgeons joined at the hip III 2011).

3. "The optimisation of polymer type and chain length for use as a biological composite graft in impaction bone grafting: a mechanical and bio-compatibility analysis."
   Tayton ER, Fahmy S, Aarvold A, Smith JO, Dunlop DG, Shakesheff K, Howdle S, Oreffo ROC.
   J Bone Joint Surg (Br) 2012;94-B(SUPP XXXIX):211 (BOA congress, Dublin, Eire, 2011).

4. "Does increasing PLA scaffold porosity using supercritical CO_2 strategies enhance the characteristics for use as an alternative to allograft in impaction bone grafting?"
   Tayton ER, Purcell H, Aarvold A, Smith JO, Dunlop DG, Shakesheff K, Howdle S, Oreffo ROC.
   J Bone Joint Surg (Br) 2012;94-B(SUPP XXXIX):212 (BOA congress, Dublin, Eire, 2011).

5. "Tantalum trabecular metal - Addition of skeletal stem cells to enhance the bone-implant interface."
   Smith JO, Sengers B, Aarvold A, **Tayton ER**, Dunlop DG, Oreffo ROC.
   J Bone Joint Surg (Br) 2012;94-B(SUPP XXXIX):212 (BOA congress, Dublin, Eire, 2011).

6. "The optimisation of polymer type and chain length for use as a biological composite graft in impaction bone grafting: a mechanical and bio-compatibility analysis."
   Tayton ER, Fahmy S, Aarvold A, Dunlop DG, Shakesheff K, Howdle S, Oreffo ROC.
   J Bone Joint Surg (Br) 2012;94-B(SUPP XXXVI):23 (BORS / BRS combined meeting, Cambridge, 2011).

7. "Enhancement of PLA for use in impaction bone grafting: the effect of production via CO_2 dissolution to increase porosity."
   Tayton ER, Fahmy S, Aarvold A, Dunlop DG, Shakesheff K, Howdle S, Oreffo ROC.
   J Bone Joint Surg (Br) 2012;94-B(SUPP XXXVI):23 (BORS / BRS combined meeting, Cambridge 2011).

8. "A tissue engineering approach with Tantalum Trabecular Metal to enhance bone-implant integration."
   Smith JO, Sengers B, Aarvold A, **Tayton ER**, Dunlop DG, Oreffo ROC.
   J Bone Joint Surg (Br) 2012;94-B(SUPP XXXVI):30 (BORS / BRS combined meeting, Cambridge 2011).

9. "Retrieval analysis of tissue engineered bone; a clinical and laboratory study."
   Aarvold A, Smith JO, **Tayton E**, Dawson JI, Briscoe A, Lanham SA, Dunlop DG, Oreffo RO.
   J Bone Joint Surg (Br) 2012;94-B(SUPP XXXVI):117 (BORS / BRS combined meeting, Cambridge 2011).

10. "A tissue engineering strategy for the treatment of osteonecrosis: evaluation of efficacy in four patients."
    Aarvold A, Smith JO, **Tayton E**, Dawson JI, Briscoe A, Lanham SA, Dunlop DG, Oreffo RO.
    J Bone Joint Surg (Br) 2012;94-B(SUPP XXXVII):436 (EFORT, Copenhagen, 2011).

11. "Optimisation of polymer and stem cell technology to produce substitute allograft for use in impaction bone grafting."
    Tayton ER, Fahmy S, Aarvold A, Shakesheff K, Howdle S, Oreffo ROC, Dunlop DG
    J Bone Joint Surg (Br) 2012;94-B(SUPP XXXVII):20 (EFORT, Copenhagen, 2011).

12. "Biological augmentation of impaction bone grafting: retrieval analysis of human tissue engineered specimens."
    Aarvold A, Smith JO, **Tayton ER**, Briscoe A, Lanham S, Dawson JI, Oreffo RO, Dunlop DG.
    J Bone Joint Surg (Br), British hip society proceedings (BHS/BORS combined meeting, Torquay, 2011).

13. "Cyst fluid and stem cells: why unicameral bone cysts are so hard to treat"
    Aarvold A, Smith JO, Edwards CJ, **Tayton ER**, Gent ED, Oreffo ROC.
    J Bone Joint Surg (Br) 2012;94-B(SUPP XXIV):12 (BSCOS, Sheffield, 2011).

14. "The development of a custom-made IM nail for use in an ovine tibial segmental defect model"
    Briscoe A, Aarvold A, Street M, **Tayton E**, Smith JO, Dunlop DG, Oreffo ROC
    J Biomech 2010;43(SUPP I):71 (OBCAS, Brunel university, London, 2010).

15. "Retrieval analysis of femoral heads after impaction bone grafting for treatment of AVN."
    Aarvold A, Smith JO, **Tayton ER**, Jones AMH, Briscoe A, Dunlop DG, Oreffo ROC.
    J Bone Joint Surg (Br) 2012;94-B(XXIV):12 (BORS, Cardiff, 2010).

Book Chapters

1. "Clinical applications for skeletal / mesenchymal stem cell therapy"
   Tayton ER, Smith JO, Aarvold A, Oreffo RO, Zaleh W, Kassem M
   In: Stem Cells: Basic Biology and Clinical Applications,
   Editor: M Kassem, Publisher: King Saud University Press, 2012

Presentations *(Presenting author unless stated)*

1. "Research from within this University; The Future of Orthopaedics?"
   Current trends in Medicine conference, University of Southampton, 30/10/13
   Podium
2. "The scale-up of a tissue engineered porous hydroxyapatite polymer composite scaffold for use in bone regenerative procedures: an ovine femoral condyle defect study"
   Wessex Sports medicine conference, Dingle, Ireland, 2/10/13
   Podium
3. "The optimisation of polymer skeletal stem cell composites for use as bone graft substitutes in impaction bone grafting"
   UoS/SUHT Translational Research Conference, Southampton, 12/11/12 (Conference 1st Prize)
   Podium
4. "The optimisation of polymer skeletal stem cell composites for use as bone graft substitutes in impaction bone grafting"
   Gauvain 15/06/12
   Podium
5. "Translational hurdles to tissue tissue engineering: an analysis of commonly used local anaesthetics on skeletal stem cell survival"
   Gauvain 15/06/12 (Conference 1st Prize)
   Podium: James Smith
6. "An *in vitro* and *in vivo* study to determine an optimal porous polymer to clinically translate for use as a living composite alternative to morselised allograft in bony regenerative procedures"
   UoS/SUHT Translational Research conference, Southampton, 16/11/11
   Poster presentation
7. "An analysis of six polymers for both the mechanical and biocompatibility characteristics required for use as an osteogenic alternative to allograft in impaction bone grafting."
   IMECHE London, 3/11/11
   Podium
8. "Does increasing polymer porosity via a novel supercritical CO2 production technique improve the characteristics for use as an alternative to allograft in impaction bone grafting?"
   IMECHE London, 3/11/11
   Poster presentation
9. "Tissue engineering strategies to extending the orthopaedic applications of Tantalum trabecular metal - Addition of skeletal stem cells to enhance the bone-implant interface"
   IMECHE London, 3/11/11
   Podium: James Smith
10. "Tantalum trabecular metal - Addition of skeletal stem cells to enhance the bone-implant interface"
    BOA, Dublin, 15/9/11
    Podium: James Smith

11. "The optimisation of polymer type and chain length for use as a biological composite graft in impaction bone grafting: a mechanical and bio-compatibility analysis"
    BOA, Dublin, 14/9/11
    Podium
12. "Does increasing PLA scaffold porosity using supercritical CO_2 strategies enhance the characteristics for use as an alternative to allograft in impaction bone grafting?"
    BOA, Dublin, 14/9/11
    Podium
13. "Exploring the pathogenesis of unicameral bone cysts"
    Gauvain, 17/6/2011
    Podium: Alex Aarvold
14. "Retrieval analysis of clinically translated human tissue"
    Gauvain, 17/6/2011
    Podium: Alex Aarvold
15. "A tissue engineered substitute for allograft to use in impaction bone grafting"
    Gauvain, 17/6/2011
    Podium
16. "The exothermic effects of setting bone cement on tissue engineering allograft"
    Gauvain, 17/6/2011
    Podium
17. "Extending the role of tantalum trabecular metal using tissue engineering strategies"
    Gauvain, 17/6/2011
    Podium: James Smith
18. "Clinical Translation of Bone Tissue Engineering"
    Medicine & Biological Sciences Postgraduate Conference, Southampton, 8/6/11
    Podium: Alex Aarvold
19. "Optimisation of polymer and stem cell technology to produce substitute allograft for impaction bone grafting"
    Medicine & Biological Sciences Postgraduate Conference, Southampton, 8/6/11
    Podium
20. "A tissue engineering strategy for the treatment of osteonecrosis: evaluation of efficacy in four patients"
    EFORT, Copenhagen, 3/6/11
    Podium: James Smith
21. "Optimisation of polymer and stem cell technology to produce substitute allograft for use in impaction bone grafting"
    EFORT, Copenhagen, 3/6/11
    Podium
22. "A tissue engineering strategy for the treatment of AVN: clinical translation and analysis of retrieval specimens"
    Orthopaedic Research Society (ORS), Long Beach, California, 13-16/1/11
    Poster presentation
23. "The optimisation of polymer type and chain length for use as a biological composite graft in impaction bone grafting: a mechanical and bio-compatibility analysis"
    British Orthopaedic Research Society (BORS), Cambridge, 27/6/11
    Podium
24. "Enhancement of PLA for use in impaction bone grafting: the effect of production via CO_2 dissolution to increase porosity."
    British Orthopaedic Research Society (BORS), Cambridge, 27/6/11
    Podium
25. "A tissue engineering approach with tantalum trabecular metal to enhance bone-implant integration"
    British Orthopaedic Research Society (BORS), Cambridge, 28/6/11
    Oral poster presentation – James Smith

26. "Retrieval analysis of tissue engineered bone: a clinical and laboratory study"
    British Orthopaedic Research Society (BORS), Cambridge, 27/6/11
    Poster presentation
27. "Biological augmentation of impaction bone grafting: retrieval analysis of human tissue engineered specimens?"
    British Hip Society (BHS), Research Prize Session, Torquay, 2/3/11
    Podium: Alex Aarvold
28. "Cyst fluid and stem cells: why unicameral bone cysts are so hard to treat"
    British Society for Children's Orthopaedic Surgery (BSCOS), Sheffield, 28/1/11
    Podium: Alex Aarvold
29. "From bench to clinic – retrieval of human tissue engineered bone"
    University of Southampton Translational Research Conference, 16/11/10
    Poster presentation
30. "The use of Impaction Bone Grafting and skeletal stem cells for the treatment of AVN of the femoral head – evaluation of efficacy in 4 patients"
    Gauvain, 16/7/2010
    Podium: Alex Aarvold
31. "The use of impaction bone grafting and skeletal stem cells for the treatment of avascular necrosis of the femoral head"
    British Orthopaedic Research Society (BORS), Cardiff, 13/7/10
    Podium: Alex Aarvold
32. "The development of a custom-made IM nail for an ovine tibial segmental defect model"
    International Conference on Orthopaedic Biomechanics, Clinical Applications and Surgery (OBCAS), Brunel University, London, 7/6/10
    Podium: Adam Briscoe

Prizes

1. Translational Clinical Research Conference 2012 (University of Southampton)
   Conference 1st Prize
   Best Presentation: "The optimisation of polymer skeletal stem cell composites for use as bone graft substitutes in impaction bone grafting"

2. Gauvain 2012 (Wessex Deanery Orthopaedic Trainees)
   Conference 1st Prize
   Best Scientific Presentation: "Translational hurdles to tissue engineering: an analysis of commonly used local anaesthetics on human skeletal stem cell survival."

3. Medicine & Biological Sciences Postgraduate Conference 2011 (University of, Southampton)
   Conference attendance award
   Commendation for podium presentation: "Optimisation of polymer and stem cell technology to produce substitute allograft for impaction bone grafting"

Chapter 1

Introduction

1.0 Introduction

As the advances in orthopaedics become ever more technically challenging, and the range of treatable conditions expands along with an increasingly aging population, the need for novel solutions is of paramount importance. One area that has been a challenge for well over one hundred years is the regeneration of lost bone stock, but more recently, especially with the unprecedented early failures of metal on metal hip replacements, the interest in this area has dramatically expanded (Langton *et al.* 2010;Langton *et al.* 2011).

Louis Xavier Édouard Léopold Ollier (2 December 1830 - 26 November 1900), a French surgeon born in Les Vans, department of Ardèche, is generally attributed as the founder of reconstructive orthopaedics (Figure 1.1). His interest in trauma was stimulated when France was invaded by Germany in 1870 and he became head of the Lyons Ambulance Service.

Figure 1.1: Louis Xavier Édouard Léopold Ollier (c1870). (Image from http://www.sciencephoto.com/media/227483/view, accessed 30/1/2014).

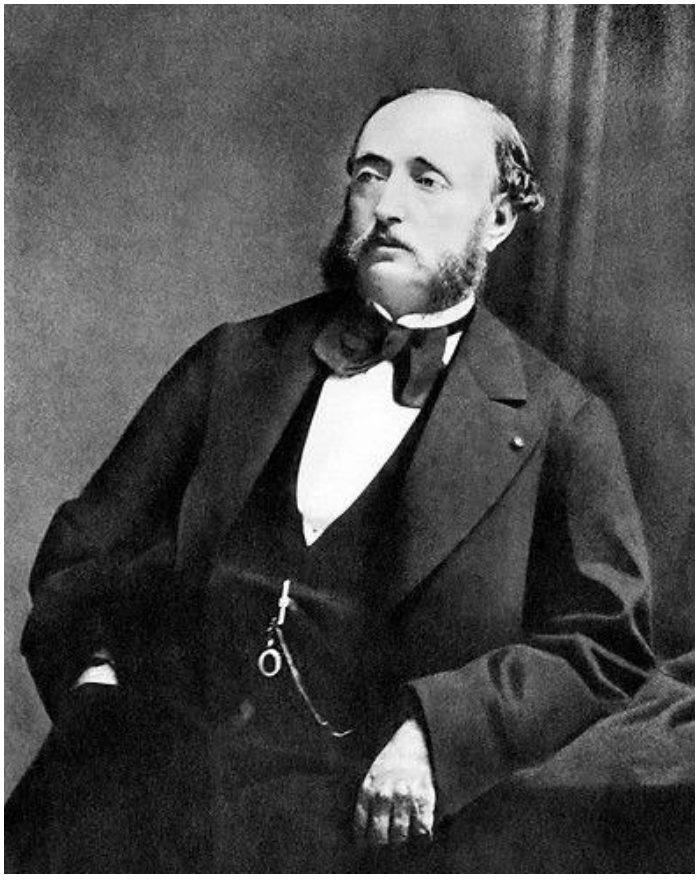

During this time he developed successful techniques of resection instead of amputation to damaged limbs, and noted how the periosteum was integral to the regeneration of bone following resection (Ollier 1867). He went on to perform seminal experiments to unravel the function of the periosteum, and the complex interaction of the periosteum with the sub-periosteal layer.

Towards the end of his life, Ollier pioneered techniques of bone grafting, comparing the relative merits of autograft, allograft and xenograft, concluding that tissue transplanted from animals was unlikely to be successful (Ollier 1891). Amazingly, although techniques have changed and our understanding of bone regeneration has evolved, bone grafting using autograft remains the gold standard for bone regenerative procedures (Marino and Ziran 2010). It is the second most common transplantation in humans and there are currently an estimated 500,000-600,000 bone grafting procedures performed annually in the United States alone (Bauer and Muschler 2000).

The technique of obtaining autograft involves removal of the hosts own bone from a donor site such as the iliac crest or a vascularised fibular graft, and placement within the required area (Taylor *et al*. 1975;Warnke *et al.* 2004). Success has been achieved due to the fact that: i) the autograft provides a osteoconductive structural scaffold with mechanical properties similar to the host area, ii) the autograft retains growth factors and nutrients essential for host integration and vascularisation, and iii) the autograft retains progenitor cells with osteogenic potential (Delloye *et al.* 2007). The fibula is particularly useful as large segments can be dissected *en bloc* together with nutrient blood vessels and periosteum. The vascularised fibular graft can then be applied to defects that require a structural or particular morphological reconstruction. The fibula, along with scapula, iliac crest, and rib transplant, have been used to repair major bony defects measuring over 50 mm (such as occur after bone tumour resections) (Warnke *et al.* 2004). There are however significant limitations to the use of autograft, including i) the risk of severe or long-term discomfort at the bone graft donor site, ii) functional or cosmetic deficit and iii) complications such as infection and nerve damage (Ahlmann *et al.* 2002). In addition to this, the volume of bone available is limited, and thus often not adequate for the recipient site (Ahlmann *et al.* 2002). Allograft provides a viable alternative for this problem. Allograft may be obtained from cadaveric donors or from patients undergoing surgery where excised bone would otherwise be discarded (for

example the femoral head during primary hip replacement surgery) (Emms *et al.* 2009). The use of fresh allograft carries significant risk of pathogen transmission so has been replaced by the introduction of regional 'bone banks' to store freeze-dried, fresh-frozen or irradiated cancellous, cortical or cortico-cancellous allograft for future use. This system has the advantage of providing a ready supply of screened and quarantined bone, although the mechanical, biological and immunological properties of the allograft may be affected differently by each storage process (Schreurs *et al.* 2004). While allograft can act as an osteoconductive scaffold, many of its osteoinductive and osteogenic properties are removed during processing, which has the benefit of reducing potential immunologic incompatibility. Allograft must be screened for bacterial and fungal contamination by validated methods in accredited laboratories. Samples for bacterial screening should be obtained aseptically and placed in appropriate culture media at the time of retrieval or processing (UK tissue transplantation guidelines 2010). However, despite such processing and rigorous donor screening, there remains the possibility of infection transmission. Some have estimated that the risk of human immunodeficiency virus (HIV) transmission alone with allograft bone is 1 case in 1.6 million population. A case of hepatitis B transmission and 3 cases of hepatitis C transmission have been reported with allograft tissue (Conrad *et al.* 1995;Tomford *et al.* 1981a;Tomford *et al.* 1981b). In addition, the acquisition, treatment, transport and storage of allograft make bone grafting a costly exercise, and as requirements increase due to the ever increasing complexity and incidence of reconstructive cases, the supply will not be adequate for the clinical demand (Delloye *et al.* 2007).

As a consequence of these disadvantages there is a need to find an alternative to allograft, for a whole spectrum of bone disorders and clinical scenarios, where the regeneration of lost bone or the *de novo* production of bone is required. The mainstay of these include traumatic bone loss from high velocity injury (such as an open tibial fracture from a motor vehicle accident), fracture non-union (which results from biological failure of normal bone healing), surgical excision of bone (as may be required for treatment of infections or during bone tumour surgery), arthrodesis (fusion of a joint such as those between vertebrae due to arthritis) and replacement of lost bone stock around prostheses such as required during revision hip replacement surgery (Marino and Ziran 2010;Schreurs *et al.* 2004;Slooff *et al.* 1984;Warnke *et al.* 2004). From a tissue engineering perspective, the ultimate solution for orthopaedic application is a bone

substitute with: i) mechanical strength comparative to that of bone, ii) a substitute that remains bio-resorbable, and iii) a material with osteoregenerative capability. However, there are currently a number of extremely successful devices and substances which do not fulfil of these criteria (McManmara *et al.* 2010, Jenis *et al.* 2010). A flow diagram depicting how the research data presented in this thesis fits into the tissue engineering paradigm is given by Figure 1.2, and the following sections of the introduction serve to elucidate the information.

Figure 1.2: Diagram showing the interrelations of tissue engineering and the clinical need for bone replacement strategies. The theme of this thesis is highlighted by the bold text within the light blue coloured boxes.

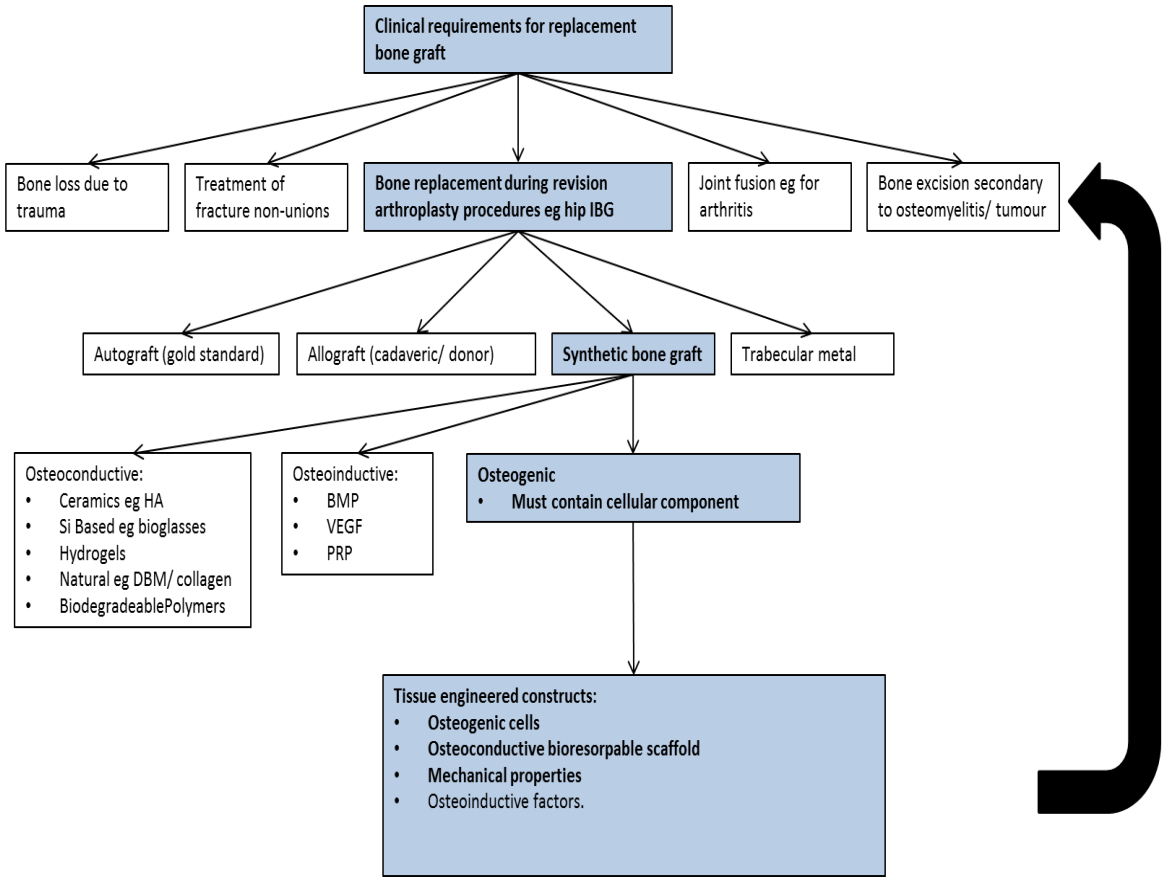

The focus of this thesis is on the need for an alternative to allograft along with skeletal stem cells to replace lost bone stock in revision hip surgery. The clinical area is very specific, along with many of the required characteristics of any tissue engineered construct (discussed in full later). However, many of the desirable characteristics are

also common to the other clinical requirements for bone replacement, and indeed regenerative medicine as a whole (thick black arrow).

1.1 Osteoconductive bone graft substitutes

1.1.1 Ceramics

Advances have been made in the generation of osteoconductive materials such as ceramics (e.g. hydroxyapatite, beta-tricalcium phosphate), where the major use for these materials has been in the coating of cementless implants to aid osseointegration. This has been extremely successful such that the use of cementless implants has now overtaken that of cemented, and there is data demonstrating successful follow up of over 20 years, with survivorship in excess of 90% (NJR 2013;Rajaratnam *et al.* 2008). Ceramics have also begun to find limited use as bone graft substitutes as well as bone graft extenders.

Wheeler *et al.* performed an ovine spinal fusion study in 18 sheep, comparing the efficacy of a silicated calcium phosphate graft (Si-CaP) to autograft (Wheeler *et al.* 2007). Outcome measures to assess fusion efficacy included computed tomography scans, radiographs, biomechanical testing, and histological analysis. The authors found that autograft provided both an osteoconductive scaffold as well as osteogenic stimuli, whereas Si-CaP provided only an osteoconductive matrix for bone infiltration. However, the Si-CaP was able to overcome the biological disadvantage and produce a robust fusion callus with osteoblast and osteoclast activity equivalent to autograft-supplemented fusion tissue at 2 and 6 months postoperatively. However, while autograft activity levels decreased from 2 to 6 months, activity in the Si-CaP group remained constant, with a subsequent increase in graft volume after 6 months compared to autograft. The authors concluded that the Si-CaP graft was equivalent to autograft in this spinal fusion model.

The concept has thus found good uptake for use during spinal fusion procedures. In a two-year clinical case series by Jenis and Banco, there was no difference in fusion rates between Actifuse (silicate substituted calcium phosphate) in combination with bone marrow aspirate and those historically gained by the same author using the standard iliac crest autograft alone (Jenis and Banco 2010).

Ceramics have also been used successfully in the fusion of other joints as well. Coralline hydroxyapatite is processed by a hydrothermal exchange method that converts the coral calcium phosphate to crystalline hydroxyapatite with pore diameters between 200 and 500 μm to produce a structure very similar to that of human trabecular bone. Coughlin *et al.* used a coralline hydroxyapatite scaffold as a bone graft substitute in a series of 10 patients undergoing hind foot fusion (Coughlin *et al.* 2006). Only nine patients were available for follow up, and eight of these reported good or excellent results. Radiographs continued to demonstrate the presence of the graft material at 6 years and also showed extrusion of the graft from the joint in all patients. However, no patient had symptoms from the extruded material. Coralline hydroxyapatite has also been used as structural graft when bone defects are associated with fractures. Bucholz *et al*. compared interporous coralline hydroxyapatite to cancellous autograft when treating the metaphyseal defects in 40 patients with displaced tibial plateau fractures (Bucholz *et al.* 1989). Roentgenographic and clinical assessments at follow-up periods averaging 15.4 months (autograft) and 34.5 months (hydroxyapatite) demonstrated no significant differences in the two groups.

Ceramics have also been used in impaction bone grafting, although ceramics do not yet have the sufficient handling characteristics that they can be used without allograft addition (Blom *et al.* 2002;Blom *et al.* 2009;McNamara *et al.* 2010). Brewster *et al.* showed the addition of bioglass particles increased the shear strength of the impacted graft mix, whereas Blom *et al*. performed an *in vitro* ovine femoral impaction study to test the strength of impacted mixtures of a porous tricalcium phosphate-hydroxyapatite ceramic (BoneSave) in differing volume mixtures with allograft, comparing ceramic against allograft alone (Blom *et al.* 2002;Brewster *et al.* 1999). Blom *et al.* found that BoneSave-allograft mixtures exhibit both much greater mechanical stability and reproducibility than the pure allograft at all tested loads (200-800 N). BoneSave was always used in combination with allograft for three reasons.

1. Bone ‘additive’ allows cohesion and adhesion of the otherwise loose mix which is crucial for surgical handling.
2. Biologically the bone adds osteoinductive potential to the otherwise only bioactive and osteoconductive ceramic.

3. Ceramic particles are hard, and can lead to host bone fracture when being impacted alone.

The issue of poor cohesion between the HA particles was also noted by Oakley and Kuiper, who used a similar technique to impact synthetic bone graft extenders alone and in combination with allograft, into discs (Oakley and Kuiper 2006). Oakley then used an unconfined compression test to assess the cohesion of the particles making up the disc, finding that although the addition of allograft to the bone graft extender improved the cohesion, the use of bone graft extender alone was not a viable option. Thus allograft is still essential during surgery when using these substances during IBG, with the associated problems including cost and availability, as well as the potential for disease transmission.

1.1.2 Silicon-based compounds

1.1.2.1 Bioactive glasses

Bioactive glasses are hard, solid (non-porous), materials which are made up of various proportions of calcium, phosphorus, and silicon-dioxide (silicate being the main component) and these glasses possess both osteointegrative and osteoconductive properties. Soluble and non-soluble forms can be made by varying the proportions of sodium oxide, calcium oxide, and silicon dioxide. When used in clinical practice, a mechanically strong bond between the bioactive glass and surrounding host bone forms through hydroxyapatite crystals similar to that of bone (Gross *et al.* 1981). Bioactive glasses are extremely strong in comparison to calcium phosphate preparations, such as ceramic-HA, but this means bioactive glasses are difficult to drill and shape. As a consequence bioactive glasses are difficult to fix to the skeleton and may fracture in the process. Nonetheless bioactive glasses have been successfully used in the fields of dental and maxillofacial surgery as coatings for implants, as well as in granular form as bone graft extenders (Kinnunen *et al.* 2000;Peltola *et al.* 2008;Mistry *et al.* 2011).

1.1.2.2 Glass ionomers

Much of the initial work involving these materials was again in the fields of dental and maxillofacial surgery. Glass ionomer cement consists of calcium / aluminium /

fluorosilicate glass powder mixed with polycarboxylic acid to produce a porous cement paste. The paste hardens in approximately 5 minutes after which it is water insoluble, and by 24 hours it has a compressive strength and modulus of elasticity comparable to cortical bone. The biocompatiblility of glass ionomers allow excellent osteointegration, with the porous structure assisting with osteoconduction and subsequent bone ingrowth, but it is non-reabsorbable thus once integrated remains in-situ. Glass ionomer has the potential for use as a replacement for polymethyl-methacrylate (bone cement) with the benefit of not having such a significant exothermic reaction during the curing process. Therefore, glass ionomers can also be impregnated with antibiotics and high molecular weight (heat labile) proteins for slow release (such as growth factors), which can occur more efficiently than with PMMA and are less likely to be damaged by the exothermic curing process (Brook and Hatton 1998;Jonck and Grobbelaar 1990;Jonck and Grobbelaar 1992).

1.1.3 Structural metals

In the last decade significant progress has been made in the generation of osteoconductive porous structural metals such as trabecular metal (Levine *et al.* 2006). These materials augment bone ingrowth but are not biodegradable, thus if subsequent surgery is required, removal is complicated and the resultant defect can be extremely difficult to manage. Metallic implants have been trialled in long bone segmental defects (Bullens *et al.* 2009). In a study using goats, a tantalum prosthesis was placed into a surgically-produced mid-femoral critical segmental defect. Bone union was induced, but only when the surrounding periosteum was preserved. This is not usually the case in clinical scenarios, such as radical tumour excisions where the periosteum is excised with the tumour, or traumatic bone loss which includes the periosteum. Tantalum in this scenario thus displays only osteoconductive potential. There are however certain clinical situations where the use of trabecular metal to fill bone defects has been deemed a good solution and the uptake is encouraging.

In the revision hip scenario, trabecular metal can act not only as a void filler, but also provides immediate stability for an associated acetabular component (Sculco 1998). Both initial and long-term stability are achieved due to the high coefficient of friction against bone with up to 80% porosity to enable ingrowth (Bobyn *et al*. 1999;Shirazi-Adl *et al.* 1993). In addition, the low modulus of elasticity of trabecular metal material can

produce more normal physiological loading and reduce stress shielding. The main indication is for use as a bone void filler in revision hip surgery is as acetabular augments as shown in Figure 1.3, where trabecular metal can provide stability to the cup in an area where the acetabulum is deficient.

Figure 1.3: Examples of trabecular metal components used in revision hip surgery. A) Trabecular metal acetabular (cup) component, B) acetabular augment, C) augment and cup *in situ*,D) post operative radiograph (images from (Bobyn *et al.* 2004)).

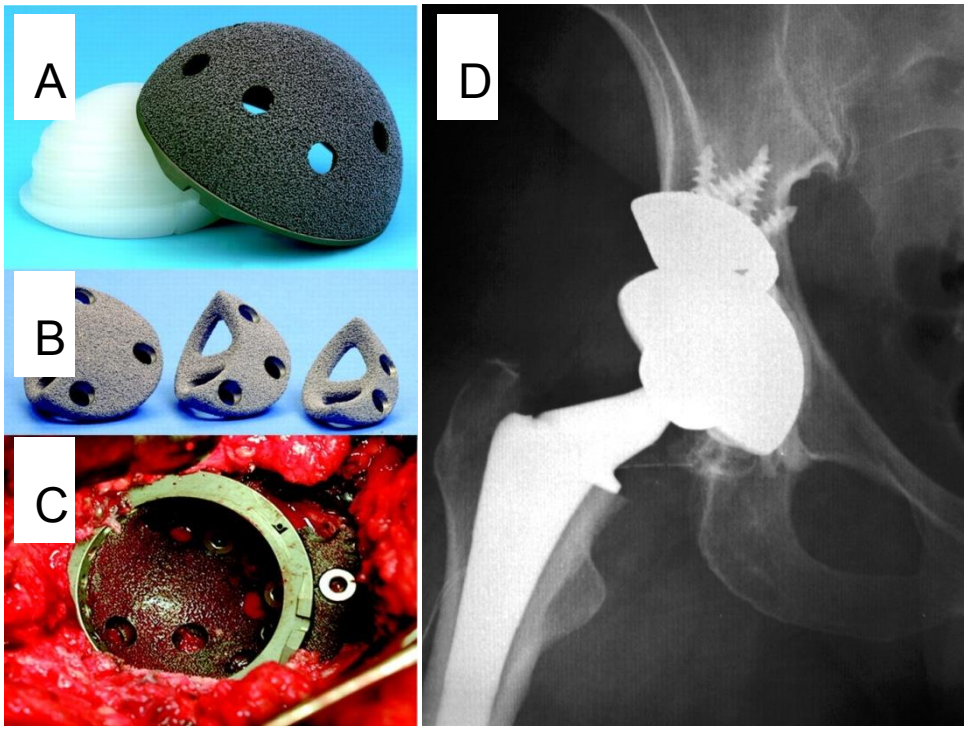

This technology is relatively new, meaning that little long-term follow up data is available, although van Kleunen J *et al.* have reviewed 97 cases of consecutive loose total hip arthroplasty with a minimum of Paprosky grade IIA pelvic bone loss treated with a trabecular metal revision acetabular component with or without modular augments (Van Kleunen *et al.* 2009). The average Harris hip score was noted to improve from 55 preoperatively to 76 postoperatively. At the time of writing, radiographic evaluation revealed that 88 cups demonstrated no lucent lines, 1 cup had lucent lines but remained well fixed and 8 cups underwent resection arthroplasty (but this was for infection). One cup was revised for chronic instability and there were no aseptic failures in the series.

Trabecular metal has also been successfully used for a number of other orthopaedic clinical scenarios, including bone defect filling and component augments in revision knee surgery, structural support for avascular necrosis of the femoral head, as well as void fillers between vertebral bodies for use in spinal fusion (Nadeau *et al.* 2007;Fernandez-Fairen *et al.* 2008;Nadeau *et al.* 2007;Lachiewicz *et al.* 2011). It is however expensive, only available in predefined shapes (so can not be shaped intra-operatively to optimally fit irregular bone defects), difficult to remove if further surgery is required and still lacks the osteoinductive and osteogenic characteristics to be considered as an optimal alternative to autograft.

1.1.4 Naturally occurring biomaterials

Naturally occurring biomaterials such as demineralised bone matrix (DBM), collagen and certain hydrogels also have been put forward as potential bone graft alternatives. DBM can be produced by decalcifying allograft. It is then processed such that the potential for infection and immunogenic host response is reduced. The remaining substance retains the collagenous structure of the original tissue, which can serve as an osteoconductive and osteoinductive scaffold (Martin, Jr. *et al.* 1999). However, due to the demineralisation process there is substantial loss of strength and clinical results are mixed (partially attributed to non-uniform processing methods) (Wang *et al.* 2007b). DBM, is available as a gel, malleable putty, flexible strips, mouldable paste with bone-chips or injectable bone paste. Due to its variable structural characteristics and concerns about its ability to withstand sustained load, DBM is widely used as a ‘‘bone graft extender’’ rather than as a bone graft substitute (Cammisa, Jr. *et al.* 2004).

Collagen can be obtained from various human or animal sources. Extracellular bone matrix is rich in collagen and it has been shown to contribute to mineral deposition, vascular ingrowth, and growth factor binding, providing a favourable environment for bone regeneration (Cornell 1999). However, due to its organic sources, collagen may carry potential immunogenicity and due to extensive processing usually provides little by way of structural support. Therefore, collagen is predominantly used in conjunction with other materials as either a carrier for bioactive materials, eg bone morphogenetic proteins, where it has been shown to significantly enhance graft incorporation or used as a composite with other bone substitutes (eg HA and tricalcium phosphate) to assist with mechanical integrity. Whilst collagen matrices have shown inconsistent results, they can

be used as effective autograft extenders (Muschler *et al.* 1996;Zerwekh *et al.* 1992). In one large randomised control multicentre trial involving the treatment of long bone injuries (249 fractures), Chapman *et al.* compared calcium-collagen graft material in combination with autologous iliac crest bone marrow to autologous bone grafting alone (<30 cm3 volume required) (Chapman *et al.* 1997). The authors observed no differences between the two groups either functionally or with regard to the union rate, and concluded that calcium-collagen graft material with autologous bone marrow is a viable alternative to autologous bone graft for patients who have an acute traumatic defect of a long bone. However, despite these good results, there remains a requirement for adequate external fracture stabilisation, and collagen matrices are thus not recommended for filling metaphyseal bone defects resulting from articular fractures as a consequence of lack of structural support.

1.1.5 Hydrogels

Hydrogels consist of a network of polymer chains that are hydrophilic, many based around the polyether compound Polyethylene glycol (PEG). Hydrogels can be reliably manufactured in large quantities, and can have characteristics tailored to the required use by controlling composition, cross-linking density and degradeable linkages (Benoit *et al.* 2006;Rice and Anseth 2004). Hydrogels are highly absorbent (they can contain over 99.9% water) natural or synthetic polymers and thus possess a degree of flexibility very similar to natural tissue and can be manufactured such that they are injectable, but can solidify in vivo (Kikuchi and Okano 2005). Hydrogels are typically biocompatible, biodegradable, and (like collagen) can also serve as carriers for additional bioactive materials (Liu *et al.* 2002;Spitzer *et al.* 2002).

1.1.6 Bioresorbable polymers

Synthetic polymers have also gained momentum as potential bone graft substitutes. Like hydrogels, by simple alteration of a monomeric unit, polymer chain length or production techniques, polymers offer the potential to vary their characteristics to suit a particular clinical need. Bioresorbable polymers are already widely utilised in other branches of medicine (heart valves, suture material, controlled release drug depo injections etc), highlighting their extreme versatility (Hyde *et al.* 1999;Langer 1983;Pillai and Sharma 2010). Polymers also have the potential to be integrated with

growth factors, drugs, and other compounds to create multiphase delivery systems. Much in vitro work has given encouraging data, and the combination of two polymers (binary blends) makes it possible to combine desirable polymer characteristics (Khan *et al.* 2010). For instance, a particular polymer may promote osteoinduction, while a second make give excellent structural support. These technologies have proved successful in animal models, but have yet to reach clinical translation.

Hutmacher stated that the ideal bone graft substitute would:

(i) have a three-dimensional and highly porous structure with an interconnected pore network for cell growth and flow of nutrients and metabolic waste;

(ii) be biocompatible and bioresorbable with a controllable degradation and resorption rate to match cell/tissue growth in vitro and/or in vivo;

(iii) have suitable surface chemistry for cell attachment, proliferation, and differentiation;

(iv) have mechanical properties to match those of the tissues at the site of implantation (Hutmacher 2000). This final property is debateable though, as some would argue that a slight mismatch in properties would stimulate bone remodelling via the 'mechanostat' mechanism. (Frost 1987)

Variation of polymer type and chain length offers this possibility although there is historical evidence that even when the breakdown products are entirely physiological (eg PLA = lactic acid), there is potential for graft failure (Bergsma *et al.* 1993;Bostman *et al.* 1990;Bostman *et al.* 1992b). Polymers of the poly(ά-hydroxy acids) group undergo a process known as bulk degradation. The molecular chains of the polymers begins to decrease in size a short time after placement in basal media, but it is not until the polymer chain length reaches a threshold value that allows the chains to freely diffuse out of the polymer matrix that mass loss can occur. This results in accelerated degradation of the polymer matrix, which in turn can lead to rapid loss of physical integrity, with an accompanying rise in potentially damaging acidic by-products.

This process has been observed in clinical case series, where significant release of acidic by-products has led to excessive inflammatory reactions (Bergsma *et al.* 1993;Bostman *et al.* 1992a). This process thus highlights the need for adequate vascularisation to occur around and throughout any polymeric grafts, such that acidic by-products can be effectively transported away.

In a large clinical case series of 2,528 patients who were operated on using pins, rods, bolts, and screws made of polyglycolic acid or polylactic acid, 108 (4.3%) were affected by a clinically significant local inflammatory, sterile tissue reaction (Bostman and Pihlajamaki 2000). In 107 patients, the reaction was elicited by a polyglycolic acid implant, but only one patient by a polylactic acid implant (incidence 5.3% and 0.2% respectively). The adverse tissue responses to polyglycolic acid were seen 11 weeks after the operation whereas the reaction to polylactic acid occurred 4.3 years after fixation of an ankle fracture. The authors concluded that the results were adequate to calculate the foreign body reaction risk for fast grading polymers such as PGA, but for slow degrading polymers such as polylactic acid, the ultimate biocompatibility still is unsettled, and additional clinical research with long follow-up is required.

A potential method to reduce the adverse effects is to incorporate basic salts within the polymer, which has given promising *in vitro* results (Agrawal and Athanasiou 1997). Furthermore, foreign body reactions have been successfully modulated in a rat model by impregnating the implants with an antibody against a macrophage- activating T-cell derived cytokine (anti-IFN-gamma) (Khouw *et al.* 1998).

1.2 The role of Tissue Engineering

Tissue engineering can be defined as the application of scientific principles to the design, modification, growth and maintenance of living tissues (Langer and Vacanti 1993). Tissue engineering strategies have built on the concept of osteoconductive graft replacements and implants, such that the production of an osteoinductive and osteogenic material is a real possibility. Principles on which bone regenerative tissue engineering strategies are based have traditionally been summarised by three principals:

1) **Osteoconduction**: a graft must promote the on-growth and in-growth of surrounding host bone.
2) **Osteoinduction:** a graft should induce host precursor cells to differentiate into mature cells required for bone generation. This may be possible through the provision of additional growth factors etc.
3) **Osteogenesis**: the graft should provide additional cells such that it has the potential for *de novo* bone regeneration in host areas where they may be in short supply eg avascular areas.

However, regarding bone regeneration these have recently been extended to a diamond concept (Figure 1.4) (Giannoudis *et al.* 2007).

Figure 1.4: The Diamond concept as described by Giannoudis *et al.* 2007. Adherence to four principals optimises the chance of successful graft incorporation.

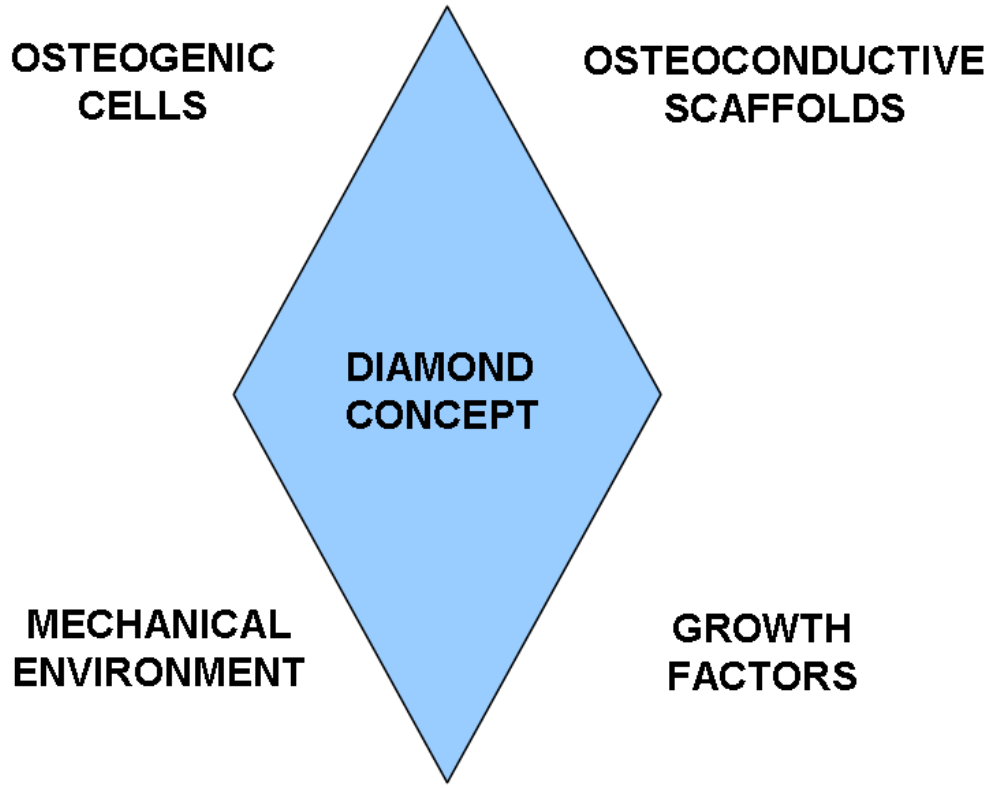

In order for optimal successful application a tissue engineered scaffold must not only supply an adequate supply of progenitor cells (which are usually deficient in areas of lost bone stock), with the appropriate growth factors to promote survival and the desired end point differentiation, but must also have appropriate structural characteristics to provide a stable local mechanical environment to promote bone regeneration. Thus in order to design an optimal tissue engineered product, a full understanding of function and biology of bone is required.

1.3 Basic Bone Biology: Structure, function and cells

Bone can be divided into two main types: cortical and cancellous bone. Cortical bone usually makes up the outer regions, whereas cancellous (or trabecular) bone is found in the inner spaces (Marieb and Hoehn 2010).

Long bones can be described as having a diaphysis or shaft, which consists of an annular of cortical bone, as well as two end regions; an epiphysis, which consists of an outer layer of cortical bone surrounding an inner volume of cancellous bone (Figure 1.5). Most bones of the limbs, including those of the fingers and toes, are long bones.

Figure 1.5: Diagram displaying the structure of a long bone. From http://classes.midlandstech.edu/carterp/Courses/bio210/chap06/lecture1.html (accessed 17/10/2013).

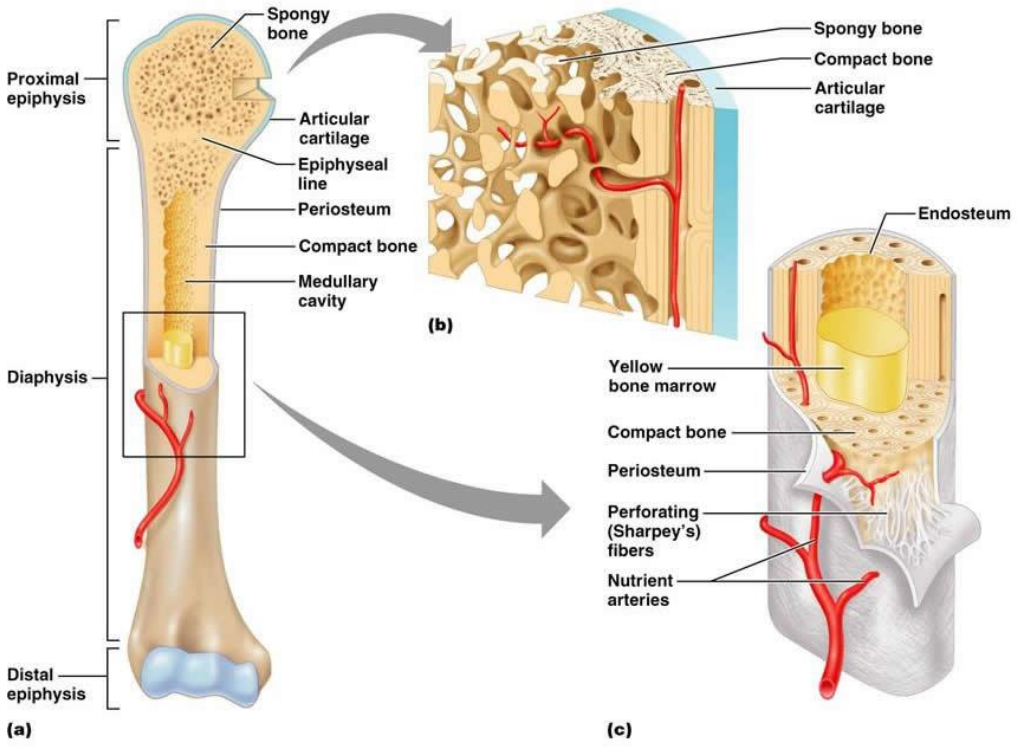

Flat bones are found where the principal requirement is either protection or the provision of broad surfaces for muscular attachment. These bones are usually broad, flat plates, such as in the cranium, the ilium and the scapula. Flat bones are composed of two thin layers of cortical bone enclosing between them a variable quantity of cancellous bone. Red bone marrow is found within the cancellous bone, and hence most red blood cells are formed within flat bones (Spence 1990).

Short bones and irregular bones consist of compact bone surrounding a cancellous interior. Short bones include those of the wrist, and irregular bones are found in areas such as the spine and hip (Marieb and Hoehn 2010).

The periosteum surrounds the external surface of most bones, and consists of connective tissue with an internal surface of a finer membrane covering spongy bone, termed the endosteum. The periosteum provides much of the bones nutrients, and is served by a number of blood and lymphatic vessels, as well as nerve fibres. The periosteum also gives rise to important muscular tendon and ligament insertions making it important for locomotion (Dunning 2002).

Cortical bone is made up of an interconnected group of subunits known as osteons, or the Haversian system. Many osteons are bundled together in parallel, which makes cortical bone optimised to handle compressive and bending forces. A single osteon consists of a hollow, laminated rod of collagen and inorganic calcium phosphates; the hollow core is a nutrient channel (the Haversian canal). At the epiphysis where the stresses become more complex, the Haversian systems diverge and branch to form a meshwork: cancellous bone. In cancellous bone the tissue consists of similar lamellae, but the lamellae are much less ordered.

Figure 1.6: The microstructure of bone. (Diagram from 'The Human Bone Manual' (White and Folkens 2005)).

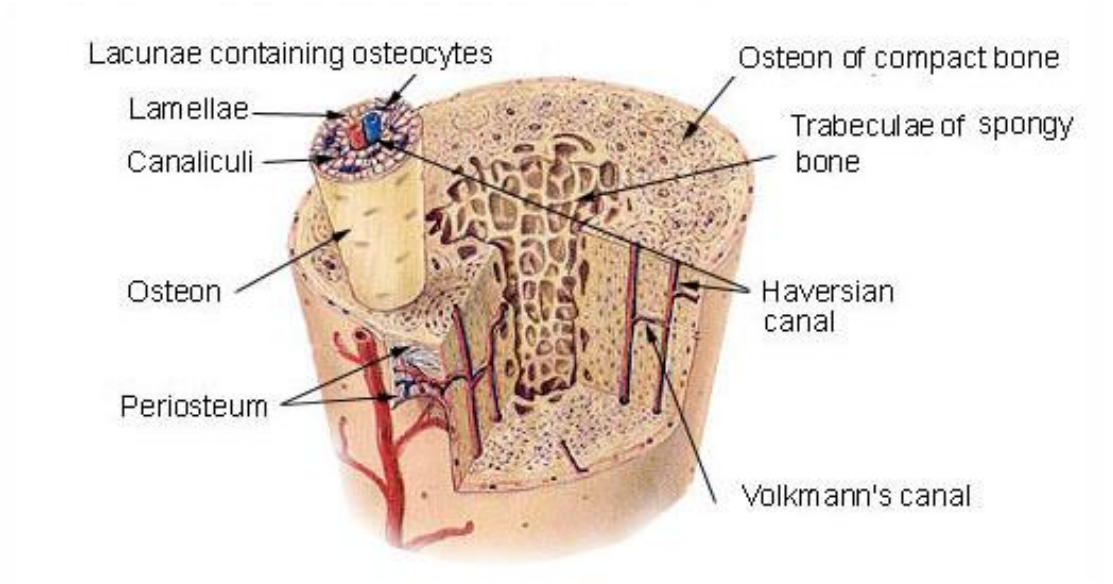

Bone is a dynamic tissue, continually undergoing a cycle of degradation and reformation. This occurs via the coordinated actions of a number of cells primarily involving osteoblasts, osteocytes and osteoclasts.

1.3.1 Osteoblasts / Osteocytes

Osteoblasts are mononucleate bone-forming cells that descend from osteoprogenitor cells. Osteoblasts are responsible for the synthesis of new bone and subsequent mineralisation (Neve *et al.* 2011). Osteoblasts are found on the surface of osteoid seams and make osteoid (the organic component of bone). Osteoid is primarily composed of fibrous protein and ground substance.(Frost 1962) The predominant fibre-type is Type-1 collagen and comprises ninety percent of the osteoid. The ground substance is mostly made up of chondroitin sulfate and osteocalcin. Osteoblasts produce alkaline phosphatase, an enzyme that has a role in the mineralisation of bone, as well as many matrix proteins (Takuwa *et al.* 1991). Osteoblasts finally become entrapped in the bone matrix and become osteocytes (Franz-Odendaal *et al.* 2006). The dendritic structures utilised by osteoblasts for communication become canaliculae as the bone hardens around them, and these allow nutrient and waste transport between different osteons (Palumbo *et al.* 1990). Osteocytes have been shown to have roles in continued formation of bone, matrix maintenance, calcium homeostasis and also have an important role as mechano-sensory receptors (Aarden *et al*. 1994).

1.3.2 Osteoclasts

Osteoclasts are derived from a monocyte stem-cell lineage, and hence have the capacity for phagocytic-like mechanisms similar to circulating macrophages (Zaidi *et al.* 1993). Osteoclasts are large, multinucleated cells and are found on bone surfaces in ‘Howship's lacunae’ or resorption pits (Dobson 1952). Osteoclasts are the cells responsible for bone resorption, and work in a coordinated fashion with osteoblasts. Osteoclasts utilise enzymes such as tartrate resistant acid phosphatase for their actions in the breakdown of mineral substrate (Marieb and Hoehn 2010).

1.4 Skeletal stem cells and their potential in tissue engineering

Skeletal stem cells (SSC), often referred to as mesenchymal stem cells, osteogenic stem cells, osteoprogenitor cell, marrow stromal fibroblastic cells, or human bone marrow stromal cells, are cells that have the capacity for self-renewal, and can differentiate into a variety of cell types, including: osteoblasts, chondrocytes, fibroblasts, myoblasts and adipocytes (Figure 1.7) (Friedenstein *et al.* 1966;Friedenstein *et al.* 1968;Lajtha 1979). SSCs differ from totipotent / pluripotent (eg embryonic) stem cells in that SSCs have the potential to give rise to cells from the stromal lineages (multipotent). There is significant work around artificially derived pluripotency from non-pluripotent cells, by inducing a "forced" expression of specific genes (c-myc, sox-2 etc) (Dimos *et al.* 2008).

Figure 1.7: Differentiation potential of skeletal stem cells (Singer and Caplan 2011).

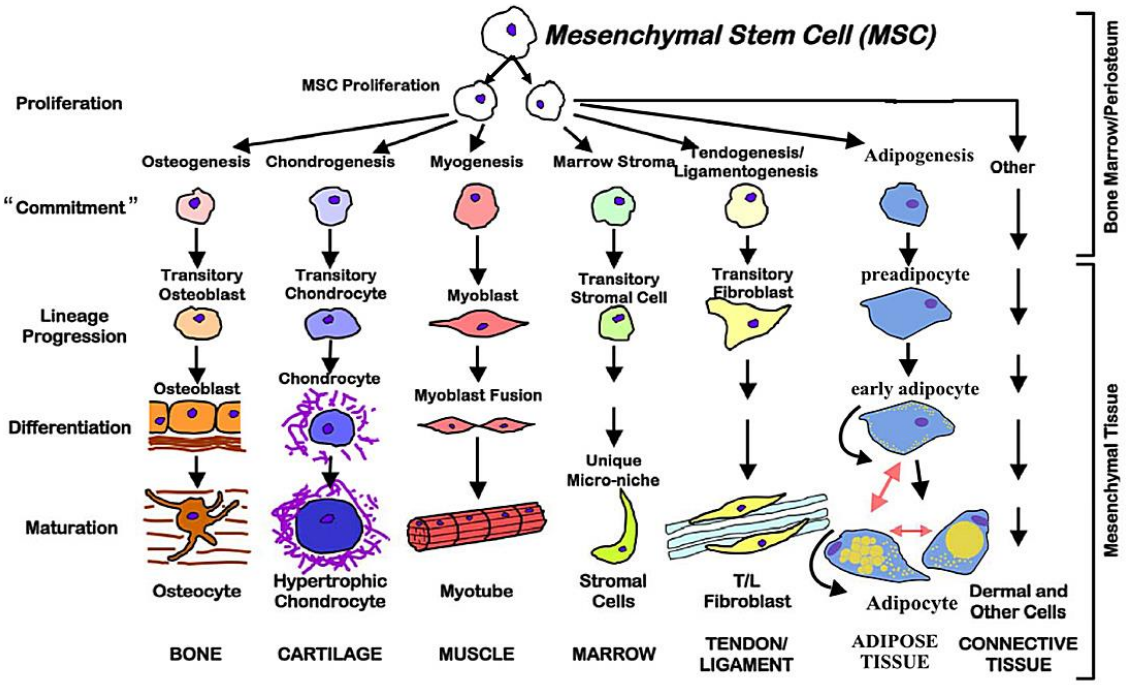

SSCs were first identified by Friedenstein and colleagues, who described a population of spindle-shaped stromal cells present in the bone marrow that had the capacity for self-renewal, differentiation into more than one cell type and maintain the ability for cell division throughout life (Friedenstein *et al.* 1974;Friedenstein *et al.* 1976). In these

original experiments SSCs were referred to as colony-forming unit-fibroblasts (CFU-f), and subsequent experiments went on to show how the differentiation potential of the cells could be altered by environmental cues. Culture of the cells in media containing ascorbic acid and dexamethasone gave the stimulus for osteoblastic differentiation (Figure 1.8), whereas the addition of factors such as transforming growth factor beta (TGF-β) stimulates the expression of chondrogenic markers (Tare *et al.* 2008).

Figure 1.8: ALP stain of SSCs on tissue culture plastic after 7 days incubation (x50) magnification A) basal media and B) osteogenic media (scale bar = 200 μm). The cells grown in osteogenic media have higher staining rate for ALP (pink) a marker of osteoblastic differentiation.

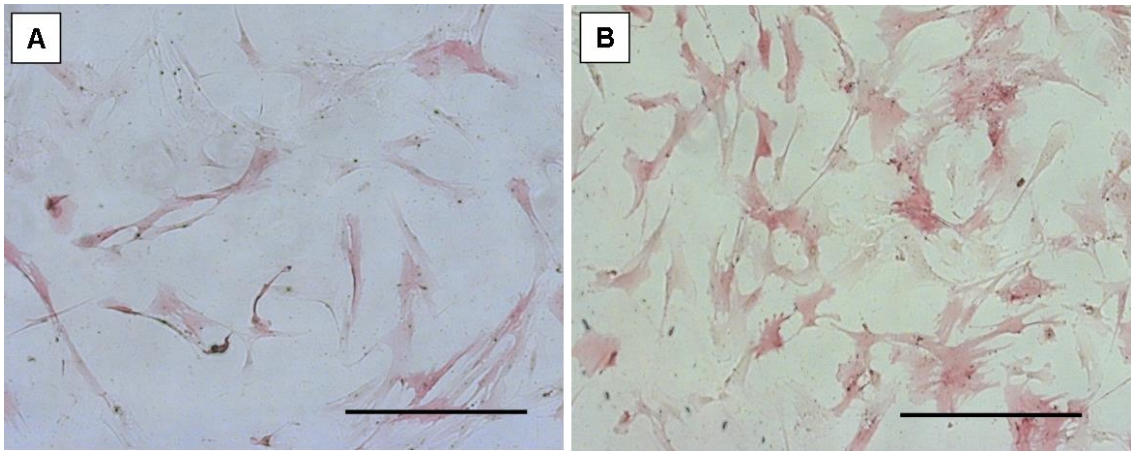

The use of SSCs is gaining momentum in the orthopaedic setting. Hernigou *et al.* have performed extensive clinical work investigating the potential of osteoprogenitor cells in the treatment of established atrophic tibial non-unions (Hernigou *et al.* 2005a;Hernigou *et al.* 2005b). The authors found injection of a concentrated fraction of autologous pelvic bone marrow aspirate into the site of non-union in sixty patients resulted in bone union in all but 7 cases. Interestingly, all these cases showed a significantly lower CFU-F (fibroblastic colony forming unit) count in the aspirate, indicating a requirement for delivery of a critical concentration of progenitor cells (significantly in excess of 1000 progenitors/ml) to the defect site. This concentration is in excess of that provided by fresh iliac crest aspirate, indicating the need for cell enrichment strategies (Hernigou *et al.* 2005a).

SSCs have also been put forward for use in cartilage regeneration. A recent equine study combined a microfracture technique with stem cell technology (Fortier *et al.* 2010). A full thickness cartilage defect was created in the lateral femoral trochlear ridge of twelve horses. The horses were treated with either microfracture alone, or microfracture augmented with a concentrated fraction of bone marrow aspirate. Results were analysed macroscopically, via imaging and histology. All scoring systems and magnetic resonance imaging data indicated that delivery of the bone marrow concentrate resulted in increased fill of the defects and improved integration of repair tissue into surrounding normal cartilage. In addition, there was improved type II collagen content and orientation of the collagen as well as significantly more glycosaminoglycan in the bone marrow concentrate-treated defects than in the microfracture-treated defects. Clinical trials are likely to follow these large animal results to confirm the efficacy observed.

SSCs have also been used for cartilage regeneration in other branches of medicine. Macchiarini *et al*. took a human donor trachea, which was then readily colonised by epithelial cells and SSC derived chondrocytes that had been cultured from cells taken from the recipient (a 30-year old woman with end-stage bronchomalacia). This graft was then used to successfully replace the recipient's left main bronchus (Macchiarini *et al.* 2008).

The addition of skeletal stem cells to joint prostheses is also under investigation in clinical practice. Ohgushi *et al.* successfully applied a tissue engineering approach to ankle arthroplasty in three patients with osteoarthritis in an attempt to reduce the rate of aseptic loosening associated with these prostheses (Ohgushi *et al.* 2005). The authors culture-expanded skeletal stem cells from iliac crest aspirate in osteogenic conditions for up to 19 days, then applied these to the alumina-ceramic bone-contacting surfaces of the prosthesis, culturing for a further 2 weeks before implanting the construct into the patient. Whilst the study had a number of limitations (lack of a control group and a small cohort with short patient follow-up) the work highlights an exciting new approach to primary arthroplasty.

1.5 Growth Factors

Growth factors are naturally occurring substances that are capable of affecting a cells growth, differentiation and behaviour. Growth factors are usually either a protein or a steroid hormone, and appear to play an important role in bone regeneration.

1.5.1 Bone morphogenic proteins

One particular group of growth factors from the Transforming growth factor (TGF- β) family, include a series of proteins known as the bone morphogenic proteins (BMPs). BMPs were originally discovered and deemed to be of interest due to their ability to induce the formation of bone and cartilage but BMPs are now considered to constitute a group of pivotal morphogenetic signals, orchestrating tissue architecture throughout the entire body (Reddi 2005). Indeed, changes to their regulation status has now been found to form pivotal roles in the signaling pathways involved in the development of Barrett's oesophagus, colon cancer and adenocarcinoma of the proximal gastro intestinal tract (Kodach *et al.* 2008;Milano *et al.* 2007).

BMPs were first discovered by Marshall Urist, who noted that demineralized, lyophilized segments of bone induced new bone formation when implanted in muscle pouches in rabbits (Urist 1965;Urist and Strates 1971). Urist proposed that proteins must be present, and coined the term bone morphogenic protein, but it was Harri Redi who first isolated them and deduced their stepwise action via the induction of chemotaxis, mitosis, and differentiation of cells (Reddi and Huggins 1972).

BMPs have found limited use clinically for application in long bone fracture non-unions and spinal fusion (infuse BMP-2 and OP-1 / BMP-7), where results have been encouraging. Stambough *et al.* examined a group of 36 patients undergoing one and two level spinal fusions using infuse BMP-2, finding a fusion rate as determined by CT, of 97.2% (Stambough *et al.* 2010).

However, due to BMPs FDA status as a class III device, regulatory approval is extremely stringent, making them prohibitively expensive, and reducing progress in this area. Furthermore, concerns have been raised as to possible side effects of BMP use, including immunogenicity, possible carcinogenicity and their ability to cross the placenta in pregnancy (Harwood and Giannoudis 2005).

1.5.2 Vascular endothelial growth factors

More recently the importance of factors influencing ingrowth of vessels has emerged. Vascular endothelial growth factors (VEGF) are a family of signal proteins produced by cells that stimulate vasculogenesis and angiogenesis (Hoeben *et al.* 2004). The most important appears to be VEGF A, which has been shown to stimulate endothelial cell mitogenesis and cell migration in vitro. It is also a vasodilator and increases microvascular permeability and VEGF mediated angiogenesis has also been shown to direct bone tissue formation at sites of endochondral ossification (Gerber *et al.* 1999;Gerber and Ferrara 2003).

Recent bone regenerative strategies have therefore attempted to promote the invasion of blood vessels and the formation of a vascular network (angiogenesis) within the forming tissue, processes which are essential to neo-bone formation. The vasculature provides for the mass transport requirements of the tissue (Colton 1995), allows for the delivery of and recruitment of circulating stem cells required for bone formation (Prockop 1997), and facilitates communication between endothelial cells and pre-osteoblasts to direct their differentiation (Villars *et al.* 2000). Even though the use of VEGF has been shown to stimulate increased callus formation and assist bone healing in animal fracture models, as well as enhance osteoregenerative scaffold integration, it has yet to make a widespread impact in clinical orthopaedic use.

Other VEGFs include VEGF-B and VEGF-C, which have roles in embryonic angiogenesis and lymphangiogenesis respectively (Claesson-Welsh 2008;Jeltsch *et al.* 1997).

Murine models have been instituted to study the effects of both BMP-2 and VEGF on bone formation in tibial segmental defects incorporating bioresorbable scaffolds. Kanczler and colleagues reported enhanced bone formation in the bone from the scaffolds incorporating BMP-2 and VEGF (Kanczler *et al.* 2010). The bone formation observed was further augmented in those scaffolds incorporating both growth factors with the additional seeding of SSCs. While these studies provide exciting and innovative developments in the regenerative potential of the critical scaffolds with SSCs for the treatment of larger bone defects, large animal studies are required prior to clinical translation.

1.5.3 Angiopoietins

The angiopoietins are another group of growth factors which are involved in the development of blood vessels. Four proteins have been discovered so far (Ang1, Ang2, Ang3 and Ang4), the first two having been shown to be essential in mature vessel formation. Knock out mouse studies revealed that Angiopoietin-2 was dispensable for embryonic vascular development, but was a requisite for subsequent angiogenic remodelling. These studies also demonstrated that members of the VEGF and Angiopoietin families collaborate during development of the lymphatic vasculature (Thurston 2003).

The mechanism of action of angiopoietins on cells is via the TIE receptor, a tyrosine kinase type receptor which leads to a series of downstream cell signals involved in key regulatory functions (Kobayashi and Lin 2005).

Clinically, angiopoietin 2 has been found to be elevated in patients with angiosarcoma, and in experimental animals injected with TIE-2 positive cells, there may be reduced atheroma formation, indicating a potential role in vascular and cardiac disease (Amo *et al.* 2004;Hauer *et al.* 2009).

From a tissue engineering perspective, angiopoietin 1 gene transfected bone marrow mesenchymal stem cells have been shown to increase the osteogenic properties of beta-TCP scaffolds by enhancing capillary regeneration, in both mice and rabbit models (Liu *et al.* 2011).

1.5.4 Platelet Rich plasma

Platelet-rich plasma (PRP) is blood plasma that has been enriched with platelets. PRP has been in clinical use for a number of years, and has been shown to assist in the treatment of orthopaedic problems such as fracture non-unions, tendon and ligament injuries (Calori *et al*. 2008;Foster *et al.* 2009). Recombinant factors (eg BMP / VEGF) are expensive, and high doses may be required to achieve any therapeutic effect. Autologous platelet concentrates, however, offer an easy, cost-effective approach to obtain high concentrations of growth factors for tissue healing and regeneration. The effects are likely mediated through the growth factors released from the α-granules of

platelets upon activation during clotting. These are known to contribute to tissue healing and include vascular endothelial growth factor (VEGF), insulin like growth factor (IGF), epidermal growth factor (EGF), transforming growth factor beta (TGF-β) and platelet derived growth factor (PDGF) (Eppley *et al.* 2004). It is also felt that PRP has anti-inflammatory properties, and this might have clinical implications in terms of cartilage regeneration (Bendinelli *et al.* 2010).

The effects of PRP have been shown both *in vitro* and *in vivo*. Lucarelli *et al.* examined the effect of increasing concentrations of PRP on the proliferation of human stem cells (Lucarelli *et al.* 2005). The authors showed a significant increase in cell numbers with an increase in concentration of PRP from 1% to 10%. Aspenberg and Virchenko showed that the injection of PRP percutaneously into transected tendo achilles of rats increased the strength and stiffness of tendon callus by about 30% after one week (Aspenberg and Virchenko 2004).

Clinical application of PRP is widespread in periodontal surgery, maxillofacial surgery and plastic surgery, but the use of PRP is also finding a place in orthopaedic procedures involving tendon and other soft tissues, as well as bone procedures. Mishra and Pavelko showed that in a cohort of 15 patients with lateral epicondylitis that had not responded to conservative treatment modalities, patients had a 60% improvement in symptoms at 8 weeks, and 81% by 6 months (Mishra and Pavelko 2006).Bielecki *et al*. examined the use of percutaneous injection of autologous platelet-rich gel as a minimally invasive alternative to open grafting in the treatment of delayed and non-union (Bielecki *et al.* 2008). In their cohort of 12 patients with delayed union, all achieved union. For the cohort of 20 patients with non-union, union was observed in 13 and the average time was 10.3 weeks after injection with PRP. Lowery, Kulkarni and Pennisi administered PRP and autogenous bone grafts during spinal fusion with good results, obtaining union in all nineteen treated patients (Lowery *et al.* 1999).

The evidence for the use of PRP in orthopaedics is however limited to small case series, and the use of PRP still lacks the support of randomised controlled trials. Further research is therefore needed to define the treatable musculo-skeletal conditions, methods of administration and the ideal patient population for PRP application.

1.6 Translation from bench to clinic for bone graft substitutes

In order to produce the optimal regenerative bone graft substitute, it is likely that the scaffold would have to combine the majority, or even all of the tissue engineering principals. Thus the graft would consist of a SSC seeded bioresorbable scaffold with structural integrity comparable to that of bone, incorporating growth factors, such that a composite graft is created that functionally fills the defect, but then dissolves or is resorbed at a rate consistent with its bone regenerative potential. Significant progress has indeed been made into this field, often with encouraging results.

When investigating the bridging of larger diaphyseal defects Quarto and co workers, translated successful animal trials of a hydroxyapatite scaffold seeded with *ex vivo* culture-expanded autologous marrow-derived osteoprogenitor cells to a small clinical series of three patients with large segmental defects (40 to 70 mm) in long bones (Quarto *et al.* 2001). Within two months of surgery abundant callus formation and new host bone integration were observed, and 6-7 year follow-up demonstrated long term durability. Similar technology has allowed the production of a distal phalanx by combining *ex vivo* culture-expanded periosteum-derived cells seeded onto a porous hydroxyapatite scaffold and encapsulated within a hydrogel coating (Vacanti *et al.* 2001).

Further clinical use of a tissue engineering strategy has also been applied in tumour surgery. Morishita *et al.* used *ex vivo* osteogenic culture-expanded autologous skeletal stem cells seeded onto a hydroxyapatite scaffold in three patients to treat a bone cavities left by excision of an aneurysmal bone cyst within proximal tibia, giant cell tumour of proximal tibia, and fibrous dysplasia of proximal femur respectively (Morishita *et al.* 2006). In all cases early weight bearing was commenced (within 2-3 weeks) with no adverse clinical or radiological sequelae, demonstrating excellent early mechanical strength. Johnson *et al*. treated twenty-five patients with resistant non-unions including partial or complete segmental defects with a composite allo-implant of human bone morphogenetic protein (h-BMP) and autolyzed, antigen-free, allogeneic bone. Union was achieved in 24 of the 25 patients, with the failed case being attributable to recurrent infection (Johnson *et al*. 1992). A summary of clinically translated tissue engineering strategies is given in Table 1.1.

Table 1.1: Clinically translated tissue engineering strategies for bone regeneration (modified from (Smith *et al.* 2011)).

RECONSTRUCTIVE STRATEGY		**SITE**	**PATHOLOGY**	**REFERENCE**
Cells	**Scaffold/ Technique**			
Autologous periosteum-derived cells	Hydroxyapatite	Thumb - distal phalanx	Trauma	(Vacanti *et al.* 2001)
Autologous marrow-derived cells	Hydroxyapatite	Long bones	Defects following osteotomy for lengthening/ trauma	(Marcacci *et al.* 2007;Quarto *et al.* 2001)
Autologous bone marrow	Hydroxyapatite & titanium	Mandible	Oral neoplasia	(Warnke *et al.* 2004;Warnke *et al.* 2006)
Autologous concentrated bone marrow aspirate	Percutaneous injection	Tibia	Non-union following trauma	(Hernigou *et al.* 2005b)
Culture-expanded skeletal stem cells	Alumina-ceramic prosthesis	Ankle	Osteoarthritis	(Ohgushi *et al.* 2005)
Autologous stem cells and platelet-rich plasma	Hydroxyapatite	Maxilla	Reduced alveolar bone crestal height	(Ueda *et al.* 2005)
Autologous bone marrow aspirate	Impaction bone grafting of allograft	Femoral head	Cyst / osteonecrosis	(Tilley *et al.* 2006)
Concentrated autologous bone marrow aspirate	Local application	Femoral head	Osteonecrosis	(Hernigou *et al.* 2009)
Culture-expanded autologous skeletal stem cells	Hydroxyapatite	Femur/ tibia	Benign bone tumours	(Morishita *et al.* 2006)
Culture-expanded skeletal stem cells and platelet-rich plasma	Titanium mesh plate	Alveolar cleft	Congenital cleft lip and alveolus	(Hibi *et al.* 2006)
Skeletal stem cells and platelet-rich plasma	Distraction osteogenesis	Femur/ tibia	Achondroplasia/ hypochondroplasia	(Kitoh *et al.* 2007)
Platelet-rich plasma	Local application	Spine/ mandible/ maxilla	Degenerative/ congenital	(Vadala *et al.* 2008;Hartmann *et al.* 2010;Alsousou *et al.* 2009)

1.7 The role of tissue engineering in hip arthroplasty

In the UK, around 2 million people per year will contact their GP with symptoms related to osteoarthritis (Arthritis Research UK 2014). Osteoarthritis of the hip is an extremely common condition throughout the western world (Figure 1.9) with approximately 12% of adults of 65 years of age or more suffering hip pain from the condition (Cecchi *et al.* 2008). Risk factors include age, female sex, obesity, previous trauma, joint laxity and family history.

The disease process involves a progressive loss of joint cartilage. As the cartilage tries to repair itself, the bone remodels, the underlying (subchondral) bone hardens, and bone cyst form. The process can be divided into distinct phases.

1. The stationary phase of disease involves the formation of osteophytes along with joint space narrowing.
2. Joint space narrowing progresses.
3. The erosive phase of the disease is marked by the appearance of subchondral cysts (cysts in the bone underneath the cartilage).
4. The final phase of the disease involves bone repair and remodelling.

Current treatment modalities involve a stepwise course of management, initially starting with conservative modalities such as weight loss, physiotherapy the provision of walking aids and behavioural changes. Pharmacological treatment also follows a standard analgesic pain ladder, ranging from simple paracetamol, and subsequent addition of anti-inflammatories and finally opioid analgesics. Other disease modifying agents and experimental agents such as matrix metalloproteinase inhibitors, cytokines, nitric oxide, growth factors and gene therapy have been tried with varied success (Fajardo & Di Cesare 2005). The use of non-prescription agents such as cod liver oil and glucosamine have not been shown to provide any relief over placebo alone (Rozendaal *et al.* 2008).

Steroid injections into the joint can give temporary relief, and are often useful for diagnostic purposes, but do not offer a long term solution (Dieppe *et al.* 1980).

Figure 1.9: AP radiograph of left hip joint, showing significant loss of joint space, sclerosis and osteophyte formation (arrow). *Image courtesy of University Hospital Southampton NHS Foundation Trust.*

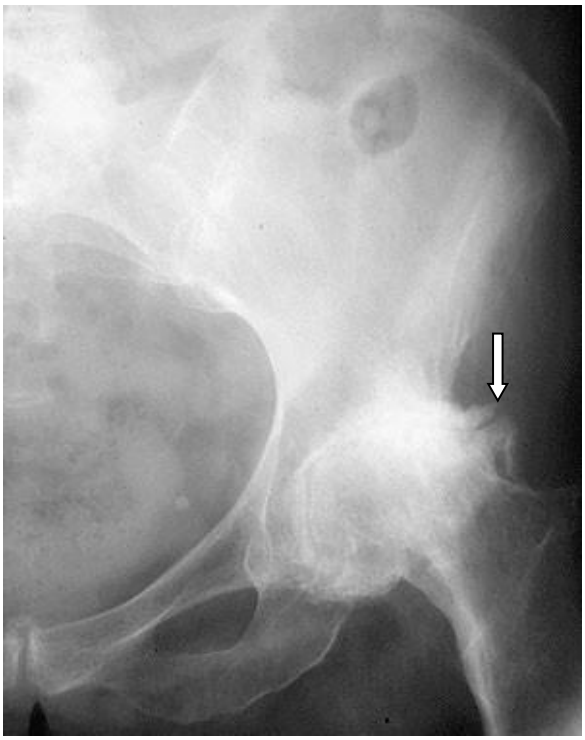

Interestingly, injections of adipose derived SSCs have been shown to be of benefit in animals with OA hip. A well conducted randomised and double blinded multicentre trial involving dogs, showed significant improvement in clinical symptoms over the study period (Black *et al.* 2007).

Injections of culture expanded SSCs into OA hips have been attempted in human populations as well with limited success. Centeno *et al.* described a case whereby a male patient suffering from a 20 year history of OA underwent a transfer of isolated nuclear cell concentrate from bone marrow aspirate into the damaged hip (Centeno *et al.* 2006). Subsequent MRI showed neocortex formation when compared to immediate pre-op MRI and objective improvements were noted that coincided with subjective reports of improvement.

Furthermore, multiple studies have described the beneficial effects of core decompression with additional implantation of autologous SSCs for treatment of early

osteonecrosis of the femoral head (a condition associated with OA of the hip) (Gangji and Hauzeur 2005).

The indication for surgery is failure of conservative therapies to control symptoms and often this will correlate with the advanced phases of the disease. Often this will involve night pain leading to loss of sleep, and day time pain meaning that activities of daily living are restricted. A range of surgical procedures are available for the treatment of advanced arthritis ranging from non-implant surgeries, including arthroscopic debridement, osteotomy, and Girdlestones excision arthroplasty, to the more routine arthroplasty options including resurfacings, hemiarthroplasty, and total joint replacement .

These final options have been attempted with varying success for almost 100 years, but it took until the 1960's, when Sir John Charnley came up with the concept of a low frictional torque arthroplasty, that advanced degenerative hip conditions have been successfully managed long-term, and in significant numbers with implant surgery (Charnley 1970). Various modifications to the original concept have been introduced over the decades, including varying head side, prosthetic shape, bearing surfaces and fixation methods, all in an attempt to enhance the longevity of the implants, but none the less little improvement has been gained over the excellent initial results of Charnley, and his early competitors (Stuchin 2008;Davidson 1993;Toth *et al*. 2010). Other than early failure due to infection, the main modality of medium to long failure is aseptic prosthetic loosening, often as a consequence of wear induced osteolysis (Zhu *et al*. 2001). Small wear particles from the bearing surfaces of the joint induce a host inflammatory reaction involving macrophages etc, leading to subsequent osteolysis of the bone in proximity to the wear particles (Amstutz *et al.*1992). The early metal on polyethylene joint replacements were particularly susceptible to this method of failure, and a large body of work has gone into designing bearing surfaces which are more resistant. Current concepts include ceramic, ultra high molecular weight and crosslinked polyethylene, as well as metal on metal bearing surfaces. However, the recent catastrophic failure and subsequent recall of the ASR metal on metal joint replacement, indicates that despite extensive *in vitro* success in this area, a proven long term clinical solution remains to be found (Langton *et al.* 2010).

Recent tissue engineering strategies are exploring novel strategies for the treatment of OA, with the intention of regenerating the joint, rather than joint excision and replacement with manufactured components. This concept represents a paradigm shift in the approach to advanced OA, and is still in the early stages of development. McMurray *et al*. have performed in vitro studies to examine the effects of surface nanotopography on SSC fate in the absence of chemical induction (McMurray *et al.* 2011). Using genetic and epigenetic analysis the authors showed that nanoscale patterns can directly modulate differentiation of human stem cells, raising the possibility that implants with specific nanotopographical surfaces, could simulate the development of biological joint surfaces. These studies have been substantiated by similar work in the area, finding that certain nanotopographies can enhance osteoblastic differentiation of stem cell populations (You *et al.* 2010).

One group has recently taken the concept a stage further with an *in vivo* model. This study in rabbits involved excision of the entire articular surface of the proximal humerus, and replacement with an anatomically correct bioscaffold spatially infused with transforming growth factor β3 (TGFβ3)-adsorbed or TGFβ3-free collagen hydrogel (Lee *et al.* 2010). Four months after surgery, TGFβ3-infused bioscaffolds were fully covered with hyaline cartilage on the articular surface whilst TGFβ3-free bioscaffolds had only isolated cartilage formation. Compressive and shear properties of TGFβ3-mediated articular cartilage did not differ from those of native articular cartilage, and were significantly greater than those of cartilage formed without TGFβ3. TGFβ3 delivery recruited approximately 130 % more cells in the regenerated articular cartilage than did spontaneous cell migration without TGFβ3. Whilst we are still along way from being able to regenerate the extremely complex human joint, this study provides proof of concept, and hints at future possibilities. The scaffolds did not have *in vitro* seeded SSCs, but did contain specific growth factors to recruit and home endogenous cells.

To date, joint arthroplasty remains the commonest final treatment choice for joint failure in OA. An ever increasing clinical problem therefore exists, in that following increasing patient numbers undergoing primary hip arthroplasty, there has now been a subsequent increase in patients who require revision arthroplasty surgery. In the UK between 2005 and 2010, the number of primary hip procedures performed increased from 56,000 to 68,000, and the number of patients undergoing revision surgery almost

tripled to eight thousand per year in that time (National Joint Registry for England and Wales 2011). Consequently, these patients now present in increasing numbers with extensive bone loss around loose implants posing a significant orthopaedic challenge for revision surgery.

1.8 Impaction bone grafting

With almost a forty year history in revision hip surgery, impaction bone grafting (IBG) using fresh frozen morcellised allograft remains the current gold standard for replacing lost bone stock (Halliday *et al.* 2003;Schreurs *et al.* 2009). This technique endeavours to recreate a solid, adaptive mantle into which the implant can sit securely, immediately able to withstand forces associated with normal implant use. The ability of the graft bed to resist shear and go on to form a new living bone construct is a critical factor in the long-term success of the revision implant. The technique was first described on the acetabular side by Sloof *et al.* in 1984, and was built on and extended to the femoral side by Ling and Gie in Exeter (Gie *et al.* 1993a;Gie *et al.* 1993b;Slooff *et al.* 1984). The process involves packing the bone defect with morcellised allograft, followed by the use of a specifically designed jig, which is impacted into place, thereby recreating the original bone morphology, but with impacted allograft where the original bone was lost. (Figures 1.10 and 1.11).

The results are encouraging, with up to 87% twenty year survivorship for acetabular components and ten year femoral component survival of 99% (Halliday *et al.* 2003;Schreurs *et al.* 2004). However, widespread adoption of this demanding technique has not always led to a repeat of these results outside of the major centres, and thus laboratory-based research endeavours to find techniques to improve the desirable characteristics of the allograft.

Figure 1.10: The use of a hammer and phantom prosthesis with morcelised allograft to demonstrate how the femoral cortex is recreated in impaction bone grafting (Oakes and Cabanela 2006). A) The use of a tamp, to ensure cortical defect filling with allograft. B) A phantom prosthesis to create an adequate space into which the prosthesis will be inserted. C) Axial view of femur post IBG.

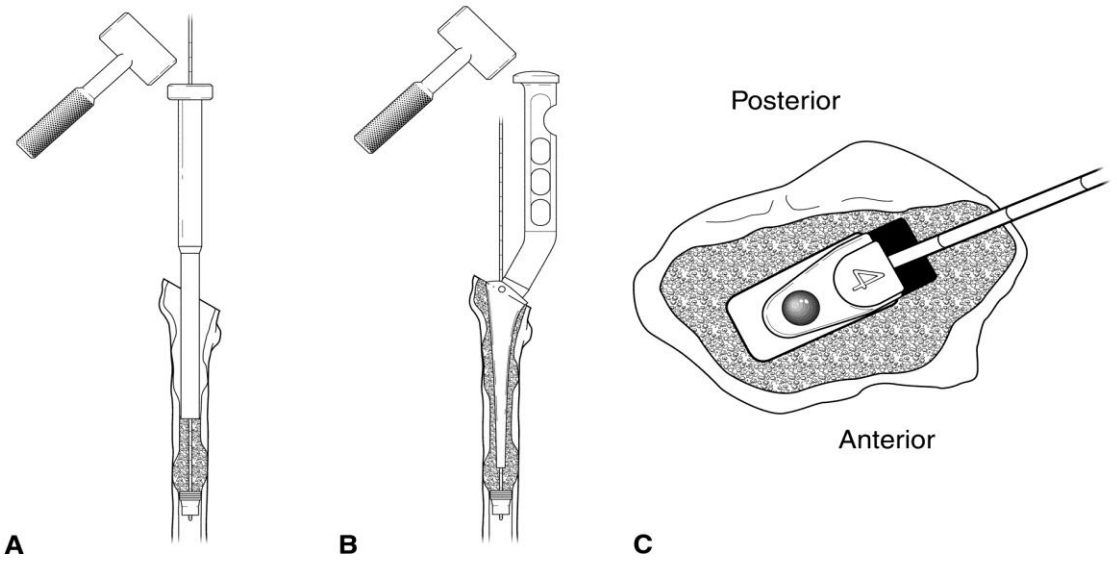

Figure 1.11: A similar technique can be used to replace acetabular bone deficit (Oakes and Cabanela 2006). A+B) Use of metalwork to create a stable base from bone discontiniuity. C-F) Use of a tamp to impact allograft and recreate acetabulum. G) Acetabular component cemented in place.

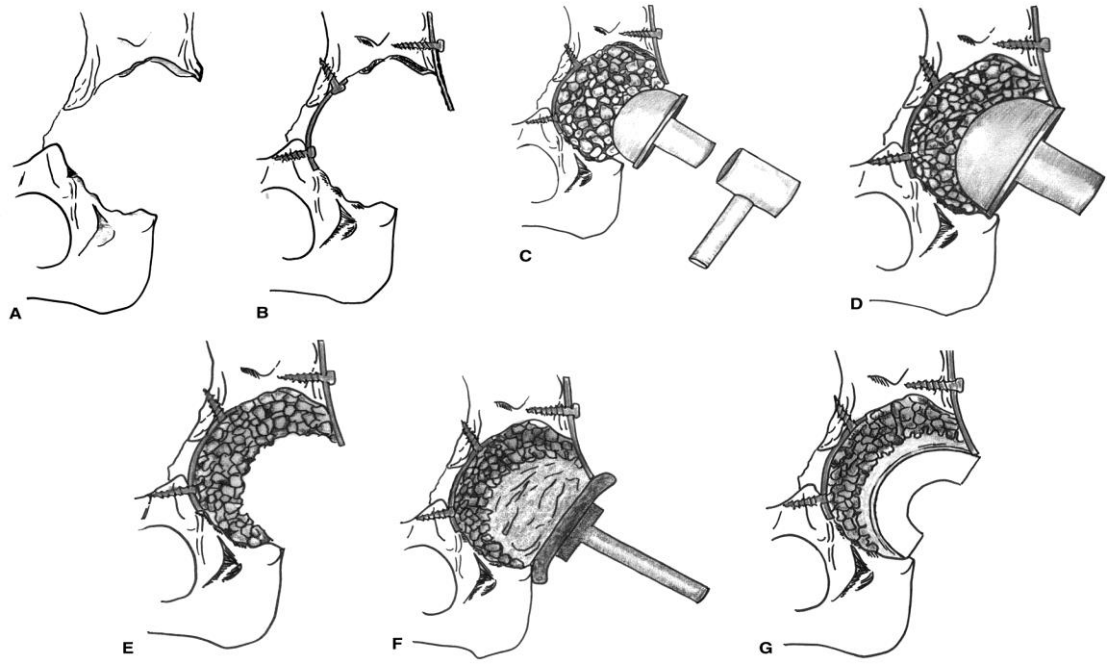

Previous in vitro studies have identified both mechanical and biological factors that can be modulated to augment the structure and performance of IBG. Dunlop *et al.* performed an in vitro study using a custom built cam shear testing rig (Dunlop *et al.* 2003). Utilising the fact that the main mode of failure of implanted prostheses into an IBG bed is due to shear failure of the allograft, they utilised soil mechanical theories in an attempt to improve the cohesion of the construct. They found that a well graded particle size and washing of the particles in order to remove the soft tissue and fat, both contributed to the shear strength of the construct. The effect of grading particle size on increasing aggregate strength has been mathematically determined via a graphical curve of particle distribution, which if carried to infinitely small size will allow the properties of an aggregate to approach those of a solid (Craig RF 1993). This effect can be visualised in Figure 1.12.

Figure 1.12: Demonstration of how a decrease in particle size will improve aggregate strength.

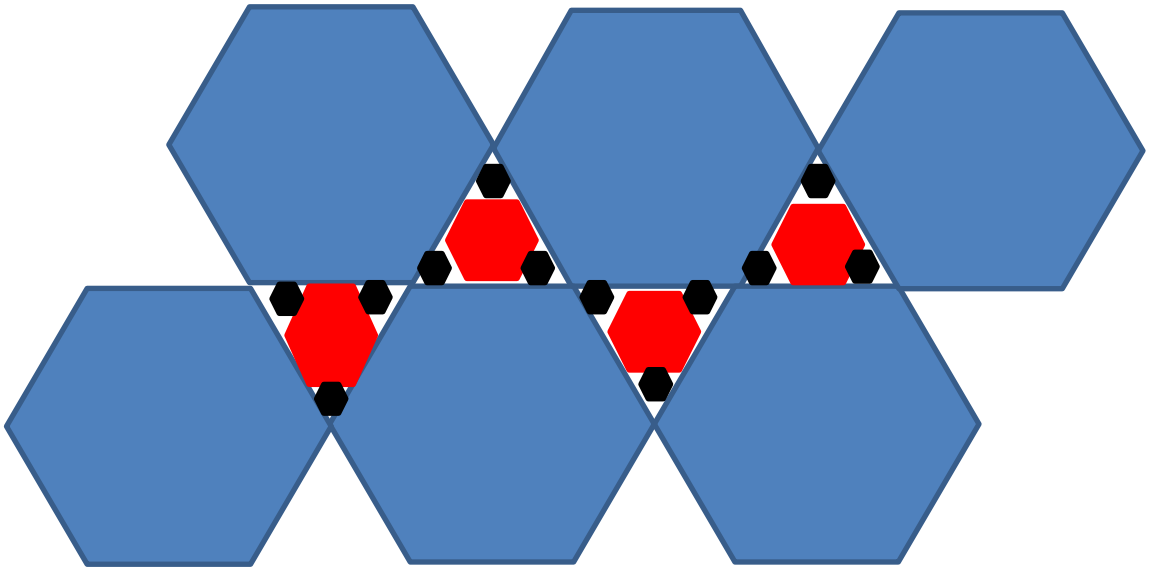

The beneficial effect of washing the graft can be explained by reducing the lubricating effects of the fluid, and by allowing effective impaction and more contact points between the solid particles, hence increasing the shear resistance. This effect can be enhanced further by local fluid drainage during the impaction process, as well as the use of a vibrating tamp. Bolland *et al.* showed that by using a modified collarless tapered stem as a tamp, with drill holes through its flanks and by attaching it to a vibrating

'woodpecker device', the authors were able to achieve a more densely packed aggregate. Furthermore, the authors found the aggregate to have enhanced mechanical shear strength, whilst at the same time reducing potentially damaging impaction loads and hoop strains to the femoral cortex, compared to a standard impaction procedure (Bolland *et al.* 2007). Jones *et al.* went on to show that a vibration device could also improve compaction of the graft on the acetabular side, whilst again reducing peak stresses (and hence fracture risk) (Jones *et al.* 2010). Similar findings have also been reported by Brennan *et al.* when using a vibration device to impact a dry aggregate, although during phase two testing (a saturated aggregate) they encountered a reduction in shear strength, which the authors attributed to the 'liquefaction' effect (Brennan *et al.* 2011). When a saturated aggregate is rapidly subjected to a vibrating load, it causes the particles to move into a denser configuration. However, the vibration also affects the fluid within the aggregate, which leads to an increase in pore pressures between the particles, forcing them apart. Thus there may be no contact between some of the particles, making the aggregate behave more like a fluid than a solid, hence decreasing both the strength and the mechanical properties of the aggregate (Seed 1979).

Figure 1.13: Example of the effects of soil liquefaction on a large scale, as occurs during earthquakes. (Image from http://7bcore2.wikispaces.com/Glossary accessed 18/10/2013).

The phenomenon of liquefaction (Figure 1.13) reinforces the need for fluid drainage and adequate preparation of the graft when using the vibration devices.

Other techniques have also been investigated, to try and improve not only the mechanical, but also the biological characteristics of impacted allograft. The combination of skeletal stem cells (SSC) with the allograft has become an area of particular interest. *In vitro* work has shown that SSC's combined with allograft can not only survive the impaction process and continue to proliferate, but also improve the mechanical (shear) characteristics (Bolland *et al.* 2006;Korda *et al.* 2006). It is surmised that the presence of cell populations, along with the extracellular matrix can act as 'cement' between particles, increasing the cohesion.

In vivo (murine) studies have reinforced these findings, and show enhanced new vessel formation within the constructs, hence raising the possibility of de-novo bone formation due to SSC survival within the graft tissue (Bolland *et al.* 2006). The accepted method for replacement of allograft in IBG is via creeping substitution (Burchardt 1983). The concept of a living graft which becomes incorporated into, rather than replaced by the surrounding host tissue presents a paradigm shift to the concept of allograft use. The addition of certain bioactive materials has also been shown to enhance the effect of the SSCs. Jones *et al.* showed that by first biologically activating the allograft with hydroxyapatite nano particles, the shear strength of the impacted composite of allograft and SSCs was significantly higher than that the allograft/SSC control composites. Similar effects have been found with the prior addition of Type 1 collagen and fibronectin (Jones *et al.* 2009). Clearly if the addition of SSCs is to make gross measurable change to the mechanical characteristics of the aggregate, the cells must be present in adequate numbers, and the initial seeding concentration of the cells is integral to this outcome. Jones *et al.* also performed multiple mechanical shear tests on impacted allograft discs seeded with increasing concentrations of SSCs. As cell seeding concentration increased, so did the allograft's ability to resist shear and to support an implant, reaching a significant difference at $2x10^5$ cells/ ml, with a 16 % increase in shear strength over allograft alone ($p<0.001$). In a clinical series Hernigou *et al.* also found a beneficial effect of increasing SSC concentration in the treatment of femoral head osteonecrosis and tibial non-union, but the numbers the authors suggested were far smaller (>1000 progenitors/ml) (Hernigou *et al.* 2005a).

The use of SSC seeded allograft has ‘bridged the gap’ from bench to clinic in a series of patients with early stage avascular necrosis of the femoral head. Tilley *et al.* described a procedure whereby a canal was drilled from the lateral femoral cortex, through the neck and into the diseased portion of the femoral head (as performed during a standard decompression procedure for the same condition) (Tilley *et al.* 2006). Donor allograft, seeded with the patients’ own cells from an iliac crest aspirate, was subsequently impacted into the canal filling the void. From the original group of six patients who underwent the procedures, five remain complication free at up to three year follow up. The disease process did however progress in one patient (both hips), and he subsequently required bilateral total hip replacements, allowing detailed investigation of the original graft material. Both μCT and histological examination away from the diseased area showed excellent incorporation of the graft into the hosts own bone, proving the success of the concept in a human subject (Aarvold *et al.* 2013).

1.9 Major Null Hypothesis:

Novel tissue engineered constructs are not as effective as allograft for the treatment of lost bone stock in impaction bone grafting.

1.10 Aims of Thesis:

The purpose of this thesis was apply tissue engineering principals to a range of polymers and polymer composites both *in vitro* and *in vivo*, in order to identify contenders with both the mechanical and biocompatibility characteristics to clinically translate for use in impaction bone grafting.

1.11 Objectives:

1. To explore techniques to optimise the protocol for successful combination of SSCs with scaffold materials.
2. To assess the effect of polymer type and chain length on polymer shear strength and biocompatibility.
3. To investigate the effect of porosity on polymer shear strength, clinical handling, biocompatibility and osteoinductivity.
4. To examine the effect of the addition of bioactive molecules on polymer shear strength, biocompatibility and osteoinductivity and hence identify two optimal polymers for detailed *in vivo* analysis.
5. To evaluate the osteogenic potential of the optimal two polymers in an *in vivo* (murine) scenario, and hence identify the best polymer for a scaled-up ovine study.
6. To identify potential pitfalls to clinical translation of the tissue engineered constructs, and explore technique to overcome them.
7. To assess the osteogenic potential of the previously identified optimal polymer in a scaled up *in vivo* (ovine) scenario.

Chapter 2

Materials and Methods

2.1 Reagents, cells, antibodies and bone graft material

2.2 Isolation, preparation, and culture of cells

2.3 Preparation of bone graft material

2.4 Polymer production

2.5 Impactor and disc design and production

2.6 Impaction procedure

2.7 Shear testing rig design and production

2.8 Histological preparation

2.9 Alkaline Phosphatase (ALP) stain

2.10 Live / Dead stain

2.11 Fluorescent immunostaining

2.12 Biochemical analysis

2.13 Confocal microscopy

2.14 Scanning electron microscopy

2.15 Micro computed tomography

2.16 Statistics

2.1 Reagents, antibodies, cells and bone graft material

Tissue culture reagents including α-MEM (Minimum Essential Medium Eagle, alpha modification), fetal calf serum (FCS), ascorbate, dexamethasone and all staining agents were purchased from Sigma-Aldrich, Poole, Dorset, UK unless otherwise stated. Phosphate buffered saline (PBS) was acquired from PAA, Linz, Austria. Fluorescent dyes and antibodies including CellTracker™ Green (5-chloromethylfluorescein diacetate) (CTG), Vybrant™, Alexa Fluor^{R} and Ethidium Homodimer-1 (EH-1) were obtained from Invitrogen, Life technologies ltd, Paisley UK apart from the polyclonal antibody to type-1 collagen which was as a generous gift from Dr Larry Fisher (NIH, Bethesda, Maryland, USA).

All human cells used for testing were obtained from the bone marrow of patients undergoing total hip replacement surgery at Southampton General Hospital with full ethical consent and approval of the local hospital ethics committee (LREC 194/99/w, 27/10/10). The bone marrow was obtained by the operating surgeon via capture of the extruded marrow in a surgical spoon during femoral canal preparation. A further piece of cancellous bone retrieved using a box osteotome when lateralising the implant was also obtained and the two specimens were then placed in a universal container and refrigerated for a maximum of forty-eight hours until used.

The femoral heads were obtained under the same consent and ethical approval (LREC 194/99/w, 27/10/10) from patients undergoing total hip replacement and hip hemiarthroplasty procedures at Southampton General Hospital. The samples were stored at -80 ºC in a tissue bank until preparation.

2.2 Isolation, preparation, and culture of cells

Cells were isolated from the marrow and cancellous bone section via repeated washes with α-MEM solution. The media was added to the universal container in order to submerge the specimens, the cancellous bone was crushed with the pipette tip, the resultant solution aspirated and put through a 70 μm filter cell strainer (in order to remove any further debris) into a separate universal container. The resultant cell solution was then put into a balanced centrifuge, and spun at 1100 rpm for four minutes. The supernatant was then carefully poured off and the cell pellet re-suspended in basal

media (α-MEM with 10% fetal calf serum with additional 1% penicillin and streptomycin). This solution was then placed into a variable number of tissue culture flasks, depending on the cell number required and incubated at 37 ºC in 5% CO_2 until confluent (Figure 2.1). Cells were washed in PBS and media changes were repeated every 3–4 days. When required for further experimentation the cells were released using 10% trypsin in ethylene diamine tetra-acetic acid (EDTA).

Figure 2.1: Growing cells in basal media. A) T150 flasks in an incubator, B) example of confluent cell population on tissue culture plastic (scale bar = 200 µm).

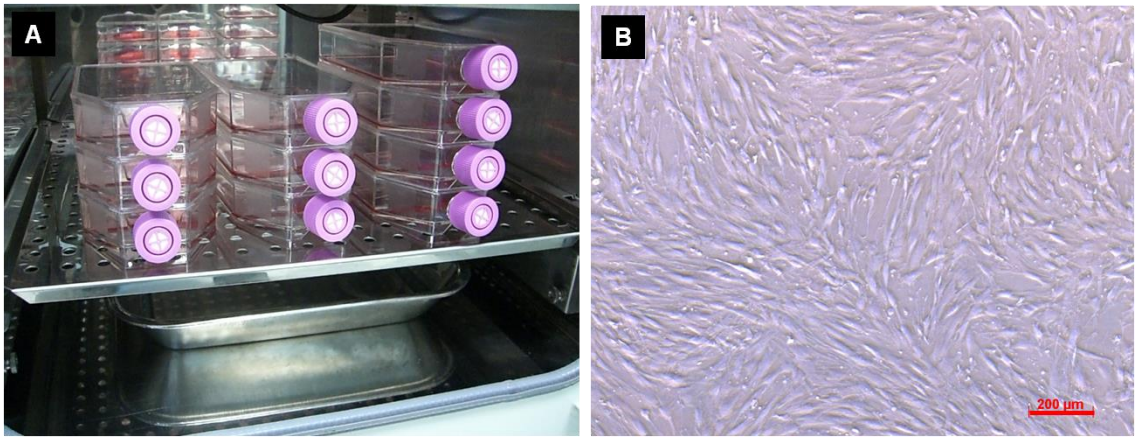

2.2.1 Storage

If not used immediately for experimentation, the expanded cell population was stored at -80 ºC. The trypsin solution containing the cell suspension was neutralised using FCS containing basal media. A cell pellet was obtained by centrifugation at 1100 rpm for four minutes, and the supernant discarded. The cell pellet was then suspended in a solution of FCS + 10% dimethyl sulfoxide (DMSO) prior to being divided into cryovials of 1 ml volume. These were then placed immediately into the -80 ºC freezer until required.

2.2.2 Culture of cells from frozen

A cryovial of the cells (P1) were reanimated by allowing the solution to thaw, adding 10 ml basal media, centrifuging at 1100 rpm for 4 minutes, pouring off the supernatant and re-suspending in basal media prior to seeding in tissue culture flasks and culturing as

described previously. Upon confluence the cells were again released using 10 % trypsin in EDTA, centrifuged and re-suspended in 5 ml basal media.

2.2.3 Dilution to required concentration

Five microlitres of cell suspension was taken via a pipette, injected into a hemocytometer counting chamber, and the cell concentration determined. Appropriate dilution with basal media was then given such that the concentration required for experimentation was obtained.

2.3 Preparation of bone graft material

When required a batch of the femoral heads was removed from the -80 ºC freezer and allowed to thaw. The femoral heads were prepared under sterile conditions in an operating theatre environment. The soft tissue, cartilage, fat and cysts were removed using a combination of sharp dissection, bone nibblers and an oscillating saw. The femoral heads were then cut into smaller pieces using the same oscillating saw, prior to being morcellised using a standard bone mill (Figure 2.2) on medium setting (Tessier Osseous Microtome, Stryker Leibinger, Freiberg, Germany) under sterile conditions.

Figure 2.2: The bone mill used for the preparation of allograft. (Image from http://www.europe.stryker.com/leibinger/90-01705_0303.pdf, last checked 19/10/2013).

Milled bone graft was subsequently prepared via repeated washes in 6% hydrogen peroxide until all the fat and the marrow was removed. The bone was then washed repeatedly (x3) in phosphate buffered saline (PBS), prior to 24 hour immersion in 5x antibiotic / antimycotic solution and UV light exposure. The bone was then re-washed in PBS and finally submerged in basal media for 24 hours prior to use.

2.4 Polymer production

2.4.1 Non- porous polymers

Dr Sherif Fahmy, post-doctoral fellow (Department of Chemistry, University of Nottingham), kindly produced all non-porous polymers used in the experimentation. These consisted of the high and low molecular weight forms of poly-caprolactone (PCL), poly(DL-lactide) ($P_{DL}LA$) and poly(DL-lactide-co-glycolide) ($P_{DL}LGA$)) .

$P_{DL}LA$ molecular weights 26 and 126 kDa, and $P_{DL}LGA$ molecular weights 35 and 110kDa were purchased from Surmodics (Surmodics Pharmaceutical, Inc. Birmingham, Al, USA), while Polycaprolactone (PCL) molecular weights 14 and 85 kDa were ordered from Sigma-Aldrich (Poole, Dorset, UK) and all were used in powder form as received. Polymers were melt casted by heating above T_m (~180C) inside Teflon cages (100 x 60 x 20 mm) and subsequently cooled to room temperature. All polymer samples were refrigerated before further processing.

2.4.2 Porous polymers

Matthew Purcell, PhD student (University of Nottingham), kindly produced and provided the porous scaffolds (Figure 2.3). Three hundred milligrams of the powder of each polymer was placed into individual cylindrical wells (11.2 mm x 10.4 mm) in a custom made PTFE mould (University of Nottingham, School of Chemistry) and placed into a 60 ml stainless steel autoclave. The autoclave was clamp sealed, heated to 35 °C, filled with CO_2, and the pressure increased to 23 MPa over a period of 20 minutes. The pressure was held for 60 minutes, and then reduced over a period of 30 minutes back to ambient conditions; heating then ceased and the mould was removed from the autoclave. The production of the hydroxyapatite (HA) composite porous scaffolds

followed exactly the same methodology, except the desired HA preparation was added to the powdered polymer in the wells prior to clamp sealing etc.

After cooling the polymer scaffolds were removed from the moulds as cylinders measuring approximately 8 mm diameter x 10 mm height.

Figure 2.3: Cylinders of porous $P_{DL}LA$. A) Close up, B) single batch (scale bar = 10 mm).

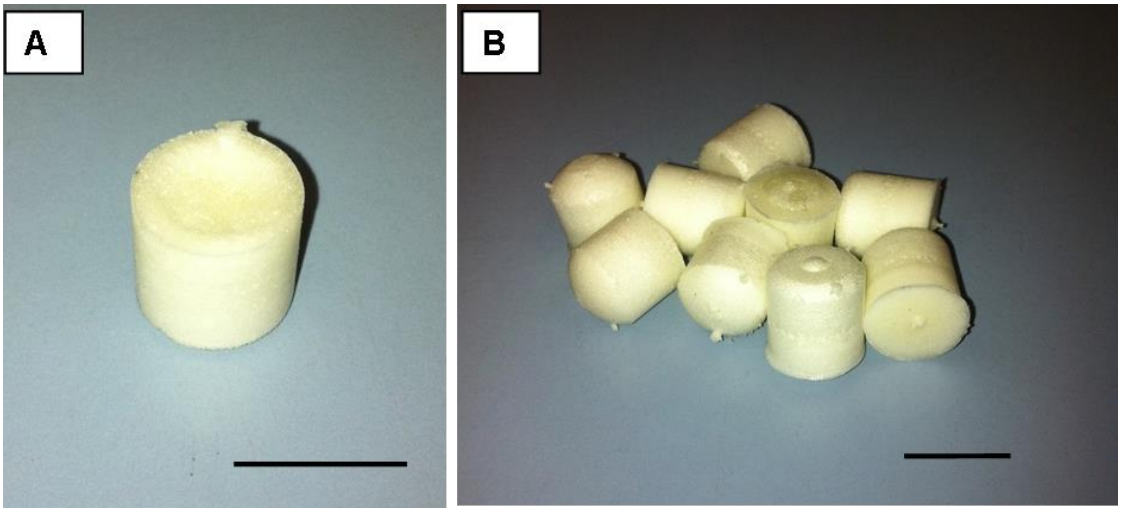

2.4.3 Preparation for use

Both porous and non-porous polymers were milled using the same standard bone mill (Tessier Osseous Microtome- Stryker Leibinger, Freiberg, Germany) on medium setting, sterilised in 5x antibiotic/ antimycotic solution and by U.V. light treatment for 24 hours and finally submerged in basal media for a further 24 hours prior to use.

2.5 Impactor and disc design and production

The studies described in this thesis utilised impactors as previously detailed by Bolland B, Jones A and Aarvold A in previous related departmental projects (Bolland *et al*. 2006;Jones *et al*. 2009). Design of impactors was based on work performed by Brewster *et al.*, whereby force plate analysis had investigated the force that allograft was

subjected to during a standard impaction bone grafting procedure (Brewster *et al.* 1999). This had been shown to be the equivalent of a 1.98 kg mass falling 65 mm onto a circular base plate 60 mm in diameter 72 times. Therefore, these figures were scaled such that two impactors were produced, one larger scale one for the *in vitro* mechanical analysis of grafts, and another scaled down version such that impacted grafts could appropriately be used for cellular and *in vivo* (murine) experimentation and analyses (Department of Engineering, University of Southampton).

Both impactors consisted of a metal cylindrical piston, with a superior sliding drop weight. The weight of the mass and the distance to fall were calculated upon the diameter of the chamber.

For example, the calculation for the scaled down impactor (weight 31g, drop height 65mm, 7.5mm diameter):

$$\text{Energy/Unit area} = mgh / \pi r^2$$

$$0.031 \times 9.81 \times 0.065 / \pi (0.000375)^2$$

$$\mathbf{474\ J/m^2}$$

The larger impactor consisted of a drop weight of 25mm in diameter and weight 344 g and a drop height of 65 mm.

For the large impactor, a based plate was designed into which a custom produced perforated perspex disc (Department of Engineering, University of Southampton) could be placed to create a chamber (Figure 2.4 A). For the smaller impactor a modified plastic electron microscopy (EM) pot served as both an impaction chamber and containment vessel. The modification involved the perforation of the pots with a twelve gauge hypodermic needle in order to allow nutrient exchange to the contained grafts.

Figure 2.4: Impactor and impaction procedure. A) Large impactor and base plate, B) filling of the perpex disc within the base plate with allograft, C) impaction by releasing the drop weight, D) an impacted disc.

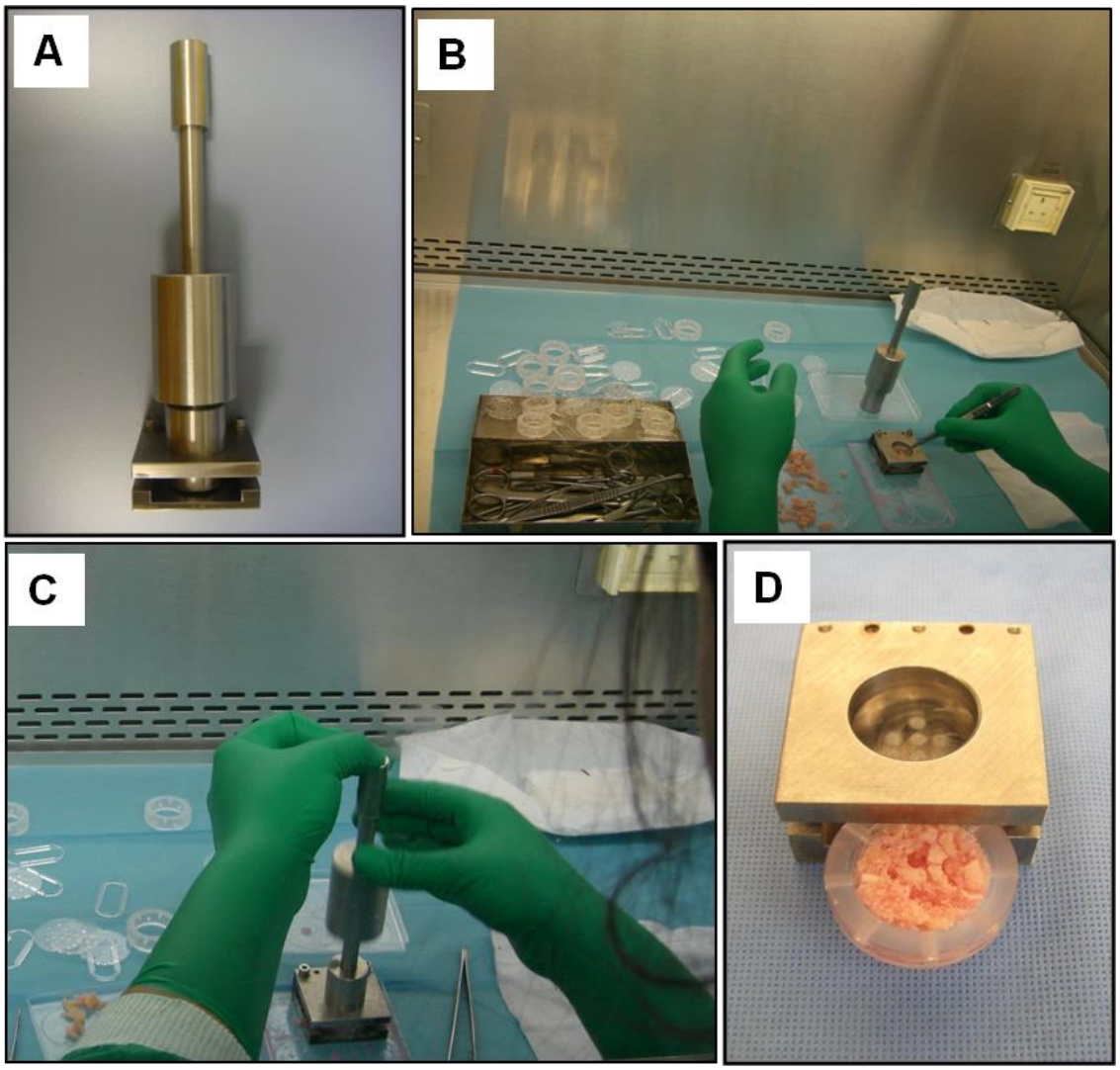

2.6 Impaction procedure

The impaction procedure used was based on a procedure developed by Dunlop *et al.*, used to investigate the mechanical effects of washing and varying particulate size of allograft in impaction bone grafting (Dunlop *et al.* 2003). The graft was placed loosely into the chamber such that it was mostly full (Figure 2.4B). The piston was then placed over the graft, making a seal at the top of the chamber. The drop weight was then released 24 times at a rate of approximately 1 Hz such that the graft was impacted into

the base of the chamber, and only fluid was able to escape through the disc perforations (Figure 2.4C). The piston was removed, and further graft was placed on top of the impacted graft, and the impaction procedure repeated. A third cycle (72 impactions in total), ensured that the chamber was full, and the volume of impacted graft was equal for all specimens. Seventy-two impactions were chosen due to the work perfomed by Brewster as discussed previously. This was performed in 3 groups of 24 impactions due to the fact that the impaction chambers were filled with loose graft, and required impaction before additional graft could be placed in, to ensure the chamber was full to the top at the end of the procedure.

For the large impactions the perspex disc containing the graft was carefully removed, and a perforated perspex base and lid attached, in order to ensure the graft remained contained and compressed (Figure 2.4D). When assembled, the three components enclosed a cylinder of scaffold 25 mm in diameter and 10 mm height, with a volume of 4900 mm^3. For the smaller impactions the EM pot had its usual lid applied, which had been previously perforated as described.

2.7 Shear testing rig design and production

The shear testing rig was based on a design validated by Dunlop *et al*., and was the same as used in previous work in the department (Bolland *et al*. 2006;Dunlop *et al.* 2003;Jones *et al.* 2009).The cam shear testing rig (Department of Engineering, University of Southampton) consisted of a chamber (of exactly the same dimensions as the impacted material) on top of which the Perspex disc was placed. Careful compression of the central impacted material allowed it to drop out of the disc into the chamber without breaking apart. The chamber had a fixed upper ring and a mobile lower ring, with the division at the midpoint of the height of the chamber (Figure 2.5 and 2.6).

Figure 2.5: Schematic demonstrating the shear testing rig setup. (Replicated from Aarvold A thesis)

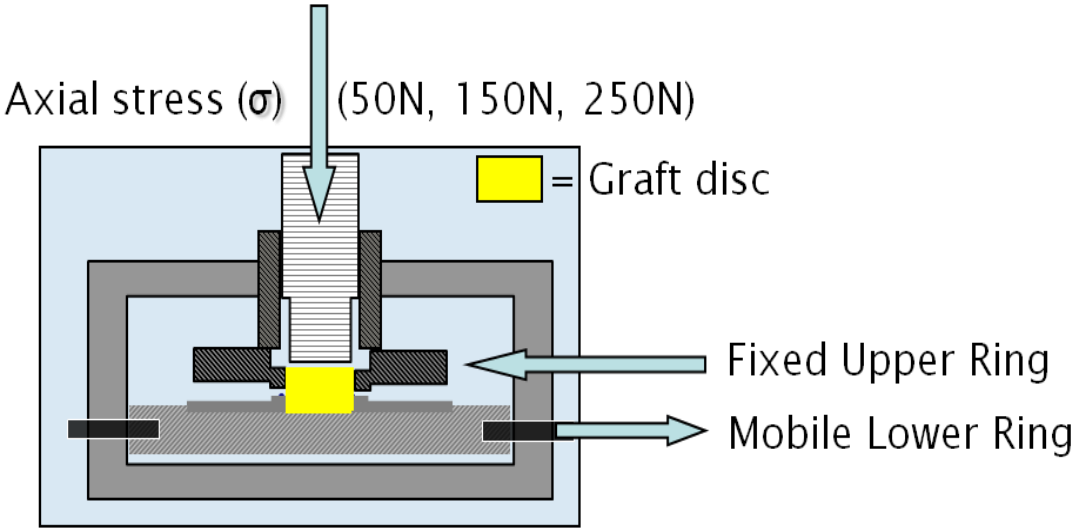

Figure 2.6: Photograph of the shear testing rig attached to the load cell.

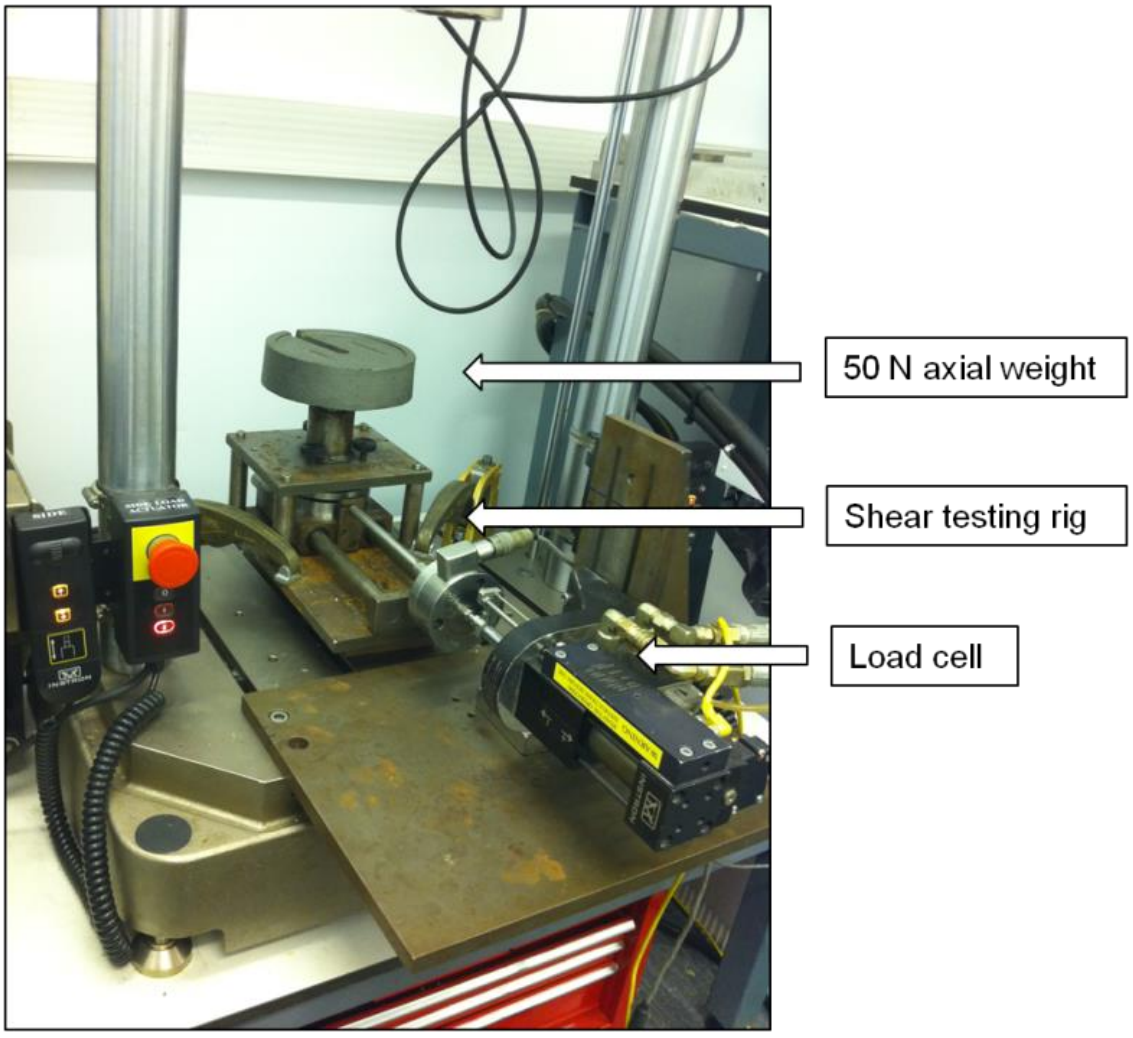

The lower ring of the chamber was attached to a hydraulic actuator (Instron Ltd, High Wycombe, UK) via a metal rod. A compressive (axial) weight was placed on top of the disc, and the set up allowed to settle for five minutes. After this time the mobile ring was pulled at a rate of 1 mm / min such that the disc of graft in the chamber was subjected to a deforming shear strain. The actuator was attached to a load cell during the shear test, and force required to maintain the constant strain rate was recorded at all time points using an attached laptop computer.

Twelve discs of each graft type under test were required for mechanical analysis. Three axial loads (50 N, 150 N and 250 N) providing compressive stresses (102 kPa, 306 kPa, 509 kPa respectively) from within the physiological spectrum were applied with four discs being tested under each load. The compressive stress value calculation consisted of dividing the compressive force in Newtons by the area of the test cell in square mm (πr^2). The resulting stress was in MPa (N / (mm^2)). To obtain stress in kPa the resulting value was multiplied by 1000.

The force measured at 10 % strain was recorded (standard engineering practice), and this was converted to a shear stress value by dividing the force by the area of the disc. The mean of the shear stress values (n=4) was plotted against normal stress and the best fit straight line (least squares technique) variation between normal stress and shear strength, represented the Mohr Coulomb failure envelope. The interparticulate cohesion could be calculated from the intersection of the best fit line with the shear stress axis and the angle of internal friction from the slope of the line (cf. $y = mx + c$).

2.8 Histological preparation

Specimens undergoing histological analysis were removed from any carrier vessels, washed in PBS before fixation in 4% paraformaldehyde (PFA) for 24-48 hours. Samples were then again washed in PBS prior to submersion in Tris / EDTA (TE) buffer solution for a variable amount of time until the de-calcification process was complete. The TE buffer was changed twice per week in order to maintain an adequate diffusion gradient for effective decalcification. Progress was assessed via faxitron analysis (Figure 2.7) at approximately two weekly intervals (MX-20, Faxitron Bioptics, Lincolnshire, USA).

Figure 2.7: Example faxitron images of specimens of bone A) two weeks and B) six weeks into the de-calcification process. The bright white areas indicate residual calcification.

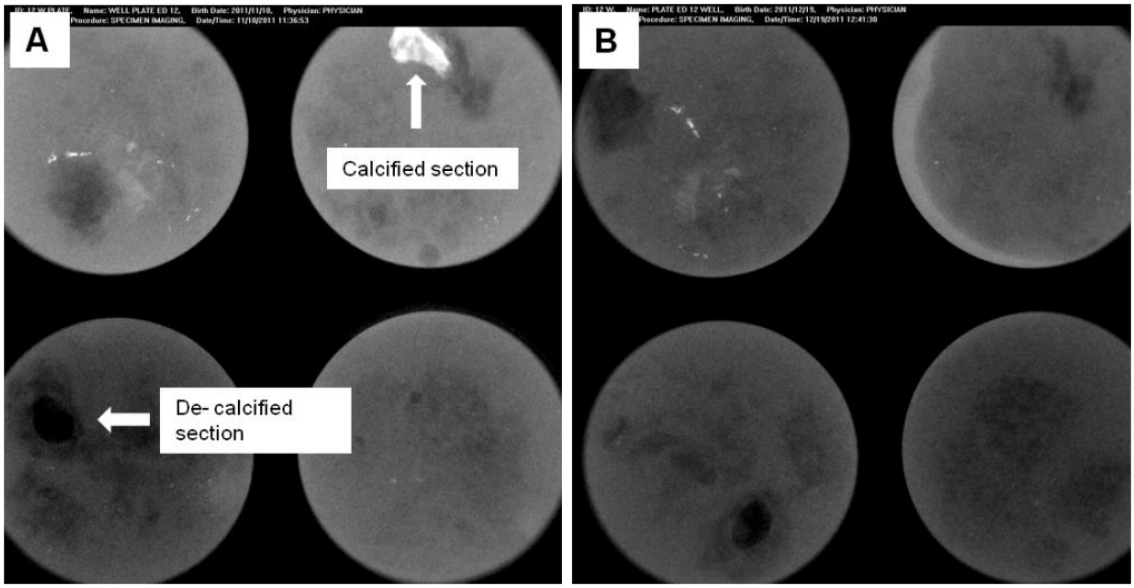

Upon completion the specimens were transferred to PBS solution prior to paraffin embedding. This process as detailed by Miao and Scutt, involved stepwise dehydration in graded ethanol solutions (50%, 90%, 100% old and 100% new) for 45 minutes in each, followed by two times one hour submersions in histo-clear solution (Miao and Scutt 2002). The specimens were then finally submerged in paraffin wax twice at 60 °C for one hour, prior to being placed into the centre of standard metallic histological wells, submerged in paraffin wax, and allowed to set by placing on a cooled surface at approximately 2-4 °C. A plastic perforated mounting plate was attached to the embedded specimen using wax. The specimens were then labelled and stored in a refrigerator at 5 °C prior to sectioning.

2.8.1 Slide preparation

When required the embedded sections were removed from the refrigerator and mounted onto a Microm 330 microtome (Microm International GmbH, Germany). Some of the specimens required one hour in the -20 °C freezer prior to sectioning to reduce the risk of a specimen coming off the mounting plate. Samples were then sectioned at 7 µm sections and carefully placed into a water-bath at 37 °C to allow the sections to spread out. The floating sections were then transferred to pre-heated glass slides and placed

onto a warming plate at 37 °C for one hour, prior to transfer to an oven set to 37 °C for 4 hours. Slides were wrapped in foil and refrigerated at 5 °C prior to staining.

2.8.2 Staining

The slide preparation for all stains utilised the following protocol. Slides were placed into a carrier vessel, and underwent stepwise submersions in histoclear solutions to remove the wax, followed by graded rehydration using methanol solutions. Any residual methanol was removed by short submersion in a water bath.

2.8.3 Alcian Blue and Sirius Red stain (A+S)

Nuclear staining was achieved by submersion in Weigert's haematoxylin solution for ten minutes. The slides were then rinsed in a water-bath, followed by a further twenty minute submersion in in Alcian Blue solution in order to stain any proteoglycan rich cartilage matrix. In order to demonstrate the presence of any collagen the slides underwent a twenty minute pre-treatment with molybdophosphoric acid, followed by staining with 0.1 % Sirius red solution for one hour.

2.8.4 Goldner's trichrome stain

Nuclear staining was performed by ten minute submersion in Weigert's haematoxylin solution. The slides were then stained with Ponceau Acid Fuschin for five minutes (cytoplasm + muscle) followed by a rinse in 1 % acetic acid. Slides were then placed in Phosphomolybdic Acid-Orange G solution until the collagen was decolorised, followed by a further thirty second rinse in 1 % acetic acid solution. The collagen was stained via a five minute submersion in Light Green Stock Solution, followed by a final rinse in 1 % acetic acid. Sections were blot dried and dipped quickly in absolute alcohol.

2.8.5 Dehydration and covering for storage

After staining all slides were dehydrated through reverse graded methanol (50%, 90%, 100%, 100%) and histoclear solutions. Stained sections were finally stabilised for long term storage by submerging in a drop of dibutyl phthalate xylene (DPX) followed by the careful placement of a glass coverslips.

2.9 Alkaline Phosphatase (ALP) stain

In order to highlight ALP positive cells within a cell population, an ALP stain was used in a number of experiments. The cell population was fixed via a five minute submersion in a 95% ethanol solution, followed with a rinse in PBS. A solution containing 40 µl/ml napthol AS-MX phosphate solution with 0.24 µg/ml fast violet salt was made up, and added to the cell population such that all the cells were covered (approximately 1 ml per well of a six well plate. A subsequent 40 minute incubation followed at 37 ºC in 5% CO_2, with a final wash in PBS and allowing to air dry prior to imaging under light microscopy.

2.10 Live / Dead stain

In order to assess the viability of the cells after experimentation, and to give a visual impression of cell number, colony characteristics and confluence, a 'live / dead' stain using the fluorescent probes Cell Tracker Green^{TM} CMFDA (5-Chloromethylfluorescein Diacetate) and Ethidium Homodimer-1 (CTG/EH-1) were used to label viable and necrotic cells respectively (Figure 2.8). The cell containing specimens were washed in PBS and then incubated (37 ºC, 5% $CO_{2)}$ for 90 minutes in 1ml of standard CTG/ EH-1 solution (10µg/ml CTG, 5µg/ml EH-1). After this period specimens were again washed in PBS, and incubated for a further 45 minutes in basal media. Specimens were then washed in PBS, fixed in ethanol for 5 minutes and stored in PBS prior to microscopic imaging under either fluorescent light through a standard FITC filter or confocal microscopy.

Figure 2.8: Live/dead stain of SSC growing on tissue culture plastic. A) Viable (green) cell population, B) compromised (multiple red) cell population (scale bar = 200 µm).

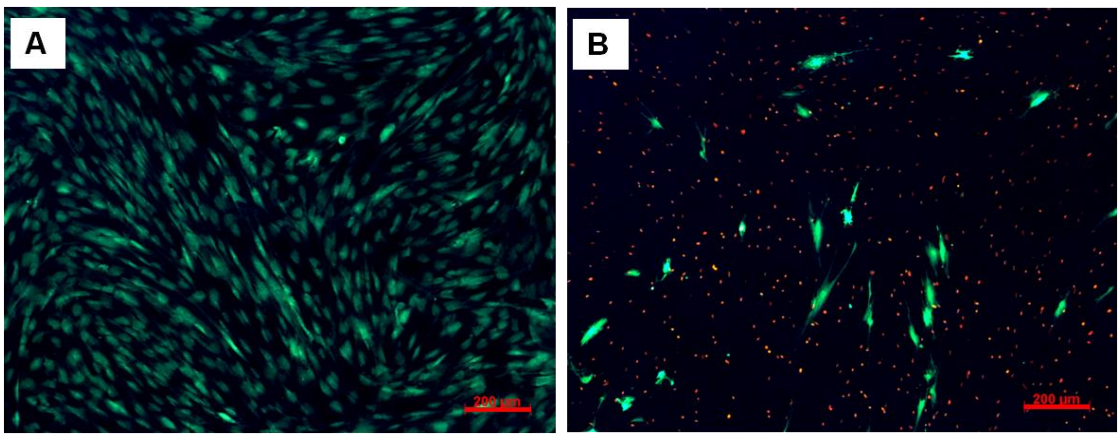

2.11 Fluorescent immunostain

Samples were removed from containers, washed in PBS and fixed for 24 hours by submersion in 4% paraformaldehyde. Samples were then transferred to PBS prior to application of immunostain. This involved a 10 minute incubation in 1% bovine serum albumin (BSA) followed by overnight incubation in 1ml of primary antibody (eg LF68 (whole rabbit serum) collagen 1 antibody (1:300 dilution with PBS/BSA)), followed by three washes in 0.1% PBS Tween. Appropriate secondary antibody (eg anti-rabbit antibody (alexafluor^{R} 594)) was then added for one hour at room temperature, followed again by three 0.1% PBS Tween washes. Finally, SYTOX^{R} blue (1:100 dilution, 10 minute incubation) was added as a nuclear counter stain. To ensure specificity of the secondary antibody a portion of the samples were treated in exactly the same way but the primary antibody was not added. The samples were stored in PBS in the dark until imaging under confocal microscopy.

The above method was used to stain for Type-1 Collagen, Bone Sialoprotein (BSP), von Willebrand Factor (vWF) and osteocalcin.

2.12 Biochemical analysis

2.12.1 WST-1 Assay

The WST-1 assay (2-(4-Iodophenyl)-3-(4-nitrophenyl)-5-(2,4-disulfophenyl)-2H-tetrazolium) was used as a measure of total cell number and viability. The WST-1 reagent provides tetrazolium salts that are cleaved to formazan by cellular mitochondrial dehydrogenases, resulting in a colour change (Figure 2.9). An expansion in the number of viable cells results in an increase in the overall enzyme activity, and hence any colour change correlates to the number of metabolically active cells in the culture (Mosmann 1983).

The incubation media was removed from the wells containing the samples and cells were washed in PBS. A solution was made up containing a 1:10 dilution WST-1 substrate (Roche ltd, Welwyn Garden City, UK) to basal media. An equal volume was added such that the samples were fully covered, and the samples were placed in the incubator at 37 ºC and 5 % CO_2. At two and four hours incubation time, three times

100µl of substrate was removed from each well and read via a Bio-Tek KC4 microplate fluorescent reader (Bio-Tek, Winooski, USA) at 410 nm. An increase in absorbance value (ie increase in optical density of the substrate) indicated increased cell number and viability.

Figure 2.9: A twelve well plate with different numbers of viable cells in each well, after 4 hours incubation in WST-1 reagent. The higher the number of viable cells, the darker the reagent colouration.

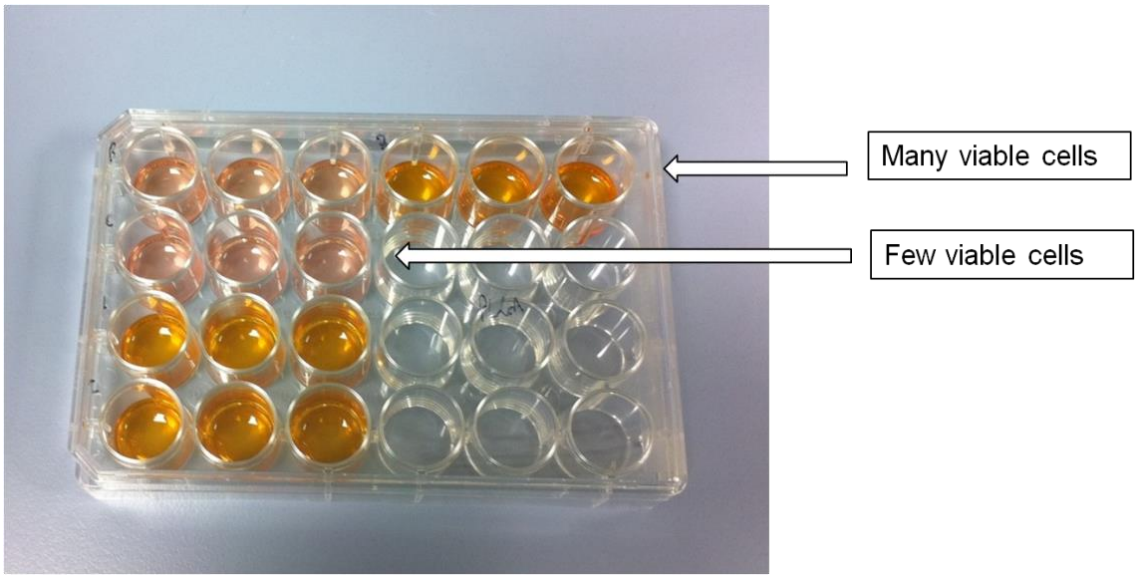

2.12.2 Alkaline phosphatase (ALP) and DNA Assays

ALP specific activity was used as a measure of osteoblastic differentiation amongst the cell population present after specific incubation periods. The specimens were washed in PBS, and then fixed by a five minute submersion in 90% ethanol prior to being allowed to air dry. Samples were then re-washed in PBS, and subsequently submerged 0.5% Triton X-100 solution. Samples then underwent x3 freeze thaw cycles with vigorous agitation (scaffold specimens) or cell scraping (cells grown on tissue culture plastic) between each freeze. Lysate was measured for ALP activity using p-nitrophenyl phosphate as substrate in 2-amino-2-methyl-1-propanol alkaline buffer solution (Sigma, Poole, UK) and DNA content was measured using Pico Green^{R} (Molecular Probes, Paisley, UK) according to routine manufacturer protocol. 10µl of lysate was run in triplicate for each sample on a plate against x2 standards, and read on an ELx 800 (ALP) and FLx-800 (DNA) microplate fluorescent reader (Bio-Tek, USA) and mean

and standard deviations calculated. The mean control values were subtracted, and specific activity was calculated by dividing the mean ALP activity (corrected to one hour incubation) by the mean DNA content of each scaffold type (expressed as nanomoles of p-nitrophenyl phosphate/hr/ng DNA) and compared to the other scaffolds using Mann–Whitney U test.

2.13 Confocal microscopy

Specimens were typically imaged using a Leica SP5 Laser Scanning Confocal Microscope and software (Leica Microsystems, Wetzlar, Germany). A small number were scanned using a Leica SP2 Laser Scanning Confocal Microscope due to technical problems with the SP5. This gave accurate and focussed three dimensional pictures of the complex surface topography of the specimens, allowing accurate visual comparison between them. The specimens were placed into custom built 'welled' coverslips and submerged in PBS. Coverslips were placed on to the platform, and an appropriate part of the specimen centralised using the standard light microscope component. An appropriate excitation light was set as per manufacturer recommendation for each fluorophore in use on the specimen, and the confocal set to receive the appropriate emission spectra. The specimen was scanned, the information recorded and the images reconstructed using Leica LAS AF Lite ver 2.0 for the SP5 scans, and Leica LCS Lite for the SP2 scans (Leica Microsystems, Wetzlar, Germany).

2.14 Scanning electron microscopy (SEM)

SEM allowed extremely detailed analysis of surface topography of scaffolds under test. The specimens for imaging were placed on SEM stubs and sputter coated. Gold sputter coating was performed using a Leica EM SCD005 sputter coater; coating at 4×10^{-2} mbar (or below) for 180 seconds. Samples were typically viewed using a FEI Quanta 200 Scanning Electron Microscope (FEI, Oregan, USA).

2.14.1 Elemental mapping

Samples containing hydroxyapatite were also imaged at the University of Nottingham using elemental mapping. Energy dispersive X-ray spectroscopy (EDX) was performed to identify HA particles within the scaffolds. Samples were prepared as for SEM prior

to sputter coating. Carbon sputter coating was performed using a Polaron SC7640 sputter coater at 4 x 10^{-2} mbar (or below) for 40 seconds. A Philips FEI XL30 SEM was used for elemental mapping with an accelerating voltage of 15 keV, and Inca Suite, version 4.14 (Oxford instruments analytical Ltd), was the software used.

2.15 Micro computed tomography (µCT)

This imaging modality gave both two dimensional and three dimensional images of internal scaffold morphology as well as an accurate means of measuring scaffold porosity and volumetric analysis. Three CT scanners were used for the work presented in this thesis (Figure 2.10). These consisted of a Bench Top CT system for microtomography (Target X-ray source 25-160Kv, 0-100µA, noncontinuous) (X-TEK Systems Ltd, Tring, Hertfordshire, UK) a Metris Xtek HMX ST 225kV CT scanning system (X-TEK Systems Ltd, Tring, Hertfordshire, UK) and a SkyScan 1176 *in-vivo* micro-CT (Skyscan, Belgium). Samples scanned at the University of Nottingham were undertaken using a Skyscan 1174 (Skyscan, Kontich, Belgium).

Figure 2.10: A) Metris Xtek HMX ST 225kV CT scanning system, B) SkyScan 1176 *in-vivo* micro-CT.

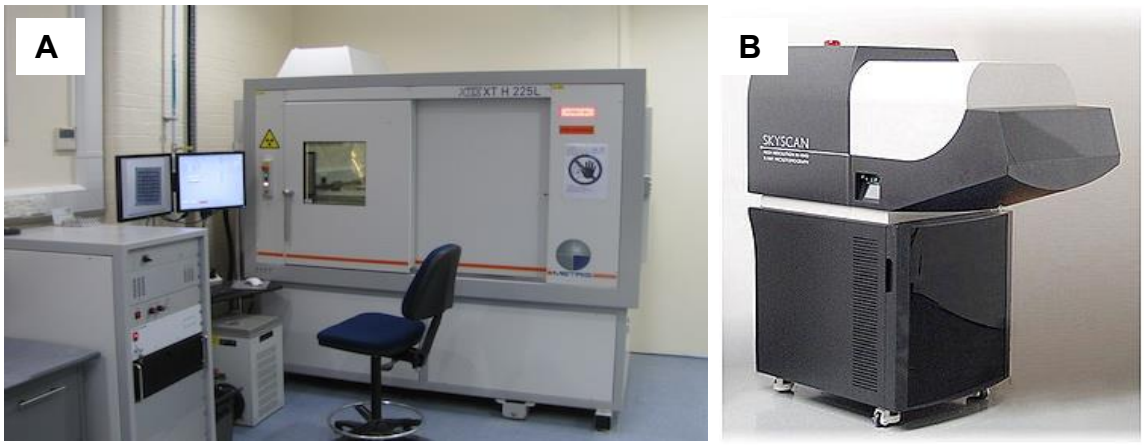

As a general method, samples were focused, calibrated and adjusted to prevent X-ray saturation. The number of frames and the approximate number of angular positions were chosen. The scans were performed with minimised ring artefacts. After the scanning process the raw data was collected and reconstructed using the appropriate software. X-TEK scans were using reconstructed using Next Generation Imaging (NGI) software packages (X-TEK Systems Ltd) with a 10µm voxel resolution. All voxels were

automatically assigned Houndsfield units via calibration against a standard water sample. The images were visualised and analysed using Volume Graphics (VG) Studio Max software (Volume Graphics GmbH, Heidelberg, Germany). The Skyscan data reconstruction was performed using NRecon (Skyscan, Belgium) and saved as 8 bit bitmaps (BMP). Analysis of the reconstructed images was performed using CTAn (Skyscan, Belgium).

2.16 Statistical analysis

When comparing shear strengths of impacted scaffolds, statistical significance was calculated by grouped linear regression analysis using Graphpad Prism software (Version 3.02). For all other statistical calculations including Mann–Whitney U test and Analysis of Variance, SPSS version 17.0 was used. Individual chapters state the specific statistics for each experiment.

All data are displayed graphically as mean ± standard deviations, and all experimental groups are repeated in triplicate unless stated otherwise. Significance values are stated as: $p < 0.05$, $p < 0.01$ and $p < 0.001$.

Chapter 3

An analysis of polymer type and chain length for use as a biological composite graft extender in impaction bone grafting: a mechanical and bio-compatibility study

Part 1: Protocol design

I am grateful to Mr James Smith for his help in the design and undertaking of the investigations to determine the accuracy of assays involving SSCs in combination with allograft.

Part 2: Study

I am grateful to Dr Sherif Fahmy (University of Nottingham) for kindly providing the scaffolds under test, to Dr Adam Briscoe (Bioengineering Science Research Group), for assistance with the mechanical testing and the Mohr-Coulomb equation calculations, to Dr David Johnston for assistance with confocal microscopy and SEM (Biomedical Imaging) and to Dr Stuart Lanham for assistance with the μCT scans and analysis.

The work detailed in Part 2 of this chapter has been published:

Tayton E, Fahmy S, Purcell M, Aarvold A, Smith J, Kalra S, Briscoe A, Lanham S, Howdle S, Shakesheff K, Dunlop DG, Oreffo RO.

An analysis of polymer type and chain length for use as a biological composite graft extender in impaction bone grafting: A mechanical and biocompatibility study.

Journal of Biomedical Materials Research Part A, 2012, 100(12):3211-9

3.1 Part 1: Protocol design

3.1.1 Introduction

A significant part of this thesis involves the *in vitro* analysis of different polymers for their biocompatibility with skeletal stem cells such that they could potentially be used as 'living' composite grafts for skeletal regeneration. Previous work from the bone and joint research group relates to this, but important aspects such as cell seeding density and time were not standardised between studies, and cell analysis investigative procedures (eg assays) were not validated. For example, Bolland *et al.* seeded allograft using a SSC seeding density of $2x10^6$ cells / ml, Khan *et al.* used a higher seeding density of 10^7 cells / ml when using Stro-1 isolated cells on binary blends of polymers, although Jones *et al.* had shown that when working with allograft in an impaction bone graft model, a seeding density of only $5x10^4$ was required to make a significant difference to the shear strength of the construct (Bolland *et al.* 2006;Jones *et al*. 2009;Khan *et al*. 2010). Provisional pilot experimentation (detailed in Appendix 1) using SSC seeding densities at a concentration of $5x10^4$ cells / ml on both allograft and a poly (DL-lactic-co-glycolide) (PLGA) followed by 28 days incubation in osteogenic media gave confusing results. Cell viability staining showed negligible survival of cells on either the allograft or the polymer, and even though quantitative assays (DNA and ALP) backed up these findings when analysing the polymer, both assays gave spuriously high readings for both the allograft SSC composites, as well as the allograft controls. Two issues therefore needed to be addressed prior to embarking on any analytical work involving allograft or polymer SSC composites: i) development of a protocol to optimise SSC adhesion, continued proliferation and viability on carrier materials, and ii) investigation of the accuracy of quantitative assays when used in combination with allograft.

Four main areas were identified for optimisation of the protocols involving the combination of SSCs with scaffolds.

1. Cell seeding density

The concentration of the cell suspension into which the allograft/ scaffolds are placed clearly has an effect on how many cells will adhere to the scaffold, and hence are likely

to survive and proliferate. Previous work had used seeding densities ranging from $5x10^4$ cells / ml to 10^7 cells / ml, with implications therein for time of culture and cost of equipment.

2. *Incubation time*

Little agreement exists concerning the optimal time for the milled allograft / scaffold to be incubated in the cell suspension prior to further experimentation such as an impaction procedure. Whereas an extended incubation could potentially increase cell adhesion, this has time and cost implications, as well as increasing the risk of contamination.

3. Supplementary media

Investigation was required to determine the efficacy of basal versus osteogenic media in the promotion of cell adhesion, proliferation and survival on different carriers.

4. Cell Type

There is significant variability between the SSC populations isolated from different patients in terms of proliferation potential (Cuomo *et al.* 2009). Identification of proliferative cells by testing an array of cells from different patients, has the potential to show measurable differences in scaffold compatibility in the experimental timeframe available.

3.1.2 Aim

To determine an optimal experimental protocol for investigating SSC compatibility with different carrier modalities.

3.1.3 Objectives

The objectives were:

1. To determine a minimum cell seeding density likely to give successful and reproducible cell adherence and proliferation on a scaffold.

2. To determine an optimal incubation time for SSCs on scaffolds such that adherence can occur, but the experiment is not unworkably lengthy.
3. To investigate whether media type has an effect on cell adherence and survival on scaffolds.
4. To identify a source of proliferative SSCs, likely to give measurable results in an *in vitro* environment in the time frame required.
5. To determine the accuracy of the DNA, ALP and WST-1 assays when used in combination with allograft.

Cell Density / Incubation time / Supplementary media

3.1.4 Materials and Methods

3.1.4.1 Cell culture

Cells were isolated from the bone marrow of a male seventy year old patient (M70) as detailed in Section 2.1, culture expanded in T150s as detailed in Section 2.2 and frozen down in individual vials for storage as detailed in Section 2.2.1. Three vials were reanimated as detailed in Section 2.2.2, and seeded onto eight T150 tissue culture plastic flasks, and grown to confluence (37 ºC, 5% CO_2) in basal media. Cells were then removed using trypsin in EDTA, centrifuged (1100 rpm, 4 minutes), the supernatant poured off, before re-suspension in basal media. This suspension was split, and diluted such that cell suspensions of concentration $1x10^5$, $5x10^5$ and $1x10^6$ cells / ml were created as detailed in Section 2.2.3.

3.1.4.2 Allograft seeding

Prepared and milled allograft (Section 2.3) was placed into these solutions (1 ml of allograft per 1 ml of cell suspension) and placed into the incubator (37 ºC, 5% CO_2).

3.1.4.3 Plate set up

After an incubation time of two hours, a portion of the allograft was removed from each of the cell suspensions, and divided into 0.5 ml aliquots, and placed into x 4 twelve well plates. Two millilitres of basal media was then added to each well in two of the plates, and 2 ml of osteogenic media added to each well of the other two plates (Table 3.1).

Table 3.1: The 12 well plate set-up of 0.5 ml aliquots of milled allograft incubated for two hours in increasing cell concentration (cells / ml) suspensions (in triplicate), followed by incubation in basal or osteogenic media. Two plates were set up in this manner for each media type, Plate 1 was later used for biochemical analysis (ALP / DNA assays) and Plate 2 for fluoroscopic (Live/Dead stain) analysis.

BASAL/OSTEOGENIC	$1x10^5$	$1x10^5$	$1x10^5$
	$5x10^5$	$5x10^5$	$5x10^5$
	$1x10^6$	$1x10^6$	$1x10^6$
	Empty	Empty	Empty

After an incubation time of 24 hours, the remaining allograft in the three cell suspensions was then removed, divided into 0.5ml aliquots and transferred to an exact duplicate of the four twelve well plates as shown in the tables.

Each plate was then placed into an incubator, underwent a wash in PBS and media change on day 4, and the experiment was stopped on day 7.

3.1.4.4 Cell viability (live / dead) stain

The allograft was analysed for cell viability via a live / dead stain, using cell tracker green (CTG) and ethidium homodimer (EH-1) as detailed in 2.10. After the incubation period the sections of allograft were washed in PBS, prior to 90 minutes incubation in CTG / EH-1 (10µg/ml CTG, 5µg/ml EH-1), a wash in PBS and further 45 minute incubation in basal media. They were then washed, fixed in ethanol, and stored in PBS prior to microscopic imaging under fluorescent light through a standard FITC filter.

3.1.4.5 Biochemical analysis

After the seven day incubation period cell number quantification and differentiation of each of the study groups was assessed via DNA and ALP assays. In brief, the specimens were rinsed in PBS, and then were fixed by submerging in 90% ethanol, followed by air drying. The specimens were then submerged in 0.5% Triton X-100 solution. Samples then underwent x3 freeze / thaw cycles with vigorous agitation between each freeze. Lysate was measured for ALP activity and DNA content as detailed in 2.11.2. Each specimen was measured in triplicate, (ie n=3, with lysate measured three times for each specimen, giving nine readings in total) and the mean measurement (along with standard deviations) calculated.

3.1.5 Results

3.1.5.1 Live / Dead stain

Cell viability as well as a visual comparison of cell number and colony characteristics were demonstrated via a live dead stain (CTG / EH-1). As initial cell seeding density increased, there was an increase in cell number and viability after the 7 days incubation period (Table 3.2). Visual inspection showed few (green) cells on any specimens initially seeded at 1 x 10^5 cells / ml, but large numbers of cells on all specimens seeded at concentrations of 5 x 10^5 cells / ml and above. Visual comparison however fails to demonstrate gross differences in cell viability or cell number when comparing different media types or initial incubation time with SSCs, and cell morphology / colony characteristics were again similar.

Table 3.2: Representative photomicrographs of allograft + SSC (M70) at indicated cell seeding concentrations, cell seeding times / hour, followed by 7 days incubation in either basal or osteogenic media (scale bars = 100 μm).

	2 hour incubation		24 hour incubation	
	Basal media	Osteogenic media	Basal media	Osteogenic media
$1x10^5$ cells/ml	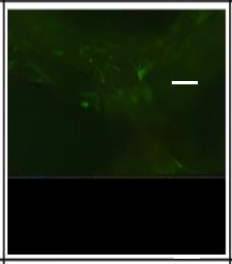	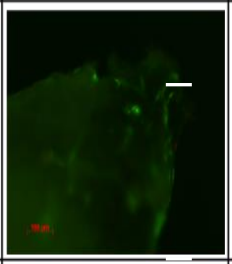	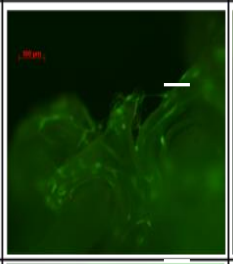	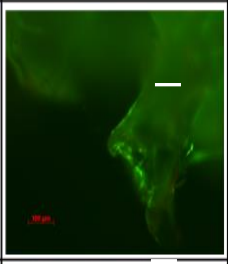
$5x10^5$ cells/ml	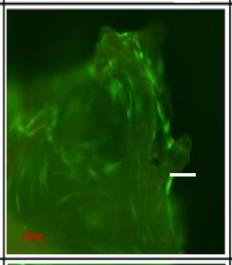	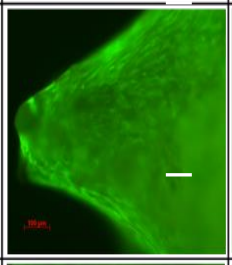	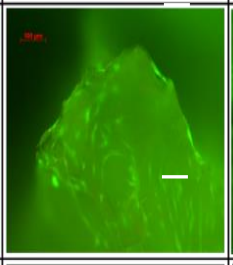	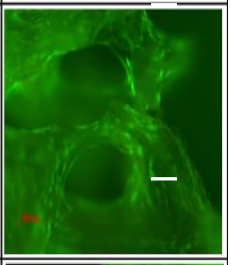
$1x10^6$ cells/ml	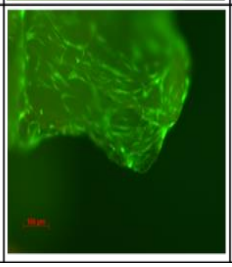	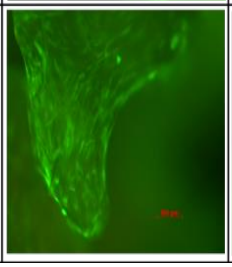	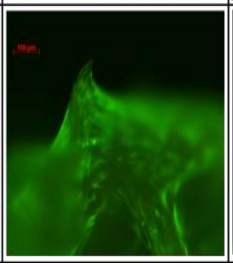	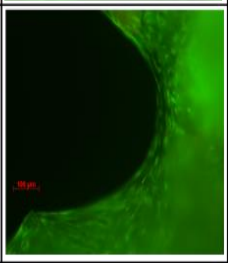

3.1.5.2 DNA assay

A DNA assay was used as a quantitative measure of cell number after the 7 day incubation period in basal media (Figure 3.1.1) and osteogenic media (Figure 3.1.2).

Figure 3.1.1: DNA assay showing mean (SD) DNA concentration of allograft + M70 (SSC) seeded at increasing concentrations for 2 and 24 hours and incubated for 7 days in basal media (n=3).

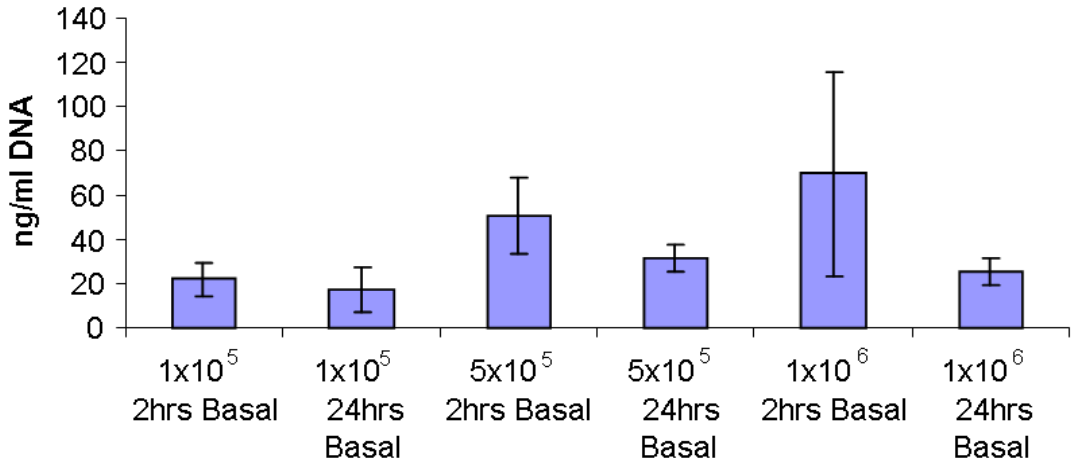

Figure 3.1.2: DNA assay showing mean (SD) DNA concentration of allograft + M70 (SSC) seeded at increasing concentrations for 2 and 24 hours and incubated for 7 days in osteogenic media (n=3).

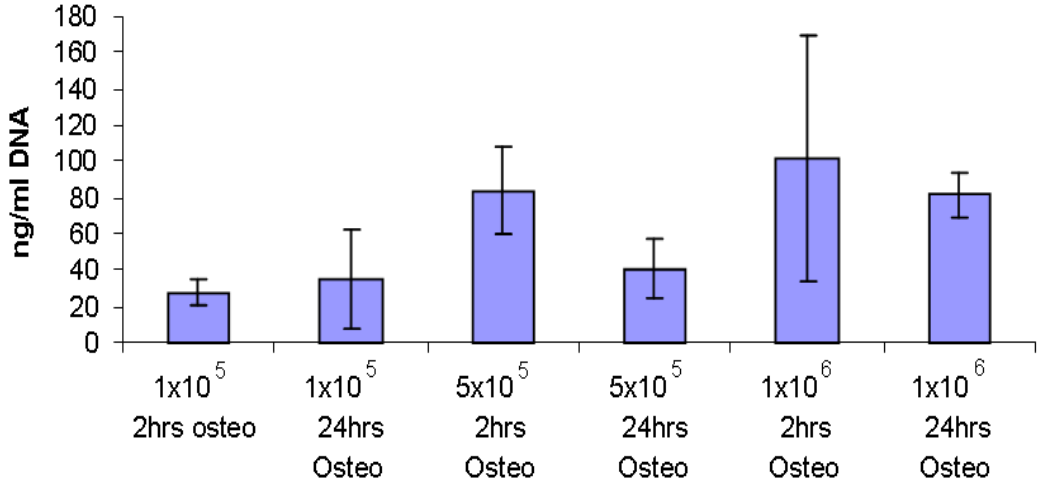

There was a trend towards increasing initial cell seeding concentration and final cell number after 7 days incubation, and (in keeping with the live / dead stain) it did not appear that seeding time or media type significantly affected this result. It should be noted at this time that the error bars were large for these samples, and some results were also spuriously low (eg allograft seeded with $1x10^6$ cells / ml for 24 hours, then incubated in basal media), despite live / dead analysis showing virtual confluent cell growth on these specimens. Reasons for this large drop in DNA content between cells seeded at $1x10^6$ cells / ml for 2 hours and 24 hours could include the fact that the nutrients and oxygen from the low volume of media were used up over the longer incubation period, although more likely is doubt as to the accuracy of a DNA assay when used in combination with *allograft*, and will be discussed in the next section.

3.1.5.3 ALP assay

An ALP assay was used as a quantitative measure of osteoblastic cell number after the 7 day incubation period in basal media (Figure 3.1.3) and osteogenic media (Figure 3.1.4).

Figure 3.1.3: ALP assay showing mean (SD) ALP activity of allograft + SSC (M70) seeded at increasing concentrations for 2 and 24 hours and incubated for 1 week in basal media (n=3).

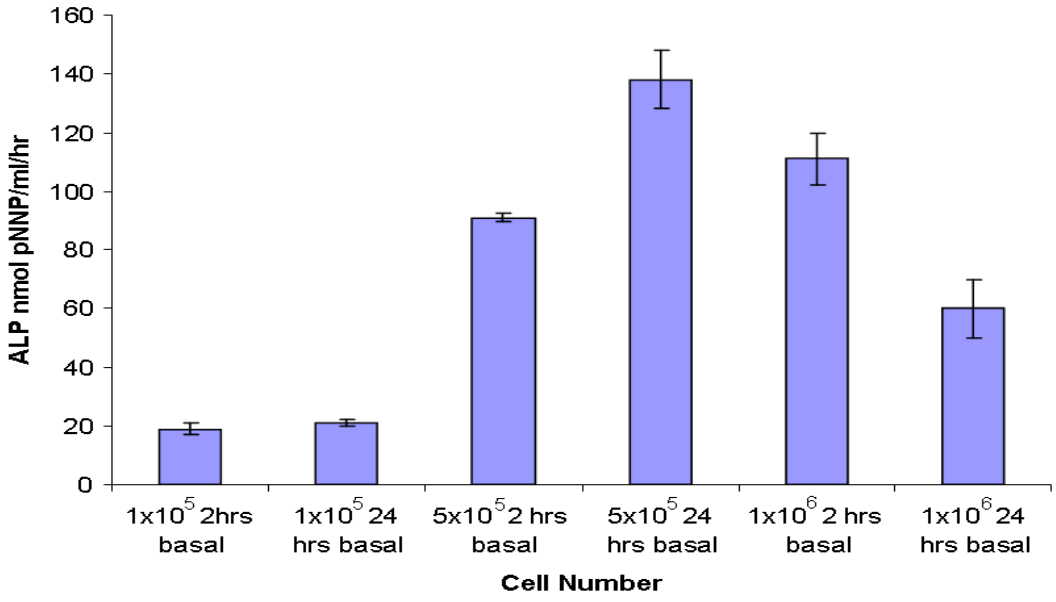

Figure 3.1.4: ALP assay showing mean (SD) ALP activity of allograft + SSC (M70) seeded at increasing concentrations for two and 24 hours and incubated for 1 week in osteogenic media (n=3).

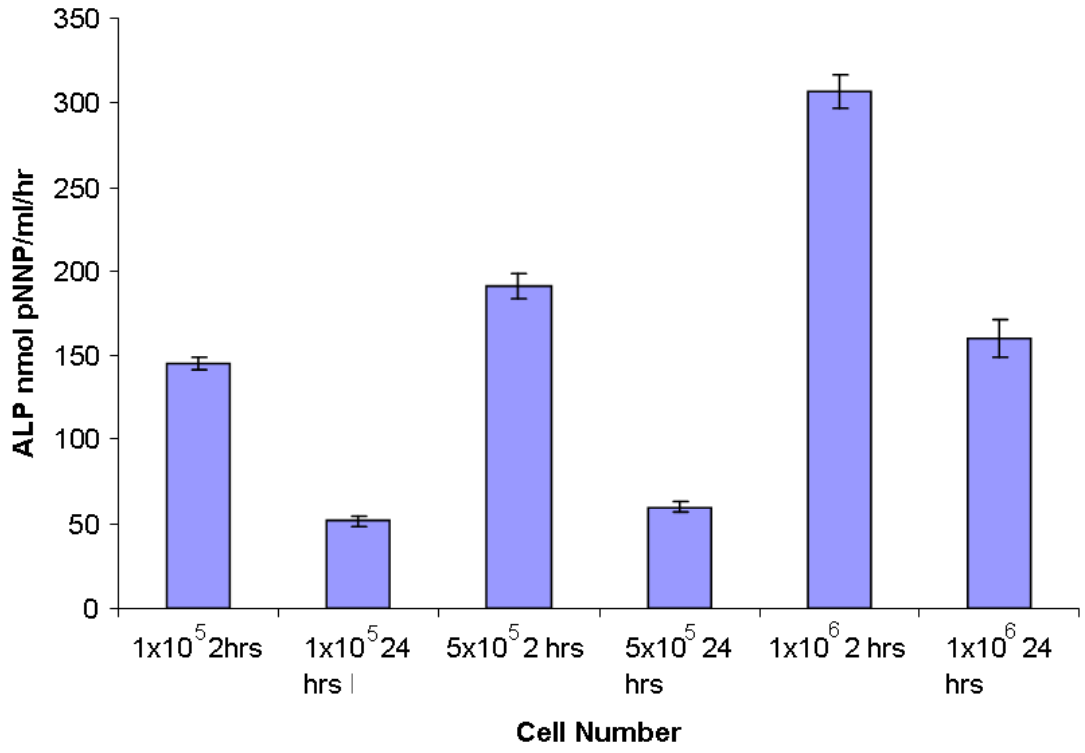

There was again a trend towards increasing initial cell seeding concentration, and total osteoblastic cell number after seven days incubation period, with a concurrent increase also noted between the allograft incubated in the osteogenic media and that in the basal media. The optimal seeding conditions for ALP activity (corresponding to osteoblast number) were 1 x 10^6 cells / ml for 2 hours followed by incubation in osteogenic media (one- way ANOVA: $p < 0.05$) and 5 x 10^5 cells / ml for 2 hours followed by incubation in osteogenic media (one- way ANOVA: $p < 0.05$). This assay also however gave some unexpected results that were not in keeping with the live / dead analysis (such as the high value obtained for the allograft seeded at 1 x 10^5 cells / ml for 2 hours and incubated in osteogenic media, and the low value obtained for the allograft seeded at 5 x 10^5 cells / ml for 24 hours and incubated in osteogenic media), again highlighting possible shortcomings of this assay when used in combination with *allograft*.

3.1.6 Discussion

Visual comparison of the representative live dead stains of the differing groups, demonstrated important factors which made a significant impact on cell survival and proliferation.

All allograft samples that were seeded with cells at a concentration of $1x10^5$ cells / ml, had poor growth of cells after seven days incubation, regardless of the incubation time or type of supporting media used. All samples seeded in cell suspension of concentration of $5x10^5$ cells / ml and 1×10^6 cells / ml showed enhanced cell survival and proliferation by visual comparison to those seeded at concentrations of $1x10^5$ cells / ml. In addition, there was also enhanced total cell number (DNA assay) and osteoblast number (as measured by ALP activity) in the groups that were incubated in the osteogenic media compared to the basal media (especially in the samples which underwent the initial 2 hour incubation with the cell suspension).

Thus from the results of this experiment it can be determined that the cell seeding concentration was the most important factor to promote total cell number adhesion, survival and proliferation over a one week incubation period. This appeared to be purely a number issue i.e. the higher the initial seeding concentration of the cells, the more likely they were going to settle on, adhere to and survive on the supporting allograft. In addition, closer proximity of surviving cells allows events such as cell signalling etc to occur, which can promote proliferation and differentiation. A seeding concentration $1x-10^5$ cells/ml was below this threshold, but both 5×10^5 cells / ml and $1x10^6$ cells / ml were above, allowing successful adhesion and subsequent proliferation to occur. This was in keeping with other studies where high concentrations of SSCs have proved successful (Kanczler *et al.* 2010;Khan *et al.* 2010;Kruyt *et al.* 2008).

As expected, the addition of osteogenic media increased survival on allograft compared to basal media. The promotion of osteogenic differentiation of the cells is likely to promote the development of cellular characteristics specific to the supporting environment i.e. a three dimensional bony scaffold.

An increase in initial incubation period in the cell suspension from two to 24 hours did not make a substantial difference in cell survival or proliferation. Thus most cell

adhesion occurred within the first few minutes to hours, and further time spent in the suspension conferred no survival advantage, but significantly increased experimental time. Using the DNA assay as a measure of cell number, there may actually be a detrimental effect of increased incubation time as demonstrated by Figures 3.1.1 and 3.1.2.. This may have been a survival issue due to limited media and gaseous requirements, although more likely an accuracy of assay issue is the cause. Anecdotally SSC adhesion is said to occur to allograft in 15 – 30 minutes, whereas haematopoietic cells have been shown to adhere to bone marrow stroma with peak adhesion at 30 minutes (Kovach *et al.* 1995).

In summary, for future experimentation a cell seeding concentration of 5×10^5 cells / ml with a seeding time of two hours will be used, to reduce cost and expedite experimental time, whilst at the same time ensuring adequate initial cell numbers for adhesion and proliferation.

Furthermore, both ALP and DNA assays should be interpreted with care, a factor that will be investigated in 3.4.1.

Identification of a proliferative cell line

3.1.7 Introduction

A significant part of the work detailed in this thesis compares a range of different scaffolds as potential osteogenic bone graft substitutes. When analysing multiple different scaffolds in terms of cell compatibility, in order to have results that can be compared quantitatively between the scaffolds, it is important to keep the number of confounding factors to a minimum. It is well known that the SSCs isolated from different patients are highly variable, both in terms of proliferative speed and differentiation potential, even under exactly the same conditions (Cuomo *et al*. 2009;Muraglia *et al*. 2000;DiGirolamo *et al*. 1999). Therefore, to reduce variables a single cell population was utilised for *in vitro* analysis. However, given the short duration and time constraints of some of the planned *in vitro* work, in order to optimise the experiments and give the highest chance of significant results, it was felt important that a proliferative cell line should be selected. Some weaknesses of this methodology are explored in the discussion (3.1.10).

3.1.8 Materials and methods

3.1.8.1 Cell extraction and expansion

Bone marrow aspirates were received in short succession from three patients undergoing primary total hip replacement at Southampton General Hospital. These were i) a male sixty six year old patient (M66), ii) a male fifty one year old patient (M51) and iii) a female sixty eight year old patient (F68). Cells were extracted using standard laboratory protocol as detailed in 2.1. The resulting cell suspension was then divided into ten T150 flasks and basal media supplemented to make the final volume up to 30 ml. The T150's were then placed into incubators at 37^{o}C and 5% CO_2, and underwent PBS washes and media changes every 3-4 days until the cells reached confluence. The cells were then released using Trypsin in EDTA, and then prepared for long term storage by suspension in DMSO in approximately 15-20 cryovials prior to rapid transfer to a -80 ^{o}C freezer (see Section 2.2.1). In this way a stock of each of the cell lines was built, such that after selection of the most proliferative line, enough was stored for all future experimentation.

3.1.8.2 Identification of proliferative cells

One cryovial from each cell population was defrosted, and the cells extracted by mixing with basal media, centrifugation for 4 minutes at 1100 rpm, careful removal of the supernatant, and re-suspension in basal media (2.2.2). A cell count was then performed, and an appropriate dilution with basal media given such that all cell lines were in a suspension of $2x10^4$ cells / ml. Ten mililitres of solution of each cell line (now P1 cells) was then seeded into three T75's ($2x10^5$ cells) and incubated for 12 days in basal media at 37^{o}C and 5% CO_2, with a PBS wash and media change on days 4 and 8. On day twelve cell growth was assessed by visual inspection and cytometry.

3.1.8.3 Visual inspection

The three T75 flasks corresponding to the cells from each patient were viewed under the light microscope, and two observers experienced in cell culture gave an estimate as to percentage cell coverage over the base of the flask.

3.1.8.4 Cytometric evaluation

The cells were released for the T75 flasks using 2 ml of trypsin in EDTA. The trypsin was neutralised using FCS containing basal media, and a cell pellet for each flask obtained via centrifugation (1100 rpm for 4 minutes). The cell pellet was then re-suspended in 5 ml basal media, and 30 µl removed and placed into a standard cell counting chamber. Appropriate calculations were made to give the total cell number in the 5 ml cell suspension, and means along with standard deviations for each cell type calculated.

3.1.9 Results.

The appearance of the T75's after 12 days incubation are given in Table 3.1.3, and expressed as percentage confluence of cell colonies over the base of the flask. The mean of the cell counts performed on each of the three flasks for each cell line is also given in the table. There was approximately x4 more cell growth in the M66 cultures compared to the M51 cultures, and x2 more cell growth compared to the F68 cultures.

Table 3.1.3: Visual estimation of cell confluence of T75 flasks of cells from each patient, and mean cell count (standard deviation) as established by haemocytometry after twelve days incubation in basal media.

	Appearance	Mean Cell Count x 10^5 (SD)
M51	50-60% confluent	6 ± 0.8
F68	90% confluent	18 ± 1.2
M66	100+% confluent	25 ± 2.8

3.1.10 Discussion

This study has confirmed significant patient to patient variability in terms of SSC proliferation potential (Muraglia *et al*. 2000;DiGirolamo *et al*. 1999). Thus when comparing carrier materials, it is extremely important to use cells of the same origin, so any differences found can be attributed to the material rather than the cells themselves. However, caution must also be exerted when translating experimental findings from one single cell population to clinical scenarios, as all patients will behave differently as well. Factors such as patient age, medications they are taking, and medical co-morbidity could affect the behaviour of the SSCs (Stolzing *et al.* 2011). Nonetheless, with limited time for multiple *in vitro* experiments, it is important to choose a cell line which will likely yield significant results, and from the comparison of the cells from each of the three patients, it was decided to use the most proliferative patient cell population (M66). Due to the nature of the process for the transfer of the patients cellular material from the hospital operating theatre to the research laboratory as well as ethical approval issues, only the sex and age of the patient was recorded. It would, however, also have been of great value to have additional patient information, as described above, when experimenting with any patient cell population.

Accuracy of Assays to be used with allograft

3.1.11 Introduction

As highlighted in Sections 3.1.5.2 and 3.1.5.3, initial experiments for assessment of cell growth via DNA assays and osteoblastic differentiation via ALP assays after incubation with *allograft* using methods described previously, gave concerns regarding their accuracy especially when the number of cells present was low.

There are two main areas where inaccuracies may arise during the preparation process for ALP and DNA assays.

1. The sample preparation process results in a cloudy solution (likely due to the breakdown of the allograft). The contaminants in this solution could potentially affect the accuracy of the PicoGreen assay,

2. The allograft used is fresh frozen morselised allograft from recent surgeries (THR/ hemiarthroplasties) at SGH. It is biological material and hence probably has residual DNA and ALP despite the preparation process. This again could strongly influence both of the assays.

3.1.12 Aim

The purpose of this investigation was to assess the accuracy and reproducibility of the DNA assay and ALP assay when used in combination with allograft. A second stage was to assess another assay, the WST-1 cell proliferation assay for its sensitivity and reproducibility for quantification of cell number when in combination with allograft.

3.1.13 Null hypotheses

1. There is no correlation between cell number and DNA assay result when used in combination with allograft.
2. There is no correlation between cell number and ALP assay result when used in combination with allograft.
3. There is no correlation between cell number and WST-1 assay result when used in combination with allograft.

3.1.14 Materials and Methods

3.1.14.1 Experimental set-up

Pre-prepared allograft (Section 2.3) was weighed out into 1g specimens and placed into individual wells of a 24 well plate in a sterile manner. A cryo vial of stored cells from the male sixty six year old (M66) patient were defrosted and grown to confluence in T150 flasks in basal media. They were then washed in PBS, trypsinised, suspended in basal media, centrifuged at 1100 rpm for 4 minutes. The supernatant was discarded and the cells were re-suspended in 10 ml basal media. Cell count was performed by haemocytometry, and then cell solutions of concentrations $5x10^3$ cells / ml, $5x10^4$ cells / ml and $5x10^5$ cells / ml via appropriate dilution with basal media. One millilitre of each solution added to the 1g allograft specimens as shown in Table 3.1.4, such that each experimental seeding group was replicated six times. The control wells contained plain,

unseeded allograft alone. Two 24 well plates were set up in this manner, one for DNA and ALP assay assessment and one for WST-1 assay assessment.

Table 3.1.4: Three 24 well plates were set up as shown, such that allograft was seeded with 3 increasing concentrations of SSC (M66), and each group was replicated six times.

1	**2**	**3**	**4**	**5**	**6**
Control	Control	Control	Control	Control	Control
$5x10^3$ cells	$5x10^3$ cells	$5x10^3$ cells	$5x10^3$ cells	$5x10^3$ cells	$5x10^3$ cells
$5x10^4$ cells	$5x10^4$ cells	$5x10^4$ cells	$5x10^4$ cells	$5x10^4$ cells	$5x10^4$ cells
$5x10^5$ cells	$5x10^5$ cells	$5x10^5$ cells	$5x10^5$ cells	$5x10^5$ cells	$5x10^5$ cells

After a two hour incubation time, five millilitres of basal media added and seven days incubation followed, with PBS washes and media changes every 2 days.

3.1.14.2 DNA / ALP assays

On day seven the samples from one of the 24 well plates were washed in PBS and fixed in 90% ethanol for 5 minutes. The ethanol was then removed and the samples left to air dry. The samples were then rewashed in PBS, and transferred to a universal container. Two millilitres of 0.5% triton was then added, and the sample then underwent x3 freeze thaw cycles with vigorous vortexing when thawed. The lysate was then tested for DNA content and ALP activity using standard laboratory protocols as described in Section 2.11.1. The lysate of each sample was tested in triplicate, and the mean for each sample calculated. There were six samples for each seeding concentration of cells, thus mean

and standard deviation for each cell seeding concentration was calculated from the previously derived data and plotted onto a graph.

3.1.14.3 WST-1 assay

After seven days incubation the seeded allograft in the second 24 well plate was tested via a WST-1 assay. The specimens were washed in PBS and then 2.5mls WST-1 (1:10 dilution with basal media) solution was added to each well. Four hundred microlitres of the substrate was taken after one and four hours further incubation, transferred into a 24 well plate and then read using Bio-Tek microplate fluorescent reader (Bio-Tek, Winooski, USA) at 410 nm. There were six samples for each seeding concentration of cells, thus mean and standard deviation for each cell seeding concentration was calculated and plotted onto a graph.

3.1.14.4 Statistical analysis

For statistical analysis of the DNA content, the ALP activity and optical density of the WST-1 solution, the difference in means for each of the cell seeding densities was calculated using a one-way ANOVA test, with post hoc Bonferroni comparison to highlight which groups the statistical differences were between (SPSS 17.0).

3.1.15 Results

3.1.15.1 ALP assay

The full results for the ALP activity of each of the six specimens at each cell seeding concentration is provided in Appendix 2 (Table 1). The mean values for each cell seeding concentration are summarised in Figure 3.1.5.

Figure 3.1.5: Mean (SD) ALP activity assay results for 1 ml allograft seeded with increasing concentrations of SSC's after 1 week incubation (n = 6).

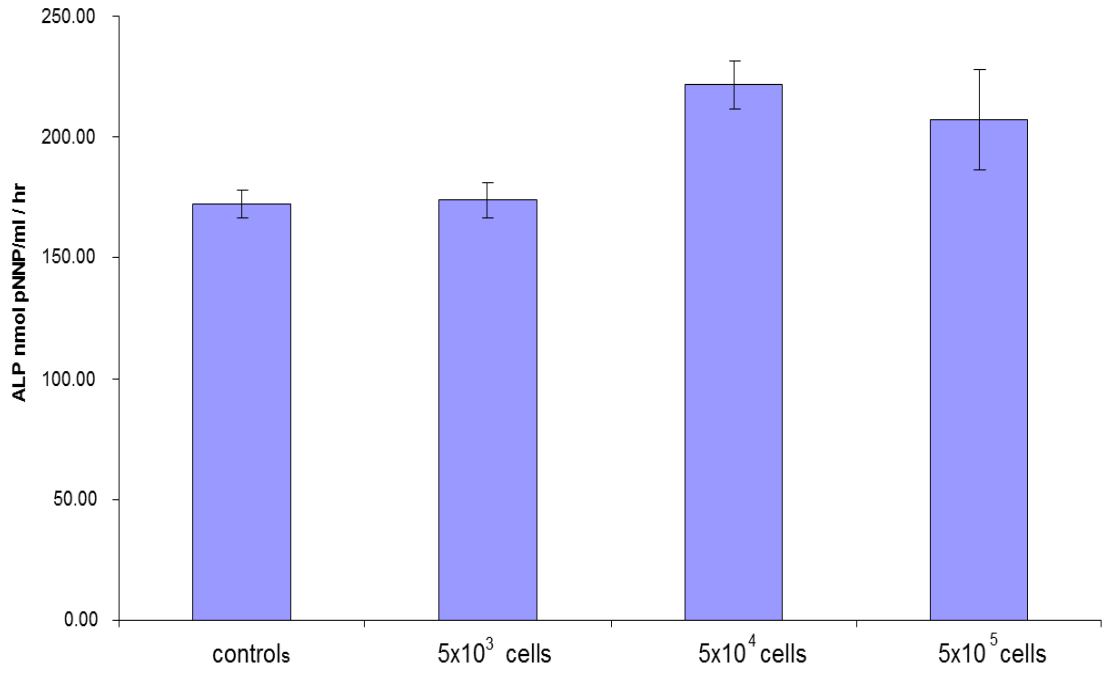

As can be seen there was an increase in ALP activity over the controls in all groups and these differences were found to be significant (One-Way ANOVA $P<0.001$, Appendix 2, Table 2). However, post hoc Bonferroni analysis showed that only the increases in ALP activity for the allograft seeded at $5x10^4$ cells / ml ($P=0.002$) and $5x10^5$ cells / ml ($P=0.04$) were significant (Appendix 2, Table 3). In addition the mean ALP activity for allograft seeded with $5x10^4$ cells / ml was found to be higher than that of $5x10^5$ cells / ml, which was not in keeping with the expected outcome.

3.1.15.2 DNA assay

The full results for the DNA content of each of the six specimens at each cell seeding concentration is provided in Appendix 2 (Table 4). The mean values for each cell seeding concentration is summarised in Figure 3.1.6.

Figure 3.1.6: Mean (SD) DNA assay results for 1 ml allograft seeded with increasing concentrations of SSCs (M66) after 1 week incubation (n = 6).

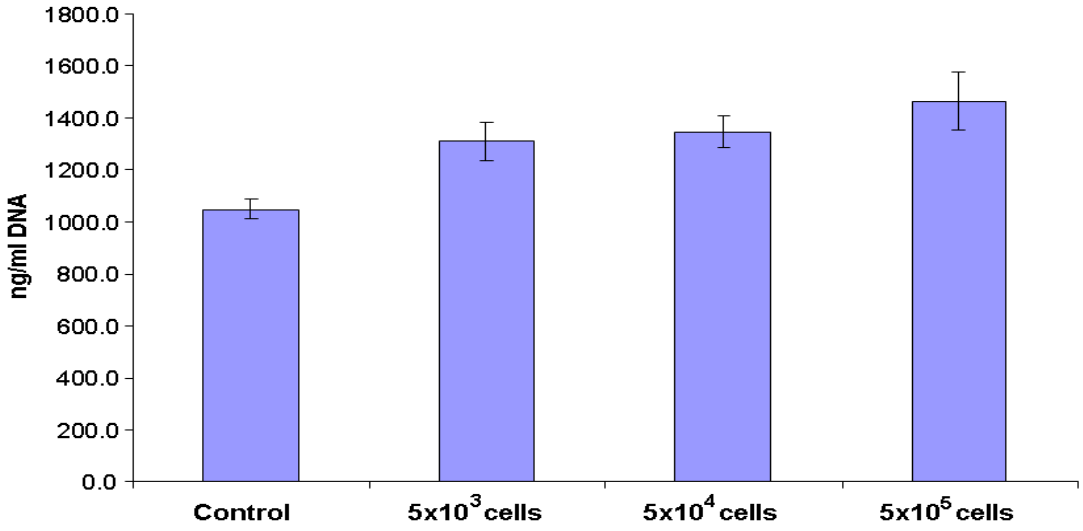

There was a stepwise increase in DNA content as initial cell seeding concentration increased. However, when the results were analysed, statistical comparison using One-way ANOVA (Appendix 2, Tables 5+6) did not find significant differences between groups at the $P<0.05$ level. It should also be noted that the control samples on to which no cells were seeded, gave significant readings of DNA.

3.1.15.3 WST-1 assay

The full results for the optical densities of the WST-1 substrate (after one and four hours incubation) of the six specimens at each cell seeding concentration is provided in the Appendix 2 (Tables 7+8). The mean values for each cell seeding concentration is summarised in Figure 3.1.7.

There was a stepwise increase in optical density achieved as initial cell seeding concentration increased, and this was more pronounced after a four hour incubation in WST-1 solution. One-way ANOVA test with post hoc Bonferroni analysis (SPSS 17.0) was used to analyse the differences in optical densities between the samples at both 1 and 4 hours. (Appendix 2, Tables 9+10).

Figure 3.1.7: Graph showing mean optical densities (and standard deviations) of WST-1 assay after one week of allograft seeded with differing cell concentrations (M66) at 1 and 4 hours.

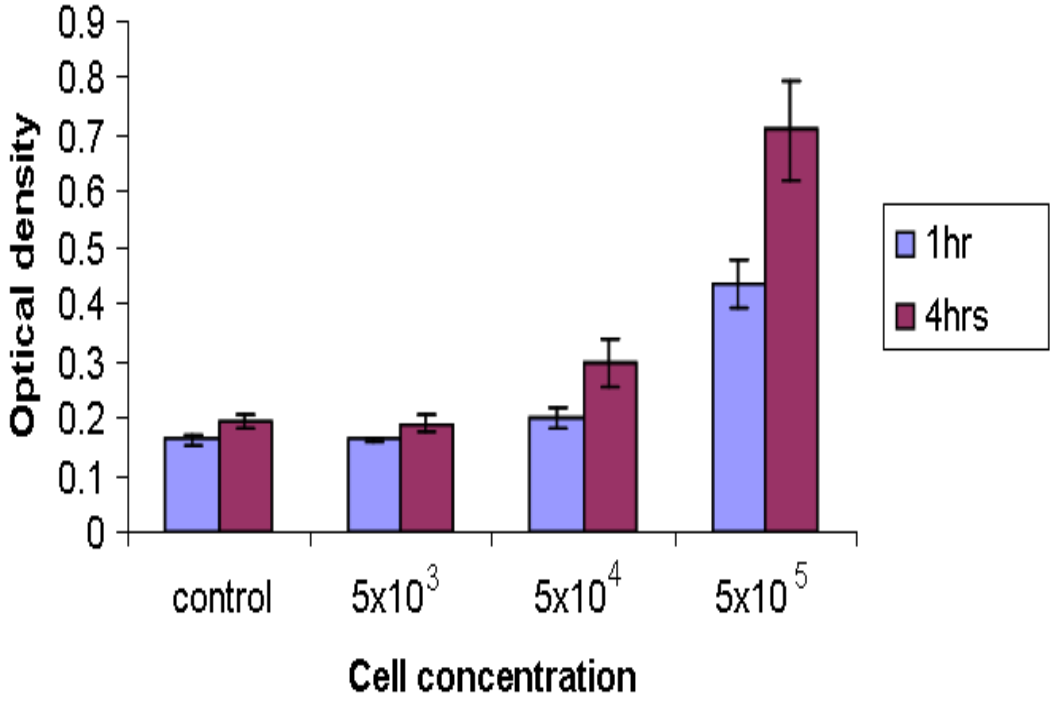

There was no significant difference in optical density after WST-1 assay between control allograft and allograft seeded with 5 x 10^3 cells / ml at 1 or 4 hours. However, results of allograft seeded with cells at a concentration of $5x10^4$ cells / ml approached significance compared to the controls at 1 hour ($p = 0.089$) and was highly significant at 4 hours ($p = 0.01$), and again approached significance compared to the allograft seeded at a concentration of $5x10^3$ cells / ml at 1 hour ($p = 0.096$) and was highly significant at 4 hours ($p = 0.007$). Furthermore results of allograft seeded with cells at a concentration of $5x10^5$ cells / ml were significantly higher than the controls at both 1 and 4 hours ($p < 0.0005$, $p < 0.0005$), allograft seeded at a concentration of $5x10^4$ cells / ml ($p = 0.0005$, $p = 0.0005$) and allograft seeded at a concentration of $5x10^5$ cells / ml ($p = 0.0005$, $p = 0.0005$).

3.1.16 Discussion

The ALP and DNA assays when used in combination with *allograft* and cells gave extremely variable results. Even the negative controls (allograft alone) gave readings in some of the samples which were higher than some of their cell seeded counterparts. Possible reasons were discussed above, and were most likely due to particulate matter in the lysate as a consequence of freeze thawing the allograft, as well as inherent residual DNA / ALP activity in the allograft, despite the thorough preparation. The WST-1 assay on the other hand, gave extremely encouraging results. There was a clear increase in cell proliferation activity on the assay at both one and four hours as the cell seeded concentration of each of the allograft specimens increases. In addition the variation in readings between the six samples seeded at the same cell concentrations was only small, making the differences between the means of the differing cell densities highly statistically significant at 4 hours for allograft seeded at densities of $5x10^4$ and $5x10^5$ cells / ml. For allograft seeded at a density of $5x10^3$ cells/ml there was no significant increase in optical density on the WST-1 assay after 1 or four hours. Either the assay was not sensitive enough to detect cells seeded at this extremely low density, or the cells did not survive the seeding process in sufficient numbers.

3.1.17 Conclusion

The results in the context of the null hypotheses were examined:

1. *There is no correlation between cell number and DNA assay result when used in combination with allograft.*

   This null hypothesis **remains unproven.**

   The experiments detailed here show a trend towards increasing cell number and increasing measured DNA content, although with the cell numbers and the experimental group numbers used the test was not sensitive enough to show a statistically significant difference.

2. *There is no correlation between cell number and ALP assay result when used in combination with allograft.*

   This null hypothesis **remains unproven.**

   Again, the experiments detailed here show a trend towards increasing cell number and increasing measured ALP content, although with the cell numbers and the experimental group numbers used, again the test was not sensitive enough to show a statistically significant difference.

3. *There is no correlation between cell number and WST-1 assay result when used in combination with allograft.*

   This null hypothesis is **false.**

   A trend of increasing cell number and increasing measured WST-1 assay result was observed, and with the cell numbers and the experimental group numbers used, the test *was* sensitive enough to show statistically significant differences.

The results of these experiments provide evidence that the results of DNA and ALP assays were inconsistent and unreliable when assessing cell viability and number in terms of survival on prepared *allograft*. The WST-1 assay was however rapid and simple to perform, and gave a reliable measure of these parameters when cells are combined with allograft, especially at an incubation time of 4 hours. For future experimentation when investigating cell number on *allograft*, this thesis will use the WST-1 assay as the **primary** measure.

An analysis of polymer type and chain length for use as a biological composite graft extender in impaction bone grafting: a mechanical and bio-compatibility study

3.2 Part 2: Study

3.2.1 Introduction

Much work has been performed investigating the combination of SSC's with biodegradable polymers. The various pros and cons for a variety of these polymers have been documented, and more recently blends have been investigated in an attempt to combine beneficial traits (Bergsma *et al.* 1993;Bostman *et al.* 1990;Khan *et al.* 2010). Furthermore, technology has allowed the combination of growth factors etc to the polymer, in an attempt to stimulate appropriately timed differentiation of cells for maximal survival and outcome (Kanczler *et al.* 2010).

From an impaction bone graft point of view, multiple studies have looked into the optimal size of particulate matter of milled allograft for maximum shear strength, the effect of washing allograft, irradiating it during the sterilisation procedure, as well as methods of optimising the surgical technique for success and longevity of the graft, but the published work surrounding the combination of SSCs with the graft is scarce (Dunlop *et al.* 2003;Gie *et al.* 1993a;Halliday *et al.* 2003;Costain and Crawford 2009). Much of this work has been performed by this department via an *in vitro* impaction bone graft model. It has been shown that when SSC's were added to allograft prior to impaction, the cells not only survived the impaction process, but were able to proliferate, and after a period of 4 weeks incubation with the allograft, they measurably improved the mechanical characteristics of the construct in terms of interparticulate cohesion and shear strength (Bolland *et al.* 2006). Early investigations into the use of biodegradable polymers in combination with SSC's as potential alternatives to allograft for use in impaction bone grafting have also been performed. The same authors analysed PLA produced via CO_2 supercritical fluid production methods in combination with SSC's both in vitro, and in a subcutaneous *in vivo* murine model, finding that the addition of SSC's not only stimulated bone production and vascular ingrowth compared to the controls, but again also improved the mechanical characteristics compared to the

controls (PLA alone) (Bolland *et al.* 2008b). This work has stimulated further avenues for investigation, which will be the basis of this thesis. There are multiple different biodegradable polymers available for use in tissue engineering strategies, and as well as polymer type, many other factors can hugely affect their material properties, including polymer chain length, crosslinking and production methods which leads to a huge diversity of morphology, strength, porosity and surface texture to name but a few (Hutmacher 2000). Current uses in surgery alone range from suture material to prosthetic heart valves, highlighting their versatility (Hyde *et al*. 1999;Pillai and Sharma 2010).

3.2.2 Aim

The second part of this chapter details the use of the protocols established Section 3.1, such that three polymers commonly used in tissue engineering could be screened in both their long and short chain forms, to find the best two polymers in terms of cellular compatibility as well as mechanical characteristics to take forward for further analysis.

3.2.3 Null hypothesis

No polymer under test has the cellular compatibility or mechanical characteristics for consideration as an alternative to allograft in IBG.

3.2.4 Materials and Methods

3.2.4.1 Polymer selection

Due to a lack of available polymer research in the IBG field, and the huge number of potential polymers to screen, the initial contenders were decided upon as likely candidates from a review of related literature by a group of experts with knowledge in chemical engineering (S.H., S.F.) tissue engineering (R.O.C.) and orthopaedic engineering (D.D., E.T., A.A., A.B.), and consisted of (polyε-caprolactone (PCL), poly(DL-lactide) ($P_{DL}LA$) and poly(DL-lactide-co-glycolide) ($P_{DL}LGA$). The high and low molecular weight versions of each polymer were tested, giving six scaffolds in total for analysis.

P_{DL}LA molecular weights 26 and 126 kDa, and P_{DL}LGA molecular weights 35 and 110 kDa were purchased from (Surmodics Pharmaceutical, Inc. Birmingham, Al, USA), while PCL molecular weights 14 and 85 kDa were ordered from (Sigma, UK) and all were used as received.

3.2.4.2 Polymer preparation

Polymers were melt casted by heating them above T_m (~180 °C) inside Teflon cages (100 x 60 x 20 mm) and subsequently cooled to room temperature. All polymer samples were refrigerated before further processing. They were then milled using a standard bone mill (Tessier Osseous Microtome- Stryker Leibinger, Freiberg, Germany), photographed, sterilised in 5x antibiotic / antimycotic solution (Sigma, Aldrich, UK) and by U.V. light treatment for 24 hours and finally submerged in basal media for a further 24 hours prior to use.

3.2.4.3 Preparation of allograft

Standard allograft was also used as a control against which each polymer could be compared and was obtained from fresh frozen femoral heads that had been stored at -80 °C (Section 2.3). Under sterile conditions the femoral heads were defrosted and milled using the same bone mill on the medium setting (Tessier Osseous Microtome, Stryker Leibinger, Freiberg, Germany). The milled bone graft was then de-fatted and prepared as described in Section 2.3. It was then soaked in 5x antibiotic / antimycotic solution and underwent UV light exposure for 24 hours, re-washed in phosphate buffered saline and then submerged in basal media for 24 hours prior to use.

3.2.4.4 Mechanical testing

Mechanical testing was performed using a method consistent to that of other IBG *in vitro* studies (Bolland *et al*. 2006;Dunlop *et al*. 2003;Jones *et al*. 2009). An acrylic disc was placed into a custom built impaction rig (Southampton University Engineering Department) designed to deliver impaction force similar to that experienced by allograft during *in vivo* IBG (Brewster *et al.* 1999). Eight millilitres of each polymer/ allograft were inserted into the centre of the disc in three equal portions, undergoing 24 impactions at a frequency of 1Hz after the addition of each portion, such that each

impacted disc had undergone 72 impactions. Twelve discs were impacted for allograft and each polymer, which then had a perforated base and lid added prior to being placed into universal pots, submerged in 30 mls isotonic solution (phosphate buffered saline-PAA laboratories, Pasching, Austria) and incubated at 37 °C, 5% CO_2 for 7 days to mimic early *in vivo* conditions. A custom made cam shear testing rig was then set up as described by Bolland *et al.* and fitted into an Instron testing machine (Instron, High Wickham, UK) (Bolland *et al.* 2006). The impacted discs were then rapidly transferred into the testing rig to prevent excessive drying. The specimens were then subjected to a constant shear strain of 1 mm/min whilst under compressive stresses of 102 kPa, 306 kPa and 509 kPa (4 discs per stress), and from this data shear strength, interparticulate cohesion and the shear stress at 350 kPa compression (a physiological load) were calculated for the allograft and each polymer using the Mohr Coulomb failure equation (see Section 2.7) at 10 % strain (standard engineering practice).

3.2.4.5 Micro Computed Tomography (µCT)

One disc of each polymer type underwent a µCT scan in order to quantify some characteristics after milling and impaction. Quantitative 3D analysis of the discs was performed using an X-tek benchtop 160Xi scanning system (Xtek Systems Ltd, Hertfordshire, UK). Raw data was then reconstructed using Next Generation Imaging (NGI) software package version 1.4.59 (X-TEK Systems Ltd) to obtain images at approximately 50 micron resolution. Visualisation and analysis was performed using Volume Graphics (VG) Studio Max 1.2.1 software package (Volume Graphics GmbH, Heidelberg, Germany) for bone/polymer: total volume ratio and bone / polymer surface area: volume ratio.

3.2.4.6 Biological Compatibility

3.2.4.6.1 Reagents, antibodies, molecular probes

For details of culture media preparation, reagents, and fluorescent probes used in this study see Section 2.1.

3.2.4.6.2 Cell culture

As described previously (Sections 3.1.7 - 3.1.10), a proliferative cell line from a male sixty six year old patient (M66) undergoing primary total hip replacement had been identified, culture expanded, and frozen for storage in cryovials. The cells from three cryovials were re-animated by allowing them to thaw, adding 10ml basal media, centrifuging at 1100 rpm for 4 minutes, pouring off the supernatant and re-suspending in basal media prior to seeding in tissue culture flasks and culturing as described previously. Upon confluence the cells were released using trypsin in EDTA, centrifuged and re-suspended in basal media and the total count using a haemocytometer determined. Appropriate dilution with basal media was then given such that the concentration was $5x10^5$ cells / ml.

3.2.4.6.3 Allograft / polymer seeding

Twenty millilitres of the allograft / polymer were then placed into a sterile universal container and seeded with 20 ml of the SSC solution ($5x10^5$ cells / ml) for two hours in an incubator at 37ºC in 5% CO_2 with agitation every 30 minutes to optimise cell adherence. Plain un-seeded allograft / polymer were used as a negative control. Thus the same concentration of Passage 2 (P2) cells from the same patient were used in all experimental arms, minimising any difference that may be observed due to different cell population characteristics.

3.2.4.6.4 Impaction of seeded allograft / polymers

Due to the cell numbers required and availability of polymers, a scaled down version of the impaction as described previously was performed. A smaller custom made impaction device was thus produced (Southampton University Engineering Department), again designed to deliver impaction force similar to that experienced by allograft during *in vivo* IBG (Brewster *et al.* 1999) (Section 2.5). Under aseptic conditions 1 ml of seeded allograft / polymer was impacted into customised electron microscopy pots in three equal portions, with 24 impactions given after the addition of each portion (72 impactions in total) (Section 2.6). The procedure was repeated 5 times for each polymer / allograft (with an additional 6 controls), and the impaction chambers were then placed individually into each well of a 6 well plate, cultured under osteogenic

conditions (basal media + 100µM ascorbate-2-phosphate, and 10 nM dexamethasone) and incubated at 37 ºC in 5 % CO_2 for 8 days, with PBS washes on days 3 + 6.

3.2.4.6.5 Cell viability

After incubation two discs were assessed for cell viability via standard incubation with Cell Tracker Green (CTG) probe and Ethidium Homodimer-1 (EH-1) (Section 2.10). This disc was then fixed in ethanol and stored in PBS prior to imaging under confocal microscopy (Leica SP5 Laser Scanning Confocal Microscope and software, Leica Microsystems, Wetzlar, Germany).

3.2.4.6.6 Cell proliferation assay

For the quantification of cell proliferation and cell viability a WST-1 assay was performed. Three discs from each group (and 1 control disc) were submerged in 2.5 mls 1:10 dilution WST-1 substrate (Roche ltd, Welwyn Garden City, UK). At 2, 4, and 6 hours 400 µl of substrate was removed and read in triplicate via a Bio-Tek KC4 microplate fluorescent reader (Bio-Tek, USA) at 410nm. An increase in absorbance value (ie increase in optical density of the substrate) indicated increased cell number and viability.

3.2.4.7 Scanning Electron Microscopy

In order to give some explanation of the different cell compatibilities for each of the polymers, small samples were taken, stub mounted and gold sputter coated in a low vacuum environment. They were then viewed under a scanning electron microscope at x50 and x200 magnification (FEI Quanta 200 Scanning Electron Microscope, FEI, Oregan, USA).

3.2.4.8 Statistical Analysis

Differences between shear strength curves were analysed statistically using grouped linear regression analysis via GraphPad Prism (ver. 3.02) software. Differences between the WST-1 activity at each time point (2, 4 and 6 hours) of each of the polymers seeded with cells was compared to that of the seeded allograft using Mann–Whitney U test, where $p < 0.05$ was deemed to be significant.

3.2.5 Results

3.2.5.1 Polymer characterisation

Macroscopic differences were observed between the different polymer types before and after the milling process, as well as after the sterilisation process, with appearance and texture ranging from clear, hard and glassy ($P_{DL}LA$ mwt 26kDa and 126kDa) to white, soft and wax-like (PCL mwt 14kDa), and ease of milling ranging from moderate ($P_{DL}LA$ mwt 26kDa and $P_{DL}LGA$ mwt 35kDa) to extremely hard (PCL mwt 85kDa and $P_{DL}LA$ mwt 126kDa) compared to allograft (Figure 3.2.1, Table 3.2.1). There were not only macroscopic differences between the different polymer types, but also between the polymers of the same type but different molecular weights. As can be seen, all polymers had irregular sized and shaped granules, which appeared grossly similar to the bone particles, but none possessed pores, a feature that will be addressed in later chapters.

Figure 3.2.1: Photomicrographs of each of the polymers after the milling process with a standard bone mill. The particles are inconsistent in size and shape, which allows effective 'packing together' during the impaction process. (A) $P_{DL}LA$ 26 kDa, (B) $P_{DL}LA$ 126 kDa, (C) $P_{DL}LGA$ 35 kDa, (D) $P_{DL}LGA$ 110 kDa, (E) PCL 14 kDa, (F) PCL 85 kDa, (G) allograft for comparision (scale bar = 20 mm).

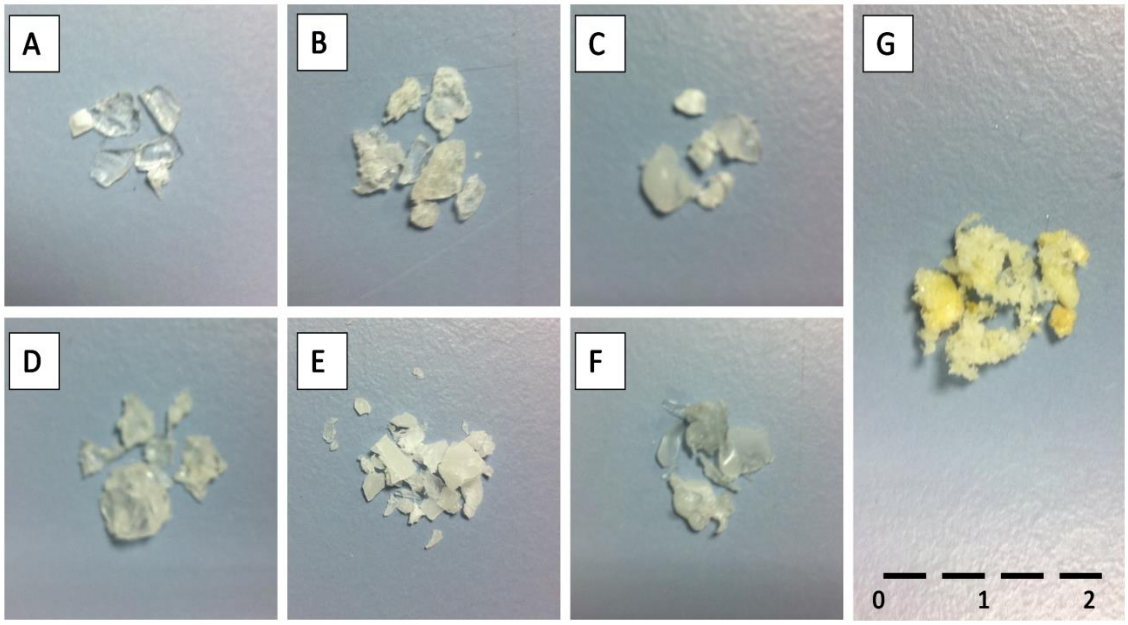

Table 3.2.1: Gross physical characteristics of the polymers during the preparation process.

Polymer	Appearance	Milling	Post antibiotic treatment
PLA 26kDa	Glassy, solid, brittle	Moderate/ hard	Adherent, structural change (softer)
PLA 126kDa	Glassy, solid	Very hard	Unchanged
PLGA 35kDa	Glassy, brittle	Moderate	Unchanged
PLGA 110kDa	Yellow, glassy, brittle	Hard	Unchanged
PCL 14kDa	White, solid, waxy	Medium	Slightly adherent
PCL 85kDa	White, solid	Very hard	Unchanged

Analysis of the CT scan of the milled and impacted allograft and each polymer is shown in Table 3.2.2.

Table 3.2.2: µCT analysis of the allograft and polymers after milling and impaction.

	Bone/polymer volume (mm)	Surface area: volume ratio	Bone/polymer volume: total volume ratio
Allograft	1602.68	14.45	0.34
PLA 26kDa	4081.55	0.67	0.94
PLA 126kDa	4999.59	0.47	0.95
PLGA 35kDa	4629.14	0.69	0.94
PLGA 110kDa	4641.22	0.50	0.88
PCL 14kDa	3037.73	0.77	0.61
PCL 85kDa	3963.98	0.90	0.72

Of note, the surface area to total volume ratio for the allograft controls was far higher and the volume to total volume ratio was less than any of the polymers, which reflected the highly irregular surface and persistent porous / trabeculated nature of the milled bone compared to the solid 'granules' of milled polymer.

3.2.5.2 Mechanical testing

Mohr Coulomb failure curves derived from the mechanical shear tests under three compressive loads for the allograft (black line), and the low and high mwt versions of each of the polymers are shown in Figure 3.2.2. As can be seen, the shear strength of the impacted constructs vary greatly between polymers, and between the same polymer type but differing molecular weight. These variations are the result of differences in material properties (eg Young's modulus), as well as differences in size, shape and surface roughness of the individual particles.

P_{DL}LGA mwt 110 kDa, P_{DL}LGA mwt 35 kDa, P_{DL}LA mwt 126 kDa and P_{DL}LA mwt 26 kDa all displayed enhanced mechanical competency compared to allograft (grouped linear regression; $p < 0.05$). The curves for the high and low molecular weight (85 kDa and 14 kDa) versions of PCL both lie inferior to that of the allograft controls ($p < 0.05$), indicating less favourable mechanical characteristics under shear. The calculated cohesion between the milled particles was significantly higher than allograft (62.51 kPa) for P_{DL}LGA mwts 35 kDa and 110 kDa (176.31 kPa and 111.59 kPa), and P_{DL}LA mwts 26 kDa and 126 kDa (72.9 kPa and 201.33 kPa), but those of PCL mwts 14 kDa and 85 kDa were less (11.3 kPa and 3.02 kPa) (Table 3.2.3). The calculated shear strength at 350kPa compression (a typical physiological force) is also displayed (along with 95% confidence interval) for each polymer type and the allograft controls. There was a trend towards the lower molecular weight version of each polymer having a higher interparticulate cohesion and it is possible that with a larger number test discs this difference would be significant. The softer nature of the lower molecular weight polymers may have allowed more polymer to be packed into the discs due to the malleable nature of the granules. This allows more surface contact between granules, increasing the shear strength of the construct as a whole.

Figure 3.2.2: Mean shear stress (and standard deviations) at 10% strain for allograft and each of the polymers under the three compressive loads. Best fit lines (least squares technique) linking the values have been added.

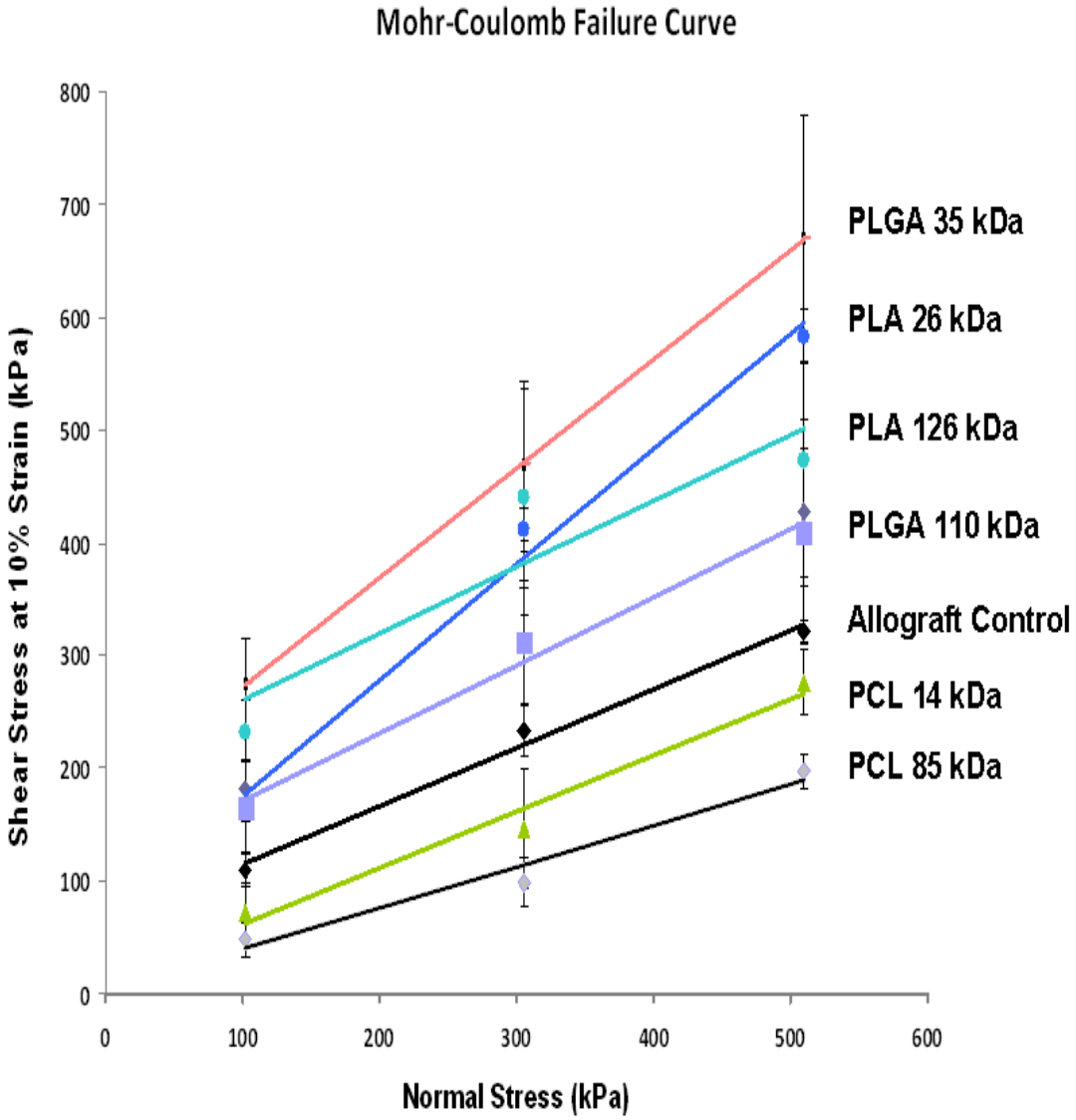

Table 3.2.3: Interparticulate cohesion, shear strength at 350 kPa (a typical physiological load during gait) and statistical significance of each of the tested polymers compared to allograft controls.

Test substance	Interparticulate cohesion (kPa)	Shear stress (kPa) at 350 kPa compression (95%confidence interval)	Statistical significance (Grouped linear regression analysis)
Allo-graft	62.5	244.8 (±12.0)	N/A
PLA 26kDa	72.9	432.3 (±22.6)	P<0.001
PLA 126kDa	201.3	407.8 (±63.7)	P<0.001
PLGA 35kDa	176.3	514.9 (±48.6)	P=0.0027
PLGA 110kDa	111.6	322.0 (±44.7)	P=0.0013
PCL 14kDa	11.3	127.2 (±25.8)	P<0.001
PCL 85kDa	3.0	131.0 (±13.0)	P=0.004

3.2.5.3 Biological compatibility

3.2.5.3.1 Assessment of cell viability

Cell viability was assessed by confocal microscopy using expression of CTG and EH-1 after 8 days incubation. This allowed focussed imaging of the irregular surfaces of both the allograft and polymer granules. Figure 3.2.3A shows a typical section of allograft in combination with SSC's. There was a moderate cluster of live cells (green), but negligible dead or compromised cells (purple/ red). Figure 3.2.3B shows allograft alone treated under similar conditions (negative control), and as expected no cells were visible.

Figure 3.2.3 (A+B): Live/dead immunostain showing (A) limited cell colonisation (arrows) of allograft seeded with SSC's after 8 days incubation in osteogenic media and viewed under confocal microscopy.(B) Allograft control treated in the same conditions but no prior SSC seeding, showing absence of live cells (scale bar = 100 µm).

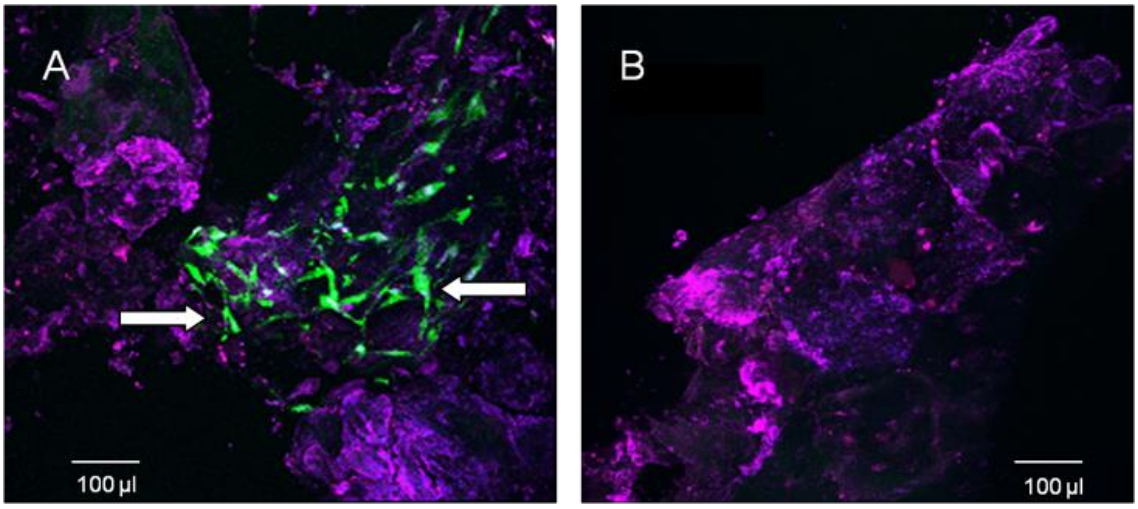

Figure 3.2.4 A-F shows the comparative typical confocal images of the six polymers under test (inset image is negative control). Excellent cell growth and viability was observed following SSC culture on P_{DL}LA mwt 126 kDa, P_{DL}LGA mwt 110 kDa and PCL mwt 85 kDa (Figure 3.2.4 B, D, F). In contrast, moderate cell growth and viability was observed on P_{DL}LGA mwt 35 kDa (Figure 3.2.4 C), and poor cell growth and viability for SSCs cultured on P_{DL}LA mwt 26 kDa and PCL mwt 14 kDa (Figure 3.2.4 A+E).

Figure 3.2.4 (A-F): Live/ dead immunocytochemistry of cell colonisation characteristics of the different polymers after 8 days incubation in osteogenic media and viewed under confocal microscopy. (A) $P_{DL}LA$ mwt 26 kDa, showing scanty cell survival along 'fissures' (arrow), (B) $P_{DL}LA$ mwt 126 kDa, displaying near confluence of cells (arrows), (C) $P_{DL}LGA$ mwt 35 kDa, showing limited cell colony survival, (D) $P_{DL}LGA$ mwt 110 kDa, displaying diffuse cell viability (E) PCL mwt 14 kDa, showing limited individual cell survival with some 'dead' or compromised cells (arrows) and (F) PCL mwt 85 kDa showing diffuse cell viability. NB inset images are controls (no SSC seeding) of same polymer (scale bar = 100µm).

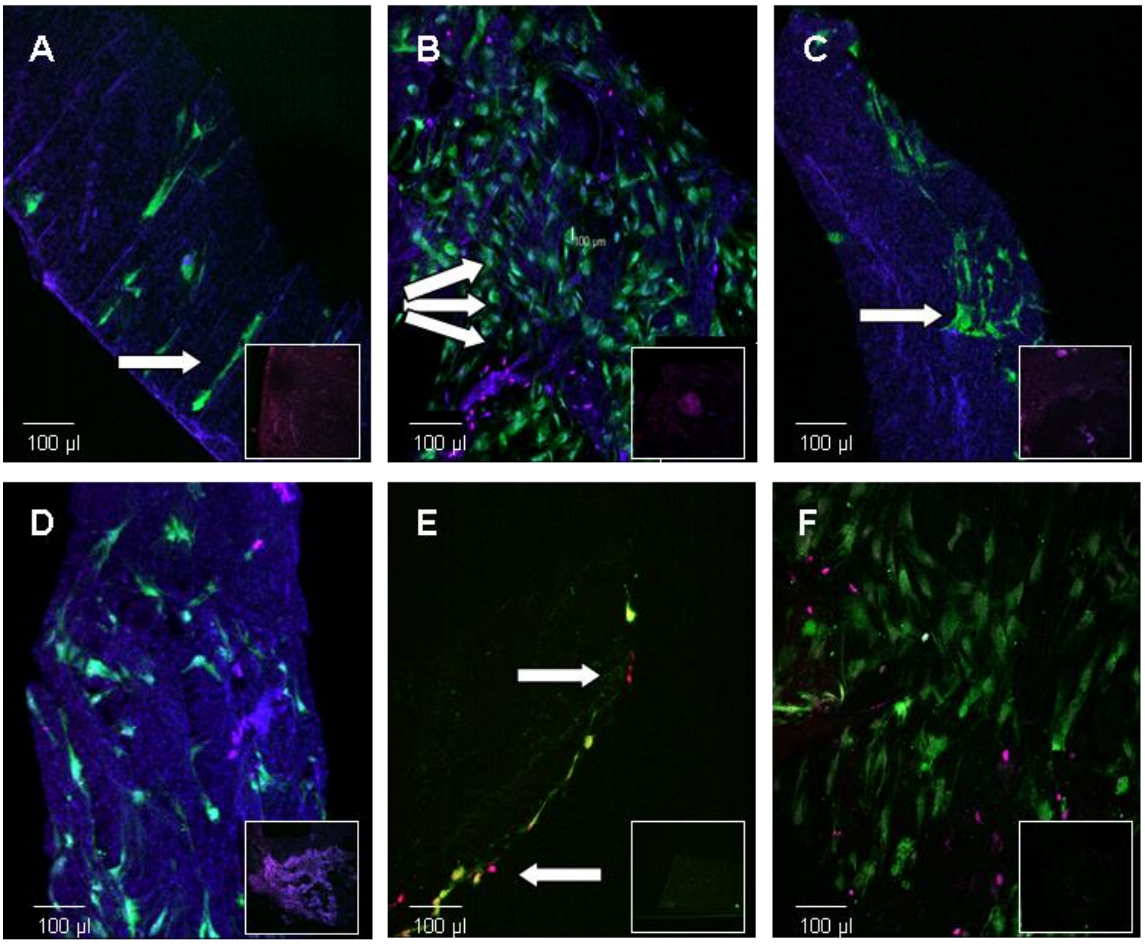

Upon further microscopic examination, those cells which had survived on $P_{DL}LA$ mwt 26 kDa (Figure 3.2.4 A) appeared to have aligned and grown along 'microfissures' on the surface of the polymer.

3.2.5.3.2 Assessment of cell number and proliferation

The WST-1 assay was used as a measure of surviving cell number and proliferative activity. Figure 3.2.5 shows the results of the assay for the 3 impacted discs of each polymer type and allograft, at the 2, 4 and 6 hour time points after the 8 day incubation period with SSCs. A significant increase in optical density (OD) indicated additional cellular activity for $P_{DL}LA$ mwt 126 kDa compared to the allograft at all time points (2hrs: OD + 0.346, $p < 0.01$, 4hrs: OD + 0.742, $p < 0.01$, 6hrs: OD + 1.060, $p < 0.01$). There was a modest increase in optical density achieved from SSCs grown on $P_{DL}LGA$ mwt 110 kDa, and these reached significance at the 2, 4 and 6 hour time points (2 hrs OD + 0.097, $p < 0.01$, 4hrs: OD + 0.282, $p < 0.01$, 6hrs OD + 0.371, $p < 0.01$). There were also modest increases in cellular activity at all time points for SSCs cultured on high molecular weight PCL which were also significant (2hrs OD + 0.124, $p < 0.01$, 4 hrs OD + 0.230, $p < 0.01$, 6hrs OD + 0.213, $p < 0.01$). The magnitude of mean cellular activity on each of the different polymers as shown by the WST-1 assay, was consistent with the visual findings of cell viability via confocal microscopy. The largest drop in cellular activity was between the high and low molecular weight versions of PLA. This may partly be explained by differences in surface topography (discussed later) or may be because the low molecular weight allows rapid breakdown of the scaffold to its cell toxic (lactic acid) by products.

Figure 3.2.5: WST-1 assay at 2, 4 and 6 hours for the allograft and 6 polymers seeded with M66 cells (minus controls) and incubated for 8 days (n = 3 ± SD, * Mann–Whitney U test vs allograft control $p < 0.01$).

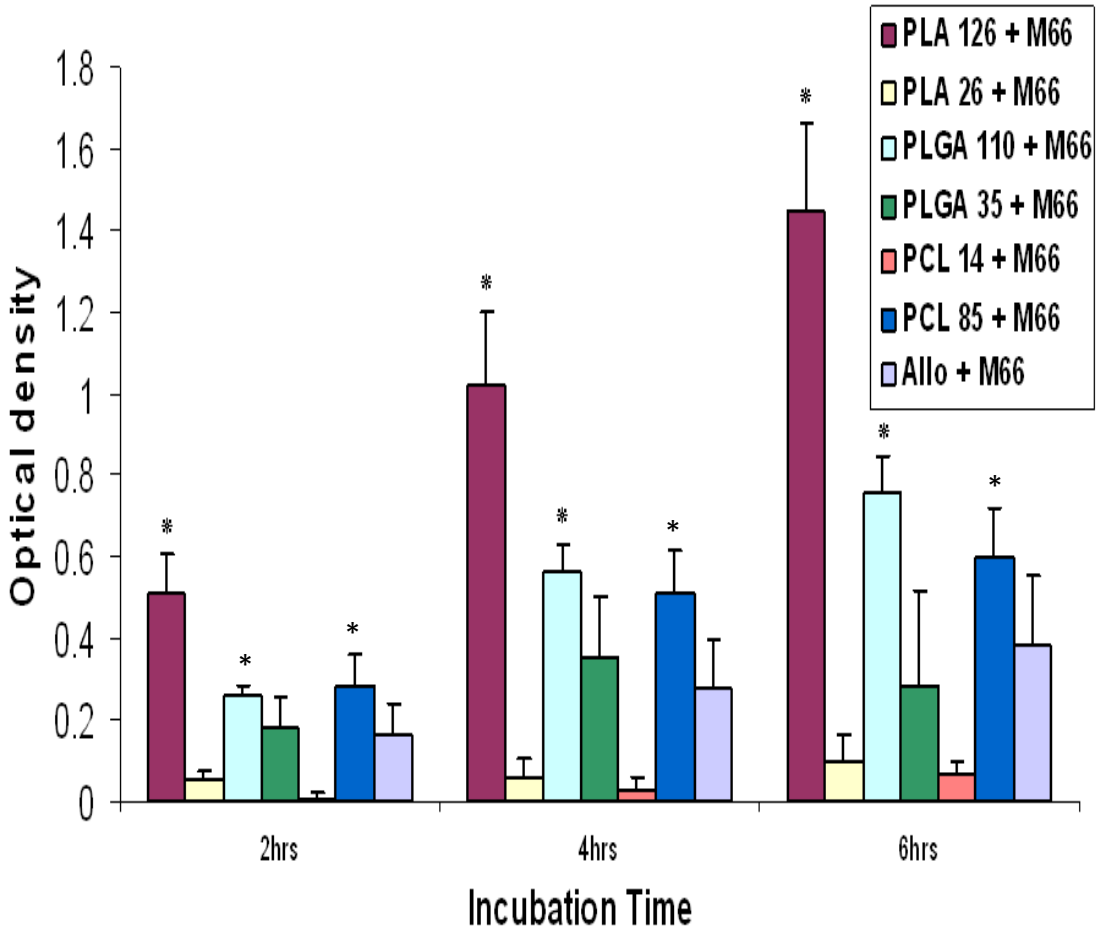

3.2.5.4 Scanning electron microscopy

Figure 3.2.6 shows typical scanning electron micrographs of the six polymers after they had been through the milling process at x200 (inset x50) magnification. There was a dramatic difference in surface texture and roughness between polymer types, and also between polymers of the same type but differing molecular weight. Thus a smooth surface was observed on $P_{DL}LA$ mwt 26 kDa and PCL mwt 14 kDa (Figure 3.2.6 A+E) in contrast to the rough and uneven surfaces of $P_{DL}LA$ mwt 126 kDa and $P_{DL}LGA$ mwt 110 kDa (Figure 3.2.6 B+D).

Figure 3.2.6 (A-F): Scanning electron micrograph images of the 6 polymers under x200 magnification (x50 inset image). (A) $P_{DL}LA$ mwt 26 kDa displaying a smooth surface with intermittent fissures (arrow), (B) $P_{DL}LA$ mwt 126 kDa displaying a surface with multiple irregularities (arrows), (C) $P_{DL}LGA$ mwt 35 kDa is fairly smooth, (D) $P_{DL}LGA$ mwt 110 kDa, displaying a rough surface (E) PCL mwt 14 kDa is even and angulated (F) PCL mwt 85 kDa displaying a course topography.

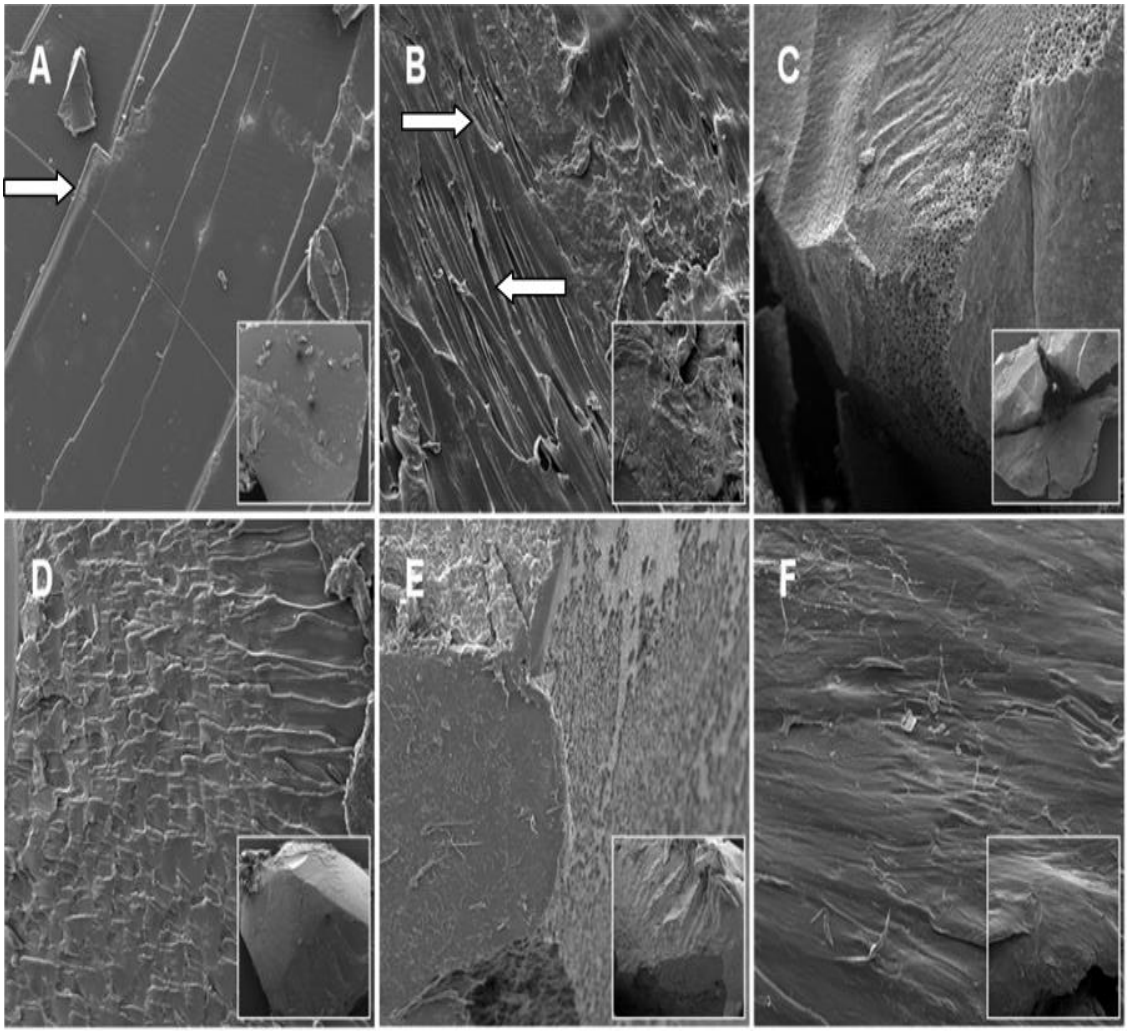

For visual comparison, a scanning electron micrograph image is shown in Figure 3.2.7. The surface area is more irregular than the surface of any of the polymers, and the porosity of the structure is clearly evident.

Figure 3.2.7: Scanning electron micrograph images of trabecular bone, demonstrating the highly porous nature. Image from http://www.ectsoc.org/gallery/ (last accessed 3/2/14).

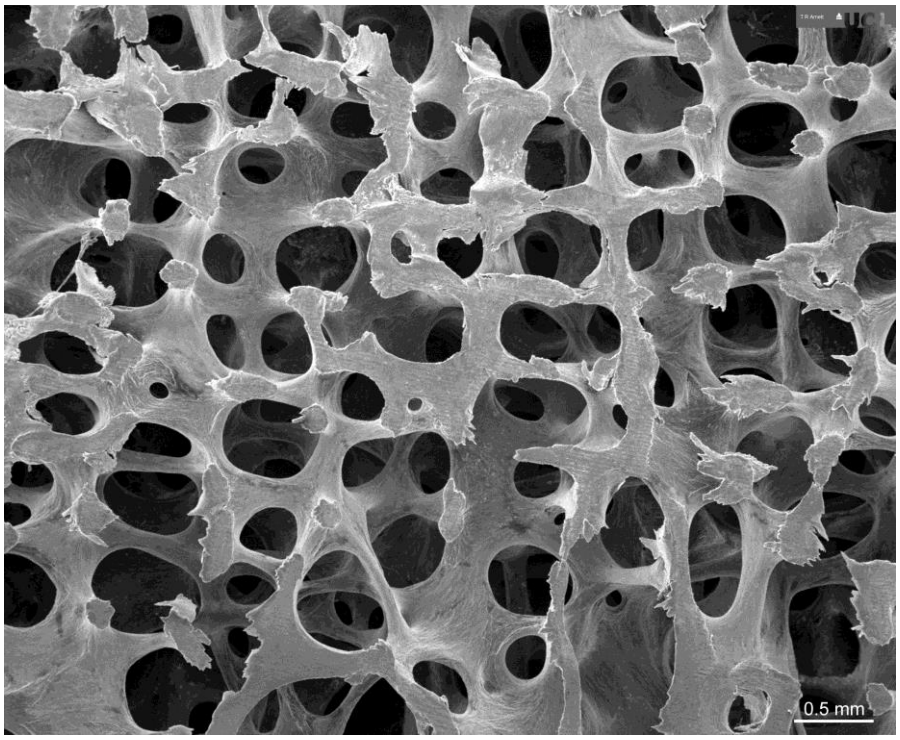

3.2.6 Discussion

Most research into alternatives to allograft for use in impaction bone grafting has centred around ceramics acting as structural bone graft extenders (Blom *et al*. 2002;Blom *et al*. 2009;McNamara *et al*. 2010). This study analysed biodegradable materials as potential substitutes not only from a mechanical point of view, but also for biocompatibility with SSC's, such that the graft could eventually fulfil the paradigm of being osteoconductive, osteoinductive and osteogenic.

Even though allograft has good mechanical strength under shear in the test rig, this study demonstrated that 4 of the polymers under test performed better from a mechanical point of view (PLGA mwt 110, PLGA mwt 35, PLA mwt 126 and PLA mwt 26), and hence would make good candidates for subsequent structural alternatives. These polymers are thus comparable to substances such as ceramics, for use in IBG.

Van hareen performed a cadaveric femoral impaction study again using a mixture of hydroxyapatite and tricalcium phosphate in comparison to allograft alone (van Haaren *et al.* 2005). However, while finding superior initial mechanical stability of the ceramic they also found increased risk of producing a fissure in the femur during the impaction procedure. Conversely, Oakley *et al*. found that pure allograft bone particles had significantly higher cohesion than when mixed with porous particles of hydroxappetite/ tricalcium phosphate extender (Oakley and Kuiper 2006). The authors however also found that the difference was alleviated by addition of clotted blood, which significantly increased the cohesion of both pure bone and mixes with pure bone and porous graft extender (and is consistent with a clinical scenario).

While all of the above studies present structural alternatives to allograft, and utilise materials with both osteoconductive and osteoinductive properties, none attempt to make the additional step to produce a composite graft with osteogenic capability.

Limited research has explored the effects of the addition of SSC's to the allograft, in an attempt to solve this problem. Bolland *et al*. performed an *in vitro* investigation, combining allograft with SSC's, showing that the cells not only survive the impaction process, but also lead to enhanced mechanical properties of the graft. Murine studies went on to show enhanced neovascularisation of the allograft indicating the ability for sustained cell survival and *de novo* bone regeneration (Bolland *et al.* 2006). Korda *et al.* also showed *in vitro* cell survival during the impaction process, going on to show increased bone formation in an ovine impaction bone graft model using SSC seeded allograft (Korda *et al.* 2006). These observations have found clinical use in the treatment of a series of patients with early femoral head osteonecrosis (Tilley *et al.* 2006). Allograft seeded with a concentrated stromal stem cell fraction of autologous bone marrow was impacted into the avascular segment of the femoral head. Early clinical results to date are encouraging, with most patients reporting improvement in up to two years follow-up, but one patient did progress to bilateral total hip replacement. Although the procedure was not successful in this patient, analysis of the retrieved specimens showed neo-bone formation in much of the cystic area, and hence gives valuable insight into the potential for SSC enhancement of allograft (Aarvold *et al*. 2013). These skeletal cell based strategies auger well for future orthopaedic use but do not dispel the need for allograft in revision hip surgery. Many studies have explored the

combination of biodegradable polymers with SSCs as potential bony regenerative strategies for use in various clinical situations, but only limited published reports use the impaction bone graft model (Bolland *et al.* 2008b). This situation differs in that the substitute graft must be in a milled form for ease of handling when used clinically, must have the ability to withstand impaction, and the resulting impacted structure must be able to withstand shear forces. The current study has taken a spectrum of possible biodegradable polymer substitutes, and compared them not only for mechanical characteristics in there milled form but also for cellular compatibility. It has also compared the high and low molecular weight versions of each polymer, and found considerable differences in both of these tested qualities. Two techniques were used to assess cell growth and viability after 8 days incubation. Confocal microscopy increases optical resolution and contrast of a micrograph and enables the reconstruction of three-dimensional structures from the obtained images (Cremer and Cremer 1978). As the specimens being viewed in these circumstances were three dimensional, it was important to view them using a technique such as this, to allow insight into growth patterns and to allow entire visual fields to be viewed in focus rather than only small areas. Furthermore, it meant that the polymers did not require extensive processing prior to visualisation, which could lead to loss of, and reduced quality of the cells, as well as changes to the morphology of the polymer. The use of CellTracker^{TM} green and Ethidium Homodimer is a well-established technique for staining live (CTG) and compromised (EH-1) cells, and in combination with confocal microscopy this has allowed visual comparison of the ability of the each polymer to support cell growth (Gantenbein-Ritter *et al.* 2011). There is a virtually confluent cell layer present on the PLA mwt 126 kDa, numerous cells present on the PLGA mwt 110 kDa and PCL mwt 85 kDa, but only patchy cell growth present on the other polymers and the allograft. Even though these are representative images, it is not, however, an accurate quantative method for assessing actual cell numbers and viability.

The WST-1 reagent provides tetrazolium salts that are cleaved to formazan by cellular mitochondrial dehydrogenases, resulting in a colour change. An expansion in the number of viable cells results in an increase in the overall enzyme activity, and hence colour change correlates to the number of metabolically active cells in the culture (Mosmann 1983). This study found significantly more cellular activity in PLA mwt 126 kDa at all time points and PLGA mwt 110 kDa at both 4 and 6 hours. The mean cellular

activity of the PLA mwt 126 kDa and PLGA mwt 110 kDa was over 5 and 3 times consecutively that of the allograft treated in the same way, and these findings are consistent with other studies examining polymer biocompatibility (Bolland *et al*. 2008b;Khan *et al*. 2010;Whang *et al*. 1999). The SEM images of the polymers after they have been milled may go some way towards explaining these findings. As can be seen there was a dramatic difference in surface textures between both polymer types, and also between polymers of the same type but differing molecular weight, ranging from very smooth eg PLA mwt 26 kDa and PCL mwt 14 kDa, to rough and uneven eg PLA mwt 126 kDa and PLGA mwt 110 kDa. This current study therefore suggests a correlation between surface roughness and cellular compatibility, with enhanced adhesion and proliferation on the uneven surfaces. The confocal image of the $P_{DL}LA$ mwt 26 kDa showed few cells, but those that were present appeared to be growing along 'microfissures', which further substantiates this concept. One explanation could be that the cells were caught by or adhered better to the uneven surface during the seeding process, and were further stimulated to proliferate by both the texture (more closely simulating that of real bone) as well as the close proximity of other cells allowing cellular signalling to occur. This was in keeping with other studies, where surface characteristics, functionalisation (eg with bioactive molecules such as collagen) and polymer type have been extensively investigated, and all shown to modulate cell adhesion, proliferation and eventual differentiation (Agrawal and Ray 2001;Hubbell 2003;Marois *et al*. 1999;Milleret *et al*. 2011;Miot *et al*. 2005).

3.2.7 Conclusion

The results in the context of the null hypothesis were examined:

No polymer under test has the cellular compatibility or mechanical characteristics for consideration as an alternative to allograft in IBG.

This null hypothesis is **false.**

The work presented in this chapter details a systematic analysis of the high and low molecular weight versions of three different biodegradable polymers as potential osteogenic composite grafts for use as alternatives to allograft in impaction bone grafting. Both the high and low mwt versions of $P_{DL}LA$ and $P_{DL}LGA$ performed better

than allograft during mechanical testing, and the high mwt versions of $P_{DL}LA$, $P_{DL}LGA$ and PCL displayed enhanced SSC compatibility. Thus the combined enhanced mechanical and biocompatible properties of high mwt $P_{DL}LA$ and $P_{DL}LGA$ indicate these polymers as strong candidates for further evaluation. Development of these biomaterials offers important potential alternatives to allograft for the treatment or replacement of lost or damaged bone stock. Therefore, the following chapters will detail research into production techniques of these particular polymers, along with the addition of bioactive materials to further optimise them as potential living composite alternatives to allograft for clinical application.

Chapter 4

Does increasing polymer porosity via a novel supercritical CO_2 production technique improve the characteristics for use as an alternative to allograft in impaction bone grafting?

I am grateful to Dr Sherif Fahmy and Mr Matthew Purcell (University of Nottingham) for kindly providing the scaffolds under test, to Dr Adam Briscoe (Bioengineering Science Research Group), for assistance with the mechanical testing and the Mohr-Coulomb equation calculations, to Dr David Johnston for assistance with confocal microscopy and SEM (Biomedical Imaging) and to Dr Mark Mavrogordato (μVIS) for assistance with the μCT scans and analysis.

The work detailed in this chapter has been published:

Tayton E, Purcell M, Aarvold A, Smith JO, Kalra S, Briscoe A, Shakesheff K, Howdle SM, Dunlop DG, Oreffo RO.

Supercritical CO2 fluid-foaming of polymers to increase porosity: a method to improve the mechanical and biocompatibility characteristics for use as a potential alternative to allografts in impaction bone grafting?

Acta Biomaterialia, 2012, 8(5):1918-27

4.1 Introduction

The *in vitro* analysis demonstrated in the second part of Chapter three, showed that the milled forms of high molecular weight $P_{DL}LA$ and high molecular weight $P_{DL}LGA$ provided both superior mechanical shear characteristics (the mode of acetabular component loosening and stem subsidence in IBG) to the allograft controls, as well as supporting cell adhesion, survival and proliferation following an extensive impaction process. These two polymers thus appeared to be the best candidates from an initial array of six polymers to take forward as potential living composite allograft alternatives for use in IBG. However, work with the polymers demonstrated that despite performing well in the *in vitro* tests, there were clearly areas where improvements could be achieved prior to *in vivo* testing. The milled forms of the polymers were observed to be granular, thus distinct from allograft in terms of handling characteristics (important if these compounds are to make clinical use), and even though SSC adherence and proliferation was supported, few indicators of osteoblastic differentiation of the cells were observed after the eight day incubation period.

The effects of varying porosity of bioactive materials has recently gained much interest, especially in terms of bone regenerative strategies, due to their mechanical strength being similar to that of bone, evidence that porosity can have beneficial effects in terms of SSC differentiation potential, and the fact that porosity allows bone ingrowth (as well as vascularisation) from adjacent bone structures (Karageorgiou and Kaplan 2005). Based on early studies the minimum requirement for pore size is considered to be ~ 100 μm due to cell size, migration requirements and transport. However, pores of > 400 μm now are recommended, due to enhanced new bone formation and the formation of capillaries (Feng *et al.* 2011).

Much work has surrounded the production processes of biodegradable polymers for use not only in the field of tissue engineering, but also for multiple other medical applications such as drug delivery systems or suture material (Langer 1983;Pillai and Sharma 2010). There are also multiple methods of achieving a structurally viable, three dimensional, porous biodegradable polymer, the main ones include solvent casting / particulate leaching, freeze drying, thermally induced phase separation, solid freeform fabrication and supercritical CO_2 foaming.

4.1.1 Solvent casting / particulate leaching

This process involves the dissolution of a polymer in a solvent to create a solution which is then mixed with water-soluble particles such as salt (Liao *et al.* 2002). This mixture is then cast in a mould and the solvent removed via a vacuum or freeze drying. Water can then be used to leach the particles from the structure creating a porous structure. The pore size can be controlled by varying the size of the particles used, and porosity can be controlled by variation of both the size and / or amount of salt particles used. Downsides to this process include the use of organic solvent and the difficulty in removing particles from inside the structure (Liao *et al.* 2002;Seebach *et al.* 2010).

4.1.2 Freeze drying

This method involves dissolving the polymer in a solvent, followed by the addition of a second immiscible liquid (Hou *et al*. 2003). This mixture is stirred to form an emulsion, which is then poured into moulds of the desired shape, and cooled in liquid nitrogen. These are then freeze dried to remove both the solvent and the immiscible liquid, leaving a porous (up to 95%) polymer with small pores measuring between 13-15 μm. The small pore sizes and use of solvents limit the application of this technique to create scaffolds for tissue engineering applications.

4.1.3 Thermally induced phase separation

For thermally induced phase separation a polymer is dissolved in a solvent with a low melting temperature (Nam and Park 1999). The solution is then fast cooled, which takes the solution from a homogeneous single-phase region into its spinodal region (the spinodal is the limit of stability of a solution, denoting the boundary of absolute instability of a solution to decomposition into multiple phases). The stability of the solution thus breaks down, which results in polymer rich and polymer poor regions and when the solvent is removed interconnected porous structures are obtained. The presence of solvent limits biocompatibility of scaffolds produced by this method.

4.1.4 Solid freeform fabrication

Novel techniques such as 3D printing, stereolithography, selective laser sintering, electron beam melting and extrusion-based systems allow 3D scaffolds to be built up in

layers (Rezwan *et al.* 2006;Puppi *et al.* 2010). CAD software is used to design the 3D model that is produced through the layering process. The advantages of scaffolds produced this way lie in extremely good reproducibility (Rezwan *et al.* 2006) and control of porosity and structure. However, high temperatures, and organic solvents may be required in processing.

All of the above techniques have significant limitations when it comes to their potential use in tissue engineering. Significantly, the use of solvents or high temperatures required for the production processes, have the potential to damage any combined or additional factors (eg growth factors / bioactive molecules) which may be designed to enhance the scaffolds function.

4.1.5 Supercritical CO_2 foaming

This technique of processing polymers does not require the use of organic solvents or excessive heating, thereby offering advantages over many of the above processing methods (Davies *et al.* 2008).

A supercritical fluid is any substance at a temperature and pressure above its critical point, where distinct liquid and gas phases do not exist. A polymer is placed into a high pressure rig and exposed to CO_2 in its supercritical phase. After a period of time the polymer becomes saturated with the fluid, which plasticises the polymer, reducing the glass transition temperature, T_g. As operating pressure is lowered to below the critical value for CO_2, areas of CO_2 gas nucleate and grow within the polymer forming pores; additionally, as CO_2 leaves the polymer the plasticising effect reduces and the T_g rises. When the T_g of the polymer rises above the processing temperature the porous polymer structure sets. The rate of growth and structure of the pores formed within various polymers can be controlled through varying operating conditions such as temperature, venting time, operating pressure and work is reported in literature demonstrating the control capable in $P_{DL}LA$ and $P_{DL}LGA$ scaffolds (Tai *et al.* 2007).

This process thus seems appealing, offering a simple technique to combine biodegradeable polymers with heat labile, or delicate growth factors and bioactive molecules, for potentially enhanced activity as tissue engineered scaffolds.

4.2 Aim

The purpose of this study was to test whether the production of porous high molecular weight $P_{DL}LA$ and $P_{DL}LGA$ scaffolds via supercritical CO_2 foaming improved their characteristics over the standard non-porous versions for translational use as living composite alternatives to allograft in IBG.

4.3 Null Hypothesis

The use of supercritical CO_2 foaming to produce porous high molecular weight $P_{DL}LA$ and $P_{DL}LGA$ confers no mechanical or biological compatibility advantage over their non-porous counterparts for use as living composite alternatives to allograft in IBG.

4.4 Materials and Methods

4.4.1 Polymer production

The polymers under test were kindly provided by Dr Sheriff Fahmy and Mr Matthew Purcell (University of Nottingham). The polymer scaffolds were produced in two ways. $P_{DL}LA$, molecular weight 126 kDa and $P_{DL}LGA$, molecular weight 110 kDa, were obtained from SurModics Biomaterials (Birmingham, USA) in powder form. The traditional form polymer scaffolds were melt processed into solid blocks as described in chapter three. For the production of the porous scaffolds 300 mg of the powder was placed into individual cylindrical wells (11.2 mm x 10.4 mm) in a custom made PTFE mould (University of Nottingham, School of Chemistry) and placed into a 60 ml stainless steel autoclave. The autoclave was clamp sealed, heated to 35°C, filled with CO_2, and the pressure increased to 23 MPa over a period of 20 minutes. The pressure was held for 60 minutes, and then reduced over a period of 30 minutes back to ambient conditions; heating then ceased and the mould was removed from the autoclave. All polymers were then milled using a standard bone mill (Tessier Osseous Microtome, Stryker Leibinger, Freiberg, Germany), sterilised in 5x antibiotic / antimycotic solution (Sigma, Aldrich, UK), placed under U.V. light for 24 hours and finally submerged in basal media for a further 24 hours prior to use.

4.4.2 Allograft preparation

For mechanical testing, standard allograft was used as a control against which each polymer could be compared and was obtained from fresh frozen femoral heads stored at -80°C. These were de-fatted, milled and sterilised as described in Section 2.3. Polymers then underwent U.V. light exposure for 24 hours, were re-washed in phosphate buffered saline and then submerged in basal media for 24 hours prior to use.

4.4.3 Characterisation

4.4.3.1 Scanning Electron Microscopy (SEM)

SEM was used to illustrate the polymers structure at the microscopic level and to examine surface characteristics such that differences in cell compatibilities of each polymer could be explained. In brief, small samples of milled polymer were taken, stub mounted and gold sputter coated in a low vacuum environment. Polymers were then viewed under a scanning electron microscope at x50 and x200 magnification (FEI Quanta 200 Scanning Electron Microscope, FEI, Oregan, USA).

4.4.3.2 Micro Computed Tomography (µCT)

Scaffolds produced via supercritical CO_2 dissolution were analysed by micro x-ray computed tomography (microCT) (Skyscan 1174, Skyscan, Kontich, Belgium) prior to the milling process. Scaffolds were mounted on a holder and placed in the scanner. The stage was set at a height of 6.5 mm and the scaffolds were scanned with the following settings: 40 kV voltage, 800 µm current and 12.0 voxel resolution. Image reconstruction was performed using NRecon (Skyscan) and saved as 8 bit bitmaps (BMP). Analysis of the reconstructed images was performed using CTAn (Skyscan) to obtain porosity values, mean pore size and surface to volume ratios.

4.4.4 Mechanical testing

4.4.4.1 Impaction procedure

The usual mode of failure for allograft in an IBG scenario is via shear. The same test as described in Sections 2.5-2.7 and 3.2.4.4 was therefore used to test the shear strength of

the milled and impacted polymers compared to allograft controls. In brief, the allograft / polymer was placed into the central chamber in the acrylic discs, receiving 24 impactions at a rate of approximately 1 Hz, and this process was repeated three times to fill the chamber, ensuring that an even and consistent volume of impacted material was achieved. The discs were then removed from the impaction device, a perforated lid and base applied, and the discs were then incubated at 37 ºC, 5% CO_2 in 30 ml of phosphate buffered saline (PBS) for one week in order to replicate early *in vivo* conditions. A total of twelve impactions (n = 12) for each polymer type and the allograft were performed.

4.4.4.2 Shear testing

After the incubation period the impacted allograft/ polymer was carefully removed from the disc as a single unit, and placed into a custom built cam shear testing rig (Southampton University Engineering Department) as described by Bolland and colleagues, and fitted into an Instron testing machine (Instron, High Wickham, UK)(see Section 2.7) (Bolland *et al.* 2006).

Each of the impacted discs was then subjected to a constant shear strain of 1.2 mm/min whilst under a compressive stress. The stresses used were 100 kPa, 300 kPa and 500 kPa, and four discs from each group of twelve were subjected to each. From this data, shear strength and interparticulate cohesion were calculated for the allograft and each polymer using the Mohr Coulomb failure equation at 10% strain (standard engineering practice). The results were annotated using a Mohr Coulomb failure envelope curve with regression analysis trendlines.

4.4.4.3 Maintenance of impacted morphology

An important aspect of polymer suitability when considering clinical translation for an IBG scenario, is the ability of the milled polymer to maintain the shape into which it is impacted. This is especially important when rebuilding the proximal femur (a medulla needs to be maintained to allow prosthesis insertion) or filling large acetabular defects. An analogy can be drawn to the difference between building a sandcastle with wet or dry sand. In order to assess the polymers ability to maintain its impacted morphology, a novel test was devised. Utilising the impaction device and protocol described previously, four discs of each milled polymer type were created. The impacted polymer

was then carefully removed from the acrylic rings so as not to disturb the shape, and placed onto a flat non-slip platform upon an agitation device (Stovall Life Science, Greensboro, NC, USA). This was then turned on such that the platform was oscillated at an orbital rate of 100 rpm for 1 minute. At the end of the time period the discs were measured for both maximum height and maximum diameter, and the mean (and standard deviations) for each polymer type calculated. A loss of height or increase in diameter corresponded to an inability of the milled polymer to maintain its impacted morphology.

4.4.5 Cellular compatibility analysis

4.4.5.2 Cell culture

As the purpose of this study was to make a direct comparison between different scaffolds, in order to minimise any difference that may have been observed due to different cell population characteristics, all experiments were again performed using the same patient cell population obtained from a male patient undergoing a routine total hip replacement surgery with the approval of the local hospital ethics committee (LREC 194/99/w, 27/10/10). These had been previously selected due to their proliferation potential, culture expanded and frozen down into vials as described in Sections 3.1.7-10.

For each test, a cryo-vial of the cells (P1) were reanimated by allowing the cells to thaw, adding 10ml basal media, centrifuging at 1100rpm for 4 minutes, pouring off the supernatant and re-suspending in basal media prior to seeding in tissue culture flasks and culturing as described previously. Upon confluence the cells were released using trypsin in EDTA, centrifuged and resuspended in basal media and the total count using a haemocytometer determined. Appropriate dilution with basal media was then given such that the concentration was 5×10^5 cells / ml.

4.4.5.3 Polymer cell seeding

Approximately 20 ml of each polymer type was used in the cellular compatibility tests. To allow cell adhesion to the scaffold 20 ml of the cell suspension (5×10^5 cells/ml) was added to each in a sterile universal tube, and the mixture placed in an incubator (37ºC,

5% CO_2) for two hours, with gentle agitation every thirty minutes. Thus each scaffold was incubated with the same cell line, of the same passage, at the same concentration, for the same time period. The solution was then aspirated and discarded. Plain un-seeded polymers were used as negative controls.

4.4.5.4 Impaction of seeded polymers

In order to recreate the conditions that the seeded scaffolds would have to undergo *in vivo* during the IBG process, a similar, but scaled down impaction process was carried out, as described previously in Sections 2.5 and 3.2.3.6.3. Under strictly aseptic conditions 1ml of seeded polymer was loaded into an impaction chamber (modified SEM pot) in three equal portions, receiving 24 impactions after the addition of each portion (72 impactions in total). The procedure was repeated 9 times for each polymer (with an additional 6 controls), and the impaction chambers were then placed individually into each well of a non-tissue culture plastic 6 well plate, cultured under osteogenic conditions (basal media + 100 μM ascorbate-2-phosphate, and 10 nM dexamethasone) and incubated at 37ºC in 5% CO_2 for 14 days, with PBS washes every 3-4 days.

4.4.5.5 Cell viability

Cell Tracker Green (CTG) and Ethidium Homodimer-1 (EH-1) were used to stain viable and necrotic cells respectively (live/ dead stain). Following 2 weeks incubation the contents of two of the impaction chambers from each group were removed and incubated for 90 minutes in 5 ml of standard CTG/ EH-1 solution (10 μg/ml CTG, 5 μg/ml EH-1). They were then fixed in ethanol and stored in PBS prior to imaging under confocal microscopy (Leica SP5 Laser Scanning Confocal Microscope and software, Leica Microsystems, Wetzlar, Germany). The procedure was repeated with the contents of one of the impaction chambers of the un-seeded scaffolds as controls.

A further experiment was run in parallel whereby SSCs (M66) were seeded onto un-milled porous scaffolds and incubated for 14 days. The cells were subjected to the same live/ dead staining process, and were then carefully sectioned using a scalpel such that an *internal* surface was exposed. Any live cells thus present on the cut surface must have penetrated the scaffold via the pores (either flowed in during the seeding process

or grown in from proliferation of surface cells). Micrographs were taken of both the outer and sectioned surfaces viewed under fluorescent light through a standard FITC filter on an Axiovert 200 inverted microscope using an AxioCam HR digital camera and Carl Zeiss Axiovision software Ver 3.0 (Carl Zeiss Ltd, Hertfordshire, UK).

4.4.5.6 Cell proliferation assay

In order to quantify cell proliferation and cell viability a WST-1 assay was performed. The contents of three impaction chambers from each group (and one control) were submerged in 2.5 ml of 1:10 dilution WST-1 substrate (Roche ltd, Welwyn Garden City, UK). At 2 and 4 hours, 400 µl of substrate was removed and read in triplicate via a Bio-Tek KC4 microplate fluorescent reader (Bio-Tek, USA) at 410 nm. An increase in absorbance value (i.e. increase in optical density of the substrate) indicated increased cell number and viability. Mean and standard deviation values were then calculated for each polymer at each time point, the mean control values at each time point subtracted, and the resultant optical densities compared to each other using a Mann–Whitney U test.

4.4.6 Osteoblastic differentiation

4.4.6.1 Alkaline phosphatase (ALP) activity assay

ALP activity was used as a measure of osteoblastic differentiation amongst the cell population present on the scaffolds after the 2 week incubation period. The contents of three of the impaction chambers of each scaffold (and one control) were removed, washed in PBS, and then fixed in 90% ethanol prior to being allowed to air dry. They were then rewashed in PBS, and subsequently suspended in 2 ml of 0.5% Triton X-100. Samples were subjected to x3 freeze thaw cycles with vigorous agitation between each freeze. Lysate was measured for ALP activity using p-nitrophenyl phosphate as substrate in 2-amino-2-methyl-1-propanol alkaline buffer solution (Sigma, Poole, UK) according to routine manufacturer protocol. Ten microlitres of lysate was run in triplicate for the three impacted cell seeded samples and single control sample of each scaffold on a plate against two standards, read in triplicate on an ELx 800 and FLx-800 microplate fluorescent reader (Bio-Tek, USA) and mean and standard deviations calculated. The mean control values were subtracted, the mean ALP activity of cells on

each scaffold type calculated via comparison with an ALP standard curve (expressed as nanomoles of p-nitrophenyl phosphate/hr).

4.4.6.2 Type-1 Collagen immunostain

Osteoblastic cells produce matrix which contains type-1 collagen. The final impacted scaffolds were removed from impaction chambers, washed in PBS and fixed for 24 hours in 4 % paraformaldehyde. The scaffolds were then transferred to PBS prior to immunostaining. This involved ten minutes incubation in 1 % bovine serum albumin (BSA) followed by overnight incubation in 1 ml of LF68 (whole rabbit serum) type-1 collagen antibody (1:300 dilution with PBS/BSA), followed by three washes in 0.1% PBS Tween^{R} (polysorbate). Secondary anti-rabbit antibody (alexafluor^{R} 594) was then added for one hour at room temperature, followed again by three 0.1% PBS Tween washes. Finally, cytox blue (1:100 dilution, 10 minute incubation) was added as a nuclear counter stain. To ensure specificity of the secondary antibody a portion of the samples were treated as detailed above, but the primary antibody was not added (negative controls).

The samples were stored in PBS in the dark until imaged under confocal microscopy (Leica SP5 Laser Scanning Confocal Microscope and software, Leica Microsystems, Wetzlar, Germany).

4.4.7 Statistical analysis

For the mechanical shear failure analysis comparisons were made between the polymers and the allograft using grouped linear regression analysis (n=4, GraphPad Prism, San Diego, California, USA).

For the cohesion analysis, comparisons were made between the standard and supercritical CO_2 produced polymers using a Mann–Whitney U test (n = 4).

For all of the described assays, comparisons were made between the standard and supercritical CO_2 produced polymers using a Mann–Whitney U test (n = 9).

4.5 Results

4.5.1 Characterisation

Figure 4.1 shows representative SEM images of the milled polymers at x50 (inset) and x200 (main) magnification. As can be seen, the surfaces of the $P_{DL}LA$ and $P_{DL}LGA$ (Figures 4.1A and B) were rough, but non porous. In contrast, the milled surfaces of the $P_{DL}LA$ and $P_{DL}LGA$ scaffolds produced via the supercritical CO_2 dissolution method (Figures 4.1C and D) consisted of irregular pores, ranging between 100-300 µm in diameter. This is similar in size to the pores in trabecular bone which relate to Haversian canals (approximately 100 µm), although those that relate to the lacunae are much smaller (< 10 µm) (Wang *et al.* 2003).

Figure 4.1: SEM images of polymers under test at x200 (main) and x50 (inset) magnification to demonstrate differences in surface textures between (A) traditional 'solid block' $P_{DL}LA$ (B) traditional 'solid block' $P_{DL}LGA$ (C) $P_{DL}LA$ produced via supercritical CO_2 fluid foaming (D) $P_{DL}LGA$ produced via supercritical CO_2 fluid foaming.

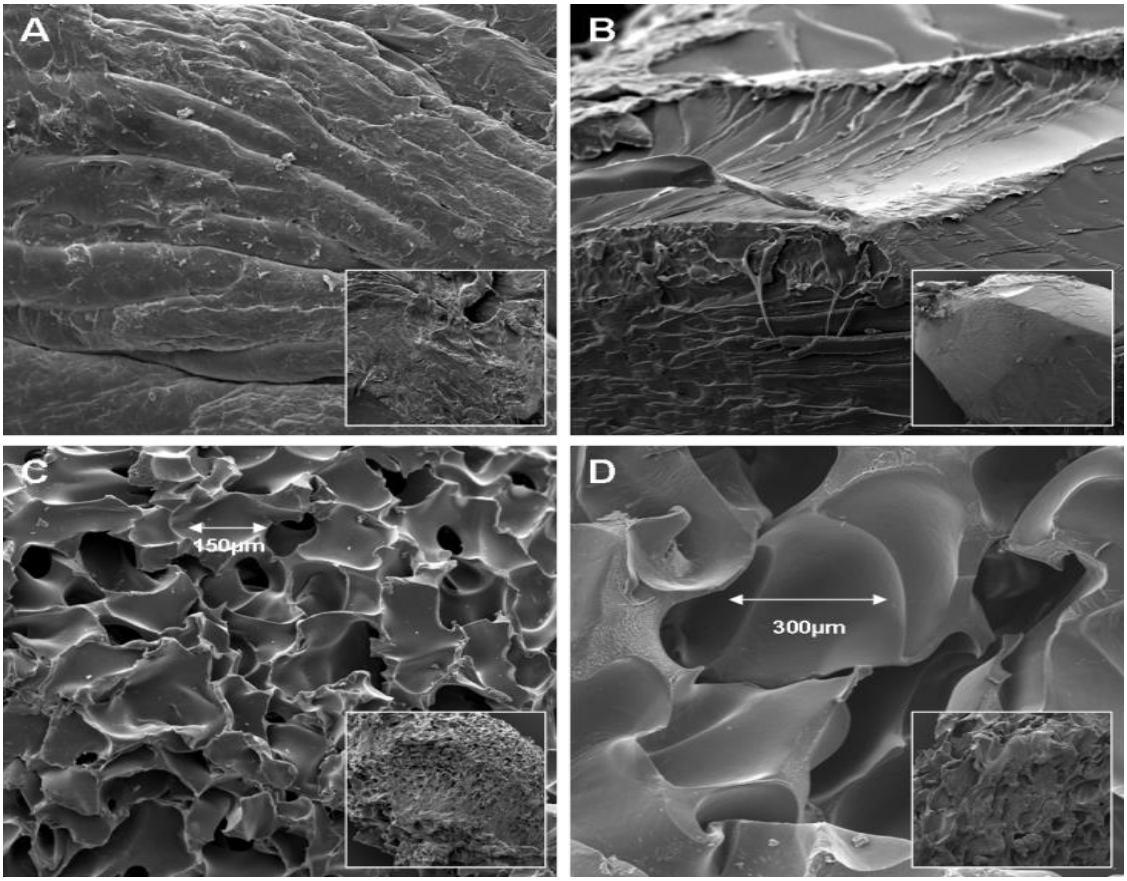

Micro CT imaging confirmed the findings (Figure 4.2), and subsequent analysis gave mean total porosity values of 58.7 % ± 0.59 % for P_{DL}LA 126 kDa and 45.5 % ± 0.56 % for P_{DL}LGA 110 kDa. Mean pore size was 155 µm ± 52 µm for P_{DL}LA, and 267 µm ± 194 µm for P_{DL}LGA, and surface to volume ratio was 0.065 ± 0.00017 for P_{DL}LA, and 0.0596 ± 0.0044 P_{DL}LGA. N.B. Total porosity involves both connected and unconnected porosity. Connected porosity is more easily measured through the volume of gas or liquid that can flow into a scaffold, whereas fluids cannot access unconnected pores.

Figure 4.2: Axial microCT images prior to milling, demonstrating porosity of (A) P_{DL}LA and (B) P_{DL}LGA, produced via supercritical CO_2 fluid foaming.

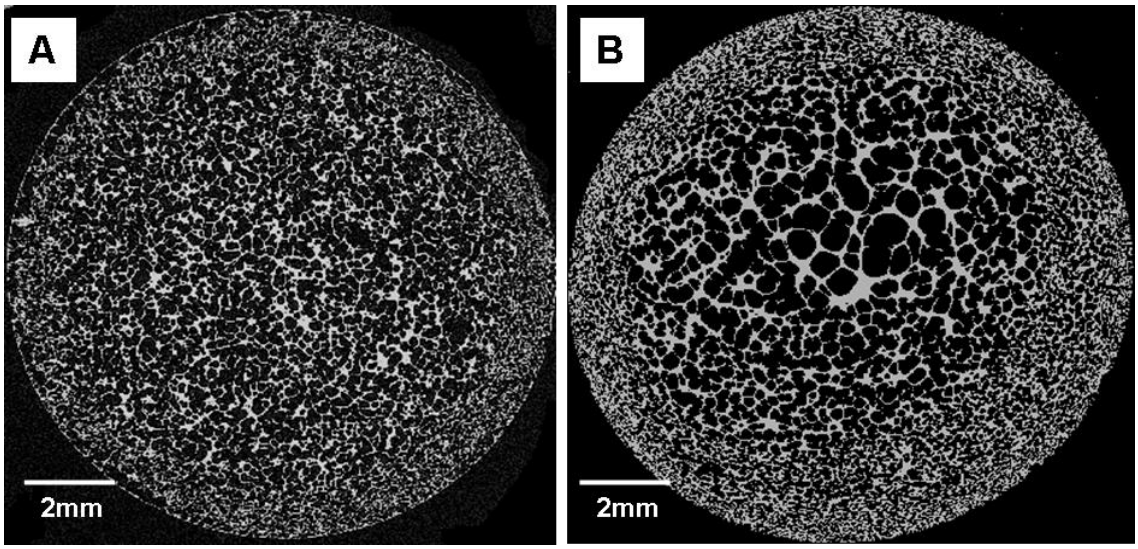

4.5.2 Mechanical analysis

Figure 4.3 shows the resultant Mohr Coulomb failure envelope curves following milling and impaction of all four polymers and the allograft controls for comparison. All four polymers displayed increased shear strength at the 3 compressive stresses tested over the allograft controls.

Table 4.1 shows the interparticulate cohesion (along with 95% confidence intervals) for all polymers and the allograft control, calculated from the same data set, and also provides the significance (linear regression analysis) of the difference of the Mohr Coulomb failure envelope curve of each polymer compared to the allograft controls. This was highly significant ($P \leq 0.001$) in all cases.

Figure 4.3: Mohr Coulomb failure envelopes for polymers under test and allograft controls, showing regression analysis trend lines and SD error bars. (n=4)

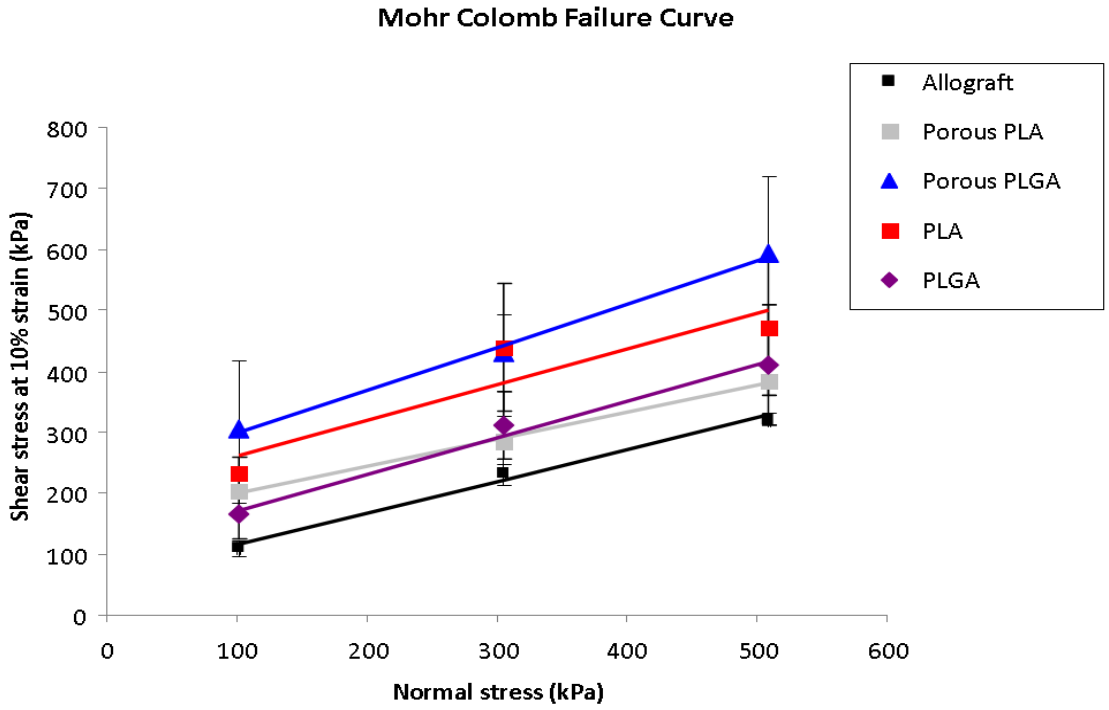

Table 4.1: Showing R^2 values and interparticulate cohesion calculated from the shear test data, as well as the results of the grouped linear regression analysis comparing the Mohr Coulomb failure envelopes of each polymer to the allograft controls.

Test substance	*R^2 value for linear regression curve*	*Interparticulate cohesion (kPa) (95% confidence interval)*	*Statistical significance (Grouped linear regression analysis)*
Allograft	0.99	62.5 (38.3-86.7)	N/A
P_{DL}LA 126	0.85	201.3 (72.7-330.0)	$p < 0.0001$
P_{DL}LGA 110	0.99	111.6 (21.3-201.9)	$p < 0.005$
Porous P_{DL}LA 126	0.99	155.1 (117.8-192.4)	$p < 0.0001$
Porous P_{DL}LGA 110	0.99	228.5 (123.5-333.5)	$p < 0.0001$

There was a significant drop in interparticulate cohesion between the porous and non porous versions of the PLGA, and although this difference was much less for the PLA polymers, the trend was reversed (ie higher interparticulate cohesion in the non porous polymer). This may be due to the differences in pore size and percentage porosity of the different polymer types after the foaming process, or may be purely a material difference. All polymers, however, out performed allograft in this shear test, so could still theoretically be useful as potential alternatives.

Figure 4.4 shows the morphology of the discs before and after agitation, displaying how a loss of maximum height and increase in maximum diameter is an effective method of assessing a change in morphology.

Figure 4.4: Photographs displaying differences in discs before and after agitation: (A) disc from above pre-agitation. Post agitation the disc has significantly changed morphology, measurable from above by (B) an increase in diameter, and sagitally from (C) a loss in height.

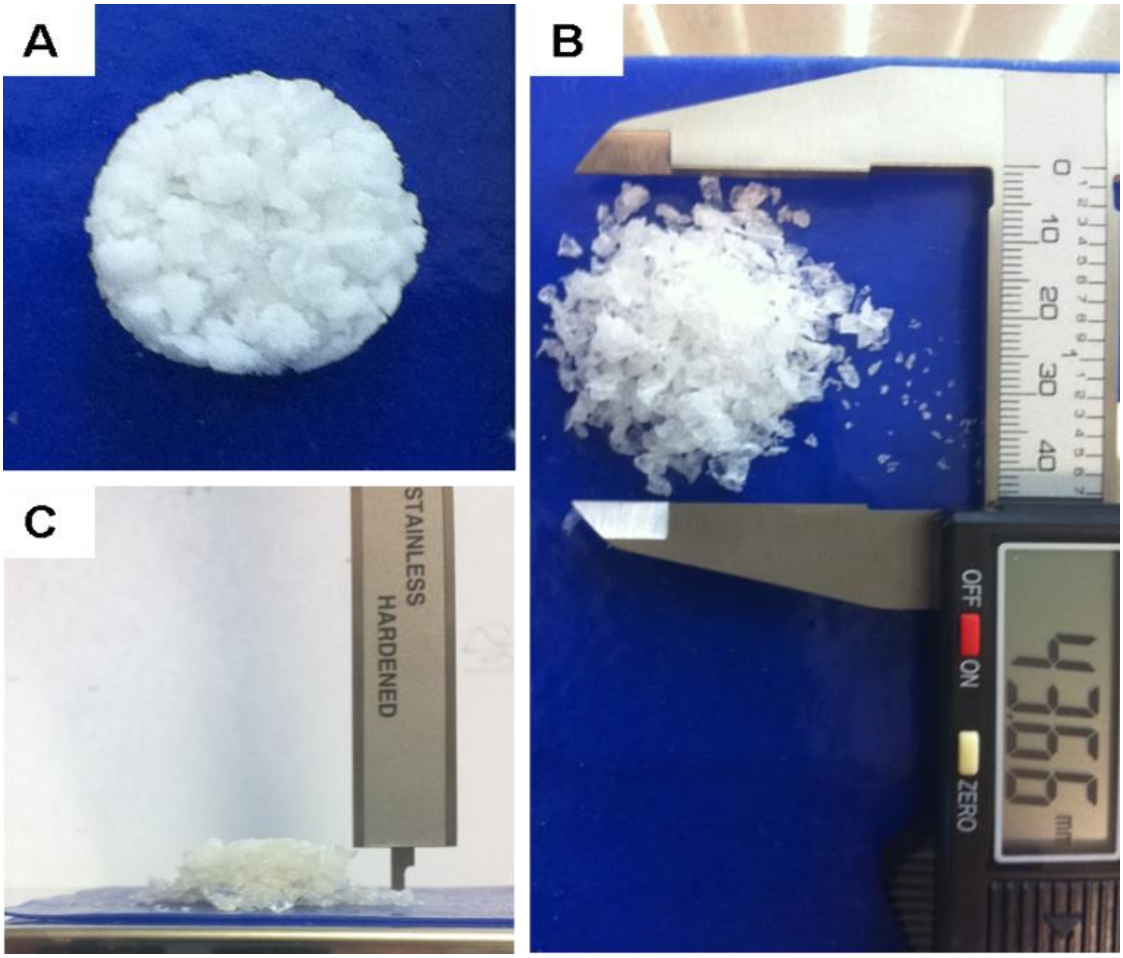

Table 4.2 shows the resultant maximum height and diameter measurements, along with the Mann Whitney analysis of the non-porous compared to the porous versions of each polymer.

Table 4.2: The resultant mean heights and widths of the discs of each polymer after 1 minute agitation, with a Mann–Whitney U test analysis comparing the traditional version of the polymer to the porous version.

	PLA 126	**Porous PLA 126**	**U test**
Mean height (mm) (S.D.)	10.00 (0.71)	11.13 (0.48)	p = 0.09
Mean width (mm) (S.D.)	42.58 (1.67)	28.00 (0.82)	p = 0.03
	PLGA 110	**Porous PLGA 110**	**U test**
Mean height (mm) (S.D.)	8.45 (0.97)	9.26 (0.62)	p = 0.2
Mean width (mm) (S.D.)	49.91 (6.89)	31.63 (2.80)	p = 0.03

There was a significant increase in diameter in the non-porous versions of both the $P_{DL}LA$ and $P_{DL}LGA$ ($p = 0.03$) as well as a loss in height in the non-porous versions of both polymers, indicating that the porosity conferred greater ability to maintain gross impacted morphology.

4.5.3 Cellular compatibility analysis

Figure 4.5 shows representative live/dead confocal images of the polymers under test after seeding, impaction and two weeks incubation in osteogenic media. There was evidence of good growth and survival of (green) cells throughout all specimens, with relatively few dead or compromised (red/purple) cells. Visual inspection showed there is a higher density of cells surviving on the porous polymers compared to the non-

porous versions (A:B and C:D), with virtual confluent cell growth on the porous $P_{DL}LGA$, and confluent cell growth with multilayering on the porous $P_{DL}LA$.

Figure 4.5: Representative live (green cells) / dead (red/purple dots) immunostain of (A) $P_{DL}LA$, (B) porous $P_{DL}LA$, (C) $P_{DL}LGA$ and (D) porous $P_{DL}LGA$ after 2 weeks incubation with SSCs viewed under confocal microscopy (x40). The inset images are corresponding controls (no cells) (scale bar = 200µm).

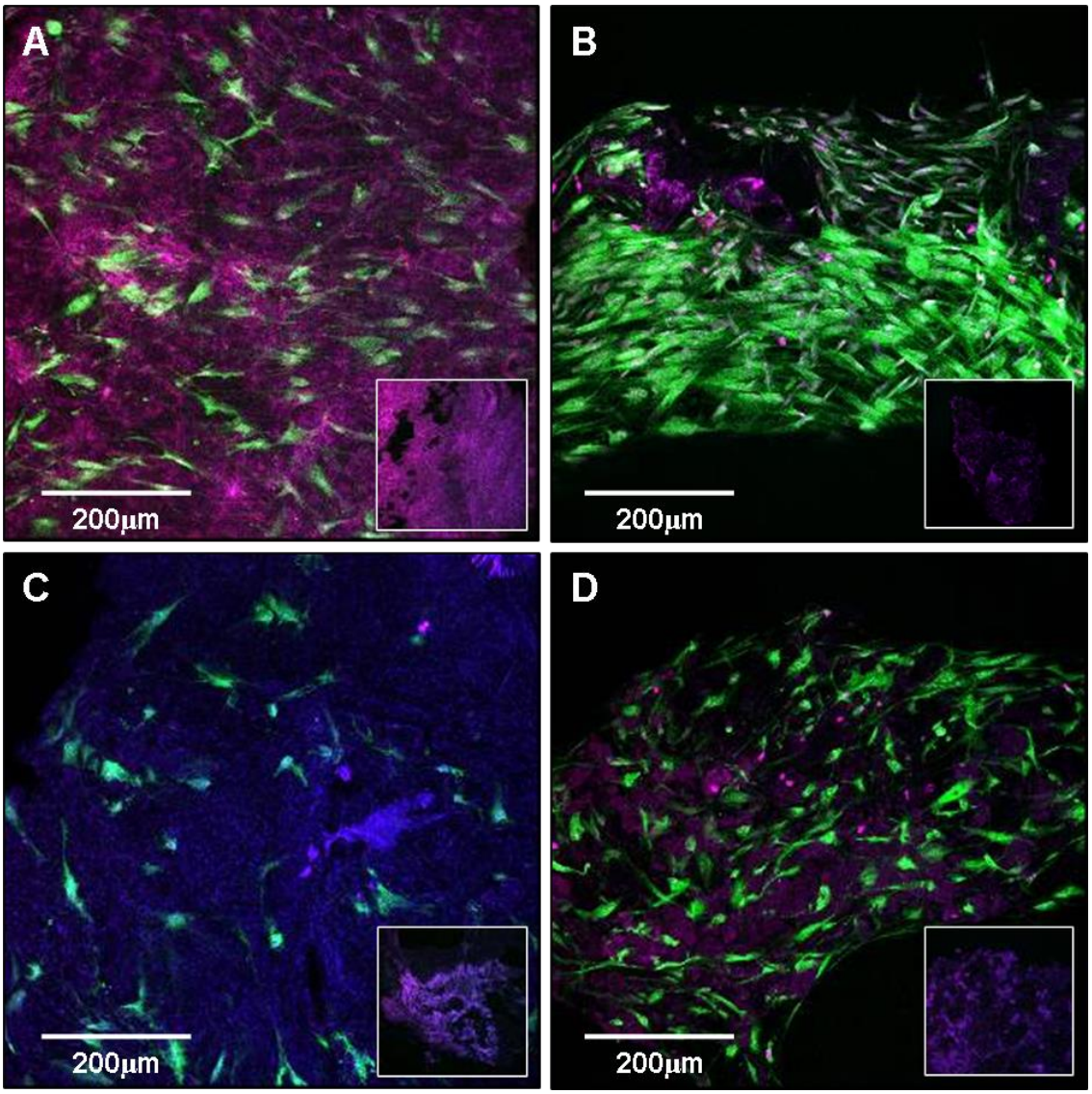

Furthermore, Figure 4.6 shows both the outer and cut surface of both of the porous polymers, demonstrating cell migration and viability within the scaffolds after the 14 day incubation period. These findings were consistent with the results of the WST-1 assay, which provided a quantitative measure of total cell number and viability.

Figure 4.6: Live/ dead stain of scaffolds after 14 days incubation with human SSCs demonstrating cell penetration throughout the scaffold. (A) Outer surface of porous $P_{DL}LA$ and (B) outer surface of porous $P_{DL}LGA$, clearly showing cell growth around and within the *connected* pores. (C) Sectioned surface of porous $P_{DL}LA$ and (D) porous $P_{DL}LGA$ demonstrating that cells have migrated internally throughout the porous structure (arrows).

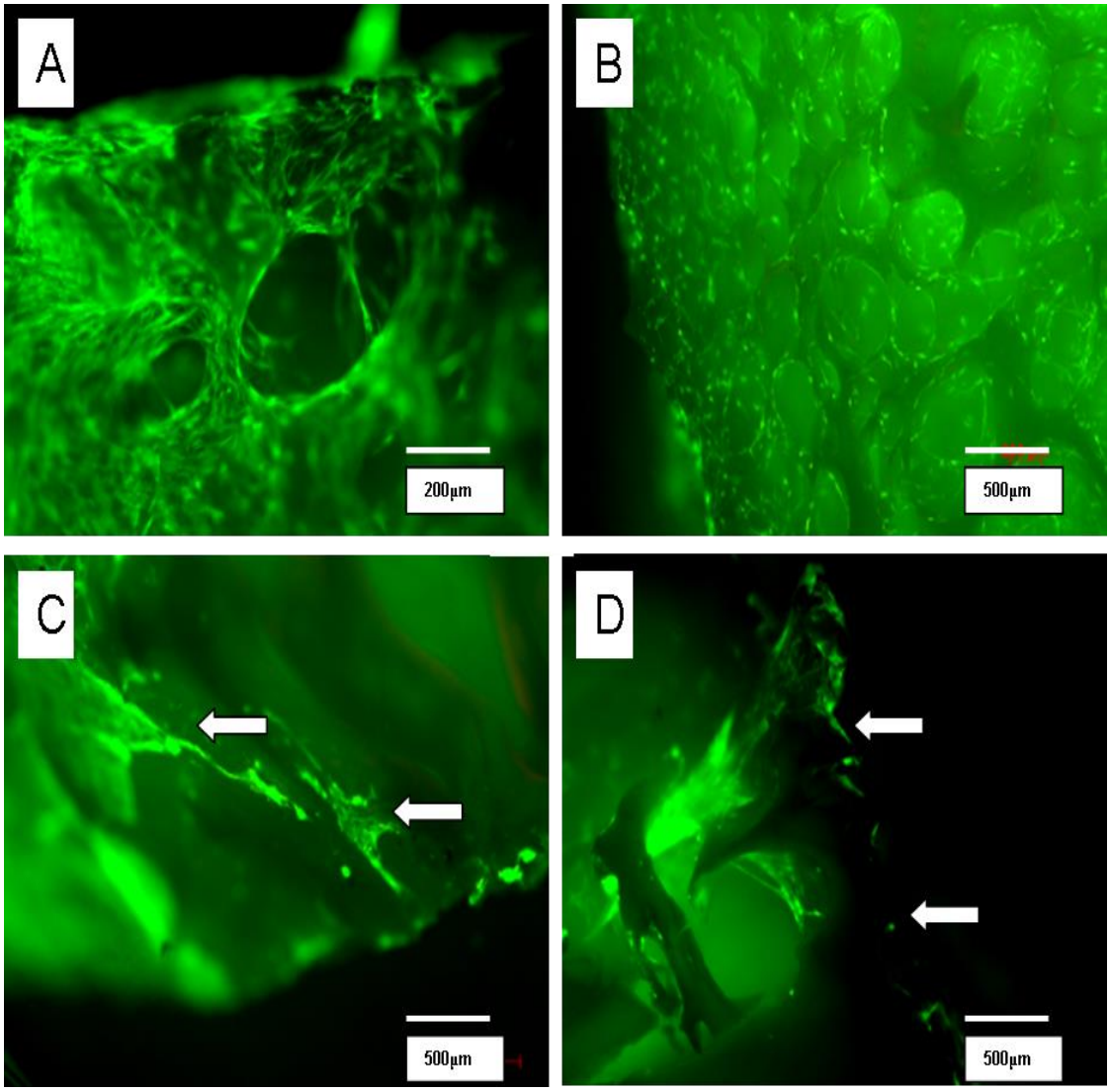

Figure 4.7 displays the results of this assay at both 2 and 4 hours incubation with the WST-1 substrate, and as can be seen there is a significant increase in mean cellular activity between the non-porous and porous $P_{DL}LA$ at both 2 and 4 hours ($p < 0.001$, $p < 0.001$) and also non-porous and porous $P_{DL}LGA$ at both 2 and 4 hours ($p < 0.001$, $p < 0.001$).

Figure 4.7: WST-1 assay showing increase in optical density (and standard deviations) of the cells grown on each of the polymers for 14 days at 2 and 4 hours (n = 3). The significance of the difference in optical density at the 2 and 4 hour time points between the porous and non-porous versions of the polymers is also shown.(* $p < 0.001$)

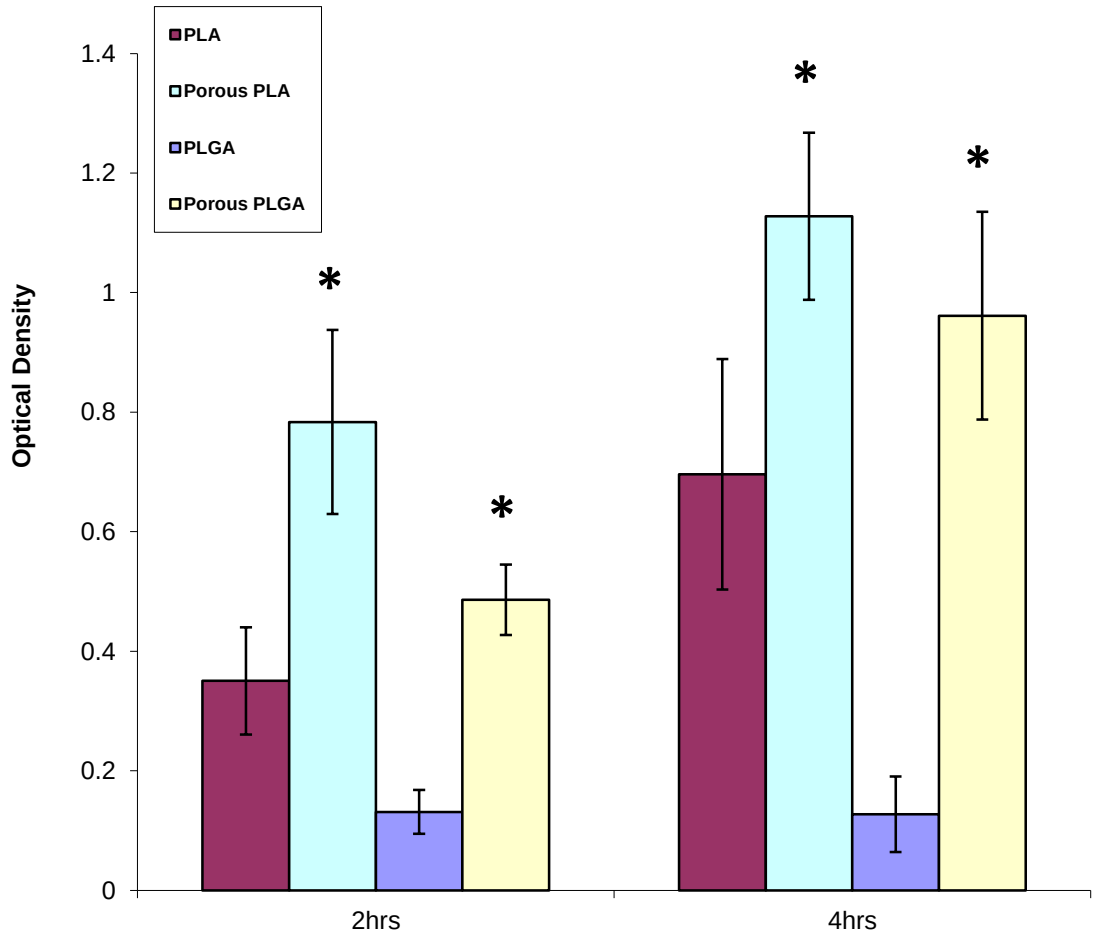

4.5.4 Osteoblastic differentiation

The total ALP activity was used as a measure of osteoblastic differentiation of the cell population on each polymer after the incubation period (Figure 4.8). There was negligible ALP activity from the cells maintained on the non-porous polymers as well as the porous version of $P_{DL}LGA$, but significant ALP activity in the cells grown on the porous $P_{DL}LA$ ($p < 0.001$). It appears as though the summative effect of the porosity in combination with the $P_{DL}LA$ polymer was enough to stimulate the cells to differentiate, but porosity alone was not enough of a stimulus to activate the cells on the more 'inert' $P_{DL}LGA$.

Figure 4.8: Mean ALP activity (+ SD, n = 9) of the cells grown on each of the different polymers after 14 days incubation (* $p < 0.001$).

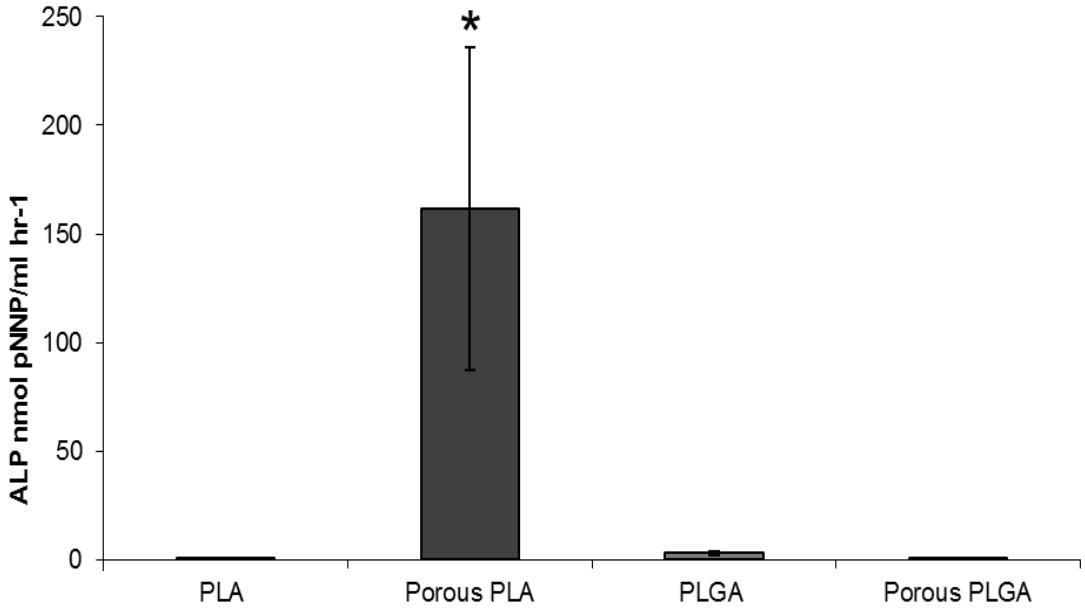

This was consistent with the type-1 collagen immunostaining observed (Figure 4.9), where all samples displayed an abundance of cells as evidenced by the DAPI (green) nuclear stains, but only the porous $P_{DL}LA$ scaffold (Figure 4.9B) stained strongly positive for type-1 collagen (red). There were patches of weak type-1 collagen staining in the other samples, more pronounced in the non-porous $P_{DL}LA$ sample.

Figure 4.9: Type-1 collagen immunostain (Alexa Fluor^{R} 594 (red), with DAPI (green) nuclear counterstain) viewed under confocal microscopy (x80). (A) $P_{DL}LA$, (B) porous $P_{DL}LA$, (C) $P_{DL}LGA$ and (D) porous $P_{DL}LGA$ after 14 days incubation with human SSCs (scale bar = 100µm).

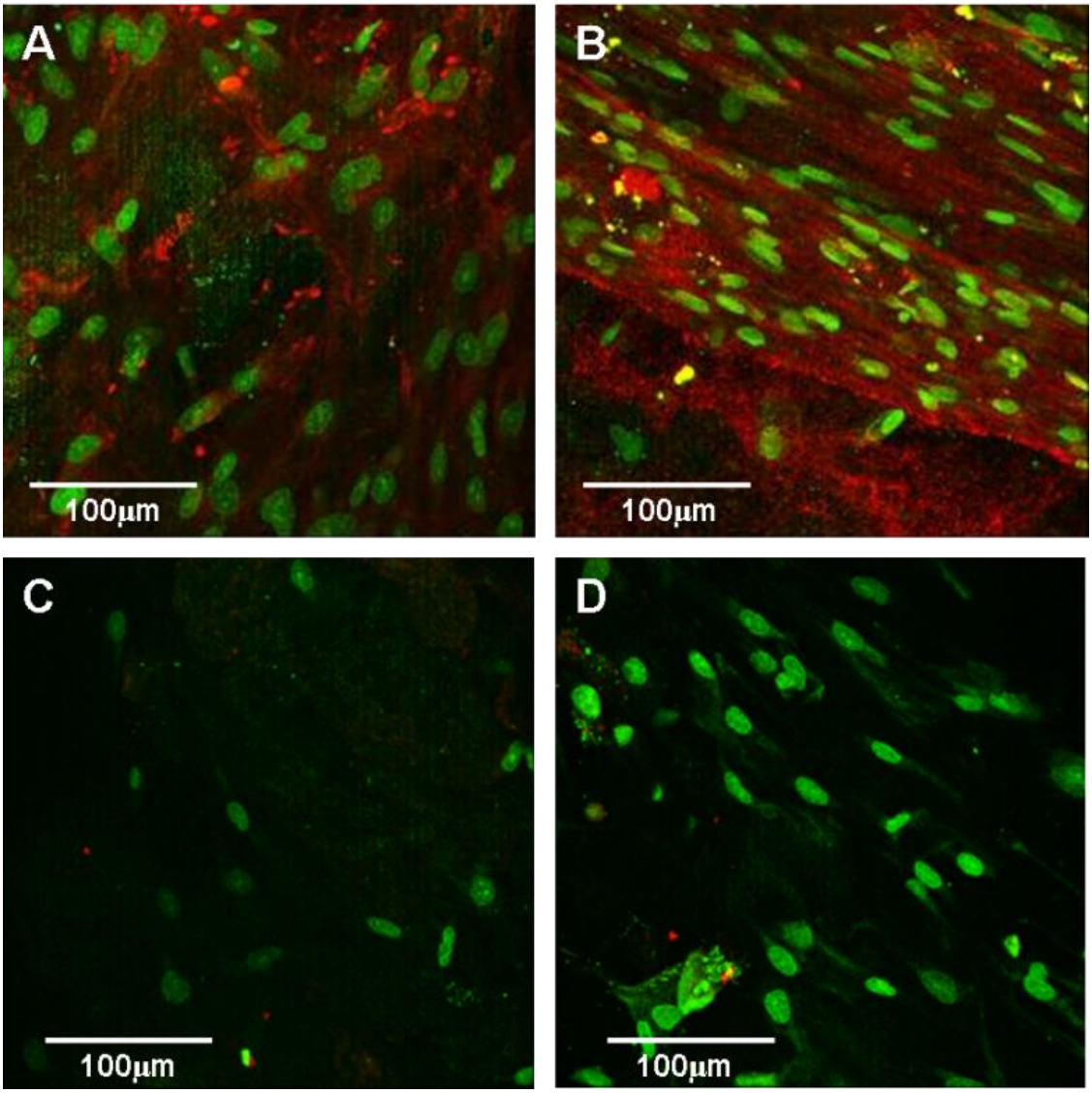

4.6 Discussion

The purpose of this study was to assess whether the production of porous polymer scaffolds via a novel supercritical CO_2 foaming process improved their characteristics over their traditional non-porous alternatives, for potential clinical translation as living composite grafts for use in impaction bone grafting. Both mechanical and biological testing modalities were used to derive a full comparison between the porous and non-porous polymers in areas which are specifically important for success in this field.

Much previous work has surrounded methods of improving allografts' ability to resist shear (the main mechanism of failure in IBG), as well as investigating potential synthetic alternatives, and most studies have used a mechanical shear test consistent with our method (Bolland *et al.* 2006;Bolland *et al.* 2008b;Dunlop *et al.* 2003). This study has shown that both the porous and non-porous versions of the polymers had significantly higher shear strengths after milling and impaction than the 'gold standard' allograft controls currently in clinical use, making these polymers potential candidates for clinical translation. Dunlop *et al.* looked into the effects of washing milled allograft prior to impaction and shearing, using a similar cam shear tester to measure the strength of the construct, concluding that removal of fat and marrow fluid from milled human allograft by washing allows the production of a stronger compacted graft that is more resistant to shear (Dunlop *et al.* 2003). Previous work in our laboratory has also used the same technique of impaction and cam shear testing to prove that the addition of SSCs to allograft increases shear strength of the construct, and that this effect is further enhanced by first functionalising the allograft with hydroxyapatite and collagen (Bolland *et al.* 2006). Bolland and *et al.* also performed initial experiments using the same rig, finding that the shear strength of a milled and impacted $P_{DL}LA$ composite was enhanced by the addition of skeletal SSCs (Bolland *et al.* 2008b). Other synthetic substances have also been trialled as potential alternatives, and found to have superior shear strength to allograft when mechanically tested. Blom *et al.* performed an *in vitro* ovine femoral impaction study to test the strength of impacted mixures of a porous tricalcium phosphate-hydroxyapatite ceramic (BoneSave) in differing volume mixtures with allograft, comparing it against allograft alone (Blom *et al.* 2002). The authors found that BoneSave-allograft mixtures exhibit both much greater mechanical stability and reproducibility than the pure allograft at all tested loads (200-800 N). It was stated in

this study though that BoneSave was always used in combination with allograft for two reasons: i) bone 'additive' allows cohesion and adhesion of the otherwise loose mix which is crucial for surgical handling and reduced fracture risk. This is likely due to a combination of the moisture provided by the biological material as well the increased elastic nature and hence ability to store compressive energy. ii) Biologically the bone adds osteoinductive potential to the otherwise only bioactive and osteoconductive ceramic. Furthermore, allograft is still essential during surgery when using this material, with the associated problems including cost, availability as well as the potential for disease transmission. The first of these issues 'handling', was addressed by the second of our mechanical tests, which assessed the ability of the impacted polymers to maintain their morphology despite agitation. This was a novel test designed to accurately quantify the polymers ability to maintain shape once milled and impacted, such that would be required clinically when recreating the femoral cortex, but maintaining the medullar into which a prosthesis will be inserted. Our results indicated the porous polymers had a significantly enhanced ability to maintain their impacted shape, making them superior to the non-porous versions when considering future potential clinical use. This is possibly due to the porosity making the milled surface of the polymer more irregular (Figure 4.1) allowing a physical interlock between the particles, as well as permitting plastic deformation of the milled particles to occur more easily, hence enhancing this effect. This aspect of translational research when considering IBG has, to our knowledge, only been investigated in one other study. Oakley *et al.* used a similar technique to impact synthetic bone graft extenders alone and in combination with allograft, into discs (Oakley and Kuiper 2006). The authors then used an unconfined compression test to assess the cohesion of the particles making up the disc, finding that although the addition of allograft to the bone graft extender improved the cohesion, the use of bone graft extender alone was not a viable option. This method of assessing the discs cohesion however required the discs to avoid collapse prior to testing (not possible with our non-porous polymers), and did not involve movement, something which is unavoidable during revision hip surgery.

The second of these issues was addressed in the subsequent cell compatibility experiments. We focused on two aspects to investigate for this part of the study, the first to quantify the ability of cells to survive and proliferate on the surface of the polymers,

and the second to assess whether polymer type or porosity could have a potential bearing on subsequent desired (osteoblastic) cell differentiation.

The WST -1 assay is a widely accepted measure of total cell metabolic activity, which is strongly related to total viable cell number (Mosmann 1983). There was a highly significant increase in total cellular activity between both the non-porous and porous $P_{DL}LA$, and the non-porous and porous $P_{DL}LGA$ at both measured time points, strongly indicating increased viable cell numbers present on the porous samples after two weeks incubation. This finding was substantiated by the representative 'live/dead' confocal images, where even though there are a good number of viable (green) cells distributed over the surface of both of the non-porous polymers, the cells are still solitary units and there is little cellular connectivity. In contrast, enhanced cell presence was observed on both of the porous polymers, with multiple colonies and intercellular connections. The porous $P_{DL}LA$ displayed a virtually confluent cell covering with evidence of cell layering, with cut sections demonstrating cell penetration within the scaffolds as well as coating the polymer surface. Thus it would appear that increasing porosity improved the ability of cells to survive and proliferate on both polymers in this impaction bone grafting model. There are a number of possible reasons as to why this is the case. As can be seen from the SEM images (Figure 4.1) the milling of the porous polymer leaves an irregular and roughened surface which potentially improves the ability of cells to adhere during the initial incubation process. This concept has been evaluated in related work, whereby methods of improving cellular attachment to scaffolds have been investigated (Agrawal and Ray 2001;Hubbell 2003;Marois *et al*. 1999;Miot *et al*. 2005;Tillman *et al*. 2006;VandeVondele *et al*. 2003;Woodfield *et al*. 2006). Both surface texture and functionalisation (using materials such as collagen, Arginine-Glycine-Aspartic acid and glycosaminoglycans), appear important to assist and improve cell adhesion via the provision of binding sites as well as directing cellular growth. Furthermore, during the impaction process the pores provide potential 'niches' where cells may accumulate so as to avoid being caught and crushed as individual granules of the polymer are compacted together. This process was quantified by Korda *et al*. who impacted ovine SSCs in allograft using different impaction forces (Korda *et al.* 2006). The authors found that with impaction forces of 3 and 6 kN there was an initial loss of cell viability, but the cell numbers recovered within 8 days; at impaction forces greater than this there was a persistent loss of cell viability over the whole experimental period.

This was substantiated by Bolland and colleagues, who showed both *in vitro* and *in vivo* that SSCs, when seeded on human allograft, were able to survive the impaction process and to continue to proliferate and differentiate along an osteogenic lineage although the authors did not quantify initial cell loss as a result of the impaction procedure (Bolland *et al.* 2006).

Another reason could be that the surface area available for cells to adhere to and proliferate on is far greater on and throughout the individual granules of the porous polymers thus supporting a higher total number of cells (O'Brien *et al.* 2005). This is evidenced via Figure 4.5 showing cell penetration within the cut surface of the scaffold, and has been replicated in multiple other studies (Agrawal and Ray 2001;Marois *et al.* 1999;Miot *et al.* 2005). However, even though Milleret *et al.* found that increasing porosity of their spun fibre scaffolds increased cell penetration, the ability of cells to adhere and proliferate was more dependent on polymer type than porosity (Milleret *et al.* 2011).

The final characteristic under investigation in our study was to assess whether the porosity could have an influence on the differentiation of the SSCs along the desired osteoblastic lineage. The modalities used to investigate this were the total ALP activity of the surviving cell population on the scaffolds and immuno-histochemically via the presence of the early bone extracellular matrix marker, type-1 collagen. We observed a dramatic increase in ALP activity between the non-porous $P_{DL}LA$ and the porous $P_{DL}LA$, although there was neglible activity in both the non-porous $P_{DL}LGA$ and the porous $P_{DL}LGA$. In addition, the porous $P_{DL}LA$ stained strongly positive for type-1 collagen in support of this finding. It would, therefore, appear that the SSCs have been influenced to differentiate along the osteoblastic lineage in these $P_{DL}LA$ samples compared to the non-porous versions, with the porosity therefore adding a further desirable property for use as potential substitute 'living' composite alternatives to allograft. This feature may be because the 3D micro architecture could distribute cellular binding sites in a variety of specific spatial locations rather than on only the single plane of rigid substrate as in traditional 2D architecture of cell culture plastic or the surface of the non-porous polymers (Chang *et al.* 2000). Cells, therefore, may have cytoskeletal adaptor proteins on 3D matrix in addition to proteins present in 2D focal adhesions (Chang *et al.* 2000;Cukierman *et al.* 2002). Such differences in cell adhesion

on the porous and non-porous polymers may therefore lead to different signal transduction and subsequent alteration in cellular rearrangement.

4.7 Conclusion

The results in the context of the null hypotheses were examined:

The use of supercritical CO_2 foaming to produce porous high molecular weight $P_{DL}LA$ and $P_{DL}LGA$ confers no mechanical or biological compatibility advantage over their non-porous counterparts for use as living composite alternatives to allograft in IBG.

This null hypothesis is **false.**

The *in vitro* study described in this chapter has compared the porous and non-porous versions of two polymers that were previously shown to have both the mechanical and cellular compatibility characteristics to be considered for potential clinical use as alternatives to allograft in IBG. Unlike other clinical uses, IBG requires the scaffold to be in a morsellised form, to undergo significant compression during the impaction process, and to maintain its morphology once impacted. These results indicate that whilst maintaining shear strength in excess of the current 'gold standard' (allograft), the porous versions of both polymers showed superior characteristics for potential clinical translation compared to their non-porous counterparts.

The following work will therefore concentrate on further improving scaffold characteristics via the addition of bioactive molecules, and *in vivo* experimentation.

Chapter 5

An in vitro and in vivo study to determine an optimal porous polymer to clinically translate for use as a living composite alternative to morselised allograft in bone regeneration.

I am grateful to Dr Sherif Fahmy and Mr Matthew Purcell (University of Nottingham) for kindly providing the scaffolds under test, to Dr Adam Briscoe (Bioengineering Science Research Group), for assistance with the mechanical testing and the Mohr-Coulomb equation calculations, to Dr David Johnston for assistance with confocal microscopy and SEM (Biomedical Imaging) and to Dr Mark Mavrogordato (μVIS) for assistance with the μCT scans and analysis.

The work detailed in this chapter has been accepted for publication:

Tayton E, Purcell M, Aarvold A, Smith JO, Kalra S, Briscoe A, Shakesheff K, Howdle SM, Dunlop DG, Oreffo RO.

A comparison of polymer and polymer-hydroxyapatite composite tissue engineered scaffolds for use in bone regeneration. An *in vivo* and *in vitro* study.

J Biomed Mater Res A. Accepted for publication Aug 2013.

5.1 Introduction

The work up to this point has concentrated on both the effects of modifying polymer type, and morphology on cell compatibility and osteoinductivity, as well as mechanical characteristics in terms of shear strength and cohesion. Much related research performed in other departments has also surrounded the search for a replacement for allograft for use in bony regenerative procedures, but most products thus far that have become available for clinical use are ceramics, based on the inorganic constituents of bone such as hydroxyapatite and tricalcium phosphate (Beswick and Blom 2011;Hing *et al*. 2006). These are both osteoconductive and osteoinductive, as well as providing good structural support in areas of bone loss (Lin *et al*. 2009;Woodard *et al*. 2007). Porous versions of ceramics have also been produced, and many authors have reported enhanced performance for these materials with increased porosity and interconnectivity (Eggli *et al*. 1988;Holmes *et al*. 1986;Holmes *et al*. 1987). This modification allows greater migration of cells such as macrophages, SSCs, osteoblasts and osteoclasts. In keeping with the beneficial findings described in Chapter 4 when comparing porous polymers to their non- porous counterparts, porous ceramics have shown enhanced cell attachment, proliferation, and differentiation, allowing for osteogenesis and angiogenesis (Kuhne *et al.* 1994;Rubin *et al.* 1994)

However, it can take extended periods of time before ceramics are resorbed, and ceramics do not clinically handle like allograft (Giannoudis *et al*. 2005;Oakley and Kuiper 2006). Ceramics are, therefore, most appropriately used as bone graft extenders meaning the problems of allograft use such as viral transmission, cost, availability and rejection are not dispelled (Blom *et al*. 2009;McNamara *et al*. 2010;Tomford *et al*. 1981a;Tomford *et al*. 1981b).

The use of biodegradable polymers as potential substitutes therefore offers an appealing alternative to ceramics. Situation specific desirable characteristics including structural strength, shape, degradation time, porostiy and cellular compatibility, can all be addressed by polymer choice and production techniques (Hutmacher *et al.* 2007;Kanczler *et al.* 2010). The experiments detailed in Chapter 3 identified high molecular weight poly (DL-lactic) acid ($P_{DL}LA$) and high molecular weight poly (DL-lactic-co-glycolic) acid ($P_{DL}LGA$) as a good contenders for use a tissue engineered living composite alternatives to allograft for use in impaction bone grafting (IBG), due

to their enhanced resistance to shear forces (the most common cause of allograft failure in IBG), and ability to support the survival and proliferation of SSCs (Tayton *et al*. 2012a). Further *in vitro* studies detailed in Chapter 4, showed that a porous version of the same polymers, produced via supercritical CO_2 foaming, enhanced both cellular compatibility as well as stimulating osteoblastic differentiation of the cells, while maintaining superior composite shear characteristics compared to allograft and improving the handling from a clinical perspective (Tayton *et al*. 2012b).

Further benefits of using porous polymers produced via the supercritical CO_2 foaming technique include the fact that it is simple to include bioactive substances, which will be distributed relatively uniformly throughout the structure (Figure 5.1), and the low temperatures required during the foaming process do not denature heat labile components such as growth factors (Davies *et al.* 2008;Kanczler *et al.* 2007). Thus with this technology and with the addition of SSCs, it is potentially possible to produce a three dimensional porous structure, with situation specific characteristics that could fulfil all constituents of the diamond concept for an ideal bone graft substitute (Giannoudis *et al*. 2007).

Figure 5.1: CT scout image of $P_{DL}LA$ + 10 % HA produced via the supercritical CO_2 foaming technique demonstrating good HA distribution (black spots) throughout the polymer scaffold structure.

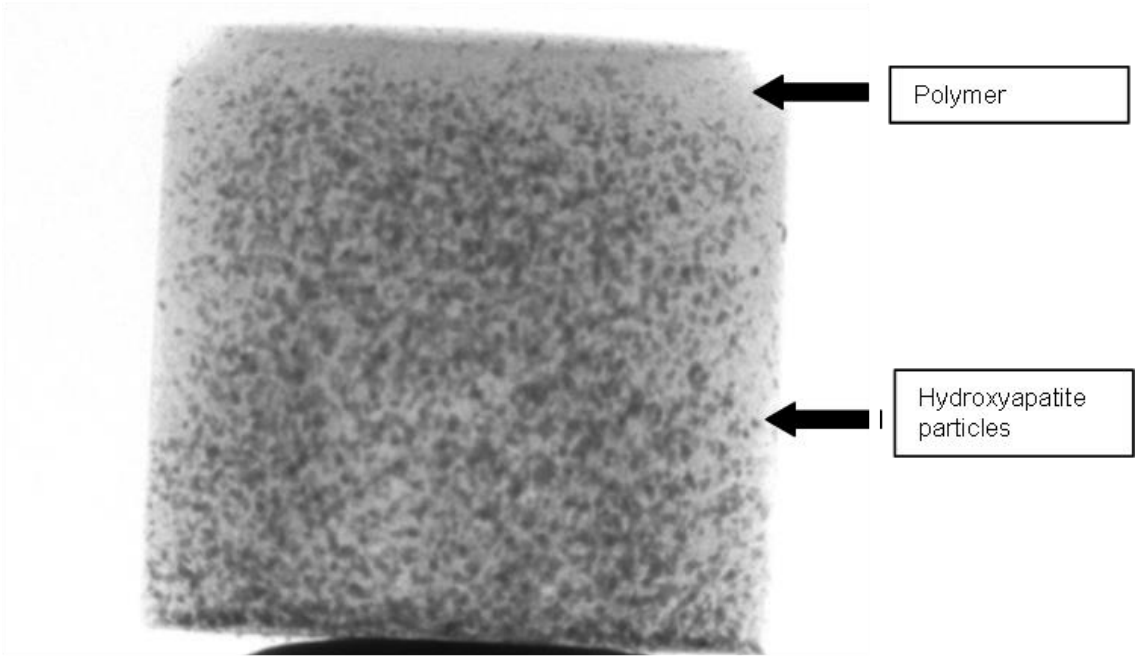

This chapter details an *in vitro* component that compared the previously selected porous polymers with similar samples incorporating a ceramic component (hydroxyapatite (HA)), to assess whether this further enhanced their desirable characteristics for use in IBG. A second stage of the study selected the best two performing polymers and translated them into an *in vivo* (murine) environment, such that a single polymer could be selected for future up scaling and potential clinical translation.

5.2 Aim

To assess the effects of the addition of hydroxyapatite particles to high molecular weight porous $P_{DL}LA$ and high molecular weight porous $P_{DL}LGA$ for use as a potential living composite alternative to allograft in IBG.

5.3 Null hypothesis

The addition of hydroxyapatite particles to high molecular weight porous $P_{DL}LA$ and high molecular weight porous $P_{DL}LGA$ has no effect on the characteristics of these polymers for use in IBG.

5.4 Materials and Methods

5.4.1 Allograft preparation

Allograft was obtained from the femoral heads of patients undergoing primary total hip replacement at Southampton General hospital under approval of the ethics committee (LREC 194/99/w, 27/10/10) (see Section 2.1). Femoral heads were stored frozen at -80°C prior defrosting and then morselisation using a standard bone mill (Tessier Osseous Microtome, Stryker Leibinger, Freiberg, Germany) under sterile condition. Samples were then de-fatted, milled and sterilised as described in Section 2.3. Samples then underwent U.V. light exposure for 24 hours, were re-washed in phosphate buffered saline and then submerged in basal media for 24 hours prior to use.

5.4.2 Polymer manufacture and preparation

The porous scaffolds were produced as described in Section 4.4.1. A 10% combination of hydroxyapatite particles with the polymers was chosen, as concentrations less than this was felt to be too low to have measurable effects in terms of exposure to cells, and a higher concentration may have significantly affected the mechanical characteristics as well as morphology of the porous structure. In brief, polymers ($P_{DL}LA$ molecular weight 126 kDa and $P_{DL}LGA$ molecular weight 110 kDa) were obtained from SurModics Biomaterials (Birmingham, USA) in powder form. Three hundred milligrams of the powder of each polymer was placed into individual cylindrical wells of a custom made mould (University of Nottingham, School of Chemistry) and placed into a stainless steel autoclave. The autoclave was clamp sealed, heated to 35°C then filled with pressurised CO_2 following the protocol described in 4.4.1. For the production of the polymers containing HA, 270 mg of each polymer was placed into each well, with an additional 30 mg HA in order to give a 90 / 10 % polymer / HA composite. The rest of the production process followed the same protocol.

All polymers and composites were then morcellised using the bone mill (Tessier Osseous Microtome, Stryker Leibinger, Freiberg, Germany), submerged in 5x antibiotic/ antimycotic solution (Sigma, Aldrich, UK) and placed under U.V. light for 24 hours, prior to immersion basal media for a further 24 hours prior to use.

5.4.3 Polymer characterisation

The polymers were characterised using micro x-ray computed tomography (Metris Xtek HMX ST 225kV CT scanning system (X-TEK Systems Ltd, Tring, Hertfordshire, UK)) prior to morcellation in order to assess mean porosity and pore size data. Samples were were also assessed via scanning electron microscopy after morcellation in order to visualise the surface available for cell adhesion. Satndard polymer samples were assessed using a FEI Quanta 200 Scanning Electron Microscope (FEI, Oregan, USA) as detailed in 2.14. Samples containing HA were imaged using elemental mapping. Energy dispersive X-ray spectroscopy (EDX) was performed to identify HA particles within the scaffolds. Samples were carbon sputter coated and a Philips FEI XL30 SEM was used for elemental mapping (FEI, Oregan, USA).

5.4.4 Mechanical testing (in vitro)

5.4.4.1 Scaffold impaction

Morcellised chips of allograft and the polymers were impacted into 12 discs as described in Sections 2.5 - 2.7 and 3.2.4.4. In brief, under sterile conditions approximately 10 mls of scaffold was placed into a perspex disc in three equal portions, each undergoing 24 impactions (72 in total) with a standardised hammer and drop weight (designed to transmit forces in the range experienced during an IBG procedure). Samples were then incubated for one week at 37°C and 5% CO_2 in 30mls of isotonic solution (PBS) for one week to mimic early *in vivo* conditions.

5.4.4.2 Shear testing

The impacted allograft/ polymers were carefully removed from the disc as a single unit, Samples were then placed into a custom built cam shear testing rig (Southampton University Engineering Department) and fitted into an Instron testing machine (Instron, High Wickham, UK). Shear testing was performed under three compressive loads (4 discs per load), as described in Section 2.7, allowing the shear strength, interparticulate cohesion and internal friction angle parameters to be calculated for the allograft and each polymer / polymer composite at 10% strain (standard engineering practice) (Bolland *et al.* 2006). The results were annotated using a Mohr Coulomb failure envelope curve with regression analysis trendlines.

5.4.5 Cellular compatibility testing (in vitro)

5.4.5.1 Human bone marrow cell culture

All experiments were again performed using the same patient cell population obtained from a male patient undergoing a routine total hip replacement surgery with the approval of the local hospital ethics committee (LREC 194/99/w, 27/10/10). These had been previously selected due to their proliferation potential, culture expanded and frozen down into vials as described in Sections 3.1.7-10.

For each test, a cryo-vial of the cells (P1) was defrosted and grown to confluence on T150 flasks using the techniques described in Section 2.2.2. Upon confluence the cells were released using trypsin in EDTA, centrifuged and re-suspended in basal media and the total count using a haemocytometer determined. Appropriate dilution with basal media was then given such that the concentration was $5x10^5$ cells / ml.

5.4.5.2 Cell seeding

The scaffolds were seeded using the same technique as described in Section 3.2.4.6.3. Twenty millilitres of the cell solution was added to 20 mls of the morcellised and sterilised polymers in a universal container, and placed into an incubator (37ºC, 5% CO_2) for 2 hours, with gentle agitation every 30 minutes, in order to allow diffuse cell adhesion. The solution was then aspirated and discarded. Thus, each scaffold was incubated with the same cell line, of the same passage, at the same concentration, for the same time period. Plain un-seeded polymers were used as negative controls.

5.4.5.3 Seeded scaffold impaction

After the incubation period the scaffolds underwent a similar impaction process to that described in Section 3.2.3.6.3. One millilitre of morcellised and seeded scaffold was placed into a modified electron microscopy (EM) pot in 3 approximately equal portions, each undergoing 24 impactions. Eight pots were filled for each polymer type, along with 4 un-seeded polymer controls. These were then transferred to non-tissue culture plastic 6 well plates and incubated at 37ºC in 5% CO_2 in osteogenic media (basal media + 100 uM ascorbate-2-phosphate, and 10 nM dexamethasone) for 14 days, with PBS washes every 3-4 days.

5.4.5.4 WST-1 assay

After two weeks incubation the contents of three of the EM pots of each polymer (and one control) were removed and each submerged into 2.5 ml 1:10 dilution WST-1 reagent (Roche ltd, Welwyn Garden City, UK). One hundred microlitres was aspirated in triplicate from each sample at 2 and 4 hours incubation time, and read via a Bio-Tek KC4 microplate fluorescent reader (Bio-Tek, USA) at 410nm. The mean values in optical densities of the solutions mixed with each polymer were calculated at 2 and 4

hours, and the mean values of the control samples subtracted in order to allow comparison between polymers (one way ANOVA).

5.4.5.5 Live / dead immunostain

The contents of one of the EM pots of each seeded polymer type (and 1 control) were removed and underwent immunostaining. One portion of each sample was stained via a traditional live / dead immunostain using Cell Tracker Green (CTG) probe and Ethidium Homodimer (EH-1) as described in Section 2.10. The samples were then fixed in ethanol and stored in PBS prior to imaging under confocal microscopy (Leica SP5 Laser Scanning Confocal Microscope and software, Leica Microsystems, Wetzlar, Germany).

5.4.6 Assessment of osteoblastic differentiation

5.4.6.1 Alkaline phosphatase assay

In order to give a quantative measure of osteoblastic cell number on each seeded polymer type, a standard Alkaline Phosphatase (ALP) assay was used. The contents of 3 of the EM pots of each type of seeded polymer (and one control) were prepared as described in Section 2.12.2. Lysate was measured for ALP activity using p-nitrophenyl phosphate as substrate in 2-amino-2-methyl-1-propanol alkaline buffer solution (Sigma-Aldrich, Poole, UK). Ten microlitres of lysate was run in triplicate for the 3 impacted cell seeded samples and single control sample of each scaffold on a plate against x2 standards, read on a Bio-Tek KC4 and FLX-800 microplate fluorescent reader (Bio-Tek, USA) and mean and standard deviations calculated.

5.4.6.1 Type-1 collagen immunostain

A second portion of each seeded polymer type separated for immunostaining underwent a type-1 collagen stain in order to illustrate and characterise early bone matrix formation (as described in Section 2.11). A final step involved the addition of cytox blue (1:100 dilution, 10 minute incubation) as a nuclear counter stain. To ensure specificity of the

secondary antibody, a control group consisted of a portion of the samples which were treated in exactly the same way but the primary antibody was not added.

The samples were submerged in PBS and stored in the dark until imaged under confocal microscopy (Leica SP5 Laser Scanning Confocal Microscope and software, Leica Microsystems, Wetzlar, Germany).

5.4.7 In vivo experimental set-up

An established murine model was set up in order to analyse the oseogenic capability of the polymers *in vivo*. In order to conform to the three Rs (reduction, refinement and replacement) of good laboratory animal practice, only $P_{DL}LA$ and $P_{DL}LA$ / HA were tested *in vivo*, as these two polymers had performed best in the *in vitro* studies; both showed enhanced ability to stimulate osteoblastic differentiation of SSCs over the $P_{DL}LGA$ and the $P_{DL}LGA$ / HA composite (see Section 5.5.4).

Another vial containing the same human SSC population (M66) was defrosted and the cells grown to confluence in basal media in T150 flasks. Cells were released using trypsin in EDTA, and seeded for two hours in an incubator at 37 ºC in 5 % CO_2 on the pre-sterilised and morcellised scaffolds at a concentration of $5x10^5$ cells / ml. After this time period each of the polymers were impacted into modified (perforated) EM pots (n = 4 per polymer) using the same protocol (Section 3.2.3.6.3) prior to being placed into individual wells of a six well plate in osteogenic media for one week. An additional 4 impacted EM pots of each polymer type were created with no cells, to act as *in vivo* controls. On day six the cells in 2 EM pots of each seeded polymer type were immunostained for long term tracking, by submerging in eight millilitres of 1: 800 dilution vybrant (Invitrogen, Paisley, UK) : PBS for 15 minutes, prior to a further PBS wash and a further 24 hour incubation in osteogenic media.

On day 7, pre-acclimatised male MF-1 nu/nu immunodeficient mice (Harlan, Loughborough, UK) were anaesthetised intraperitoneally using fentanyl fluanisone (Janssen-Cilag Ltd, High Wycombe, UK) and midazolam (Roche Ltd, Welwyn Garden City, UK). Small (10 mm) incisions were made into the subcuticular tissue over the loin

area bilaterally, and pockets created into which the EM pots containing the polymers were placed. The incisions were closed under aseptic conditions, the mice allowed to recover, and were subsequently allowed *ad libitum* access to standard mouse chow and water.

After 35 days the mice were euthanased, and half were perfused with radio-opaque contrast (a mixture of Barium sulphate and 2% laponite solution) via the left ventricle (Bolland *et al.* 2008a), in order to display the neo-vasculature around and throughout the EM pots.

5.4.8 Micro Computer Tomography (µCT) analysis (in vivo)

Quantitative 3D analysis of the pots was obtained using Metris Xtek HMX ST 225kV CT scanning system (X-TEK Systems Ltd, Tring, Hertfordshire, UK). Raw data was collected and reconstructed using Next Generation Imaging (NGI) software package (X-TEK Systems Ltd) with a 10.6 µm voxel resolution. All voxels were automatically assigned Houndsfield units via calibration against a standard water sample. The images were visualised and analysed using Volume Graphics (VG) Studio Max software (Volume Graphics GmbH, Heidelberg, Germany). The regions of interest (contents of the EM pots) and thresholds for new bone, polymer and hydroxyapatite were selected manually, and the volumes of new bone calculated via the software. From this data, the mean and standard deviations for bone volume were calculated for each experimental group. Both 2D and 3D images (saved as TIFFS) were created, with different colour assignments to certain greyscale value ranges in order to highlight areas of interest.

5.4.9 Histological analysis (in vivo)

Following µCT analysis, the specimens were removed from the EM pots, and sections of each specimen underwent histological analysis (Section 2.8). In brief, they were washed and decalcified as detailed by Miao and Scutt (Miao and Scutt 2002), followed by dehydration in a graded series of alcohols, low melting point paraffin wax embedding and finally cut into 7 µm sections. Staining included an Alcian Blue and Sirius Red stain for proteoglycan rich extracellular matrix and collagen respectively, and Goldners Trichrome stain for bone and osteoid, using standard protocols (Sections 2.8.3 and 2.8.4).

5.4.10 Immunostaining (in vivo)

Post removal from the EM pots, sections of each specimen also underwent immunostaining as described in Section 2.11. Immunostains involved type-1 collagen, bone sialoprotein (BSP), osteocalcin (OC) and Von Willibrands factor (vWf) for evidence of vascularisation, with a DAPI nuclear counterstain added to all samples. The sections were not wax embedded to preserve polymeric architecture, and imaging via confocal microscopy (Leica SP5 Laser Scanning Confocal Microscope and software, Leica Microsystems, Wetzlar, Germany) allowed 3D topographical visualisation of the surface of the polymers.

5.4.11 Statistical analysis

All measurements were calculated as mean ± standard deviation. Grouped linear regression analysis (GraphPad Prism, San Diego, California, USA) was used to compare failure curves of the polymers against the allograft controls. Differences between groups were assessed by a Mann–Whitney U test or one way ANOVA with post hoc Bonferroni analysis depending on group number, and $p < 0.05$ was considered to be significant.

5.5 Results

5.5.1 Polymer characterisation

The mean porosity for $P_{DL}LA$ was 58.7 % ± 0.59 % with pore size 155 μm ±52 μm. $P_{DL}LA$ in combination with HA had a mean porosity of 63.4% ± 5.4 % with pore size 192 μm (SD ±51). For $P_{DL}LGA$ the mean porosity was 45.5 % ± 0.56 % with mean pore size 267 μm ± 194 μm, whereas the porosity of $P_{DL}LGA$ in combination with HA was 59.3 % ± 2.1 % with mean pore size 156 μm ± 37 μm. These small differences were due to the different behaviours of the polymers/ composites during the supercritical foaming process, even though the production conditions were the same, and are visualised by μCT in Figure 5.2.

Figure 5.2: Characterisation of polymers prior to milling via µCT. Axial slices are shown in all specimens to demonstrate porosity throughout the structure A) $P_{DL}LA$, B) $P_{DL}LA$ + 10 % HA, C) $P_{DL}LGA$ D) $P_{DL}LGA$ + 10 % HA (scale bar = 3 mm).

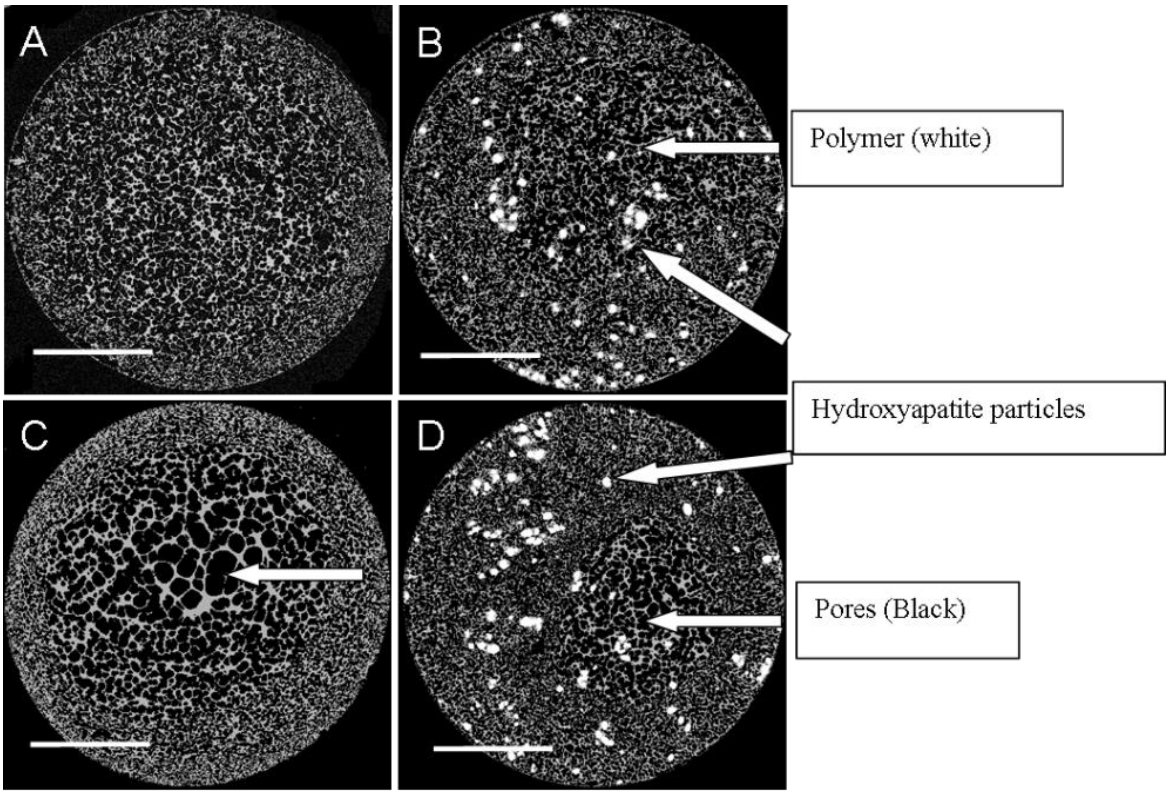

Scanning electron microscopy after the milling process revealed irregular surface topography in all samples, providing excellent cell binding sites (Figure 5.3). The HA particles were also visible (Figure 5.3 C + D), and hence available for cell adhesion and attachment.

Figure 5.3: Characterisation of polymers after the milling process via SEM. A) $P_{DL}LA$, B) $P_{DL}LGA$, C) $P_{DL}LA$ + 10 % HA, D) $P_{DL}LGA$ + 10 % HA (scale bar = 300 μm). NB A + B are replicated from Figure 4.5.1 C + D. White arrows = HA particles.

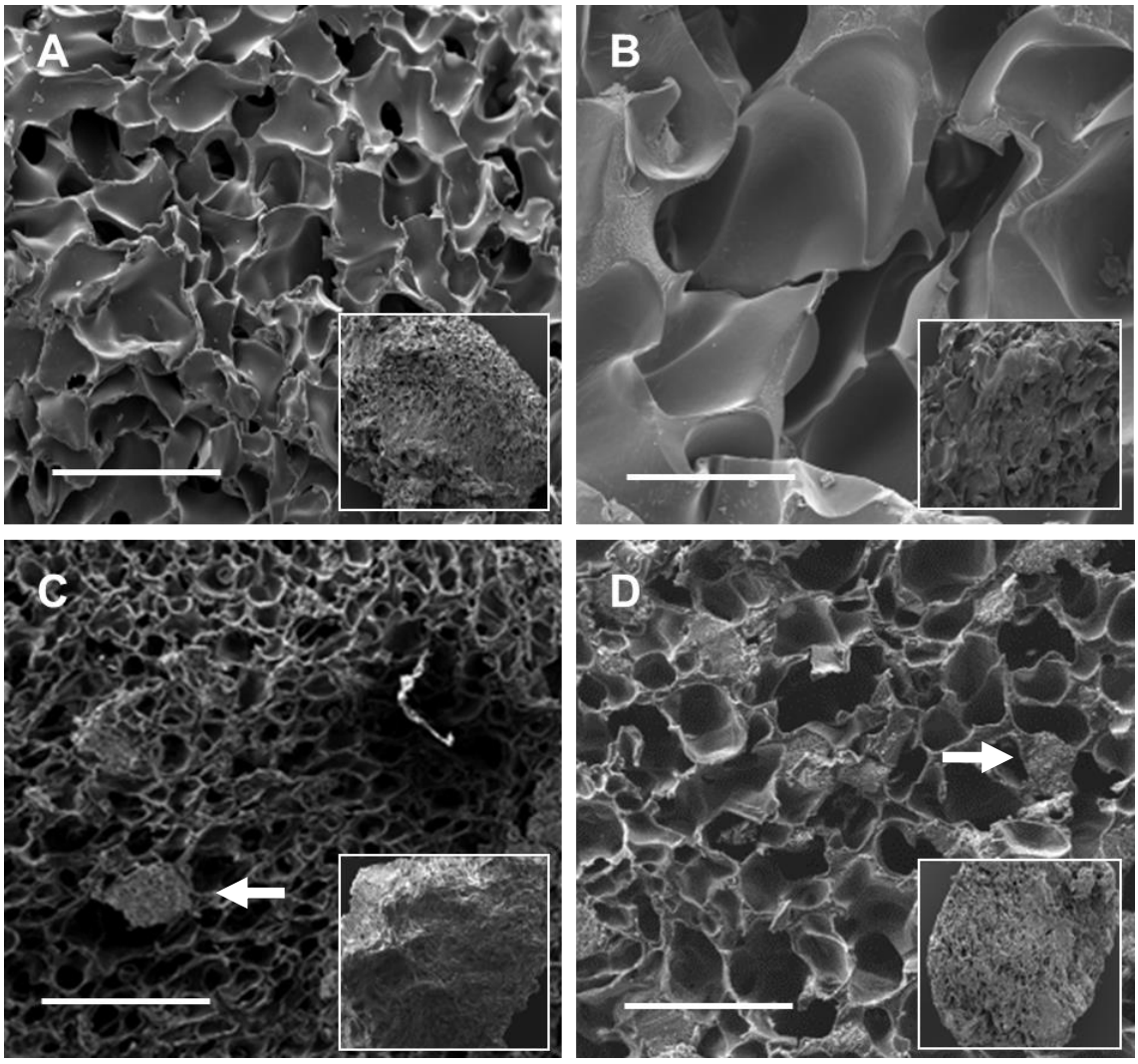

5.5.2 Mechanical testing (in vitro)

There was a linear increase in shear stress of the discs of impacted allograft (controls) and each of the polymers with an increase in compressive stress, in keeping with the Mohr Colomb failure law (Figure 5.4).

Figure 5.4: Mohr Coulomb failure envelopes for polymers under test and allograft controls (black line), showing regression analysis trend lines and SD error bars. All polymers show significant increases in shear stress over allograft at all compressive stresses ($P<0.001$, $n = 4$).

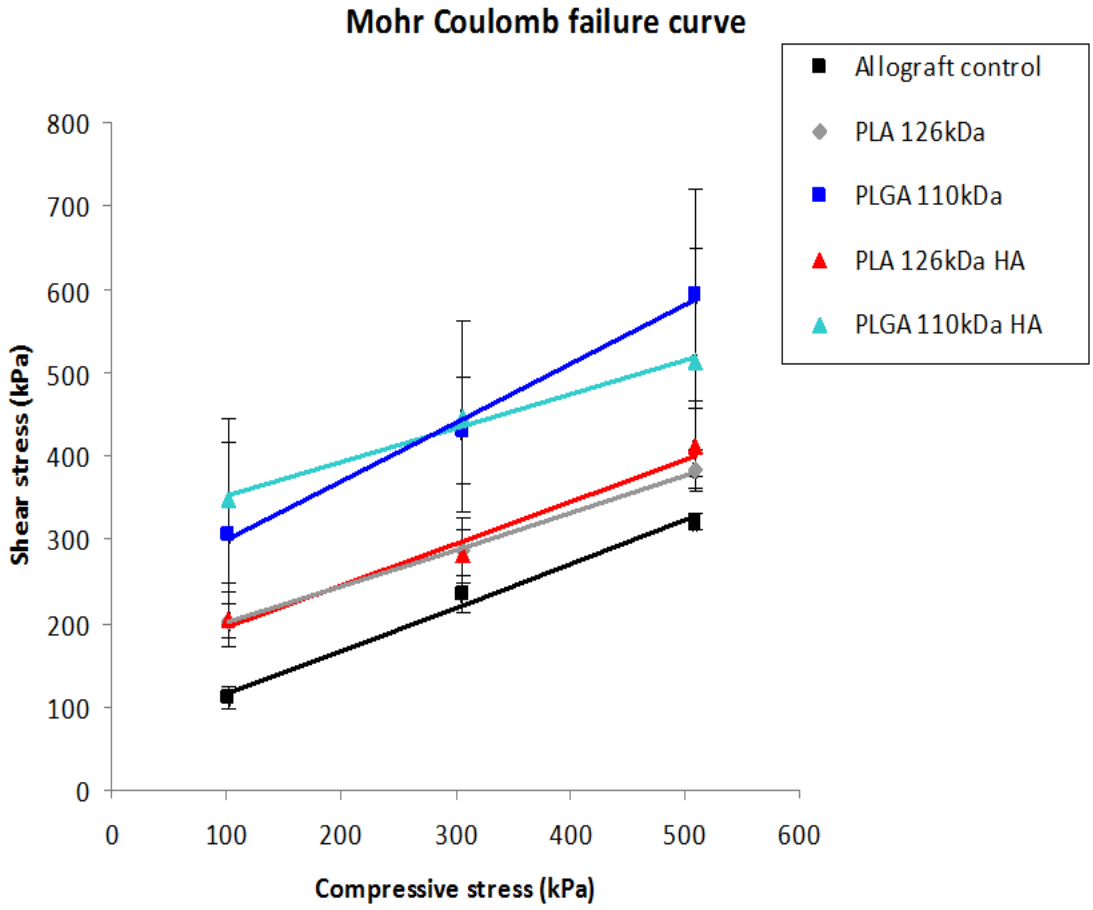

When comparing each of the polymers to the allograft controls (Grouped linear regression (GLR) ($R^2 > 0.9$ all cases)) there was significant increase in shear strength for all ($p < 0.001$). Table 5.1 displays this data with additional interparticulate cohesions (along with 95% confidence intervals) for all morcellised polymer composites and the allograft controls. Interestingly, there was no difference in the shear strength of the $P_{DL}LA$ discs compared to the $P_{DL}LA$ / HA discs (GLR: $p = 0.585$) or the $P_{DL}LGA$ discs compared to the $P_{DL}LGA$ / HA discs (GLR: $p = 0.842$), indicating that hydroxyapatite in the concentrations used for the composite polymers (10%), had little effect the mechanical characteristics.

Table 5.1: Showing R^2 values and interparticulate cohesion calculated from the shear test data, as well as the statistical significance of the grouped linear regression analysis comparing the Mohr Coulomb failure envelopes of each polymer to the allograft controls, and the HA composite polymers to their corresponding counterpart.

Test substance	*R^2 value for linear regression curve*	*Interparticulate cohesion (95% confidence interval)*	*Statistical significance (Grouped linear regression analysis)*
Allograft (Group 1)	0.98	62.5 (38.3 - 86.7)	N/A
Porous PLA 126 (Group 2)	0.99	155.1 (117.8 - 192.4)	vs group 1: $p < 0.001$
Porous PLA 126 10% HA (Group 3)	0.97	144.2 (91.2 - 197.1)	vs group 1: $p< 0.001$ vs group 2: $p = 0.585$
Porous PLGA 110 (Group 4)	0.99	228.4 (123.5 - 333.5)	vs group 1: $p < 0.001$
Porous PLGA 110 10% HA (Group 5)	0.98	311.7 (161.0 - 462.4)	vs group 1: $p< 0.001$ vs group 4: $p = 0.842$

These findings were in keeping with the previous data, confirming that the porous versions of the polymers maintained their increased shear strength when milled, impacted and compared to allograft controls. The integral material properties, in combination with the irregular and porous architecture of the granules after the milling process, thus maintained a structure after impaction with desirable characteristics for clinical translation. As can be seen from the µCT and SEM images, the HA particles make up only a small proportion of the volume of the polymer, and also appear to have only a minimal effect on the porous architecture of the composite, hence have little impact on the mechanical behaviour of the polymers.

5.5.3 Cell viability (in vitro)

5.5.3.1 WST-1 assay

Following impaction into EM pots and 14 days in culture, a WST-1 cell proliferation assay was used as a quantitative measure of total cell viability. This timed assay (measurements taken at 2 and 4 hours) showed a substantial increase in mean optical density for WST-1 solutions mixed with all 4 polymer and cell composites, indicating excellent cell growth and ongoing cell survival (Figure 5.5). There was no significant difference in optical densities attained at either 2 or 4 hours assay time in any group (one way ANOVA: 2 hours $p = 0.07$, 4 hours $p = 0.197$).

Figure 5.5: Graphical representation of results of WST-1 assay of polymers in combination with SSCs (M66) after 14 days incubation. Mean optical densities (minus control values) are displayed with standard deviations of WST-1 solutions after scaffold submersion for 2 and 4 hours (n=3).

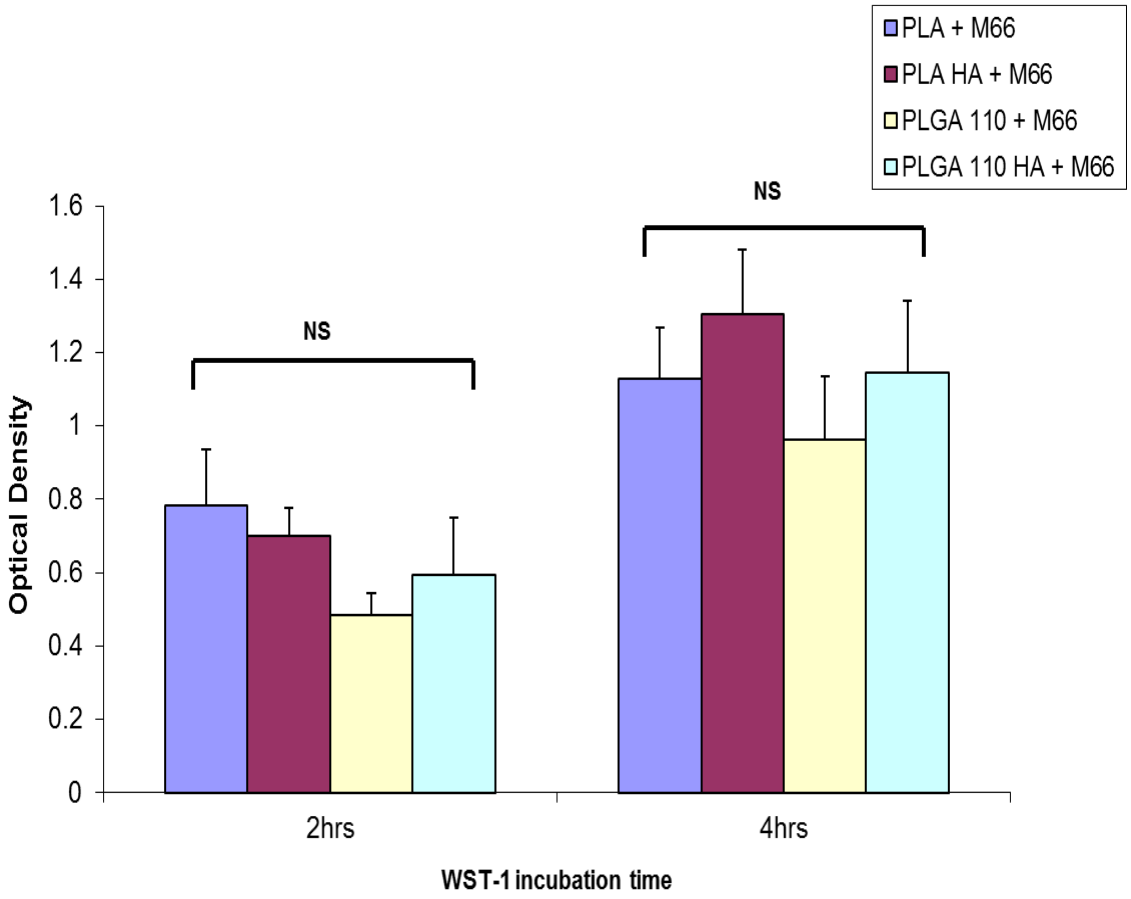

5.5.3.2 Live / dead immunostain

A standard live / dead immunostain was performed using CTG probe and EH-1 on one of the samples of each polymer after the 2 week incubation period, in order to illustrate the findings of the WST-1 assay. Confocal images (Figure 5.6 A-D) display representative areas of the polymers, where live cells stain green and dead or compromised cells stain red / purple. There was abundant live cell staining in all samples, with near confluent cell growth on both the $P_{DL}LA$ and $P_{DL}LGA$ samples (Figure 5.6 A+C), and confluent cell growth with evidence of cell layering on both the $P_{DL}LA$ HA and $P_{DL}LGA$ HA samples (Figure 5.6 B+D). There were a small number of dead or compromised cells (red / purple) on all samples, in keeping with a healthy cell population with cells at all points of the cell cycle. The inset images display the corresponding controls for each polymer (no cells), and as expected there was no evidence of cell growth.

5.5.4 Cell differentiation (in vitro)

5.5.4.1 ALP assay

An ALP assay was used as a measure of cellular osteoblastic differentiation (Figure 5.7). There was substantial ALP activity in cell populations grown on both the $P_{DL}LA$ and the $P_{DL}LA$ / HA with negligible activity measured in the cell populations grown on the $P_{DL}LGA$, and only very minor activity measured from those grown on $P_{DL}LGA$ / HA. One way ANOVA analysis revealed these differences to be significant ($p < 0.001$), and the results of the post hoc (Bonferroni) analysis between the groups is given in Appendix 3. Importantly, the ALP activity measured in the cell population growing on the $P_{DL}LA$ / HA was significantly higher than in all other groups ($p < 0.01$), and that measured in the cell population growing on the $P_{DL}LA$ was significantly higher than that measured from either the $P_{DL}LGA$ or the $P_{DL}LGA$ HA ($p < 0.05$).

Figure 5.6: Representative image stacks showing live (green cells) / dead (red/purple dots) immunostain of (A) $P_{DL}LA$, (B) $P_{DL}LA$ / HA, (C) $P_{DL}LGA$ and (D) $P_{DL}LGA$ / HA after 2 weeks incubation with SSCs viewed under confocal microscopy (x200 magnification, scale bar = 200μm). The inset images are corresponding controls (no cells).

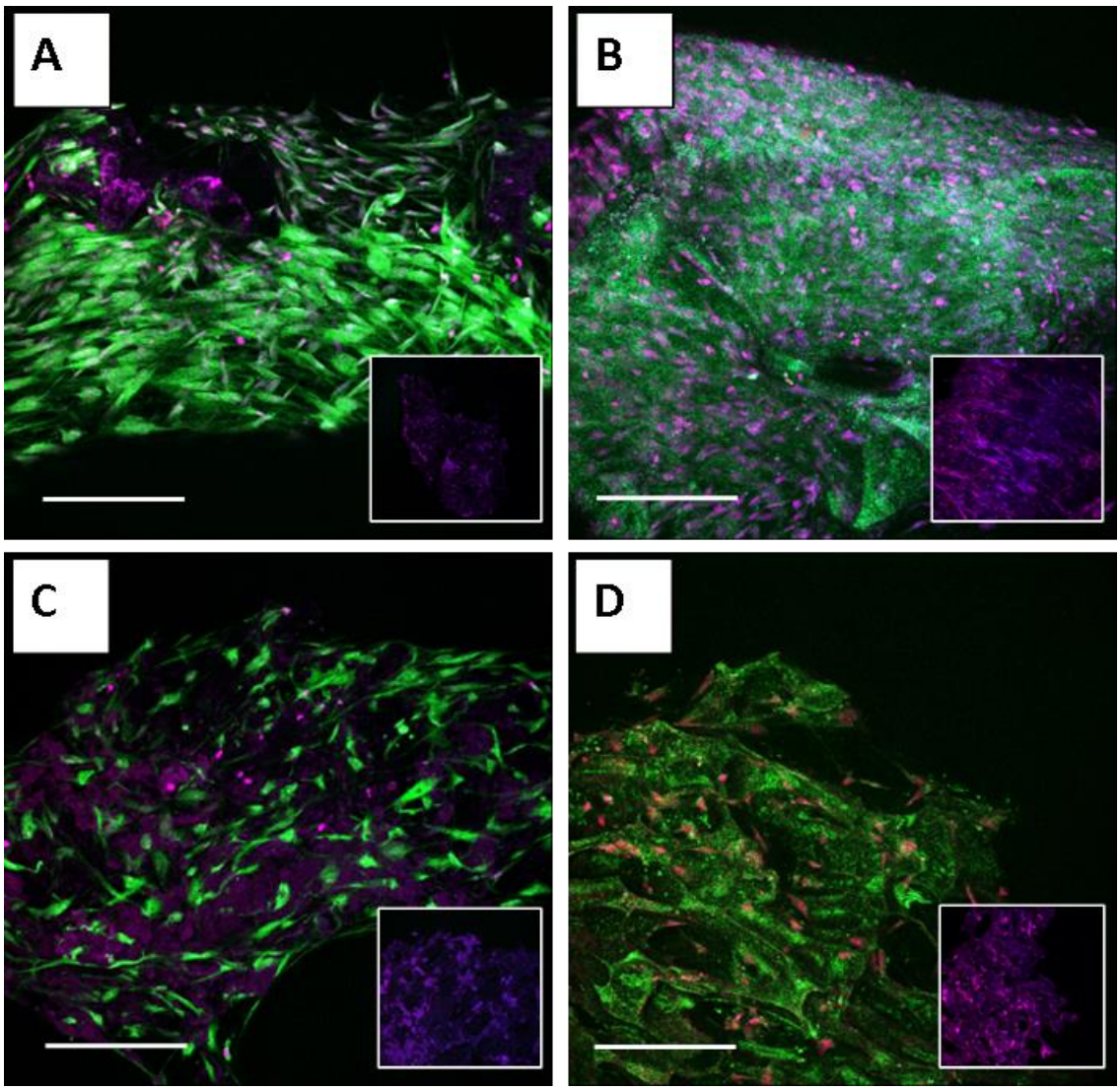

Figure 5.7: Graphical representation of mean (standard deviation) alkaline phosphatase activity (minus control values) of polymers in combination with SSCs (M66) after 14 days incubation. (* $p < 0.05$, ** $p < 0.01$, $n = 3$)

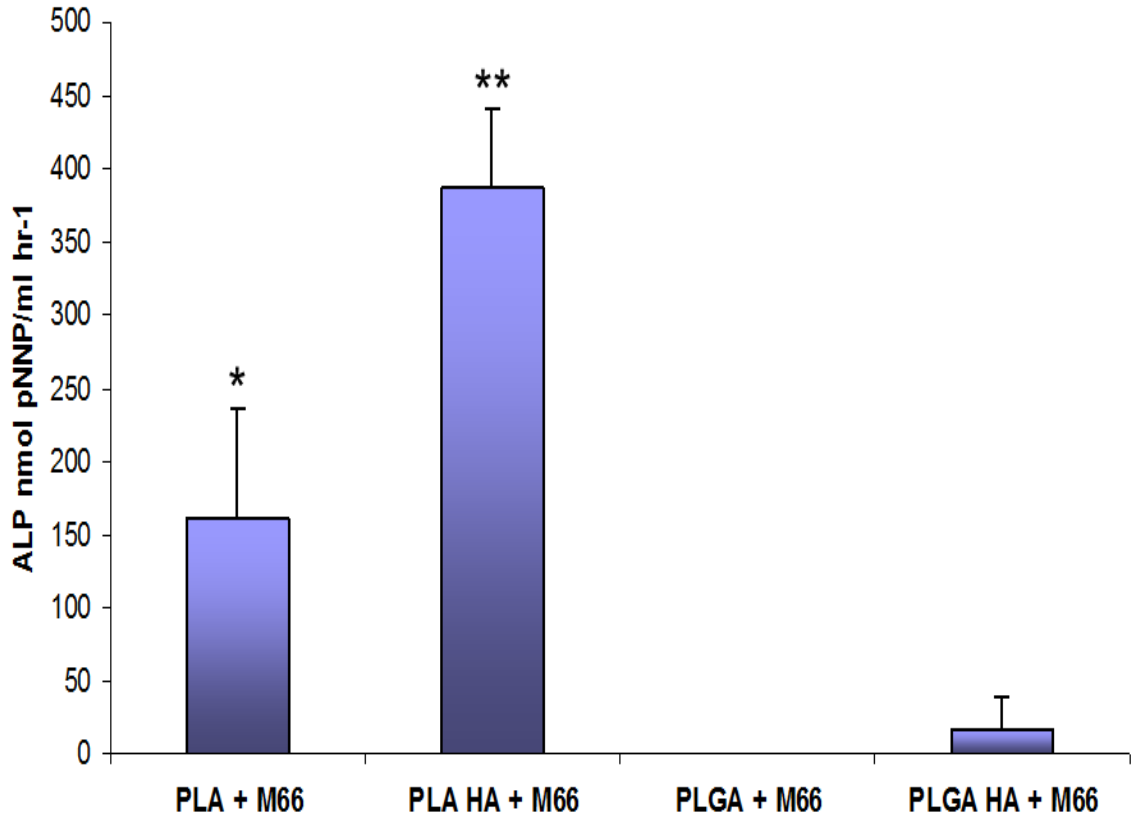

5.5.4.2 Type-1 collagen immunostain

Type-1 collagen immunostaining imaged via confocal microscopy (Figure 5.8) confirmed the enhanced osteoblastic nature of the cells grown on the $P_{DL}LA$ and $P_{DL}LA$ / HA scaffolds. Cell nuclei were counterstained with cytox blue (shown as green), and were diffusely present on all 4 polymer samples (Figure 5.8 A-D), but there was enhanced extracellular staining (red) on both the $P_{DL}LA$ and $P_{DL}LA$ / HA scaffolds (Figure 5.8 A+B), indicating the presence of type-1 collagen in these samples.

Figure 5.8: Reconstructed image stacks of type-1 collagen immunostain (red), with cytox blue nuclear counter stain (green) produced via confocal microscopy (x400 magnification, scale bar = 100μm) showing representative areas of (A) $P_{DL}LA$, (B) $P_{DL}LA$ HA, (C) $P_{DL}LGA$ and (D) $P_{DL}LGA$ HA after 2 weeks incubation with SSCs. The inset images are negative controls (no primary antibody added).

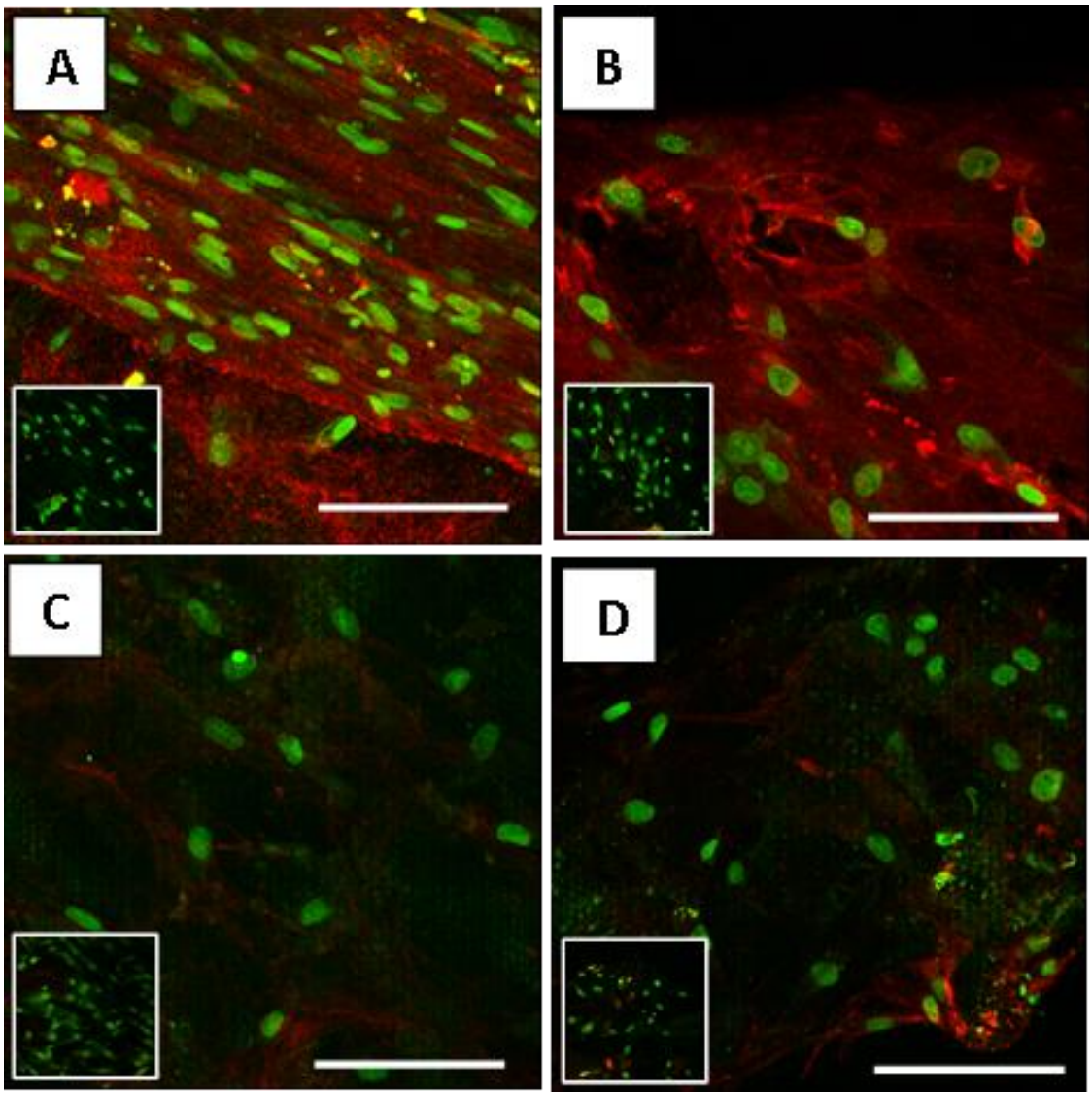

As a result of these findings of enhanced osteoinductivity, only the $P_{DL}LA$ and $P_{DL}LA$ / HA scaffolds were taken forward for *in vivo* testing (see section 5.4.7).

5.5.5 µCT analysis (in vivo)

MicroCT was performed on all samples and controls after one week *in vitro* incubation followed by 5 week *in vivo* incubation (6 week total) as described in Section 5.4.8. Quantitative analysis (Table 5.2) revealed a significant increase in new bone formation between the control $P_{DL}LA$ and that pre-seeded with human SSCs (U test: $p = 0.03$) and the increase in new bone between the $P_{DL}LA$ / HA and that pre-seeded with SSCs approached significance (U test: $p = 0.1$). There was a large increase in new bone when comparing the $P_{DL}LA$ / HA to the $P_{DL}LA$ both in the control groups and in the groups seeded with SSCs (U test: $p = 0.03$, $p = 0.03$).

Table 5.2: Displaying the mean bone volume (n = 4) formed on each polymer after a 5 week *in vivo* study.

	Mean bone vol (mm^3)	**SD**
PLA cells	0.66	0.31
PLA cont	0.08	0.03
PLA/HA cells	24.62	3.98
PLA/HA control	18.18	4.63

Figure 5.9 demonstrates the 3D reconstructed µCT image of (A) the EM pot containing $P_{DL}LA$ + SSCs post *in vivo* incubation, and (B) the same image but with the low density EM pot and $P_{DL}LA$ extracted in order to show the higher density new bone formation only. As the polymer, EM pot and original cellular material were all of low density, the specificity of the remaining high density areas for volumetric bone calculations is high.

Figure 5.9: 3D reconstructed μCT images of A) EM pot containing PLA + SSCs post 5/52 *in vivo* (murine) incubation, and B) same image but with EM pot and PLA extracted to show only new bone formation (Scale bar = 5mm).

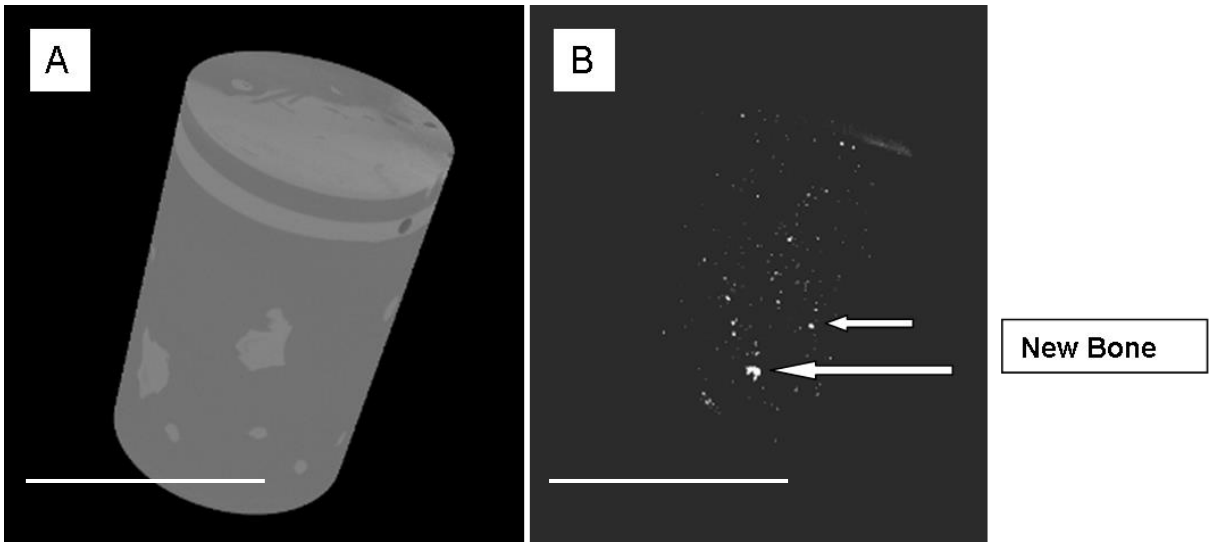

Figure 5.10 (A-C) demonstrates typical axial (A+B) and coronal (C) μCT sections of $P_{DL}LA$ / HA + SSCs after the 5 week in vivo incubation. The HA was clearly visible as bright white round and ovoid particles (A). In B+C the lower density new bone has been highlighted by colouring it red. As the range of densities of new bone (predominantly medium) and HA (predominantly high) have slight crossovers, there was unavoidable potential for inaccuracies when calculating bone volumes. Figure 5.10 (D-F) show similar axial and coronal sections of the $P_{DL}LA$ / HA control specimens after the 5 week *in vivo* period. The medium density range has again been enhanced by red colouring (E,F); the new bone was less abundant, and more localised to the HA particles than the SSC seeded counterparts.

Vasculature was also visualised via contrast injection into the left ventricle (Figure 5.11A) and subsequent μCT imaging. This difficult technique relies on micro-vessel perfusion around and throughout the construct before harvest, and is not appropriate for volumetric analysis. However, there was good evidence of excellent neo-vessel formation in both the $P_{DL}LA$ (Figure 5.11B) and $P_{DL}LA$ / HA (Figure 5.11C) constructs.

Figure 5.10: Axial (A + B) and coronal (C) μCT sections of $P_{DL}LA$ / HA + SSCs after 5/52 *in vivo* incubation.). In B + C the lower density new bone has been highlighted by colouring it red, and is visible diffusely throughout the sections. Axial (D + E) and coronal (F) sections of $P_{DL}LA$ / HA controls, where the same lower densities have again been coloured red (E + F) (scale bar = 5mm).

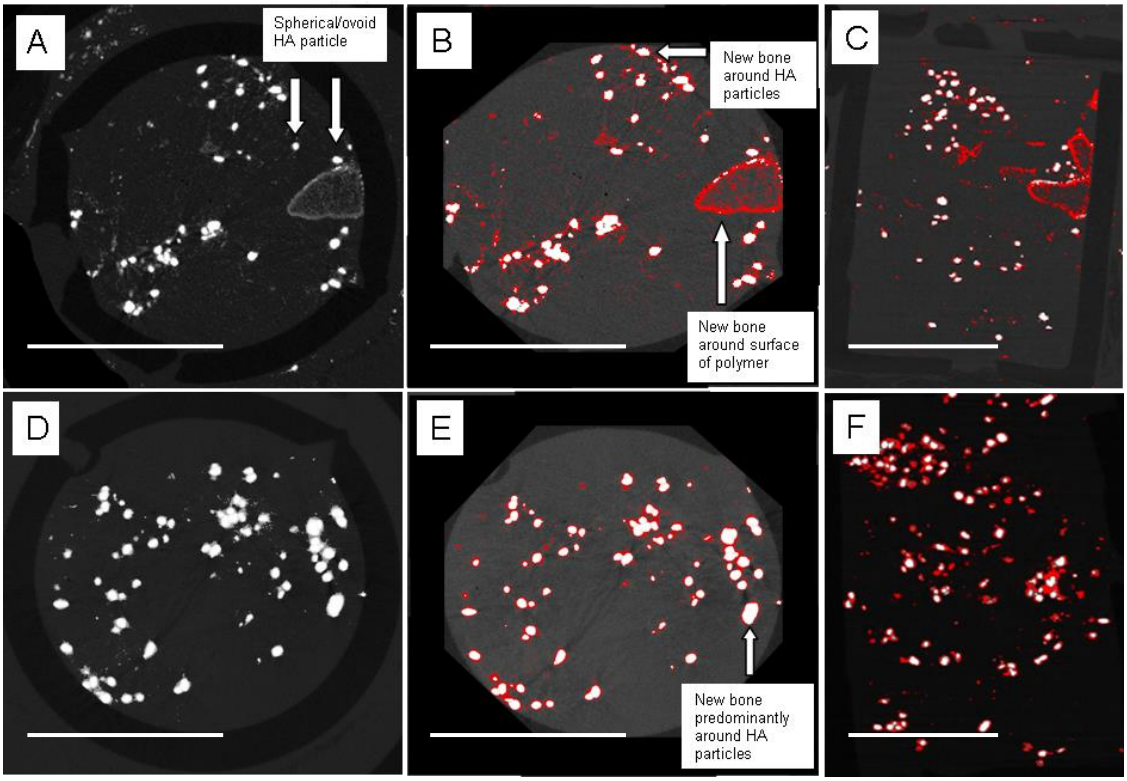

Figure 5.11: Demonstration of neo vessel formation in and around the scaffolds. (A) injection of radio opaque contrast into the left ventricle. (B+C) 3D reconstructed μCT images demonstrating good evidence of neovascularistion in both the $P_{DL}LA$ (B) and $P_{DL}LA$ / HA (C) samples (scale bar = 5mm).

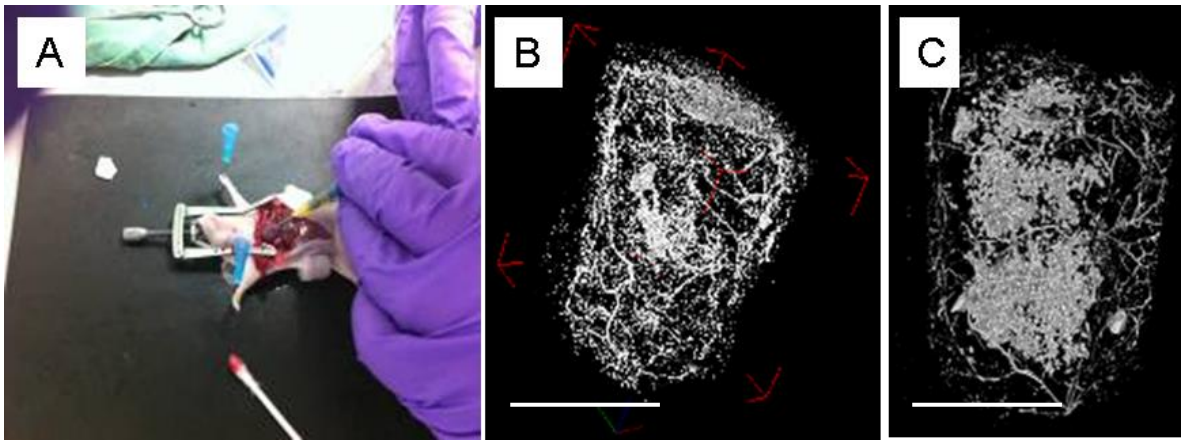

5.5.6 Cell viability (in vivo)

The human SSCs from two samples per group were pre-labelled with fluoro-markers (vybrant) prior to murine subcutaneous implantation. After the *in vivo* period there was evidence of on going cell survival as demonstrated by the confocal images shown in Figure 5.12. The pre-labelled cells stained green, and they were present in both the $P_{DL}LA$ samples (Figure 5.12A) and the $P_{DL}LA$ / HA samples (Figure 5.12B), but in the latter they had a more osteoblastic (spindle shaped) appearance.

Figure 5.12: Reconstructed image stacks obtained via confocal microscopy showing representative images of the cells stained with vybrant prior to subcutaneous murine implantation on $P_{DL}LA$ (A) and $P_{DL}LA$ / HA (B) after 5 weeks *in vivo* culture (x 400 magnification, scale bar = 100μm) (inset pictures x100 magnification).

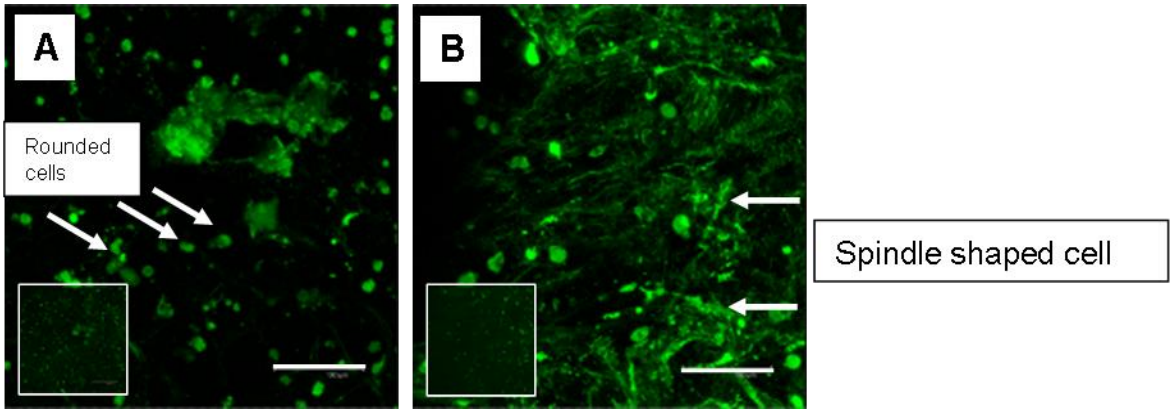

5.5.7 Histological analysis (in vivo)

Alcian Blue and Sirius Red staining showed the presence of collagen and proteoglycan deposition amongst both the human SSC seeded $P_{DL}LA$ and $P_{DL}LA$ / HA scaffolds (Figure 5.13 B+D), although it was more abundant on the latter. Interestingly, there was also evidence of cells, along with collagen and proteoglycan deposition on the $P_{DL}LA$ / HA controls, indicating the ability of this scaffold to stimulate *de novo* bone formation from the host cells (Figure 5.13 C). These results were reinforced by Goldners' Trichrome staining positive for osteoid (Figure 5.13 F-H). The $P_{DL}LA$ control scaffold showed no histological evidence of neo-bone formation (Figure 5.13 A+E).

Figure 5.13: Histological sections of specimens viewed under light microscopy (x20 magnification, inset = x50 magnification, scale bar = 100 μm) post 5 week *in vivo* period. (A-D) Alcian blue and Sirius red staining for collagen and proteoglycan deposition is negative for the $P_{DL}LA$ controls (A) but positive for other specimens (B-D). Similar findings when assessing for osteoid using Goldner's Trichrome stains (E-H).

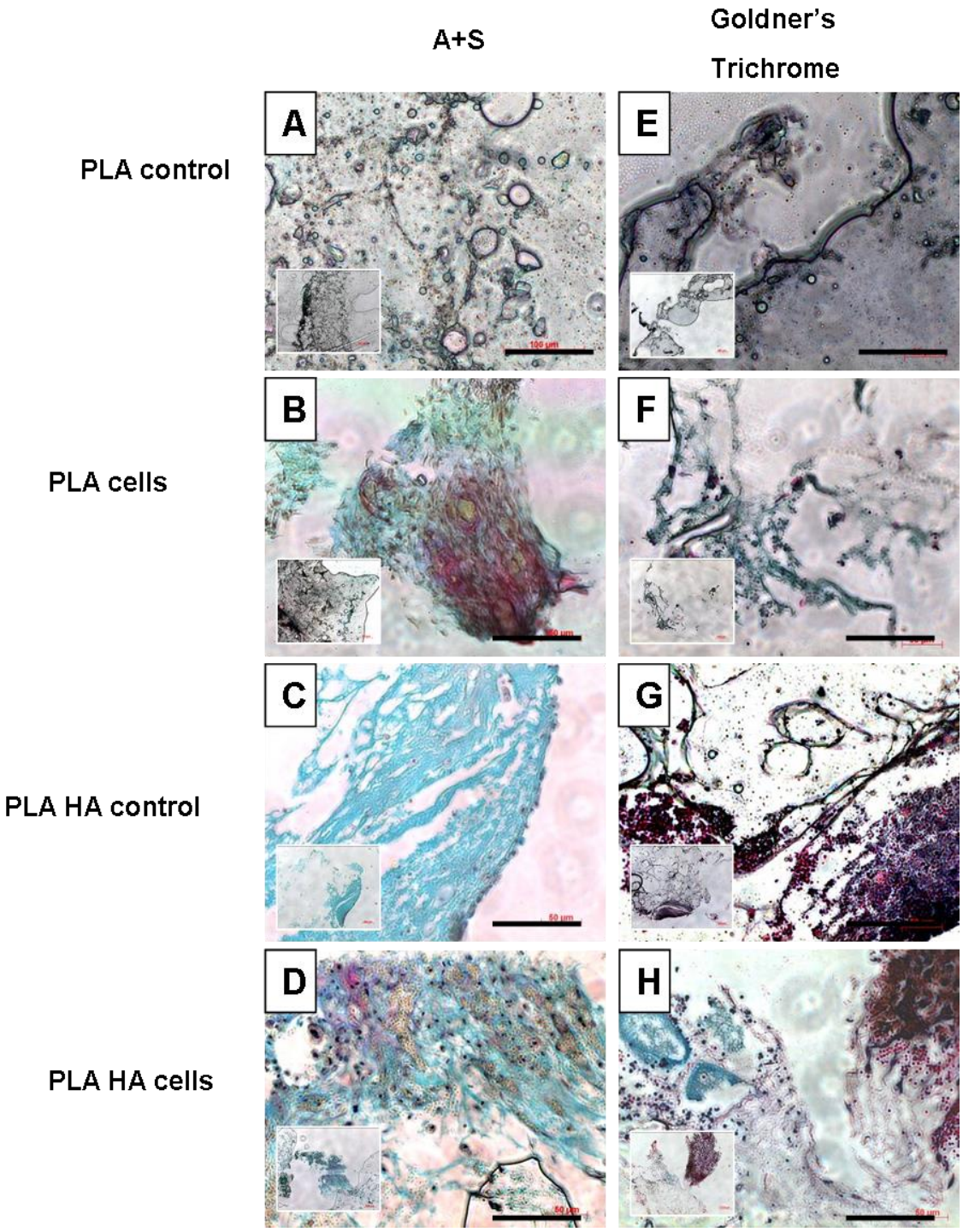

5.5.8 Immunostaining (in vivo)

Both the $P_{DL}LA$ and $P_{DL}LA$ / HA seeded with human SSCs, along with the $P_{DL}LA$ / HA controls stained positive for type-1 collagen and bone sialoprotein, and had scattered positivity for vWF (Figure 5.14), in keeping with the evidence for widespread new bone formation and a more localised vascularisation process. All samples were negative for the late marker osteocalcin, possibly due to a relatively short (5 week) incubation period. As expected the $P_{DL}LA$ controls stained negative for all markers of bone formation. The DAPI nuclear counter stain was positive (green spots) throughout all samples, even the controls to which no human cells were added. This explains the positive collagen staining not only in the cell seeded specimens ($P_{DL}LA$ + M66, $P_{DL}LA$ / HA + M66) but also the $P_{DL}LA$ / HA controls, indicating that host cells have not only grown into the construct, but have also been stimulated by the presence of HA to differentiate and to produce bone matrix.

Figure 5.14: Reconstructed image stacks obtained via confocal microscopy (x200 magnification) displaying immunostains (coloured red) for bone markers (type-1 collagen, bone sialoprotein, ostreocalcin) and vascular markers (Von Willebrand's factor). All specimens had DAPI nuclear counterstains (green). The negative controls have no primary antibody added, to prove specificity (scale bar = 200 μm).

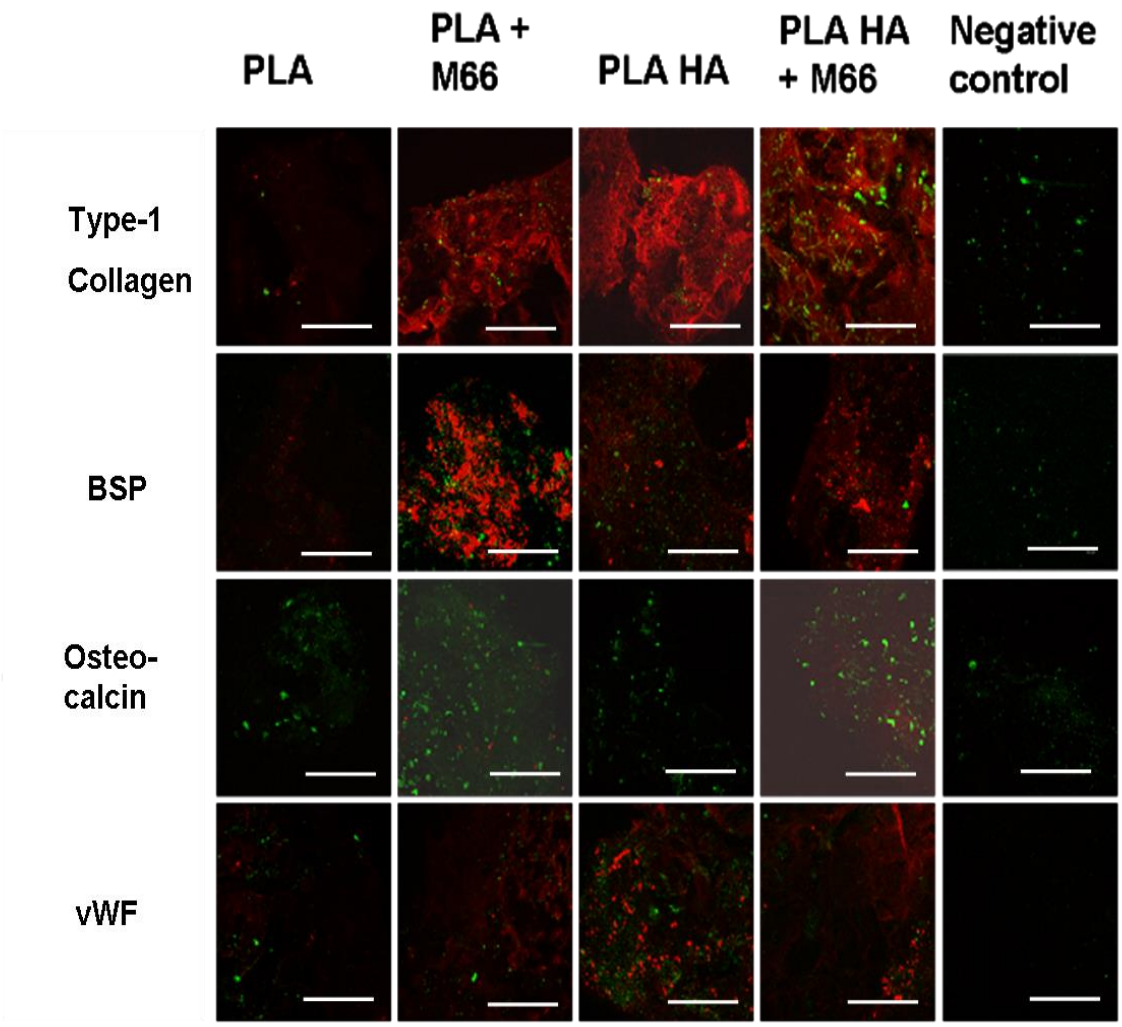

5.6 Discussion

The *in vitro* studies detailed in the previous chapters have highlighted that porous high molecular weight $P_{DL}LA$ and $P_{DL}LGA$ have both the mechanical and cellular compatibility characteristics to be good potential osteogenic substitutes to allograft for use in impaction bone grafting. This study has now shown that the addition of 10 % hydroxyapatite to the scaffold improved the osteogenic potential by up regulating osteoblastic differentiation of accompanying SSC populations, with no measureable changes to cellular compatibility or the mechanical shear strength of the composite.

In this study, an increase in total ALP activity was used as measure of osteoblastic cell number after the incubation period. This technique provides a reliable and reproducible measure that has been cited in a number of other related studies (Bolland *et al*. 2006;Bolland *et al*. 2008b;Jones *et al*. 2009). Molecular analysis of the cell polymer composites was also attempted utilising multiple techniques, but unfortunately the interaction of the required chemicals with the polymer, as well as total cell number required for accurate results, meant that an unreliable and incomplete data set was produced. Current work is underway to optimise molecular protocols for use with these novel scaffolds. Furthermore, the findings of the assay were backed up by the type-1 collagen immunostain: a commonly used extracellular marker for early bone matrix deposition (Bolland *et al.* 2006;Bolland *et al.* 2008b;Kanczler *et al.* 2010;Kanczler *et al.* 2007). Not only was there abundant type-1 collagen positivity on both of the $P_{DL}LA$ scaffolds, on close observation of the $P_{DL}LA$ / HA scaffold it appeared as though the collagen is more organised - a feature only made visible by viewing the 3D reconstructed image stack acquired by confocal microscopy.

The WST-1 assay acts as a standard quantitative measure of total cell activity, and hence number (Ishiyama *et al.* 1996). Due to previous studies highlighting the excellent biocompatibility of these particular polymers, the fact that there was no significant difference observed between the samples after the incubation period was to be expected (Bolland *et al*. 2008b;Tayton *et al*. 2012a;Tayton *et al*. 2012b). The live / dead stains imaged under confocal microscopy confirmed these findings, with near confluent cell growth over the surface of all of the polymers.

The shear test used was consistent with the previous investigations detailed in this thesis as well as other published studies in this field (Bolland *et al*. 2008b;Brennan *et al*. 2011;Dunlop *et al*. 2003). It used standard engineering principals and practices to gain an accurate and reproducible measure of the impacted composites true shear strength; the compressive stresses chosen were consistent with physiological loads. However, it was a static model, so did not submit the impacted polymer composites to the constantly changing loads experienced *in vivo.* Other studies have attempted this with IBG implanted simulated sheep bones under cyclical loading conditions, but thus introduce a large number of variables such as implantation technique and implant position (Blom *et al*. 2002).

$P_{DL}LA$ polymers significantly outperformed the $P_{DL}LGA$ polymers during *in vitro* studies, and hence only these polymers were subsequently tested *in vivo.* The second part of this study has now shown that SSCs in combination with these novel porous $P_{DL}LA$ scaffolds survived the impaction process, were subsequently able to proliferate *in vivo,* and form *de novo* bone throughout the $P_{DL}LA$ constructs. Furthermore, there was evidence that the SSC seeded $P_{DL}LA$ / HA scaffold stimulated more bone production than its $P_{DL}LA$ counterpart, and also stimulated *de novo* bone production by the host, even when implanted without pre-seeded SSCs.

MicroCT was used as the primary measure of new bone volume formation and is gaining increasing value in regenerative fields (Ho and Hutmacher 2006;Kanczler *et al*. 2010). The samples were imaged at a 10.6 μm resolution, minimising volumetric measurement inaccuracies due to voxel size and making imaging of tiny structures such as individual HA particles and micro-vessels possible. The large difference in densities between the $P_{DL}LA$ and new bone formation also meant that effective threshold ranges for each could be assigned such that volume calculations for each were accurate. As hydroxyapatite is one of the constituents of mature bone, there was an unavoidable crossover between threshold ranges of the new bone formed and the HA already present in the scaffold, which resulted in inaccuracies when calculating new bone volumes in the scaffolds containing HA. However, the colour enhanced CT images (Figure 5.12 B+C) showed that it was still possible to manually select a threshold range corresponding to new bone, where it could be seen in abundance both in contact with and distributed away from the characteristic ovoid and spheroid HA particles.

Interestingly, when using the same threshold values for the un-seeded $P_{DL}LA$ / HA controls, there also appeared to be an abundance of new bone formation, but this time distributed predominantly around and in contact with the HA particles (Figure 5.10 D-F). It is possible that the host (murine) cells had been stimulated to differentiate and to produce bone, and it was the HA particles which directly provided this stimulus. This would explain the HA localisation and was also substantiated by both histological and immuno-histological findings. Other studies have described this effect when assessing the osteoinductive effect of HA in heterotopic sites in various animal models (Ripamonti 1996). However, it was the periphery of the HA that was exposed to extracellular fluid etc, and it was therefore also possible that early degradation of the HA particle was occurring, which lead to a reduction in HA density at these points, at least contributing in part to these findings.

Concern has been raised as to the cellular toxicity of the acidic breakdown products of $P_{DL}LA$ scaffolds (Athanasiou *et al*. 1996;Taylor *et al*. 1994). This study did not observe this to be the case even after a prolonged combined *in vitro* and *in vivo* (6 week total) period. Possible explanations include the high molecular weight of the $P_{DL}LA$, meaning degradation was slower and more controlled, and the fact that the polymers were both porous and milled prior to being impacted into the desired shape, meaning that a constant fluid diffusion gradient and eventual vascular network could develop throughout and within the individual $P_{DL}LA$ particles allowing the effective removal of the lactic acid as it is produced (Hutmacher 2000).

There are various techniques of producing porous polymers, including salt leaching and gas foaming (Murphy *et al*. 2002;Nam *et al*. 2000). However the novel production by supercritical CO_2 means that the polymer can easily combined with a bioactive material such as HA, can be kept within a physiological temperature range and is not subjected to damaging organic solvents (Tai *et al.* 2007). Therefore, future heat labile additions such as vascular endothelial growth factor or bone morphogenic protein-2 are possible, which have been shown to increase both the bioactivity and vascularisation of related scaffolds (Kanczler *et al.* 2010;Tai *et al.* 2007;Kanczler *et al.* 2010). The presented *in vivo* analysis found significant increases in bone formation on the $P_{DL}LA$ scaffolds seeded with SSCs compared to the controls, and that of the $P_{DL}LA$ / HA scaffolds approached significance. With the addition of further bioactive molecules in addition to

the HA, there is thus future potential to dispel the need for *ex vivo* SSC seeding due to effective recruitment of the hosts own progenitor cells.

The murine model presented has significant limitations, including small scale and lack of loading conditions. However, it is an excellent and reproducible starting point to provide the *in vivo* conditions for assessment of mid-term biocompatibility, osteoinductive / osteogenic capability, and vascularisation potential of the different scaffolds. Histological and immuno-histological examination of the contents of the EM pots after the *in vivo* period has confirmed the ability of the polymers to support and even stimulate host *de novo* bone formation, without substantial inflammatory or toxic effects.

5.7 Conclusion

The results in the context of the null hypothesis were examined:

The addition of hydroxyapatite particles to high molecular weight porous $P_{DL}LA$ and high molecular weight porous $P_{DL}LGA$ has no effect on the characteristics of these polymers for use in IBG.

This null hypothesis is **false.**

This study completes a series of investigations whereby an array of porous and non-porous polymers, of low and high molecular weights, and in combination with hydroxapatite, have been compared to find the optimal polymer for use with SSCs as an osteogenic alternative to allograft in impaction bone grafting. The summation of the *in vitro* and *in vivo* findings showed that porous high molecular weight $P_{DL}LA$ in combination with hydroxyapatite has the mechanical, biocompatibility and osteoinductive characteristics required, and out performs all other polymers (as well as the control allograft) under test. This work therefore provides a platform from which up-scaled (ovine) models can be planned prior to eventual clinical translation.

The following chapters will focus on overcoming the translational issues surrounding these tissue engineered scaffolds as well as up scaling these findings via an ovine femoral condylar defect model.

Chapter 6

The effects of setting bone cement on tissue engineered bone graft; overcoming barriers to clinical translation.

I am grateful to Mr Matthew Purcell (University of Nottingham) for kindly providing the scaffolds under test, and to Mr James Smith for his help with the design of the experimental protocol, as well as technical assistance when combining the allograft with the cement. I am also grateful to Mr Nicholas Evans and Dr Alex Dickinson for their assistance with the temperature analysis of the setting cement.

The work detailed in this chapter has been published:

Tayton E, Smith J, Evans N, Dickinson A, Aarvold A, Purcell M, Howdle S, Dunlop D, Oreffo ROC.

The Effects of Setting Bone Cement on Tissue-Engineered Bone Graft: a Potential Barrier to Clinical Translation?

The Journal of Bone and Joint Surgery, 2013, 95, (8), 192-197.

6.1 Introduction

The previous chapters have detailed the development of polymers (Chapters 3+4) and polymer composites (Chapter 5) that are specifically tailored for use in IBG, and both the *in vitro* and *in vivo* trials showed encouraging results for potential clinical translation of these polymers.

The beneficial effects of the addition of SSCs to allograft has already been proven via both *in vitro* and *in vivo* impaction bone graft (IBG) models in terms of improving aggregate shear strength, increasing new bone formation and improving vascularisation (Bolland *et al.* 2006;Korda *et al.* 2008). This technique has been successfully translated into a small cohort of patients undergoing core decompression procedures for avascular necrosis of the femoral head (Tilley *et al.* 2006). Application has been made for a multicentre trial (including Southampton General Hospital), to compare the efficacy of allograft seeded with SSCs against the current gold standard of allograft alone.

There remain however important differences between experimental models and the actual clinical application of tissue engineered materials, and these need to be addressed prior to the incorporation of novel technologies, to ensure optimal and successful implementation. As described in the introduction and depicted in Figure 1.10 and 1.11, the IBG process involves building a new layer of cortical bone from impacted allograft to replace the lost bone stock and to provide a stable base into which an implant can be inserted (Figure 6.1).

The next stage of the procedure involves the injection, and pressurisation of bone cement into the newly created femoral medullary canal, followed by the insertion of the definitive prosthesis (Figure 6.2). The curing process of the cement involves a significant exothermic reaction (Anselmetti *et al.* 2009).

Figure 6.1: Clinical photograph showing the IBG procedure. Figure 6.1A depicts the proximal femur transversely. A wire mesh has been used to surround the extremely thin shell of cortical bone. Figure 6.1B shows the same femur after the IBG procedure. The cortical bone has been reinforced with allograft and the medullary canal recreated such that a new implant can be inserted.

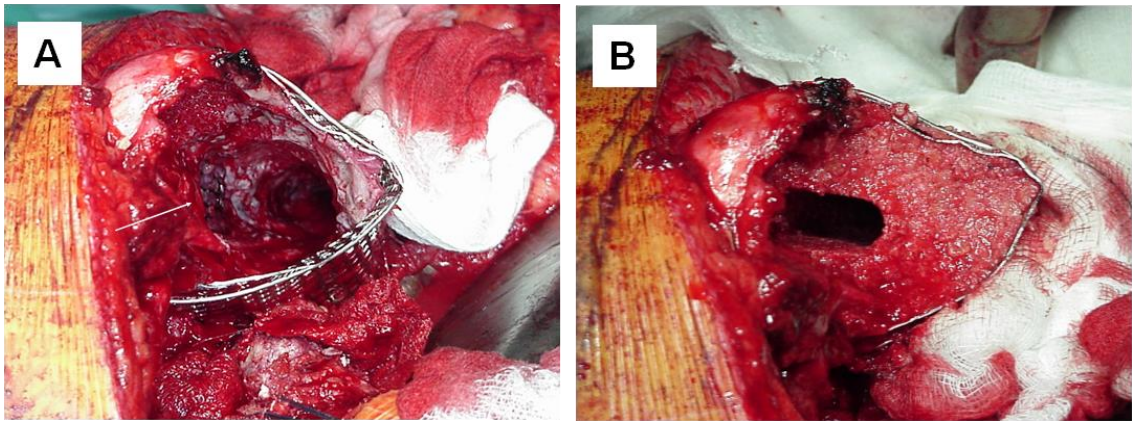

Figure 6.2: Injection of the femoral canal with cement prior to insertion of the prosthesis.

Thus in revision arthroplasty, a possible pitfall to the successful implementation of tissue engineered allograft and polymers in IBG involves the potential damaging

exothermic effects of setting bone cement to the SSCs in the near-by vicinity, as would occur during the fixation of the femoral stem.

Laponite is a novel clay-gel from the Smectite Group (Neumann and Sansom 1971), that has been shown to support SSCs, and to provide beneficial microenvironments for ongoing proliferation and differentiation. In the clinical situation it could potentially provide the cell nutrition required prior to host vascular ingrowth, reducing cell loss in tissue engineered constructs (Dawson *et al*. 2011;Dawson and Oreffo 2013). If SSCs are damaged by the cement curing process, it is possible that the addition of laponite to the graft may also protect the cells due to the insulating properties of the clay-gel.

6.2 Aim

The purpose of this study was to investigate the effects of setting bone cement on both tissue engineered SSC / allograft composite and a novel SSC / polymer composite designed for translational use in IBG. A second stage of the experiment entailed investigating potential methods (including the addition of laponite) to reduce the damaging exothermic effects of the cement on the SSCs.

6.3 Null hypotheses

6.3.1

The exothermic reaction caused by the setting of bone cement has no effect on a surrounding tissue engineered construct.

6.3.2

The addition of laponite to SSC seeded graft, pre-cooling the graft, or a combination of the two methods has no effect on cell survival when exposed to the exothermic effects of setting bone cement.

6.4 Materials and Methods

6.4.1 Cell culture

Bone marrow was obtained from fully consented patients undergoing a routine total hip arthroplasty at Southampton General Hospital with local hospital ethics committee approval (LREC 194/99/w 27/10/10). The cells used in the first stage of the study were from an 89 year old male (M89) and the cells used in the second stage of the experiment were from a 66 year old male (M66). Progenitor cells were extracted as described in Section 2.2.2, and then culture expanded on standard tissue culture plastic (T150) flasks in basal media and incubated at 37 ºC in 5 % CO_2, with phosphate buffered saline (PBS) washes and media change every 3-4 days. Upon confluence the cells were released using trypsin in ethylene diamine tetra-acetic acid (EDTA), suspended in basal media, centifuged at 1100rpm for 4 minutes, and the supernatant discarded. The remaining cell pellet was re-suspended in basal media to give a concentration of 5×10^5 cells / ml, as determined by a haemocytometer.

6.4.2 Allograft preparation

Femoral heads were obtained with patient consent and under local hospital ethics committee approval from patients undergoing total hip arthroplasty (LREC 194/99/w 27/10/10) and were defatted, milled and prepared as described in Section 2.3. The resulting allograft was then submerged in 5x antibiotic solution, and placed under a UV light for 24 hours to ensure sterility, prior to further 24 hour incubation in basal media.

6.4.3 Polymer preparation

The previous work detailed in this thesis had identified high molecular weight poly (DL-lactide) ($P_{DL}LA$) in combination with 10% hydoxyapatite (HA) to have desirable characteristics for potential translation as an allograft alternative in IBG. The polymer was obtained from SurModics Biomaterials (Birmingham, USA) in powder form and porous scaffolds were produced using a novel supercritical CO_2 foaming technique as detailed in Section 5.4.2. Samples were then milled and sterilised in 5x antibiotic solution and 24 hours U.V. light exposure, followed by further 24 hours incubation in basal media.

6.4.4 Allograft / polymer seeding

The basal media was removed from both the milled allograft and polymer, and the cell suspension added at a ratio of one millilitre solution to one millilitre of allograft / polymer. The composites were then incubated for 2 hours (37 ºC, 5 % CO_2) in universal tubes, with gentle agitation every 20-30 minutes in order to allow diffuse cell adhesion. For the first stage of the experiment the seeded allograft / polymer was used immediately for experimentation, as would be the case when applied clinically. For the second stage of the experiment the seeded allograft and polymer were transferred to individual wells of 6 well plates (approximately 2-3 ml of each per well), and incubated in basal media at 37 ºC, 5 % CO_2, with standard PBS washes and media changes every 3-4 days until the cells reached confluence at approximately 14 days. Cell numbers involved for experimentation were thus higher, and hence any beneficial effects on cell survival of pre-treatment methods would be more pronounced and critically detectable and quantifiable.

6.5 Study 1

A protocol for the methodology used in Study 1 is shown in Figure 6.3. Sixteen 5ml syringes were customised such that the tips were removed, and markings were made at 5 mm intervals longitudinally. Eight of these were filled to the 20 mm mark with SSC (M89) seeded allograft (Group 1), and eight with SSC (M89) seeded polymer (Group 2). Cement was prepared (Surgical Simplex P, Stryker, Newbury, UK) as per manufacturers protocol and was placed in four of the syringes of each group in apposition with the graft prior to setting such that a cement mantle of 5 mm was created. The syringe plunger was then used to apply a compressive force to the cement against the graft, in order to mimic the compression that occurs during cement pressurisation and as an implant is placed into the proximal femur during IBG (Figure 6.4A). Simple pressure was applied to the plunger with the thumb blocking extrusion of cement. Roughly equal pressures were applied but there was no formal standardisation of this process. The graft containing syringes were placed into a custom made polystyrene holder, such that the heat from the setting cement was directed towards the SSC seeded graft. The remaining four syringes from each group were used as positive controls. The cement was moulded into cylinders, allowed to set and cool, and then placed in apposition with the seeded allograft and polymer such that the SSCs were not exposed

to the exothermic reaction. The syringes were then separately submerged in basal media prior to analysis.

Figure 6.3: Diagram displaying protocol for Study 1.

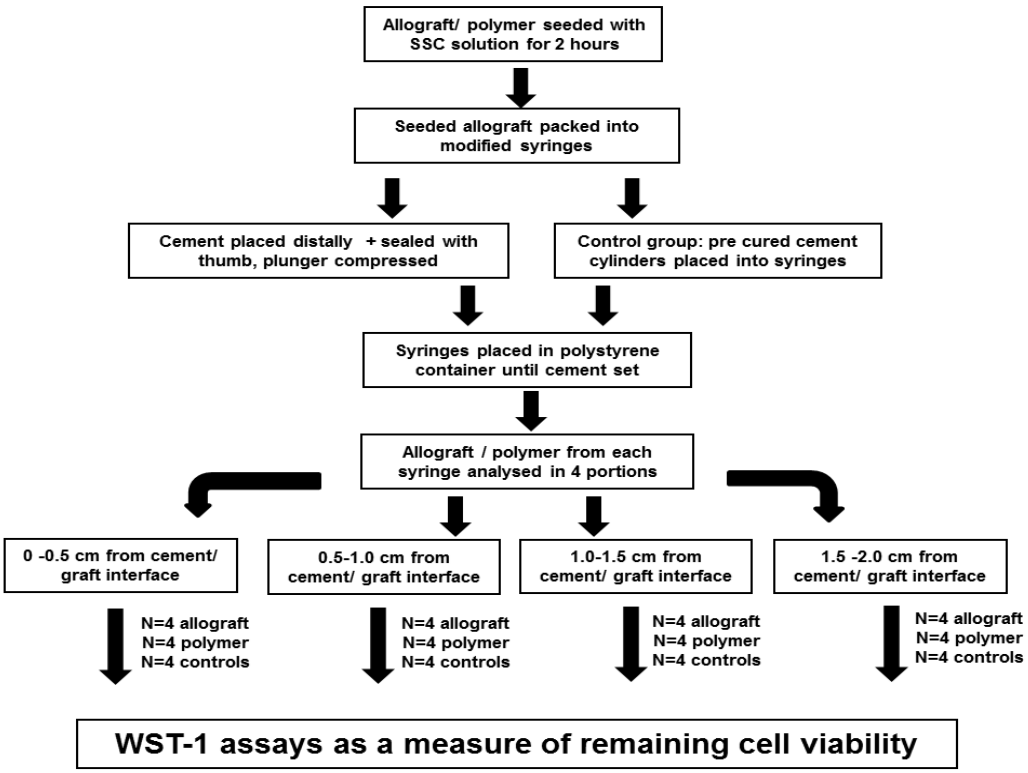

Figure 6.4: Addition of cement to SSC seeded constructs. A) Photograph demonstrating the compression procedure of the allograft onto the curing bone cement by using the syringe plunger (study 1), B) Placement of cement into a modified EM pot containing SSC seeded allograft as described in Study 2.

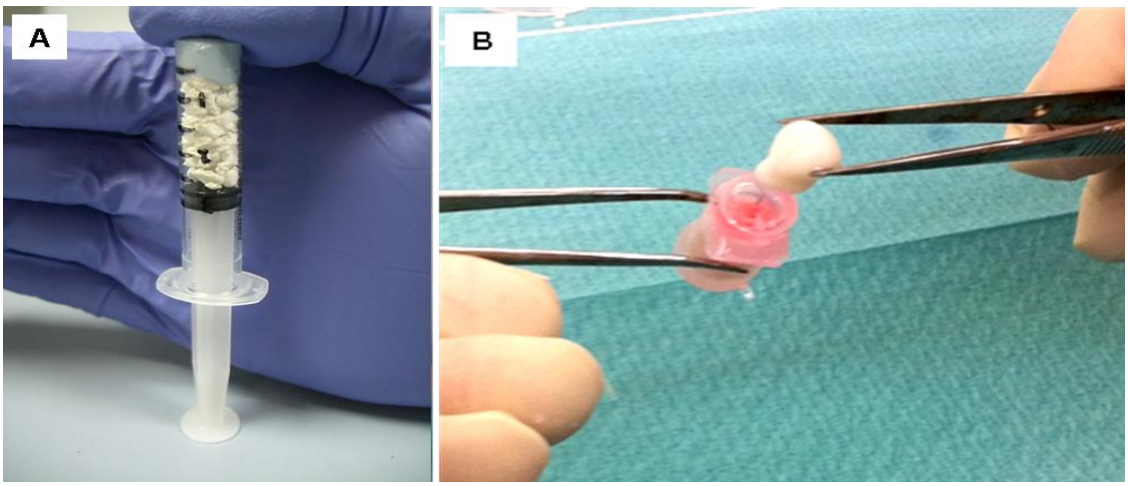

6.5.1 Assessment of cell viability

6.5.1.1 WST-1 cell proliferation assay

After one hour (the time required for experimental setup) the contents of the syringes were analysed. The plungers were used to expel the graft in 5 mm incremental distances from the cement graft interface. Each 5 mm section was analysed separately such that the exothermic effects of the cement could be quantified by distance. This would provide a range from the cement that resulted in 50 % cell survival (LD 50). The graft from each section was submerged in 2 ml 1:10 dilution WST-1 substrate (Roche ltd, Welwyn Garden City, UK). Blank WST-1 samples were run in parallel (negative controls). At 4 hours, 3 x 100 µl substrates were removed from each test section (4 test sections per 5mm increment) and analysed via a Bio-Tek KC4 microplate fluorescent reader (Bio-Tek, USA) at 410 nm. An increase in absorbance value (i.e. increase in optical density of the substrate) indicated increased cell number and viability. The mean absorbance value was then calculated for both the allograft and the polymer at each 5 mm incremental distance from the cement / graft interface, the mean negative control WST-1 absorbance value subtracted, and statistical comparison (one way ANOVA) made with the mean positive control values.

6.5.1.2 Standard Curve

In order to calculate a LD 50 distance a standard curve for the WST-1 assay was established using the same (M89) cell line. Known numbers of cells were seeded into individual wells of a twelve well plate in 1 ml basal media. One millilitre of 1:10 dilution WST-1 reagent was added and 3 x 100 µl of substrate was removed at 4 hours, read as described previously and the mean absorbance value calculated. After subtraction of the negative control value a change in absorbance value could be related to a known cell number and hence the distance (in 5 mm increments) from the cement graft interface, at which 50% of the cells survived the exposure, calculated.

6.5.2 Temperature assessment

A supplemental test was conducted to assess the temperature profile through the graft as a function of the distance from the cement-graft interface. As before, 2.5 ml syringes

were loaded with graft material up to 5 mm from the open end, and instrumented using K-type thermocouple wires (RS Components Ltd., Corby, UK). Thermocouples were placed to measure the temperature at four locations throughout bone cement curing: in the cement, 5 mm, 10 mm and 15 mm above the cement-graft interface. Data was recorded using a Micro-Measurements 7000 Series Data Acquisition System and StrainSmart® Software (Vishay Measurements Group UK Ltd., Basingstoke, UK), at a sample rate of 10Hz. The cement was mixed and introduced to fill the remaining 5mm of the syringe after 2 minutes when doughy, and pressed in with light thumb pressure. The syringe was then pressed into a block of expanded polystyrene for thermal isolation, and data was recorded for 20 minutes, at which point a temperature peak associated with cement curing had been recorded by all thermocouples. The experiment was repeated in triplicate for both PLA and allograft specimens.

6.6 Study 2

A protocol for the methodology used in Study 2 is shown in Figure 6.5.

Figure 6.5: Diagram displaying protocol for Study 2.

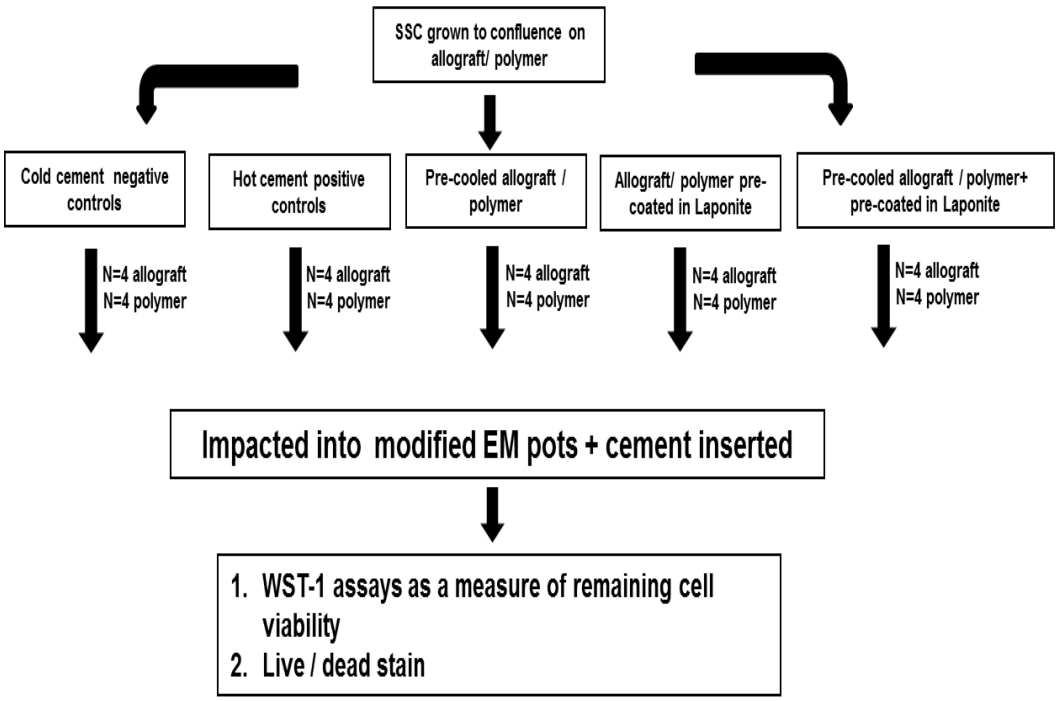

Having established the effects of setting bone cement on tissue engineered constructs, changes to pre-treatment protocols were initiated in an attempt to reduce the toxicity. A modified experiment was designed due to the increase in experimental groups and to maintain all grafts in close proximity (< 10 mm) to the cement / graft interface, after which distance negligible loss of cell viability was observed (established by Study 1). Cells were grown to confluence on milled polymer and allograft as previously described, before being impacted into modified electron microscopy (EM) pots (1 ml volume). A total of 20 pots of allograft and 20 pots of polymer, were subsequently divided into 5 groups of 4 pots. One group was treated as a negative control group, and these were subjected to cold, pre-set cement only. A second group acted as a positive control, and these had 0.5 ml of mixed cement added to the EM pot (Figure 6.3), which was subsequently allowed to set via its normal exothermic reaction. A third group of 4 pots acted as the first of the treatment groups. These pots were pre-cooled to 5 ºC for one hour prior to cement exposure as in Group 2. The allograft/ polymer from the fourth group were dipped in 1 % laponite (a bioactive clay with the potential for protecting the cells) prior to setting cement exposure, and a final group was both cooled to 5 ºC for one hour and dipped in 1% laponite prior to cement exposure.

6.6.1 Cell Viability

6.6.1.1 Live/ dead immunostain

Small portions of polymer were taken from the graft cement interface and at a 10 mm distance, in order to illustrate visually the effects of the setting bone cement. Samples were incubated for 90 minutes in 5 ml of standard Cell Tracker Green probe (CTG)/ Ethidium homodimer (EH-1) solution (10 µg / ml CTG, 5 µg / ml EH-1, Invitrogen, Life technologies ltd, Paisley UK) as described in Section 2.10. They were then fixed in ethanol and stored in PBS prior to imaging under confocal microscopy (Leica SP5 Laser Scanning Confocal Microscope and software, Leica Microsystems, Wetzlar, Germany).

6.6.1.2 WST-1 assay

Cell viability was tested using a WST-1 cell proliferation assay. After one hour incubation in basal media post cement exposure, the contents of each of the EM pots were removed, and placed individually into 1 ml of 1:10 dilution WST-1 substrate (Roche ltd, Welwyn Garden City, UK). At 4 hours incubation, 3 x 100 µl of substrate was removed and analysed using a Bio-Tek KC4 microplate fluorescent reader (Bio-Tek, USA) at 410 nm. After subtraction of the blank WST-1 absorbance values, mean and standard deviations in optical densities were calculated for each of the treatment groups, and compared to the controls.

6.7 Statistical Methods

All experimental groups were replicated four times, and statistical comparison was made using one way ANOVA tests with post hoc Bonferroni analysis (SPSS ver. 17.0), with $p < 0.05$ taken to be significant.

6.8 Results

6.8.1 Study 1: cell viability

Mean cell viability as measured by an increase in optical density using a WST-1 assay was observed to rise as distance from the cement bone interface increased in both the SSC seeded allograft (Figure 6.6) and the SSC seeded polymer (Figure 6.7) groups. The effect was more pronounced in the allograft group. In the allograft group there was a reduction in mean optical density (OD) compared to the control group of 84 % between 0 - 5 mm from the cement bone interface and 48 % between 5 -10 mm although this was only statistically significant between 0 - 5 mm (*One way ANOVA*, $p < 0.01$ (Table 6.1)).

Figure 6.6: Graph showing mean optical density values (± SD, n = 4) of WST-1 substrate after 4 hours incubation with each 5 mm section of SSC seeded allograft post cement exposure (* $p < 0.05$, Control = pre-cured cement at ambient temperature).

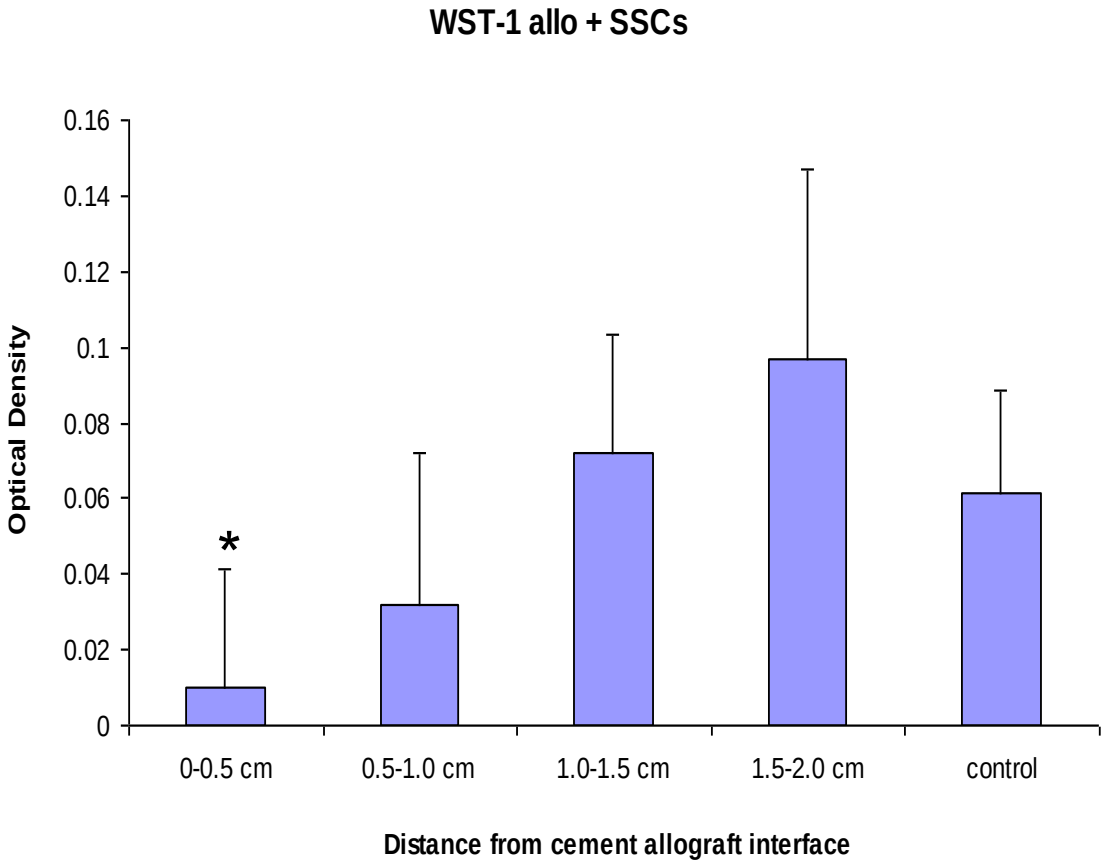

Table 6.1: Mean optical density value (+ SD, n = 4), percentage comparison to control and significance (one way ANOVA) value of each 5 mm section of SSC seeded allograft post cement exposure.

Distance	Optical Density ± SD (n=4)	Percentage control (%)	P value (*One way ANOVA*)
0 - 5 mm	0.01 ± 0.03	16	<0.01 *
5 - 10 mm	0.03 ± 0.04	52	0.26
10 - 15 mm	0.07 ± 0.03	117	0.62
15 - 20 mm	0.09 ± 0.05	158	0.26
Control	0.06 ± 0.02	N/A	N/A

When relating absorbance values to actual cell numbers via the standard curve (Figure 6.8) it could be seen that the mean control value (OD = 0.06) related to approximately 38000 cells. In comparison, the value for 0 - 5 mm from the cement graft interface (OD = 0.01) related to approximately 4000 cells, the value for 5 - 10 mm from the cement graft interface (OD = 0.03) related to approximately 18,000 cells, whereas that for 10 - 15 mm (OD = 0.07) related to over 40,000 cells. There was thus no measurable loss of cells between 10 - 15 mm compared to controls and hence in this experiment the LD 50 distance was observed to lie between 5 mm and 10 mm from the cement graft interface.

In the polymer group there was a reduction in mean OD compared to the control group of 32 % between 0 - 5 mm from the cement bone interface and 16 % between 5 - 10 mm (Figure 6.7) although these changes were not significant (Table 6.2).

Figure 6.7: Graph showing mean optical density values (± SD, n=4) of WST-1 substrate after 4 hours incubation with each 5 mm section of SSC seeded polymer post cement exposure.

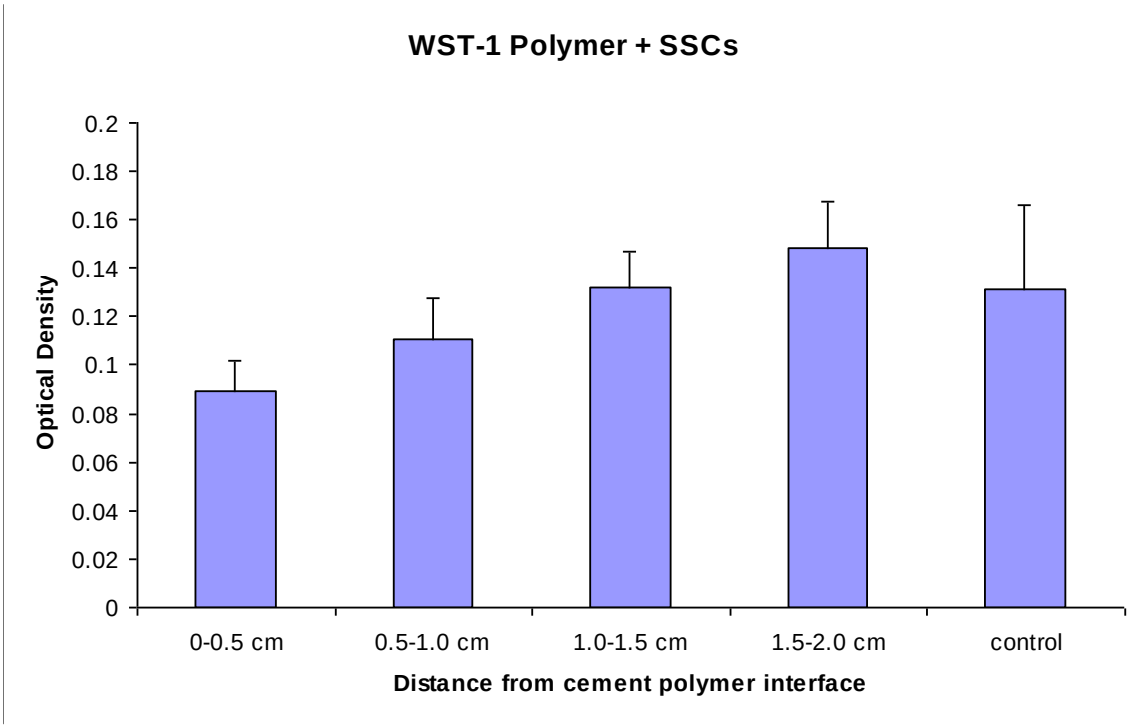

Table 6.2: Mean optical density value (SD), percentage comparison to control and significance value of each 5 mm section of SSC seeded polymer post cement exposure.

Distance	Optical Density ± SD (n=4)	Percentage control (%)	P value (*one way ANOVA*)
0 - 5 mm	0.09 ± 0.01	68	0.06
5 - 10 mm	0.11 ± 0.02	84	0.31
10 - 15 mm	0.13 ± 0.01	100	0.97
15 - 20 mm	0.15 ± 0.02	113	0.42
Control	0.13 ± 0.03	N/A	N/A

When relating absorbance values to actual cell numbers (Figure 6.8) the mean control value (OD = 0.13) related to approximately 90,000 cells, the value for 0 - 5 mm for the cement graft interface (OD = 0.09) related to approximately 59,000 cells. Thus in this group the LD 50 distance was noted to lie between 0 mm and 5 mm from the cement graft interface.

Figure 6.8: Graph showing standard curve for mean optical density values (± SD, n = 3) of WST-1 substrate after 4 hours incubation with M89 cells of increasing number. Black line = best fit.

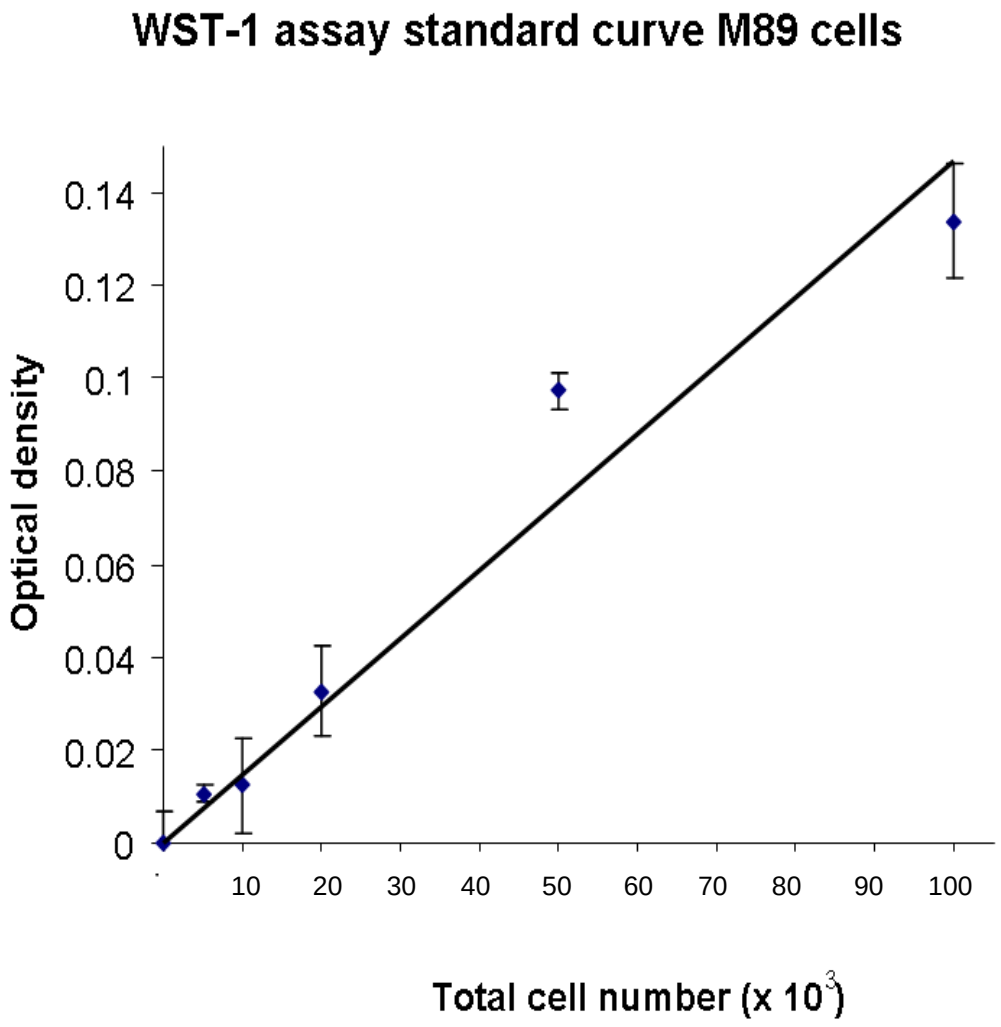

6.8.2 Temperature assessment

A typical graph displaying change in temperature against time for each of the 5 mm increments as the cement cured is displayed in Figure 6.9, and the mean increase in temperature values for these locations are shown in Table 6.3. Temperatures in excess of 75 ºC were measured within the cement mantle, confirming the exothermic reaction of the polymerisation process to be sufficient to cause localised cellular damage. However, in keeping with the results of the cellular experiments, there was only a moderate mean temperature rise (9.1 ± 3.9 ºC PLA and 8.4 ± 3.8 ºC Allograft) at a distance of 5 mm from the cement, and negligible temperature rises at distances further than this.

Figure 6.9: A typical graph displaying temperature change against time at incremental distances from the cement in one of the polymer specimens during the curing process.

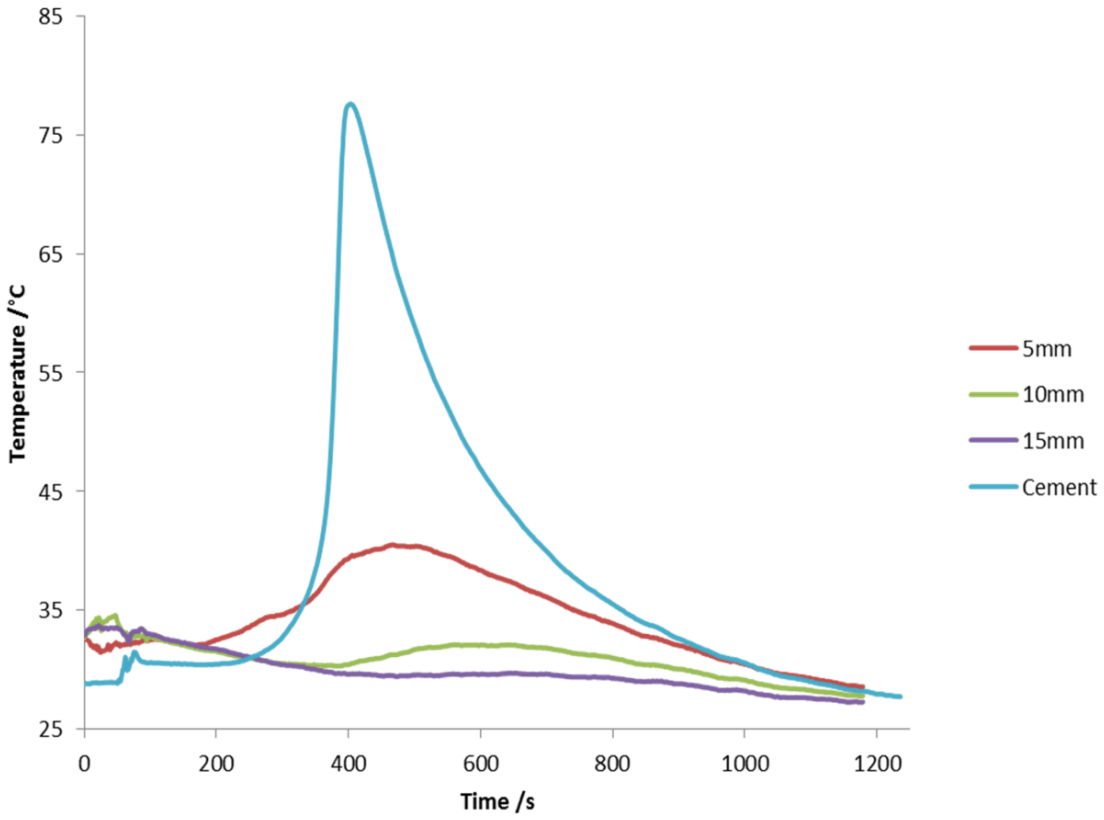

Table 6.3: Displaying mean maximum (±SD) temperature rise at the cement and at 5mm incremental distances in both the polymer and allograft constructs during the curing process.

	Mean temperature rise (°C)	
	PLA	**Allo**
Cement	49.6 ± 1.6	51.3 ± 3.8
5 mm	9.1 ± 3.9	8.4 ± 3.8
10 mm	2.9 ± 0.1	2.8 ± 2.1
15 mm	1.3 ± 0.6	0.6 ± 1.3

6.8.3 Study 2

6.8.3.1 Live dead stain

Cell viability was examined using a standard live / dead stain. Samples were taken from the cement graft interface and at 10 mm distal. There was a reduction in the density of viable (green staining) cells at the cement bone interface and an increase in the number of dead or compromised (red) cells. One centimetre distal to the cement there was confluent live cell coverage, and very few dead cells observed (Figure 6.10).

Figure 6.10: Photomicrographs of allograft after CTG / EH-1 immunostain, demonstrating A) limited live (green) and multiple dead (red) cells at the cement bone interface (arrows = dead cells), and B) predominantly live (green) cells on the allograft 10 mm from the cement (scale bar = 200 μm).

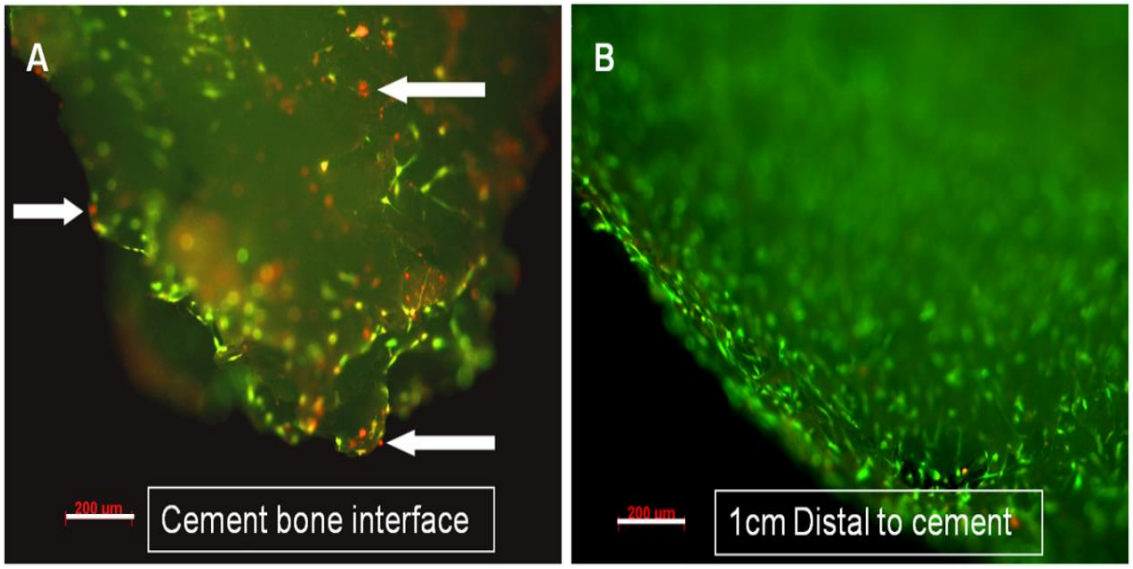

6.8.3.2 WST-1 assay

Mean cell viability as assessed using the WST-1 assay, showed a significant decrease in all groups when compared to that of the negative control group subjected to cold, pre-set cement only in the seeded allograft and polymer (Figures 6.11 and 12, $p < 0.05$). There was no significant increase in cell viability for any of the treatment groups compared to the positive control (hot cement only) group, indicating that none of the pre-treatment protocols effectively protected the cells from the exothermic and toxic effects of the setting cement. Interestingly, the addition of 1 % laponite actually appeared to significantly reduce cell activity on both the allograft and the polymer, in both the ambient temperature and pre-cooled forms ($p < 0.01$).

Figure 6.11: Graph showing mean optical density values (± SD, n = 4) of WST-1 substrate after 4 hours incubation with the pre-treated portions of allograft post cement exposure (* $p < 0.05$).

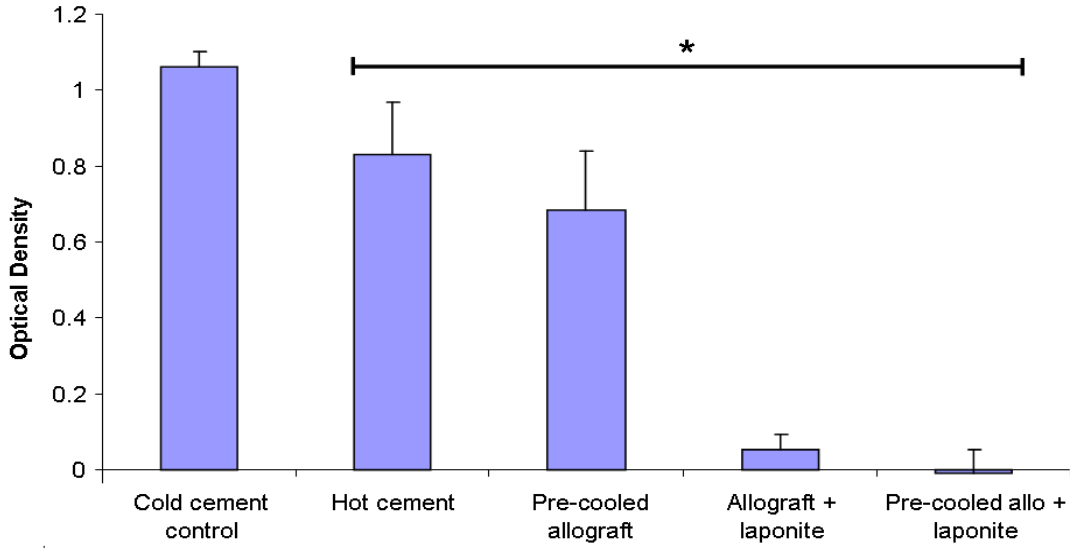

Figure 6.12: Graph showing mean optical density values (± SD, n = 4) of WST-1 substrate after 4 hours incubation with the pre-treated portions of polymer post cement exposure (* $p < 0.05$).

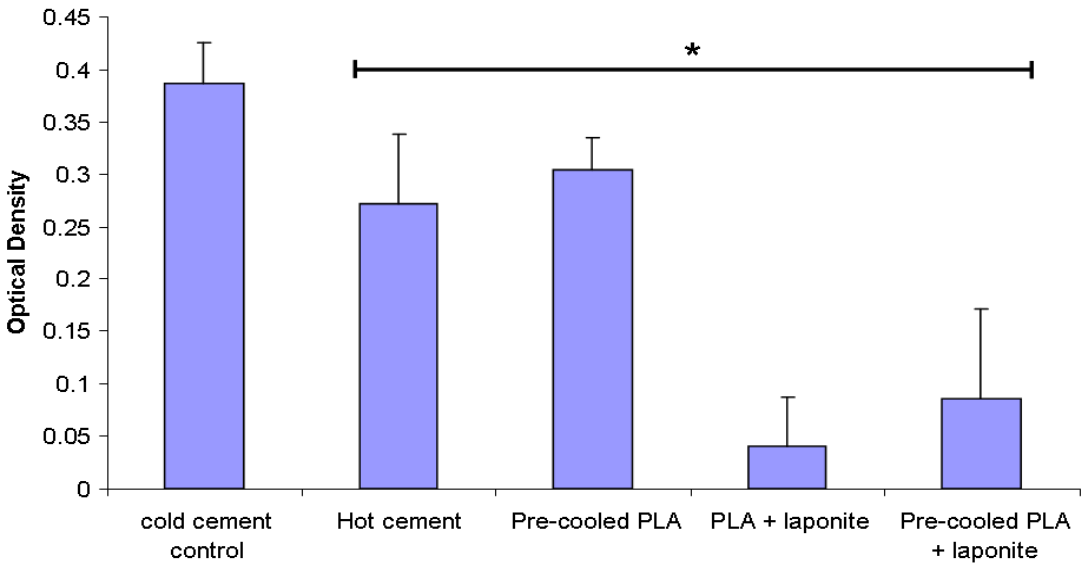

6.9 Discussion

The addition of skeletal stem cells to allograft for use in impaction bone grafting has been shown to enhance the cohesive strength of the allograft *in vitro*, as well as to improve vascularisation and bone formation *in vivo*, both in a murine and a scaled up ovine model (Bolland *et al.* 2006;Korda *et al.* 2008). However, none of these studies exposed the graft to the exothermic effects of bone cement, a factor used in the vast majority of clinical cases, especially when implanting the femoral component (Halliday *et al.* 2003). This *in vitro* study has examined the impact of setting bone cement on two skeletal stem cell seeded constructs, both of which have the potential for clinical translation. The present study demonstrated that there was a loss of cell viability associated with the rise in temperature as occurs during cement polymerisation, but this only occured significantly within 5 mm of the cement graft interface. Only one (unpublished) study has to our knowledge addressed the question of SSC heat tolerance before, whereby cell cultures were exposed to cell media of increasing temperatures for differing time periods, and assessed for viability (Reissis *et al.* 2011). The authors concluded that cells could survive exposure of up to 48 ºC for 150 seconds, which covers many situations in which cement is used, but over 58 ºC for the same incubation period, most cells die. The data from this study compliments this research, but adds a model more consistent with the clinical situation with the use of actual bone cement as the toxicant and cell seeded allograft for the analysis, and also allowed the calculation of quantitative distance for the harmful effects to occur.

Much related work has however previously been performed surrounding the use of bone cement in hip replacement / orthopaedic surgery. Due to the lack of actual adhesive bonding between cement and bone, third generation cementing techniques advise the use of pressurisation which allows cement to mechanically interlock into the bone lacunar and trabecular spaces (Oishi *et al*. 1994). Therefore not only cells at the initial cement bone interface are at risk of significant heat exposure, but also those in the surrounding bone into which the cement extrudes. *In vitro* impaction bone graft models have subsequently shown cement to penetrate the graft in a variable manner, but it can occur over the entire thickness of the graft up to the original endosteal surface (Frei *et al.* 2004). There are however large areas (especially in Gruen zones 1 and 7), where there is graft without cement penetration. This study attempted to mimic the

pressurisation procedure via the use of the syringe plunger, but clearly this was a limitation of the current experimental set up.

Analysis from cadaveric retrievals of patients previously undergoing IBG procedures using standard allograft, have shown allograft replacement by host bone around the periphery of the construct, but the central areas in close proximity to the cement consisted of necrotic bone and fibrous tissue only (Linder 2000;Ling *et al*. 1993). This current study indicated that this is still a possibility despite the addition of SSCs to any construct due to the high loss of cell viability in these regions. However, whilst reduced, these experiments demonstrated measurable cell viability within close proximity (5 mm) of the cement / graft interface (especially in the polymer graft substitute). The finding of continued viability indicated that the cellular components of the constructs were not completely destroyed, hence leaving the potential for cell colony recovery via subsequent surviving cell proliferation. It is not known whether the surviving cells retain the potential to divide or differentiate as a consequence of the heat exposure, and future experimentation is directed towards the investigation of these questions.

Actual cement mantle thickness can affect the final temperature obtained during the polymerisation process. A recent finite element analysis study attempted to correlate cement mantle thickness to surrounding thermal necrosis of bone, concluding that a 7 mm mantle (thicker than used in most standard practice) was required (Li *et al.* 2003). However this was a theoretical model, and failed to consider the relative frailty of the seeded SSCs in loose impacted bone as opposed to native bone.

In Study 2, attempts were made to protect the cells from the exothermic effects of the cement. None of the pre-exposure techniques produced a significant increase in cellular viability when compared to the positive controls, either in the allograft or the polymer groups. It was hypothesised that pre-cooling the construct to 5 ºC could potentially improve cell survival in two ways: i) if starting from a lower initial point, it is likely that the maximal temperature reached by the graft (and associated cells) would be lower, and hence fewer cells would perish and ii) a pre-stress to the cells for an extended period could initiate the production of protective proteins (eg heat shock proteins), which can have protective effects on cell survival in adverse conditions (Samali and Cotter 1996). This did not however appear to be the case; it is possible that the pre-cooling treatment itself damaged the cells irreversibly, or that the time period chosen was not sufficient

for the stimulation of the proteins. Furthermore, it is possible that an increased number of cells did survive the exposure, but were not as active as the cells not subjected to pre-cooling due to being in a different part of the cell cycle. It should also be noted that the cement graft interface was affected by the pre-cooling procedure, in that interdigitation was not as effective, and hence this method of potentially improving cell survival is not recommended.

Laponite is a novel smectite clay-gel with potential use in tissue engineering (Dawson *et al.* 2011). It was hypothesised that pre-coating the SSC seeded grafts in this substance could protect the cells due to an insulation effect. However, there was a significant loss in cellular viability in all groups pre-coated with laponite compared to the grafts exposed to the cement alone. It is possible that this additional loss in cell viability was a consequence of reduced effective gaseous exchange to the cells.

6.10 Conclusion

The results in the context of the null hypotheses were examined:

1. The exothermic reaction caused by the setting of bone cement has no effect on a surrounding tissue engineered construct.

This null hypothesis is **false.**

As the evidence supporting the use of tissue engineered constructs becomes more commonplace, the uptake into clinical practice is rapidly developing. Care is required in their incorporation into well established surgical procedures, to ensure that the processes involved are investigated to establish any detrimental action on the grafts subsequent function. The heat produced by polymerising bone cement has the potential to denature proteins and hence kill or attenuate cells. In this model, exothermic effects occurred significantly within 5 mm of the cement graft interface, but were not sufficient to terminate all cells in this region, hence leaving the potential for cell recolonisation.

2. The addition of laponite to SSC seeded graft, pre-cooling the graft, or a combination of the two methods has no effect on cell survival when exposed to the exothermic effects of setting bone cement.

This null hypothesis is **false.**

The results of these studies indicated that laponite had a detrimental effect on cell survival, and using the described protocols, should *not* be considered a potential method of protecting tissue engineered products from exothermic damage.

Studies that explore translational aspects of novel technologies are essential prior to clinical translation. Tissue engineering essentially involves the incorporation of living tissue constructs, and thus any processes (surgical or otherwise), which have detrimental effects on cell survival, must be kept to a minimum. Surgeons should be made aware of the relative frailty of the constructs, and specialist training would likely be of paramount importance before widespread use.

These studies indicated that, with care, the combination of SSCs with allograft and bone graft substitutes can be effectively implemented in procedures (such as IBG) involving cement.

Chapter 7

The scale-up of a tissue engineered porous hydroxyapatite polymer composite scaffold for use in bone regenerative procedures: an ovine femoral condyle defect study.

I am grateful to Mr Matthew Purcell (University of Nottingham) for kindly providing the scaffolds under test, and for assistance with the analysis of the specimens, to Mr James Smith for assistance with surgical procedures, to Dr David Johnston for assistance with confocal microscopy and to Dr Stuart Lanham for assistance with the μCT scans and analysis. I am particularly grateful to Professor Allen Goodship and Professor Gordon Blunn for their expert guidance in the design and execution of this study, as well as the use of the facilities both at the Royal Veterinary College and Stanmore. I would like to thank all members of their team, especially Miss Gillian Hughes, for help with the care, anaesthesia and recovery of the animals. I am also grateful to Dr Darren Fowler, consultant pathologist, for help with analysis of the lymph node specimens.

7.1 Introduction

Despite multiple novel basic science breakthroughs over the last decade, especially in the field of tissue engineering, there have been very few that have actually made the transition from the laboratory into clinical practice. Hollister *et al.* state that despite 25 years of research, funding totalling hundreds of millions of dollars, over 12,000 papers on bone tissue engineering (BTE) and over 2000 papers on BTE scaffolds alone in the past 10 years, "the translation of these therapies to clinical use remains, bluntly, a failure" (Hollister and Murphy 2011). This theoretical barrier to progress has been termed "the valley of death", and is present for a number of reasons, the most pertinent including: i) There is a dramatic increase in funding required to scale-up from relatively inexpensive small animal studies to large animal studies, ii) large animal studies are of paramount importance when considering bone regenerative strategies, and whilst small animal studies may have shown a particular technology to be encouraging, these traits may not be reproduced when scaled-up and a multitude of other confounding factors are introduced, iii) even if successful, there is a substantial funding requirement during the transition from product / technology development to regulatory approval and subsequently commercialization (Reichert *et al.* 2010). In addition, further issues may arise surrounding the scale-up and reproducibility of manufacturing processes, as well as the subsequent pre-clinical approval and undertaking of pilot and clinical trials. In a recent review article, Evans discussed the sociological elements surrounding tissue engineering, stating "perfect as the enemy of good" as a reason for poor clinical uptake of these strategies (Evans 2011). Evans states that given the multiple intersecting components (cells, scaffolds, morphogenic stimuli and bioreactors) required for successful tissue engineering, and the tendency amongst scientists to attempt to optimise each of these, the task becomes operationally unachievable.

A diagram displaying the multitude of hurdles to be overcome during the stepwise translation of novel technologies is displayed in Figure 7.1.

Figure 7.1: The collaborative tissue engineering ‘‘life-cycle.’’ The process is driven at all stages by informed allocation of funding (denoted by $). Reproduced from (Smith *et al.* 2011).

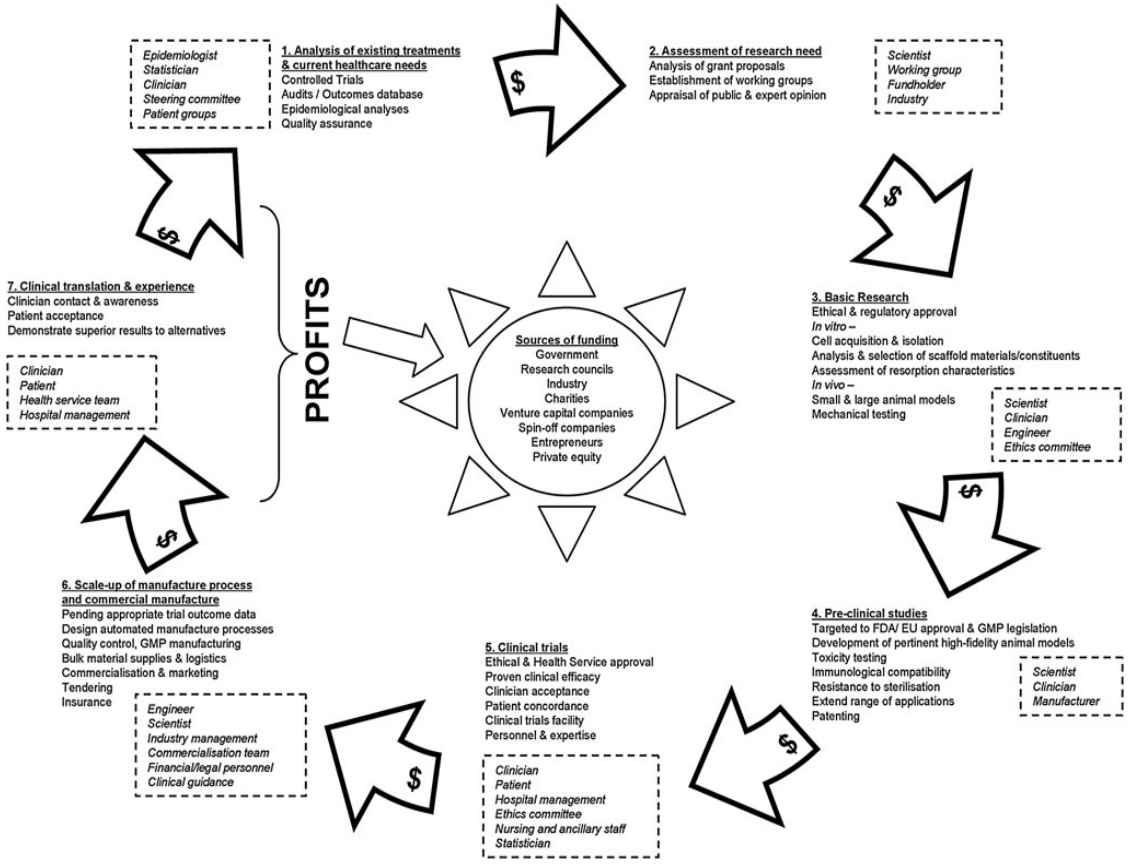

Despite the difficulties surrounding clinical translation, some strategies have been successfully brought to market. Recombinant human bone morphogenic protein-2 (rhBMP-2) has been the most commercially successful tissue engineered product to be used in orthopaedics, being used in up to 25 % of all spinal fusion procedures. InFUSE™ is a bone graft substitute which consists of genetically engineered rhBMP-2 along with a Type-1 (bovine) collagen scaffold. It has been combined with a spinal fusion cage and has gained FDA approval for use in lumbar spinal arthrodesis. This approval was based on the results of a prospective, randomised, multi-centre clinical trial in which 279 patients with degenerative disc disease were randomised to receive either the scaffold or autologous bone graft (Burkus *et al.* 2002). Based on computed tomography (CT) evaluation, the reported 2-year fusion rates were 94.5 % versus 88.7 % for the scaffold and autograft, respectively.

Autologous cartilage implantation (ACI) is also becoming more commonplace, especially in the treatment of cartilage defects in the knee, and is now also been trialled in other joints such as the ankle (Mitchell *et al*. 2009). As described in previous sections, the use of SSCs has also been shown to be of benefit in a cohort of patients in the treatment of fracture non-unions as well as being a useful adjunct to allograft in patients with AVN undergoing core decompression procedures (Hernigou *et al.* 2005a;Hernigou *et al.* 2009;Tilley *et al.* 2006). In addition, SSCs have been combined with carrier matrices in the treatment of cartilage defects. Haleem *et al.* have translated this to a small clinical series of five patients will full thickness cartilage defects of the femoral condyle (Haleem *et al.* 2010). Platelet-rich fibrin glue was used as a scaffold to deliver autologous culture-expanded bone marrow derived skeletal stem cells to the defect site. All patients' symptom scores improved significantly over the follow-up period of 12 months, and arthroscopic scores were essentially normal for the two patients who consented to arthroscopy after the procedure. MRI of three patients at 12 months postoperatively revealed complete defect filling and surface congruity with native cartilage, whereas MRI of two further patients showed incomplete congruity. Wakitani *et al*. treated two patients with a patellar cartilage defects with collagen gels containing SSCs, which were subsequently covered with a periosteal flap (Wakitani *et al.* 2007). Fibrocartilaginous filling of the defects was found after 1 year, and both patients showed significantly improved clinical outcomes. However, despite these encouraging case series, the combination of SSC with carrier modalities has certainly not had widespread uptake.

As indicated to earlier, the use of large animal models is essential when investigating bone regenerative strategies. Whilst small animal studies can be of some use when investigating osteogenic potential of constructs, as well as allowing an array of substances to be tested relatively cheaply and quickly, there are a number of essential factors which are severely compromised, and need careful consideration when interpreting any findings. In 1892, Julius Wolff noted that external forces have an impact on skeletal form: "Every change in the form and function of bones, or of their function alone, is followed by certain definite changes in their internal architecture and equally definite secondary alteration in their external conformation, in accordance with mathematical laws" (Wolff J 1986). This law has not been superseded today, and thus any small animal model either ignores, or has significant limitations to this fundamental

issue, when comparing any force experienced within a small animal such as a mouse or rabbit, to those experienced by certain bones in humans. Furthermore, the amount of new bone produced, or distance of any bone defect bridged in a small animal model is not usually of significance in a larger animal, and given that cell size does not proportionally increase as animals increase in size, it is not appropriate to assume that bone bridging distance or bone volume production will increase proportionally either. Other issues surrounding distance and time for ingrowth of blood vessels, and the related survival of any pre-seeded cells are not typically addressed by small animal models.

Traditionally, animals used as appropriate sized models in orthopaedic research have included pigs, goats, horses and sheep (Newman *et al*. 1995;Reichert *et al*. 2010). Goats and sheep are most commonly used for bone regenerative research, due to their comparable body weight, and dimensions of long bones allowing for the use of human implants and fixation techniques, whereas horses are useful for cartilage repair strategies, due to the thick cartilage layer in the equine knee (Chu *et al*. 2010;Reichert *et al*. 2010). The availability, cost, nature and ease of husbandry of sheep make them particularly popular (Muschler *et al.* 2010).

7.2 Aim

The purpose of this investigation was to compare the osseointegration and bone regenerative capacity of the previously identified optimal polymer composite ($P_{DL}LA$ + 10 % HA) both with and without the addition of SSCs in a scaled-up ovine critical sized femoral condyle defect model.

7.3 Null Hypotheses

1. There is no difference in the bone regeneration between either of the composite polymers or the (historical) empty femoral condyle defect controls.
2. There is no difference in the bone regeneration or the osseointegration of the polymer composite with and without the addition of SSCs.

7.4 Materials and Methods

A timeline depicting the important stages of the study is given in Figure 7.2.

7.4.1 Sheep selection

Six healthy skeletally mature (>2 years old) Welsh mule ewes weighing between 60 and 90 kg were obtained, vetted and acclimatised in a barn for at least four weeks prior to use. This was a common and standard sheep breed, previously used by the senior author (A.G), with docile characteristics and body weight comparable to humans.

Figure 7.2: Timeline depicting the stages of the study. A) Aspiration of iliac crest, B) SSCs grown to confluence *in vitro*, C) scaffold seeded with each sheep SSCs in universal tubes.

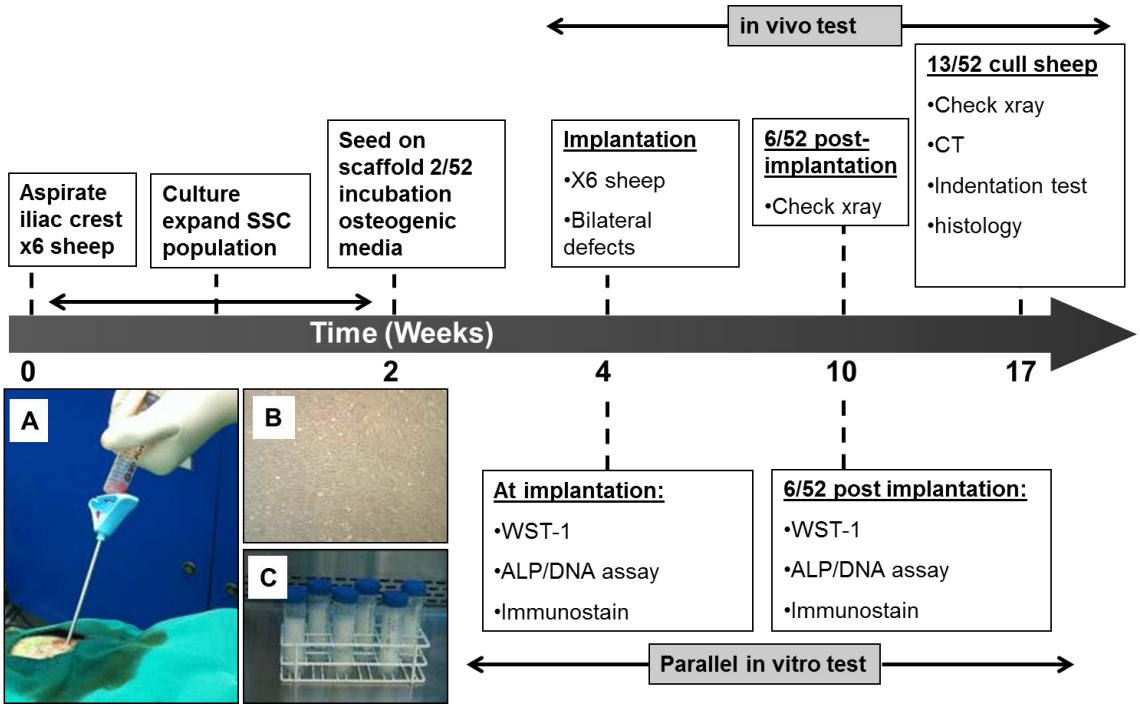

7.4.2 General anaesthesia

All sheep underwent general anaesthesia prior to any interventional procedure, which followed a routine protocol (Appendix 4). Premedication consisted of 0.1 mg/kg intramuscular xylazine injection (Rompun, Bayer PLC, Bury St Edmunds, UK) and the prophylactic antibiotic 5mg sodium cefalexin (Ceporex, Schering-Plough, Welwyn Garden City, UK).

Anaesthesia was induced using 2.5 mg intravenous (IV) Midazolam (Hypnovel, Roche, Welwyn Garden City, UK) and 2 mg/kg IV ketamine hydrochloride (Ketaset, Fort Dodge Animal Health Limited, Southampton, UK). The sheep were then intubated, and general anaesthesia was maintained using inhaled isoflurane, oxygen and nitrous oxide (Figure 7.3).

Figure 7.3: General anaesthesia of sheep. A) Intubation, B) fully anaesthetised sheep maintained on inhaled isoflurane, oxygen and nitrous oxide.

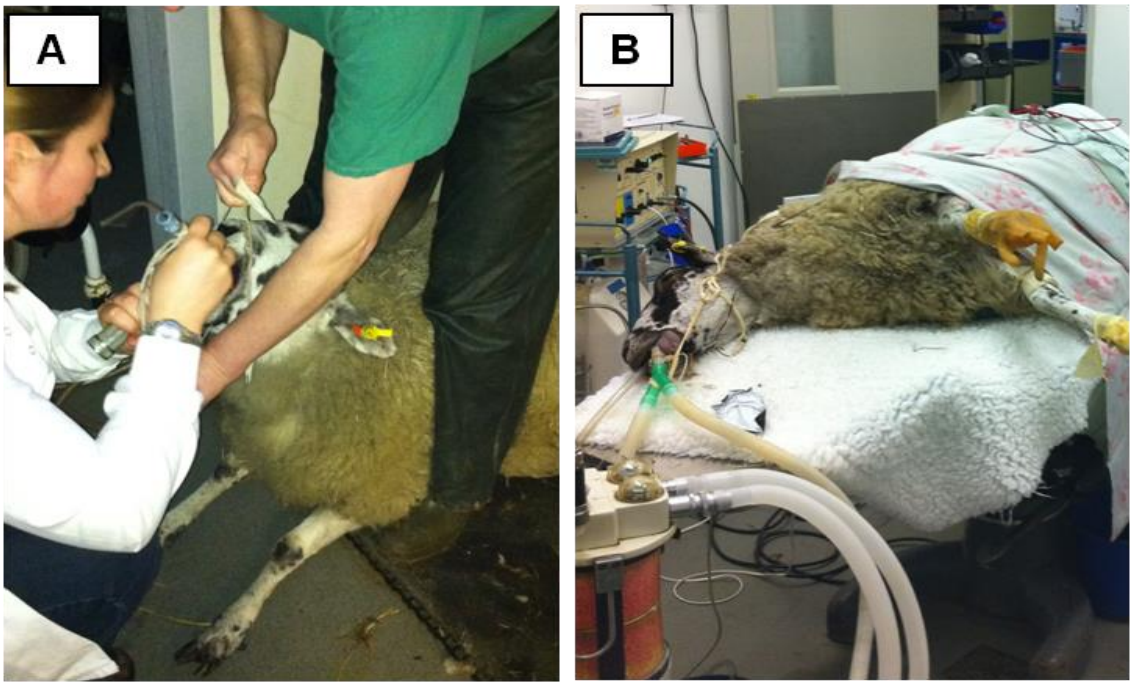

7.4.3 Harvest of skeletal stem cells

Once fully anaesthetised the sheep were placed in the left lateral position. An area measuring approximately 200 mm x 200 mm directly over the iliac crest was shaved and thoroughly cleaned using 10 % povidone-iodine (betadine) solution followed by 2 % chlorhexidine gluconate solution. A trochar was then inserted through the cortical bone (Figure 7.2A), and approximately 5 – 10 mls aspirated. The aspirate from each sheep was then placed into a separate universal container and into a cool box for transportation to the laboratory. The sheep were then recovered, and given analgesia as required. Sheep were housed in a barn, penned and fed standard food until further use.

7.4.4 Expansion of SSC populations

Ten millilitres of basal media (α-MEM with 10% fetal calf serum with additional 1% penicillin and streptomycin) was added to the universal tubes containing the aspirates, and the resultant solutions were put through 70 μm filter cell strainers and into a separate universal containers. The resultant cell solutions were then put into a balanced centrifuge, and spun at 1100 rpm for four minutes. The supernatants were carefully poured off and the cell pellets re-suspended in 40 ml basal media. These solutions were then placed into four T75 tissue culture flasks (10 ml per flask), incubated at 37 ºC in 5 % CO_2 until confluent (Figure 7.2B). Cells were washed in PBS and media changes were repeated every 3–4 days. When required for further experimentation the cells were released using using 10% trypsin in ethylene diamine tetra-acetic acid (EDTA). The trypsin was neutralised via the addition of basal media, and cell pellets obtained via centrifugation (1100 rpm for four minutes). The supernatants were carefully poured off, the cell pellets resuspended in basal media and the total counts determined using a haemocytometer. Appropriate dilution with basal media was then given such that the concentration was 5 x 10^5 cells / ml.

7.4.5 Scaffold Seeding

The polymer composite ($P_{DL}LA$ + 10% HA) was produced, milled and sterilised as described in Section 5.5.2. Twenty millilitres of each of the cell solutions was added to 20 mls of the polymer in a universal container (Figure 7.2C), and placed into an incubator (37ºC, 5% CO_2) for 2 hours, with gentle agitation every 30 minutes, in order to allow diffuse cell adhesion. The solution was then aspirated and discarded. The seeded scaffold was then placed into individual wells of a six well plate, and cultured in osteogenic media (basal media + 100 μM ascorbate-2-phosphate, and 10 nM dexamethasone) for 14 days, with PBS washes every 3-4 days.

***In vivo* ovine study**

7.4.6 Operative procedure

Twelve hours prior to surgery the sheep were given two analgesic Fentanyl patches (75mcg/hr) and were randomised to receive scaffold + SSC or scaffold alone to either the right or left side. The sheep underwent full general anaesthesia as described in Section 7.4.2. They were placed in the supine position, with surgical gloves placed over their hooves. The hind legs were both secured to the operating table with rope, shaved, and cleaned thoroughly using 10% povidone-iodine (betadine) solution followed by 2 % chlorhexidine gluconate solution. Each sheep was then covered with sterile drapes such that only the surgical sites were exposed. Ten centimetre longitudinal incisions were made centred over the palpable bony protuberances located on the medial sides of the medial femoral condyles of each leg, with careful dissection through subcutaneous tissue, fascia, muscle and periosteum to expose the underlying bone. A customised 8mm drill bit was then used to create a hole with a consistent depth of 15 mm into the underlying cancellous bone (Figure 7.4 A + B). After the hole was created a reamer was used to give the hole a flat bottom. The scaffold was tightly packed into the hole on its allocated side, and the scaffold seeded with SSCs was tightly packed into the hole on the contralateral side such that the holes were filled (Figure 7.4 C + D). Two stainless steel guide wires were placed superior and inferior to the holes for radiographic location purposes at a later stage. The periosteum and other layers were then closed over the filled holes using 2/0 Vicryl in order to contain the scaffold, and the skin was closed with interrupted sutures using 2/0 Ethilon and op-site spray. The wounds were subsequently covered with betadine soaked gauze, wool and crepe bandage. The sheep received a five day post-operative antibiotic regime (Ceporex 5ml OD) with Fentanyl patches and buprenorphine (0.6 mg) for 72 hours after application of the patches (for analgesia) and regular wound checks. After surgery the sheep were housed individually in pens for 5 days, followed by group housing in pens for the remainder of the study. The sheep were fed according to standard practice, with free access to water from troughs.

No control (empty defect) sheep were utilised due to experimental cost and the fact that the critical defect nature of the model had been previously demonstrated (Lo *et al.* 2007).

Figure 7.4: The operative procedure for the femoral condyle defect ovine model. A) Creation of a cavity on the medial femoral condyle using the customised drill bit, B) the hole (arrow), C) the scaffold, D) packing the scaffold into the hole. E) Medial side and F) posterior of sheep femur demonstrating the location of the drill hole (arrow).

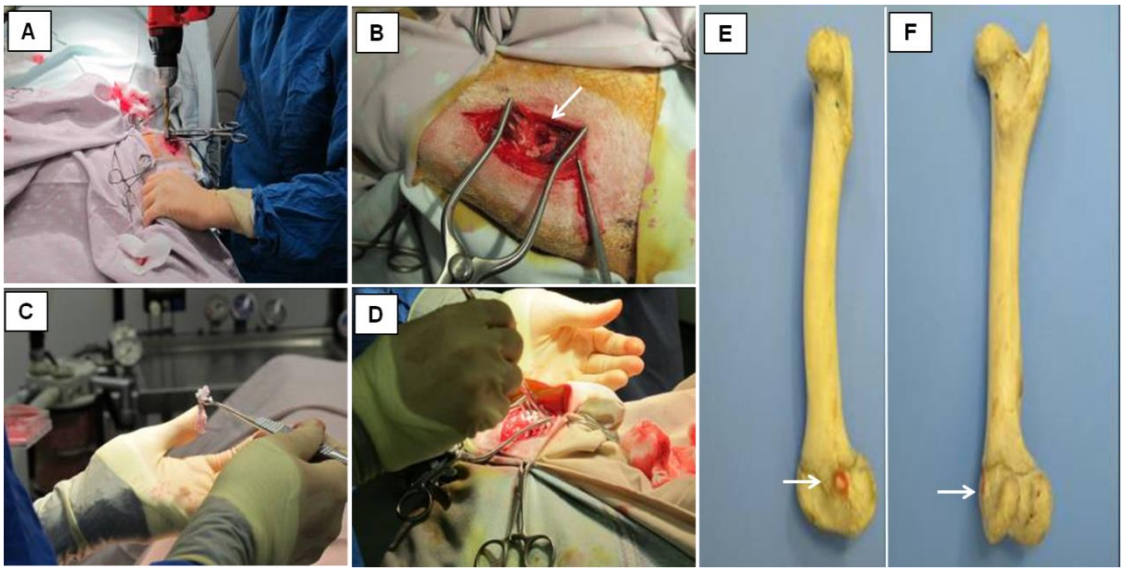

7.4.7 Radiographic analysis

Craniocaudal radiographs were taken using a portable x-ray unit (PLH Medical Ltd, Watford, UK). Radiographs were taken directly after the surgical procedure, after six weeks and after 13 weeks. Under general anaesthesia, the sheep were placed in appropriate positions for antero-posterior (AP) and lateral radiographs with the hip and knee fully extended. The plate was positioned dorsal with the source ventral (AP) and the plate lateral with source medial (lateral) using standardised distances (800 mm) and exposure times.

7.4.8 Retrieval of specimens

The sheep were euthanased with barbiturate overdose (0.7 mg / kg) 13 weeks post implantation of the specimens. The femoral condyles were harvested, along with the popliteal lymph nodes as previous studies have highlighted potential inflammatory reactions associated with *in vivo* polymer use (Bergsma *et al.* 1993;Bostman *et al.* 1990).

7.4.9 Peripheral quantitative computed tomography (pQCT) evaluation

Immediately after harvest the femoral condyles were scanned using an on-site pQCT scanner (XCT 2000, Stratec Medical, Pforzheim, Germany). Longitudinal slices through the centre of the defects were obtained, and mean density (mg/cm^3) of each specimen calculated. The mean densities of two other sections (designated bone areas 1 and 2) of normal trabecular bone within the condyles was also obtained, and these were compared statistically with the mean densities of the control scaffold defects and scaffold + SSCs using Mann–Whitney U test.

7.4.10 Preparation of condyles

After pQCT scan the condyles were rapidly transported to the Stanmore site, and all were prepared and mechanically tested within six hours of harvest. The condyles were placed in a jig and carefully orientated via the use of the radiographs and marker wires, such that when cut with a diamond-edged EXAKT band saw (EXAKT, Hamburg, Germany), the specimen filled drill holes were transected longitudinally in the coronal plane at the midpoints (Figure 7.5). One half of each specimen was subsequently taken for immediate mechanical testing and µCT evaluation, and the other half was prepared for histology.

Figure 7.5: A femoral condyle after preparation with the band saw. The original hole containing the scaffold has been transacted longitudinally (ring).

7.4.11 Mechanical testing

One half of each of the femoral condyles was used for mechanical testing. Due to the size of the test area, an indentation test was used. The specimen was placed onto the stage of the a Z005 static materials testing machine (Zwick/ Roell, Leominster, Herefordshire, UK), and a flat ended metal indentation rod (diameter 4 mm) was placed in opposition to the desired test area, and a preload of 10 N applied with a speed of 5 mm / min. The test areas are shown in Figure 7.6A, where areas 1 and 2 correspond to the superficial and deep areas of the scaffold within the drill hole, and areas A and B correspond to proximal and distal areas of normal cancellous bone. The test was started and the indentation rod was advanced at a rate of 10 mm / min, and the force required at each second time point recorded via a load cell.

Figure 7.6: Mechanical indentation test. A) The four areas of each specimen used, B) the specimen under test.

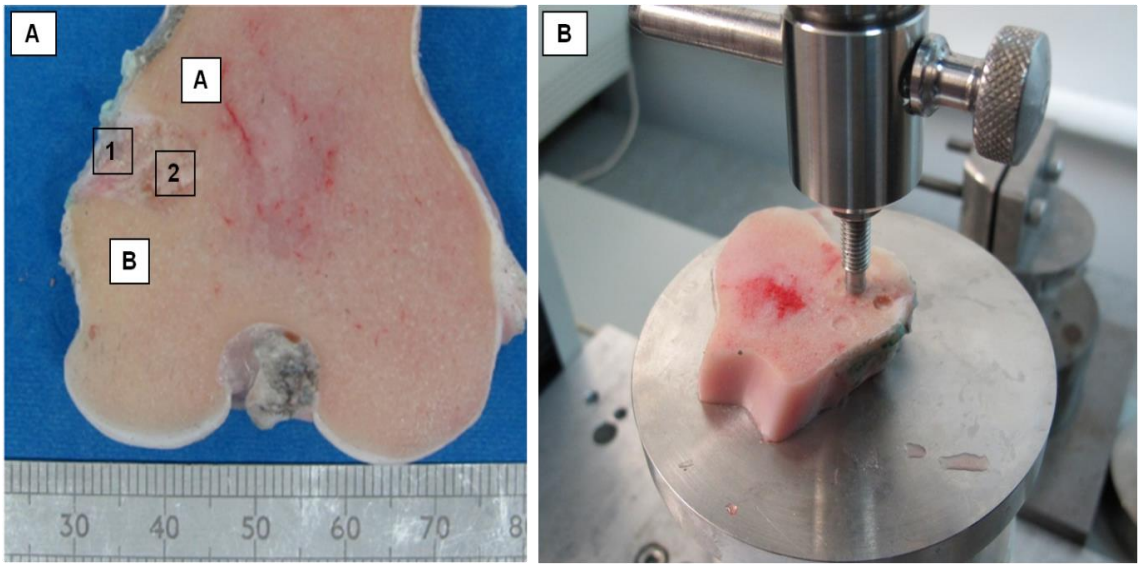

The data was transferred to a spreadsheet (Excel 2007) and graphs of force against strain plotted (load deformation curve). From these graphs a peak was visible, which corresponded to the failure of the test area. The force required at this peak was recorded for each area under test, and converted into a stress value. Mean stress values (along with standard deviations) were calculated for each area of the femora implanted with the scaffold alone, and those implanted with the scaffold + SSCs, and they were compared using Mann–Whitney U test.

7.4.12 µCT evaluation

After indentation the specimens were frozen until µCT evaluation could be performed. Samples were individually defrosted and scanned using a SkyScan 1176 micro-CT. Samples were focused, calibrated and adjusted to prevent X-ray saturation. The scans were performed with minimised ring artefacts to give an 18 µm voxel resolution. Data reconstruction was performed using NRecon (Skyscan, Belgium) and saved as 8 bit bitmaps (BMP). Analysis of the reconstructed images was performed using CTAn (Skyscan, Belgium). The region of interest (corresponding to the volume within the original drill hole) was extracted manually using the software, and via comparison with standard phantoms, new bone was deemed to correspond to all density values over 0.25. Mean volume of new bone within the region of interest was calculated for the femora implanted with the scaffold alone, and those implanted with the scaffold + SSCs, and were compared using a Mann–Whitney U test.

7.4.13 Histological examination

7.4.13.1 Femoral condyle

The other half of the femoral condyle samples were fixed in buffered formal saline (pH 7.2) for one week followed by dehydration through an ascending alcohol series over a three week period. The samples were then infiltrated with JB4 resin (Ted Pella, Inc., Redding, CA, USA) for three weeks, changing the solution weekly, and were then embedded in the same resin. Using the band saw, longitudinal slices measuring 5 mm thick were taken through the specimens and from these slices thinner sections measuring between 50 and 80 µm thick were made. The sections were attached to an acrylic slide using UV curable cyano-acrylate glue, before being grinded and polished on an EXACT grinding machine. Sections were stained with toluidine blue to stain the soft tissue followed by paragon to stain the bone, before being viewed by light microscopy.

7.4.13.2 Popliteal lymph node

The lymph nodes were prepared as described in Section 2.8. In brief lymph nodes were fixed in formaldehyde, and dehydrated in graded ethanol solutions prior to wax

embedding on a mounting plate. Seven micrometer sections were cut, transferred to a water bath and mounted on slides, prior to transfer to an oven set to 37 °C for 4 hours. Samples were subsequently stained using a standard Haematoxylin and Eosin (H + E) stain, and assessed by a consultant pathologist (D.F.) for the presence of abnormal inflammatory cells.

Parallel *in vitro* Study

7.4.14 WST-1 cell viability assay

At the start of the study, the remaining SSC seeded scaffold was kept for parallel *in vitro* evaluation.

The seeded scaffold from each sheep was weighed out into multiple, separate one gram portions, and each portion was placed into an individual well of a 24 well plate and cultured at 37 ºC, 5% CO_2 in osteogenic media with PBS washes every 3-4 days. Fourteen days post SSC seeding (day 1 of ovine experiment), and at 8 weeks post SSC seeding (midpoint of ovine experiment) three portions from each sheep (18 in total) were assessed for cell viability via a WST-1 assay.

Each portion was submerged in 1 ml 1:10 dilution WST-1 substrate (Roche ltd, Welwyn Garden City, UK). Unseeded scaffolds were run in parallel (controls). At 4 hours, 3 x 100 µl substrates were removed from each portion and analysed via a Bio-Tek KC4 microplate fluorescent reader (Bio-Tek, USA) at 410 nm. An increase in absorbance value (i.e. increase in optical density of the substrate) indicated increased cell number and viability. The mean absorbance value was then calculated and the mean control WST-1 absorbance value subtracted.

7.4.15 ALP / DNA assays

ALP specific activity was used as a measure of osteoblastic differentiation amongst the cell population present on the scaffolds after 2 weeks and 8 weeks of incubation. Three portions of SSC seeded scaffold from each sheep were tested at each time point. The scaffolds were individually washed in PBS, and then fixed in 90% ethanol prior to being allowed to air dry. Samples were then re-washed in PBS, and subsequently suspended in 2 ml of 0.5% Triton X-100. Samples were subjected to three freeze / thaw cycles with

vigorous agitation between each freeze. Lysate was measured for ALP activity using p-nitrophenyl phosphate as substrate in 2-amino-2-methyl-1-propanol alkaline buffer solution (Sigma, Poole, UK) and DNA content was measured using Pico Green (Molecular Probes, Paisley, UK) according to routine manufacturer protocol. Ten microlitres of lysate was run in triplicate for each cell seeded sample and control samples on a plate against two standards, read in triplicate on an ELx 800 and FLx-800 microplate fluorescent reader (Bio-Tek, USA) and mean and standard deviations calculated. The mean control values were subtracted, and specific activity was calculated by dividing the mean ALP activity by the mean DNA content (expressed as nanomoles of p-nitrophenyl phosphate/hr/ng DNA).

7.4.16 Immunostaining

SSC seeded specimens from two sheep also underwent immunostaining after eight weeks incubation time, as described in Section 2.11. Immunostains involved type-1 collagen, bone samples. The sections were not wax embedded to preserve the polymeric architecture, and imaging via confocal microscopy (Leica SP5 Laser Scanning Confocal Microscope and software, Leica Microsystems, Wetzlar, Germany) allowed 3D topographical visualisation of the surfaces.

7.5 Results

In vivo ovine study

7.5.1 Radiographic analysis

Standardised AP and lateral radiographs were taken at day 0, day 21, 6 and 13 week time points (Section 7.4.7) and representative lateral images of one sheep at day 42 are shown in Figure 7.7. There was little evidence of new bone within the defects at the 21 day time point, but by six weeks some of the defects appeared to be filling in, as evidenced by increased opacity within the hole, and loss of the definition of the margin (Figure 7.7 B). This appeared to be more evident in defects into which the scaffolds alone were implanted, as opposed to those in combination with SSCs.

Figure 7.7: Representative lateral radiographs of a single study sheep's knees taken six weeks after the scaffold insertion date. A) Scaffold + SSCs, the margins of the drill hole are still clearly evident (white arrow), B) scaffold control, the hole margins are less defined (white arrow). The black arrows indicate the metallic guide wires used for later processing.

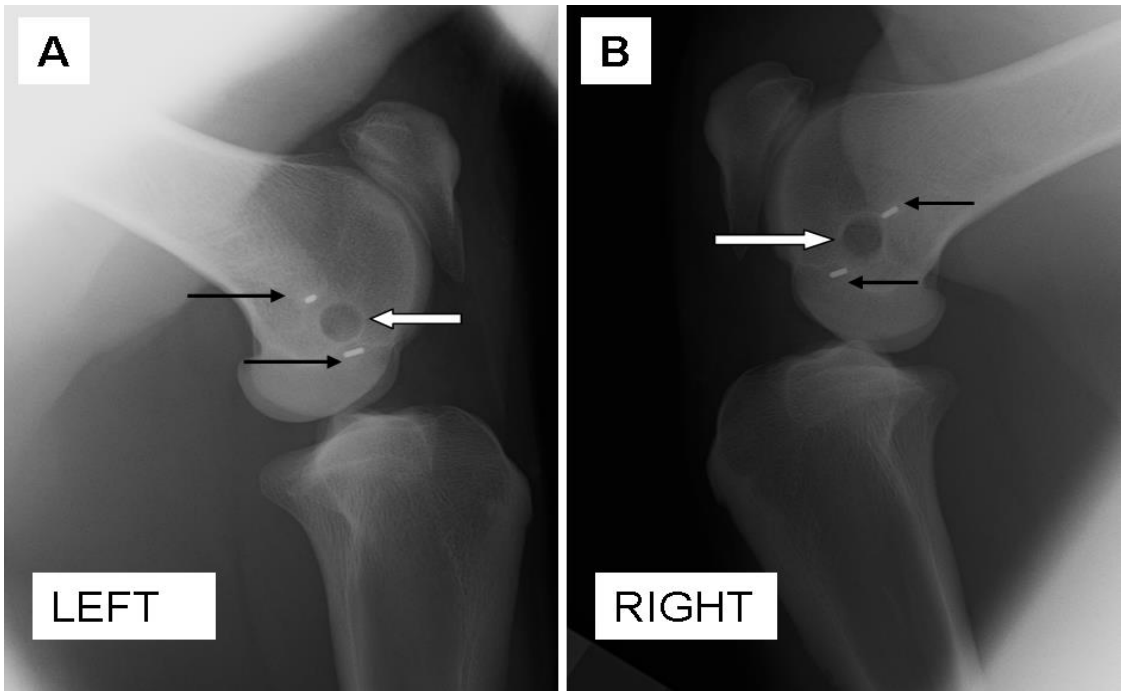

7.5.2 pQCT analysis

On-site pQCT was used as an immediate method to compare bone density within the defects to normal cancellous bone of the same sheep femoral condyle, as well as to compare the bone densities within the defect filled with the scaffold alone and those filled with scaffold + SSCs (Section 7.4.9). Figure 7.8 displays these results graphically. A 58 % decrease in mean bone density between cancellous bone area 1 and the scaffold + SSC defects (U test: $p < 0.01$) and a 44 % reduction between bone area 2 and the test area (U test: $p < 0.01$) was observed. There was a 48 % decrease in mean bone density between cancellous bone area 1 and the scaffold alone defects (U test: $p < 0.01$) but only a 20 % reduction between bone area 2 and the scaffold alone defects, and this was not significant (U test: $p = 0.13$). There was a 30 % reduction in bone density between the femoral condyle defects filled with scaffold + SSCs, compared to those filled with scaffold alone after the 13 week incubation period, but this was not significant at the $p < 0.05$ level (U test: $p = 0.09$).

Figure 7.8: Graph displaying bone densities of the named bone and defect areas (± SD, n=6) after the 13 week *in vivo* incubation as measured by pQCT.

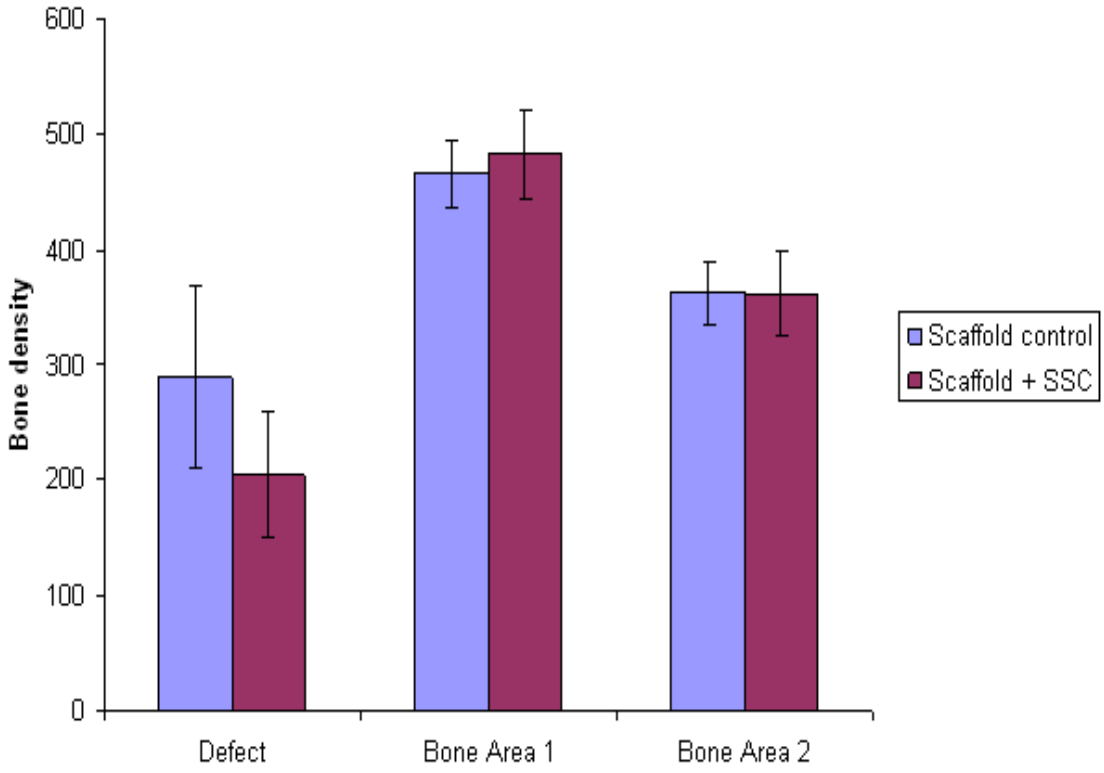

7.5.3 Mechanical testing

An indentation test (Section 7.4.11) was used to assess the mechanical strength of the defect areas containing the scaffolds, and two areas of cancellous bone as demonstrated in Figure 7.6. The mean failure stress of the defect area containing the scaffold controls was 20% that of the mean strength of the cancellous bone areas (U test: $p < 0.001$), and the mean mechanical strength of the defect area containing the scaffold + SSCs was 11 % that of the mean strength of the cancellous bone areas (U test: $p < 0.01$). When comparing the mean mechanical stress at failure of the defects containing the scaffold to those containing the scaffolds + SSCs, the addition of the SSCs lead to a 41 % reduction in stress at position 1(U test: $p < 0.01$), and a 72 % reduction in stress at position 2 (U test: $p < 0.01$).

Figure 7.9: Graph demonstrating the mechanical stress at failure during the indentation test for each of the designated areas (± SD, n=6). Positions 1 and 2 refer to the defect areas containing the specimens and Positions A and B refer to normal cancellous bone.

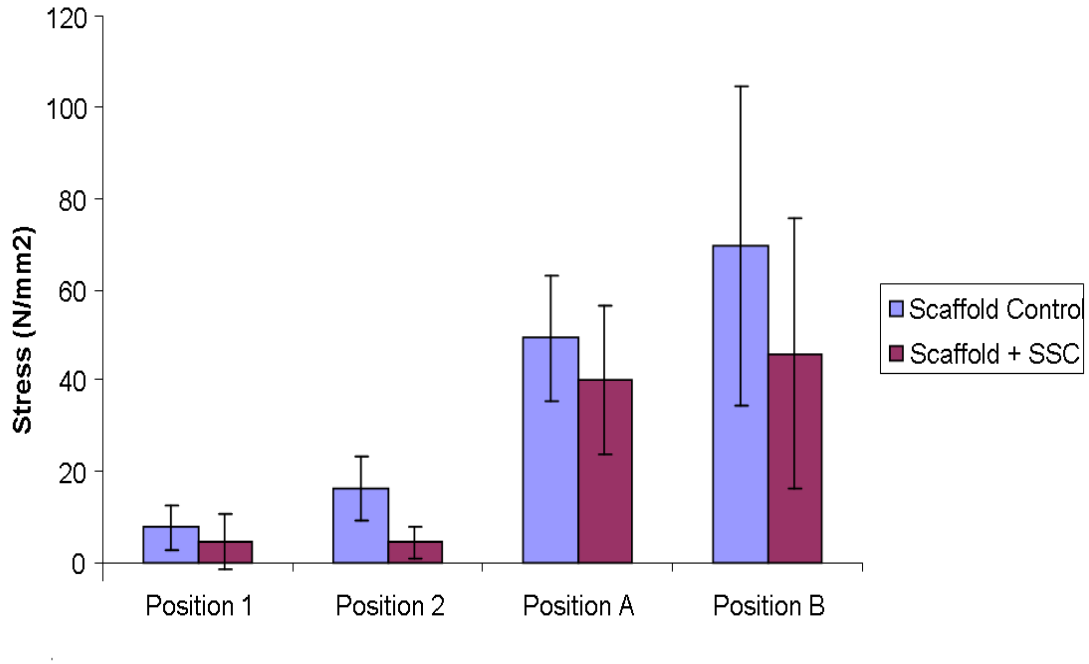

7.5.4 µCT evaluation

Representative images of the µCT reconstructions of the defects containing scaffold controls and scaffold + SSCs are given in Figure 7.10. The 3D reconstruction images (inset) showed that the defects were still visible in both samples after the three month incubation period, which was to be expected as not all of the scaffold would be fully resorbed by this time. However, the axial slices showed that there was a sclerotic margin around the samples seeded with SSCs (indicating that full integration would be unlikely), but within the defects filled with the scaffold alone there was evidence of normal trabecular bone, indicating that given more time the defect would have completely filled in.

Figure 7.10: Representative μCT images incorporating the defect site (transected longitudinally) and surrounding host bone of A) 3 D reconstruction scaffold + SSCs, B) axial slice through (A) demonstrating sclerotic margin around defect site (arrow), C) 3 D reconstruction scaffold controls and D) axial slice through (C) demonstrating new trabecular bone within defect site (arrow). Scale bar = 10 mm.

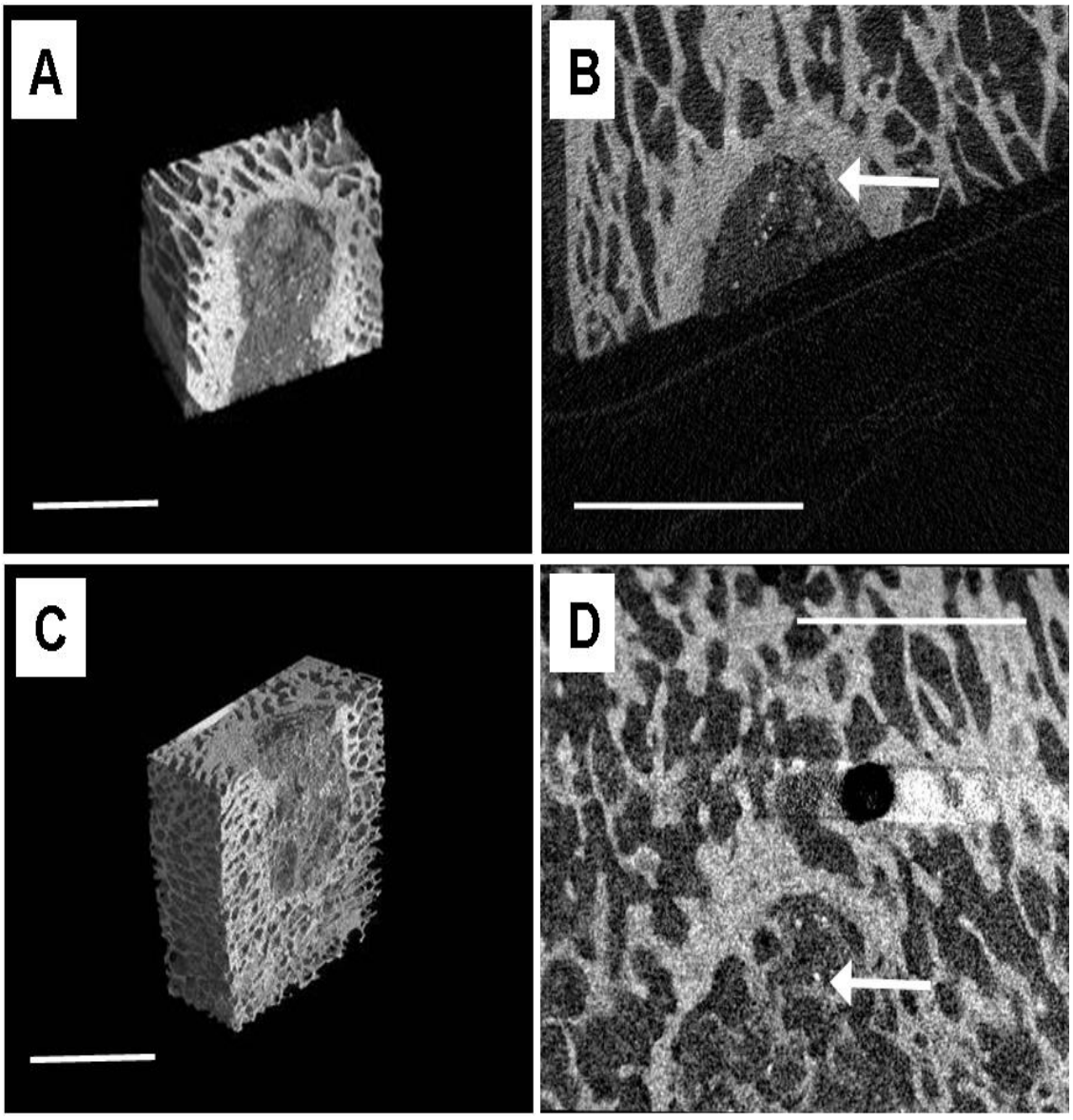

The mean percentage bone volume content of the defects filled with scaffold alone and scaffold + SSCs was calculated from the raw μCT data, and is displayed graphically in Figure 7.11. There was a reduction in percentage bone volume within the defect of 13.4% when comparing the scaffold to the scaffold + SSCs, but this was not significant (U test: $p = 0.13$).

Figure 7.11: Graph displaying mean percentage bone (± SD, n=6) within the defect areas after the 13 week *in vivo* incubation period.

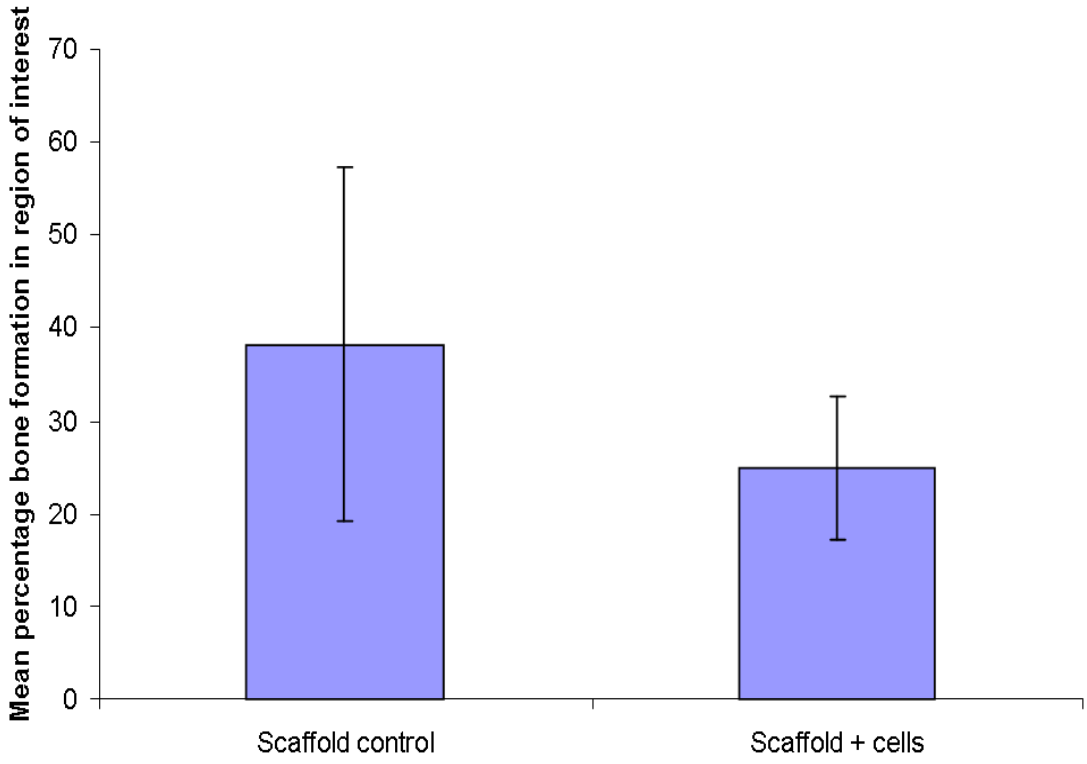

7.5.5 Histological examination

7.5.5.1 Femoral condyle

Representative images displaying the histological appearance of the femoral condyle defects filled with scaffold controls and scaffold + SSCs are displayed in Figure 7.12. In keeping with the μCT findings, there was evidence of new bone formation in both the groups, although the new bone in the scaffold alone packed defects appeared more diffusely throughout the defect, and appeared to integrate more closely with the remaining scaffold material. Figure 7.13 displays representative sections of normal sheep condylar cancellous bone, for comparison.

Figure 7.12: Micrographs displaying histological sections (toluidine blue and paragon stain, x25 magnification, scale bar = 500 μm) of the defect areas of each of the sheep condyles packed with polymer (PLA HA) alone (left side: A,C,E,G,I,K) and polymer + SSCs (right side: B,D,F,H,J,L). There was evidence of new bone formation (purple) in all specimens, but was more abundant in the control samples (thick white arrows), with more fibrous tissue formation in the samples containing SSCs (thick black arrows). The thin white arrows (Figure 12B) depict the external margin of the defect, and show that very little osseointegration has occurred in this region. The thin black arrows represent the remaining polymer. The numbers represent those assigned to each sheep for experimentation recording purposes.

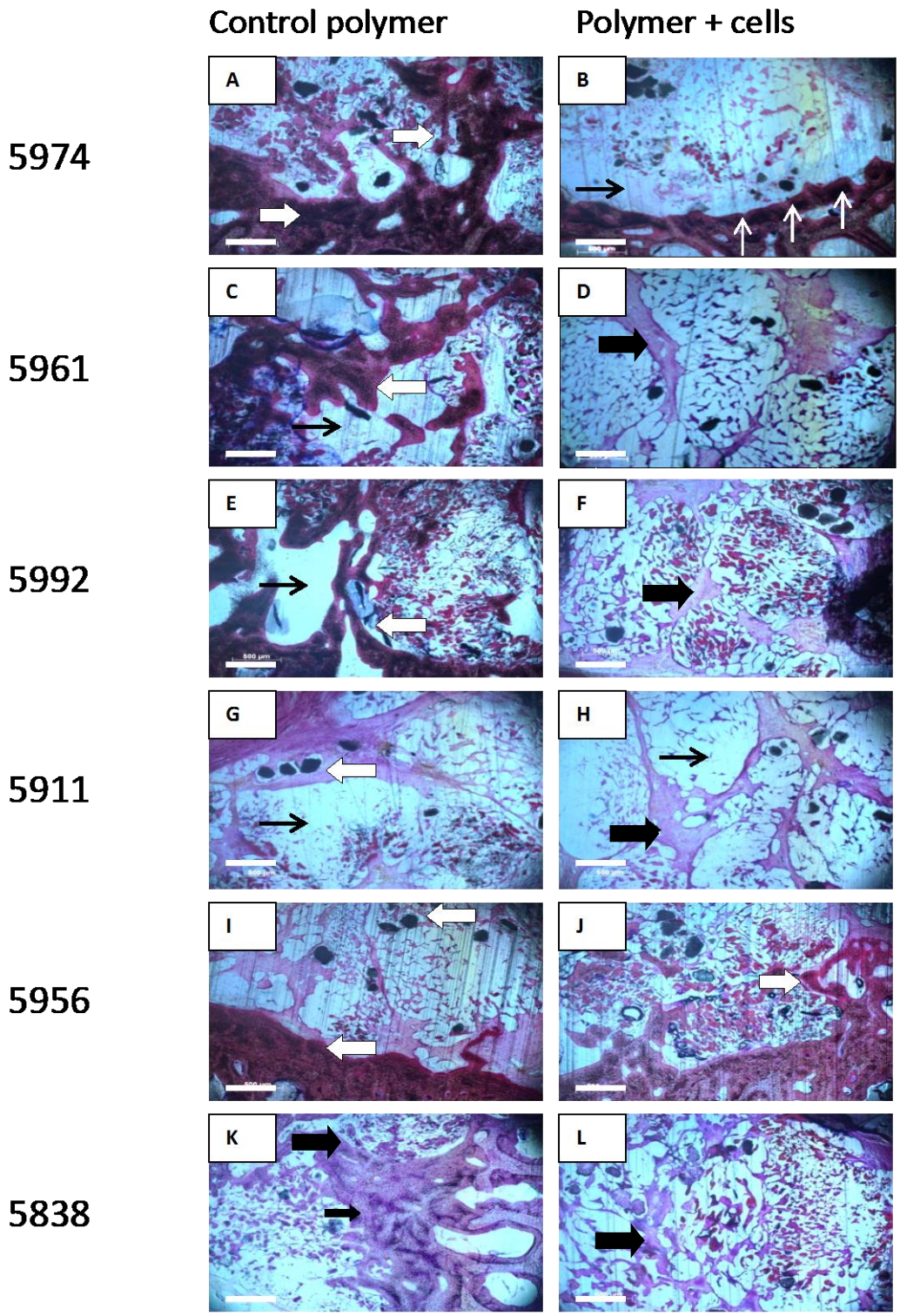

Figure 7.13: Micrographs displaying histological sections (toluidine blue and paragon stain), of normal sheep condylar cancellous bone. A) Displaying gross architecture (x25 magnification, scale bar = 500 μm), B) higher magnification image (x100 magnification, scale bar = 200 μm).

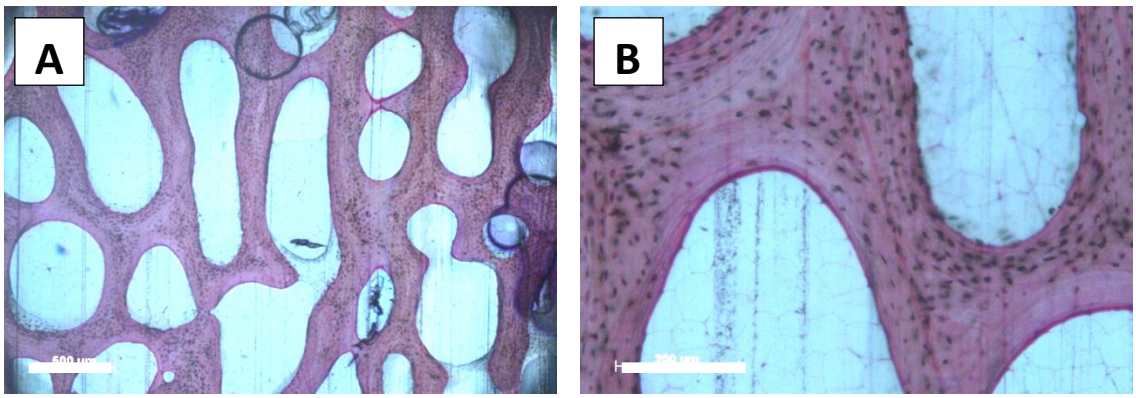

With higher magnification of the areas of new bone formation it was possible to identify the hydroxyapatite particles that were originally from within the polymer scaffold, and there was evidence of the osteoinductive/ osteoconductive nature of these particles, as shown in Figure 7.14.

Figure 7.14: Micrograph displaying histological section (toluidine blue and paragon stain) taken from within an area of new bone formation (x200 magnification, scale bar = 100 μm). A hydroxyapatite particle (white arrow) is shown to be completely encompassed by new bone.

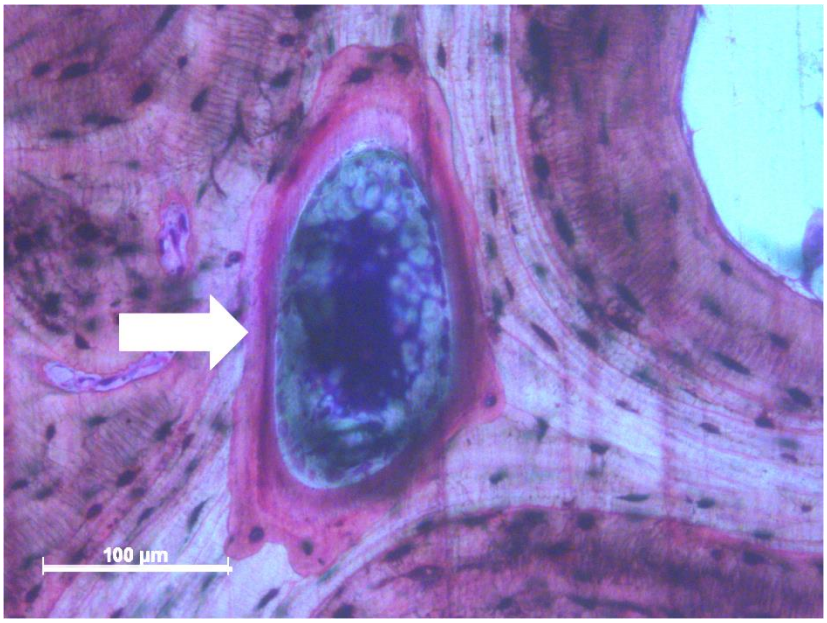

7.5.5.2 Popliteal lymph node

The popliteal lymph nodes serve the region including the operative site, and were therefore examined histologically for evidence of an abnormal inflammatory reaction. This has been noted previously in some studies, and is of importance when considering potential clinical use (Bergsma *et al.* 1993;Bostman *et al.* 1990). Osteolysis as a result of polyethylene wear debris in total hip replacement has been reported for some time, but the recent widespread failure of metal on metal bearing total hip replacements (Langton *et al.* 2010; Amstutz *et al.*1992) (due to an adverse inflammatory reaction to metal debris (ARMD)) has highlighted the need for meticulous *in vivo* testing prior to clinical translation.

Representative examples of H + E stains of the lymph nodes are displayed in Figure 7.15. All lymph nodes had an essentially normal appearance (Figure 7.15 A), but did contain occasional small circular spaces probably representing material which had been lost through processing, but critically had not stimulated an overt inflammatory response (Figure 7.15 B + C). In one peri-lymphatic fat area of a single lymph node there was a small focus of regular circular spaces surrounded by fibrous tissue containing macrophages, lymphocytes and plasma cells (Figure 7.15 D). There were however no neutrophils, no polarisable material, and no well formed granulomas. This was similar to the histology seen around surgical biodegradeable sutures, and hence was likely to be of no clinical significance.

Figure 7.15: Micrographs of H + E stains of lymph nodes and peri-lymphatic fat after the study period. A) Normal lymph node tissue appearance (x 25 magnification, scale bar = 1000 μm), B) occasional small circular spaces (arrows) (x 25 magnification, scale bar = 1000 μm), C) high magnification (x400) of small circular space, showing no increased inflammatory response around it (scale bar = 50 μm) and D) small focus of fibrous tissue from within the peri-lymphatic fat, containing macrophages, lymphocytes and plasma cells (x 50 magnification, scale bar = 500 μm).

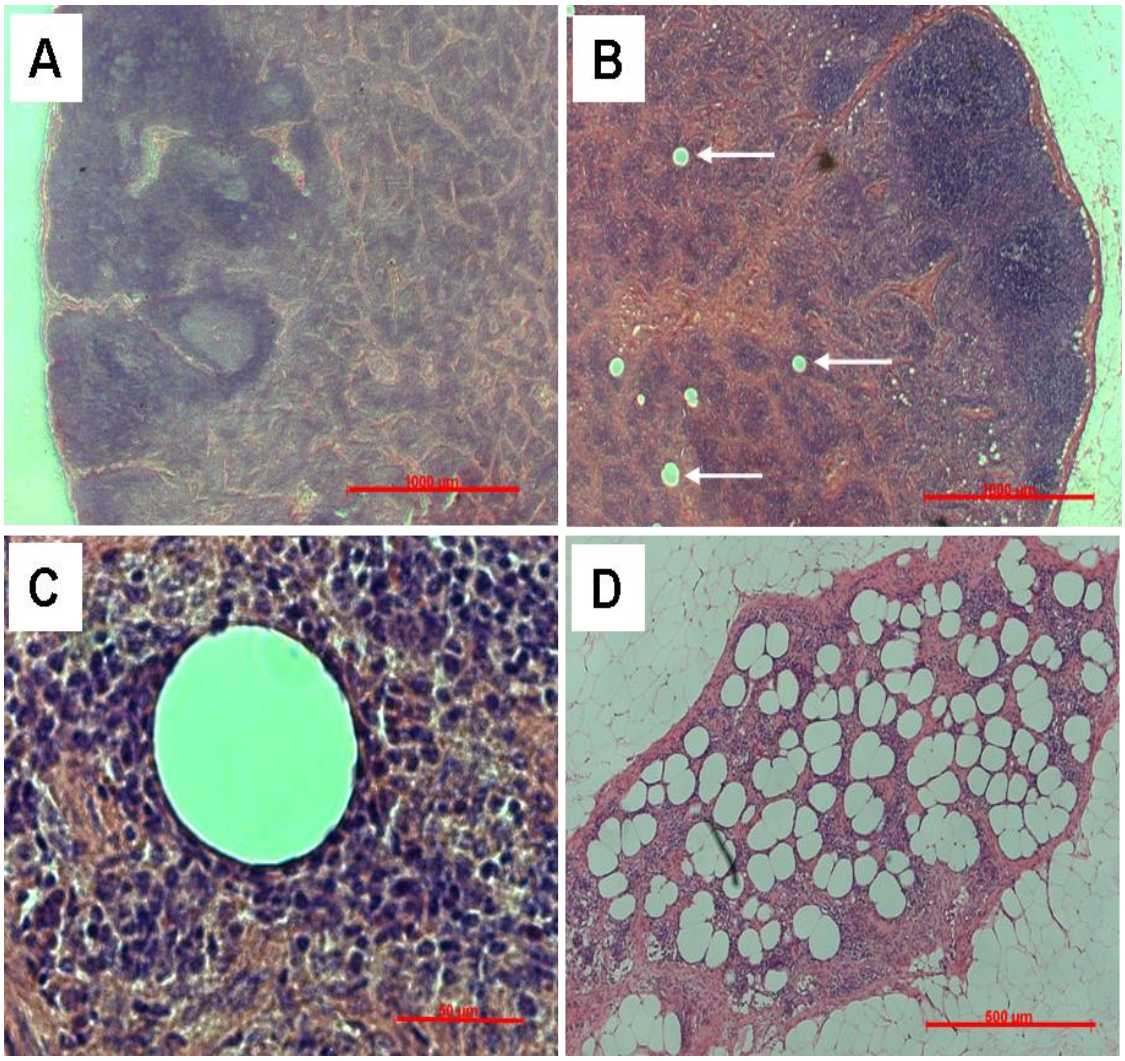

Parallel in vitro study

7.5.6 WST-1 assay

A WST-1 assay was used as a measure of cell viability on the scaffolds at the 14 days and 8 weeks time points and this data is displayed graphically in Figure 7.16. There was excellent cell growth and viability at both time points as demonstrated by the large change in optical density over the four hour assay period. There was however a decrease in final optical density achieved when comparing the 8 weeks sample to the two weeks sample (although this was not significant ($p = 0.16$)), either reflecting a decrease in viable cell number at this time point or a reduction in cell metabolic activity (as occurs post differentiation).

Figure 7.16: Graphical representation of mean increase in optical density (minus controls) of the scaffolds seeded with sheep SSCs at the 2 week (*in vivo* implantation) and 8 week (*in vivo* mid point) stages (± SD, n = 6).

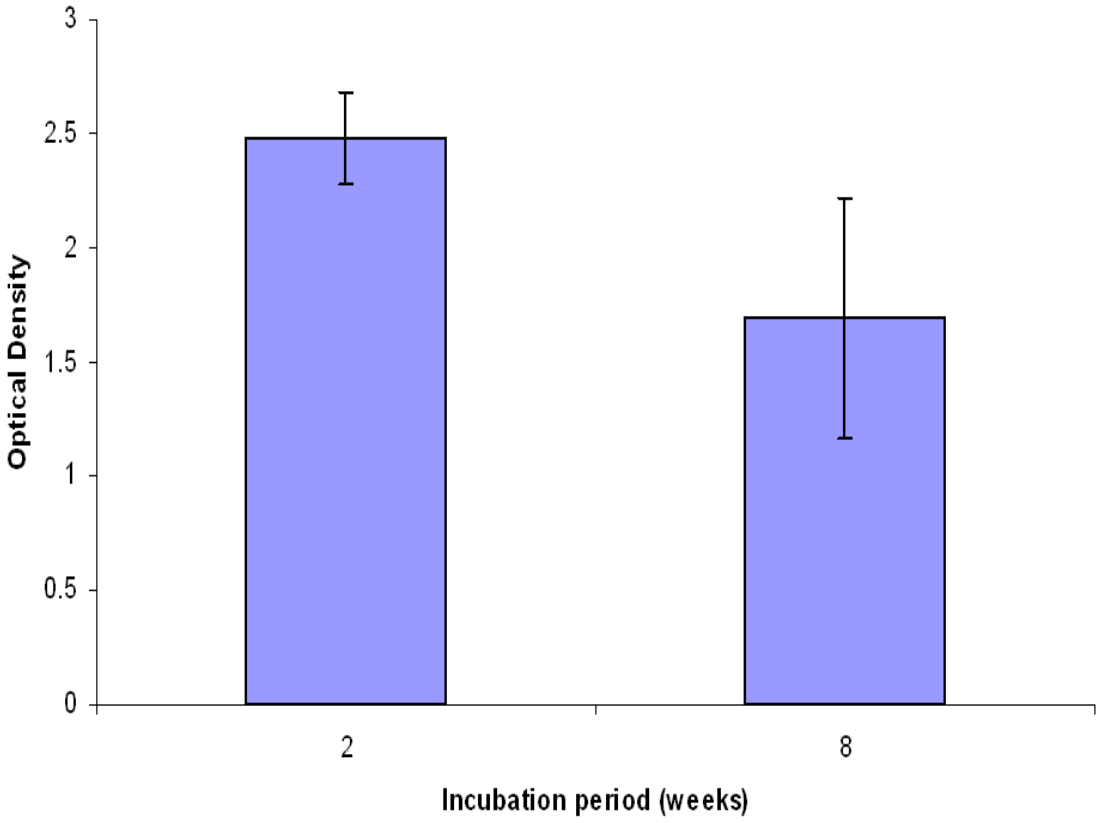

7.5.7 Biochemical analysis

The mean ALP specific activity at the two and eight weeks time points was used as a measure of osteoblastic differentiation amongst the SSC population (Figure 7.17). There was negligible ALP specific activity at the 2 weeks time point, and even though there was a significant increase to 0.04 nmol pNNP/ ml / hr/ ng DNA at the 8 weeks time point (U test: $p < 0.05$), the value obtained is still very low, indicating only minimal osteoblastic differentiation amongst the cell population.

Figure 7.17: Mean ALP specific activity of the sheep SSC population on the scaffolds at the 14 days and 8 weeks time points (± SD, n=6).

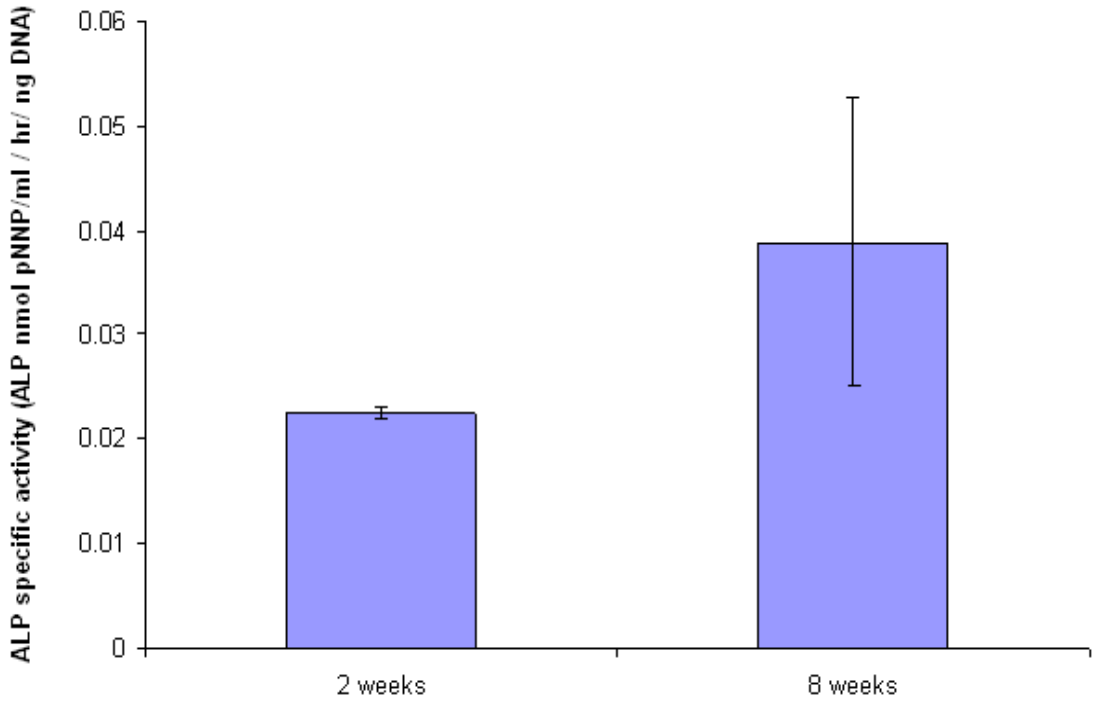

7.5.8 Immunostaining

Scaffolds underwent immunostains for type-1 collagen, osteocalcin and bone sialoprotein, as potential markers of osteoblastic differentiation and bone matrix formation. These were imaged under confocal microscopy and are displayed in Figure 7.18. There is poor evidence for good bone formation in this *in vitro* study as evidenced

by the moderate positivity for BSP, but only minimal positive staining for both type 1 collagen and osteocalcin.

Figure 7.18: Reconstructed 3D image stacks obtained via confocal microscopy displaying immunostains of scaffold + sheep SSCs after 8 weeks *in vitro* incubation. Nuclei are shown as red (DAPI) and positivity for the marker is green (alexafluor 594). A) control (no primary antibody added), B) type 1 collagen, C) osteocalcin and D) bone sialoprotein.

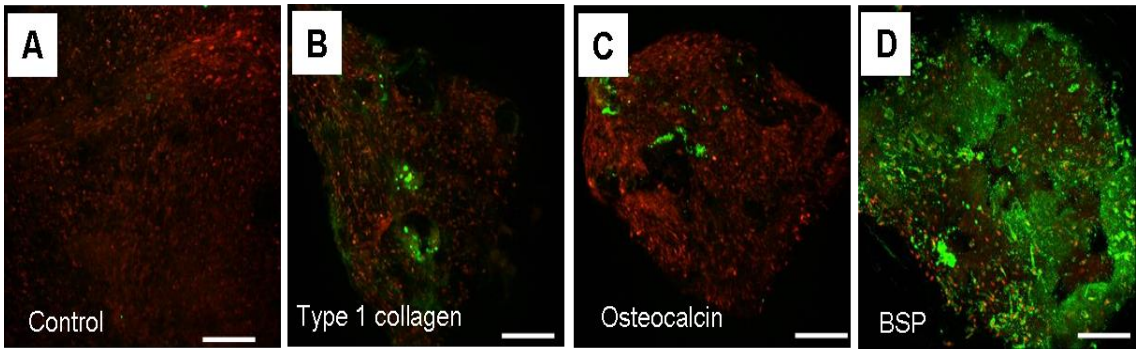

7.6 Discussion

The ovine femoral condyle defect offers a good model for the formation analysis due to the size of the defect, the surrounding tissue coverage and blood supply, as well as the nature of the surrounding trabecular bone being similar in nature to those of human counterparts (Reichert *et al.* 2010). Due to their size, sheep also provide models whereby constructs can be exposed to loads and forces comparable to the human clinical setting, but this model was not loaded and hence realistically provided a transitional model to a more complicated loaded model, prior to any human clinical trials (Bergmann *et al.* 1984). This limitation does however mean that it was less complicated, quicker to perform and subject to fewer variables, providing a cost effect method to screen, and hence further improve and enhance constructs and experimental protocols prior to more expensive loaded models. This factor has proved important in this case, whereby the scaffold has provided some encouraging results, but has also

introduced important factors for investigation surrounding the potential of the SSCs and the protocols for their use.

The scaffold, consisting of porous high molecular weight $P_{DL}LA$ in combination with 10 % HA has shown, after a three month *in vivo* incubation period, the potential to stimulate new bone formation within a critical sized defect of cancellous bone. Both histological and µCT analysis have shown good evidence for neo bone formation around and within the constructs, although this was incomplete in all cases. The mechanical indentation tests have confirmed these findings, whereby there was structural integrity within the defects, although it was approximately only one fifth of the strength of that of the neighbouring cancellous bone. This structural issue is of paramount importance when considering a fully bioresorbable scaffold for use in various loaded clinical situations such as IBG. Previous *in vitro* mechanical tests (chapter 5) found the composite to have comparable strength to milled allograft (the current gold standard for large bone defect filling), but the comparison in this model is to native cancellous bone. Ideally, a control defect group containing milled allograft, along with a more standardised impaction procedure, would allow an accurate comparision to the current gold standard for IBG procedures. Unfortunately financial constraints limited the experimental group numbers in this project, but it should be considered and explored in future models. Furthermore, over time in the *in vivo* situation, the breakdown of the polymer reduces the mechanical integrity. Importantly, this model has shown little inflammatory reaction associated with any polymer breakdown products, making it a contender for further optimisation and testing. The perfect solution would achieve a balance whereby the bioresorption and hence loss of strength of the scaffold is matched by the ingrowth and increase in strength provided by new bone formation. Shikinami *et al*. investigated this process using $P_{L}LA$ / HA composites in a rabbit model, concluding that composites containing 30 % and 40 % HA particles are clinically effective for use in high-strength bioactive, bioresorbable bone-fixation devices with the capacity for total bone replacement (Shikinami *et al*. 2005).

Consistently throughout the *in vivo* analyses, this study has shown that the addition of SSCs was detrimental to both the volume and quality of new bone formation in the defect site, as well as the mechanical strength of the construct / new bone composite

after the three month incubation period. This was inconsistent with a multitude of other *in vitro* and *in vivo* studies. The addition of SSCs have been shown to have additive effects in terms of enhanced bone formation when combined with a host of different scaffolds in murine, lapine and ovine models (Fialkov *et al*. 2003;Kanczler *et al*. 2010;Kanitkar *et al*. 2011;Korda *et al*. 2008).

The previous chapters detail both the *in vitro* and small animal *in vivo* work surrounding the production, optimisation and choice of this composite scaffold. Of note, all previous work was performed with the addition of human SSCs, even in the murine models, where the immuno-compromised status of the mice made this possible. It has however been shown that the osteoinductivity of certain substances or culture conditions is different between human and ovine SSCs (Zannettino *et al*. 2010). The parallel *in vitro* section of this study elaborated on this theory, and gave some indication as to why the SSCs may have been detrimental in this case. The WST-1 assay showed excellent cell viability on the scaffolds at both the 14 day and 8 week incubation times indicating biocompatibility, but the ALP assay was negative at the 14 day stage and only weakly positive at the 8 week stage, despite culture in standard osteogenic media. This indicated a lack of osteoblastic differentiation amongst the SSC population and this finding was re-inforced with the negative immunostains for both type-1 collagen and osteocalcin at the 8 week incubation stage. There are two potential explanations for these phenomena; either the scaffold was not osteoinductive to ovine SSCs, or the culture conditions were not conducive to osteoblastic differentiation of the SSC population. These factors could potentially favour differentiation into undesirable cell types such as fibroblasts, which could actually block osteoconduction or osteoinduction of surrounding host cells when implanted *in vivo*. Given the fact that the control scaffolds performed well during the *in vivo* study, indicating both osteoinductivity and osteoconductivity, it is likely that it is the initial SSC isolation and seeding protocols which need to be addressed in order to achieve potential SSC benefits. Future work will therefore concentrate on this area, with culture expansion of ovine SSCs in strongly osteogenic conditions (such as in the presence of BMP-2), and scaffold seeding at the time of *in vivo* implantation, such that the cells are immediately exposed to the regional growth factors and stimulatory microenvironments.

Furthermore, multiple studies have shown enhanced osteoinductivity of biodegradeable scaffolds with increasing HA concentrations. Zannettino *et al*. found that a 15 % concentration of HA was required, whereas Shikinami *et al.* found that over 30 % was effective (Shikinami *et al*. 2005;Zannettino *et al*. 2010). Chapter 5 detailed the murine *in vivo* study performed with the $P_{DL}LA$ / HA composite scaffold, and μCT analysis clearly showed enhanced bone formation in areas that were in contact with the HA particles. This therefore introduced two potential means of improving the scaffold prior to a second ovine study: i) The HA content could be increased and ii) the availability of the HA to the SSCs could be enhanced. The first issue can be addressed by increasing the proportion of HA to $P_{DL}LA$ during the initial foaming process, and the development of nano HA particles offer a potentially exciting solution to the second. By foaming $P_{DL}LA$ with nano HA, rather than the $P_{DL}LA$ having large particles of HA distributed randomly throughout its structure, such that only some of the cells growing over it are in contact with the HA, it becomes matrix with HA distributed diffusely throughout the whole porous structure; a truly synthetic bone graft with $P_{DL}LA$ acting rather like collagen and the nano HA as the inorganic components of bone.

7.7 Conclusion

The results in the context of the null hypotheses were examined:

1. There is no difference in the bone regeneration between either of the composite polymers or the (historical) empty femoral condyle defect controls.

This null hypothesis is **false.**

2. There is no difference in the bone regeneration or the osseointegration of the polymer composite with and without the addition of SSCs.

This null hypothesis is **false.**

These studies showed that significant bone regeneration occurred in the defects filled with both the scaffold / SSC composites and the scaffold controls. However, there was significantly more bone regeneration in the scaffold controls.

These studies have made progress towards the successful translation of a tissue engineered product previously shown to have encouraging capability via both *in vitro* and small animal *in vivo* studies. The potential of this fully bioresorbable composite scaffold to stimulate bone regeneration in a critical defect has now been demonstrated in a scaled up large animal study. However, there are areas for improvement prior to any clinical trials, and thus significant further testing and scaffold optimisation is required. These include optimisation of cell seeding protocols, including pre-differentiation of SSCs or inclusion of osteoinductive stimuli within the scaffolds, the need to address vascularisation of the graft or techniques to enhance cell survival prior to host vascular ingrowth, and the investigation of HA concentration and bioavailability. Further research in these areas is on-going such that future studies should improve the regenerative capacity of the scaffold, and clinical use of a tissue engineered product is one step closer.

This study has also raised issues as regards the actual need for SSCs in a successful allograft alternative (given the relative success of the control scaffolds), as well as the validity of ovine models in tissue engineering (discussed in Section 8.3).

Chapter 8

Conclusions, weaknesses and future perspectives

8.1 Conclusions

Musculoskeletal disease remains the worldwide leading cause of ongoing morbidity, pain and disability (Mason and Manzotti 2010). As predicted, the last decade has seen much effort and expense directed towards all aspects of addressing these problems, with huge recent interest in the realm of regenerative strategies (Horan 2011).

The work detailed in this thesis has ruled out the major null hypothesis:

Novel tissue engineered constructs are not as effective as allograft for the treatment of lost bone stock in impaction bone grafting.

Throughout a series of *in vitro* investigations it has been shown that novel tissue engineered polymer constructs have consistently out-performed allograft from both a mechanical and biocompatibility perspective. Important composite polymers have been identified with enhanced osteogenic capability, such that the potential for clinical translation is a real possibility. The University of Southampton Bone and Joint research group (along with collaborators) remains the only group to have published work surrounding the specific use of tissue engineered polymer/ polymer composites in an impaction bone graft model (Bolland *et al.* 2008b;Tayton *et al.* 2012a;Tayton *et al.* 2012b) although multiple studies have shown the promising use of tissue engineered polymer composites in other bone regenerative strategies (Berner *et al.* 2013;Reichert *et al.* 2012) and certain ceramic bone graft extenders have shown mechanical superiority over allograft for use in impaction bone grafting in both *in vitro* and *in vivo* experimentation (Aulakh *et al*. 2009;Blom *et al*. 2009;McNamara *et al*. 2010).

The conclusions from the experimental strategies used to investigate the thesis objectives are summarised below:

8.1.1 Chapter 3: Techniques to optimise the protocol for successful combination of SSCs with scaffold materials.

Cell seeding density was of optimal importance to ensure successful SSC construct combination. A concentration of 5 x 10^5 cells / ml was deemed both adequate in terms of cell number required, efficiency of culture and reproducibility. Culture in osteogenic

conditions improved cell proliferation and osteoblastic differentiation on scaffolds, but initial cell seeding time was not important.

8.1.2 Chapter 3: The effect of polymer type and chain length on polymer shear strength and biocompatibility.

Both the high and low molecular weight versions of $P_{DL}LA$ and $P_{DL}LGA$ had superior mechanical shear strength when compared to the allograft controls, but those of PCL were significantly less. The high molecular weight versions of $P_{DL}LA$, $P_{DL}LGA$ and PCL showed improved biocompatibility over the allograft controls. Thus only the high molecular weight versions of $P_{DL}LA$ and $P_{DL}LGA$ performed well in both tests, and were highlighted for further analysis. Throughout the literature, many polymers have been tested for biocompatibility with encouraging findings, but Polylactic acid and Poly (lactic-co-glycolic) acid are amongst the most commonly cited (Tare *et al*. 2009;Whang *et al*. 1999). However, no published research is available directly comparing the effects of altering the molecular weight of the polymers under test.

8.1.3 Chapter 4: The effects of porosity on polymer shear strength, clinical handling, biocompatibility and osteoinductivity.

It was shown that the porous versions of high molecular weight $P_{DL}LA$ and $P_{DL}LGA$ had improved clinical handling and biocompatibility over their non-porous counterparts, whilst significantly maintaining shear strength over the allograft controls. The porosity also induced further osteoblastic differentiation amongst the SSC population on the $P_{DL}LA$ scaffolds, but this effect was less pronounced on the $P_{DL}LGA$ counterparts. This is in concordance with the literature, and has also been shown to have further beneficial effects in terms of vascular and bone ingrowth (Feng *et al*. 2011;Karageorgiou and Kaplan 2005).

8.1.4 Chapter 5: The effects of the addition of bioactive molecules on polymer shear strength, biocompatibility and osteoinductivity and identification of two optimal polymers for detailed in vivo analysis.

The addition of 10 % hydroxyapatite to the porous versions of high molecular weight $P_{DL}LA$ and $P_{DL}LGA$ had no effect on biocompatibility or mechanical shear strength of

the polymers. It did however increase the (desired) osteoblastic differentiation amongst the SSC population as measured via an Alkaline phosphatase assay and confirmed via type-1 collagen immunostaining. The osteoinductive influence of HA was an expected finding and consistent with multiple studies (He *et al*. 2013;Lin *et al*. 2009). High molecular weight $P_{DL}LA$ and $P_{DL}LA$ + 10 % HA performed the best from the array of polymers tested, and hence were selected for *in vivo* testing.

8.1.5 Chapter 5: The osteogenic potential of the optimal two polymers in an in vivo (murine) scenario, and subsequent identification of the best polymer for a scaled up study.

Both $P_{DL}LA$ and $P_{DL}LA$ + 10 % HA displayed biocompatibility characteristics and showed osteogenic potential when tested via a subcutaneous murine model. The addition of SSCs to the constructs further increased the volume of new bone formation over the control scaffolds. There was excellent vascularisation of all constructs despite an absence of angiogenic growth factors. Consistent with other studies (He *et al*. 2013;Lin *et al*. 2009) the addition of 10 % HA to the $P_{DL}LA$ improved the osteogenicity of the scaffold in terms of volume of new bone formed during the study period. MicroCT analysis showed that the new bone was largely localized around the HA particles indicating an intrinsic osteoinductive capacity of this substance. $P_{DL}LA$ + 10 % HA was hence identified as the optimal polymer composite for scaled up *in vivo* (ovine) testing.

8.1.6 Chapter 6: The identification potential pitfalls to clinical translation of the tissue engineered constructs, and exploration of techniques to overcome them.

The use of bone cement is integral to the technique of impaction bone grafting when fixing both the acetabular and femoral prostheses to the newly constructed bone platform. The exothermic reaction caused by the curing of the bone cement caused significant loss of cell viability on tissue engineered allograft and $P_{DL}LA$ + 10 % HA in close proximity. Pre-cooling, or pre-coating the constructs with 1 % laponite did not moderate this effect, and caused changes to the important construct / cement interface. However, the harmful effects of the heat on the cells only occurred within 5 mm of the cement construct interface, and even within this region there was substantial remaining cell viability. Published studies in this area corroborate the finding that heat damage

from curing cement is localized (Linder 2000;Ling *et al*. 1993) and in addition, the exothermic effects of the setting cement are further decreased as the metallic implant acts as a heat sink (Mjoberg 1986). The results of these studies would therefore indicate that cell loss due to exothermic toxicity would be minimal, and the surviving cell population would thus have the capacity to fully recolonise the scaffold. The use of bone cement is therefore not contraindicated when used in close proximity to tissue engineered constructs. Further testing is required to assess whether the differentiation capacity of the SSCs is affected by the heat exposure.

8.1.7 Chapter 7: The assessment of the osteogenic potential of the optimised polymer composite ($P_{DL}LA$ + 10 % HA) in a scaled up in vivo (ovine) model.

The significant potential for the tissue engineered composite polymer to produce bone was displayed. New bone formation in critical sized defects was demonstrated both histologically and volumetrically via microCT scanning. Indentation testing demonstrated mechanical integrity of the constructs at the three month time point, although this was significantly less than the surrounding cancellous bone. This finding is in line with mechanical results from other large animal studies incorporating tissue engineered constructs (Reichert *et al.* 2012).

The addition of skeletal stem cells to the polymer composite was not shown to enhance bone formation or mechanical strength of the construct at the three month time point. This was an unexpected finding and in contrast to most published large animal studies in this area, and may therefore suggest a problem with this model (Bruder *et al.* 1998;Field *et al.* 2011;Kon *et al.* 2000;Korda *et al.* 2008). However, a group in Brisbane has made significant progress in this area, finding good bone regenerative capacity with scaffolds impregnated with osteoinductive factors, but have had similar negative results with the addition of a cellular component to the construct (Reichert *et al.* 2012). More work is required towards cell seeding protocols, pre-differentiation strategies, and the provision of a microenvironment within scaffolds in order to support cellular survival prior to vascular ingrowth (Dawson *et al*. 2011;Dawson and Oreffo 2013).

8.2 Weaknesses

The fundamental objective of this work was to produce a bone graft substitute that could realistically be translated into clinical practice. This process involves laboratory based experimentation, small animal experimentation, scaled up large animal work and eventually small human trials. In order to ensure continued progress of the study, and avoid getting caught endlessly at one stage of this process (termed the 'valley of death' (Reichert *et al.* 2010)) certain assumptions had to be made, as well as decisions based on likely best outcomes, which unfortunately introduced shortcomings to some of the studies.

8.2.1 Polymer choice

There are a multitude of biodegradeable polymers available, many of which have found clinical use in various medical disciplines ranging from drug administration to cardiac surgery. It is also noted that variation of the molecular weight (as well as isometry) of the specific polymer type also dramatically alters mechanical characteristics, degradation time as well as cellular compatibility. Initial testing of the three polymers (polyε-caprolactone, poly(DL-lactide) and poly(DL-lactide-co-glycolide)), based on expert guidance as well as related literature reviews, therefore opened up the possibility of missing an important polymer type which may have had optimal characteristics. Furthermore, the testing of only the high and low molecular weight versions (and DL isomers) of each was clearly restrictive for the same reasons, but did maximize the difference in individual characteristics obtained by this process, and avoided the need to test the virtually endless polymer/ molecular weight permutations that it is possible to produce.

8.2.2 Hydroxyapatite concentrations

Hydroxyapatite is available in many different forms, ranging from nano-particles and particulate matter, all the way through to porous solid structures. In addition, other ceramic bone substitutes (including calcium tricalcium phosphate and calcium silicates) are also available, all of which could have been combined with the chosen polymer. For the same reasons as above, the number of possible permutations in terms of ceramic type and combination concentration is again virtually endless, and hence a 10%

combination of hydroxyapatite particles with the polymers was chosen, as concentrations less than this was felt to be too low to have measurable effects in terms of exposure to cells, and a higher concentration may have significantly affected the mechanical characteristics as well as morphology of the porous structure. It was subsequently shown that this composite did display enhanced osteoinductive capacity without significant change to mechanical shear strength over polymer controls, but clearly there is significant scope for further research in this area, and indeed preliminary work into nano-particle composites has already been commenced (see future perspectives).

8.2.3 Single cell line

One significant weakness of the study was the fact that culture expanded cells from only a single patient were used for each of the stages of the study. It was important that the same cells were used, as the main comparisons were between polymers, and hence if different cells had been used between polymers, the heterogeneity of cell behaviour would mean that any comparisons would be subject to great variability. Ideally therefore, each stage of the experiment would be repeated multiple times using the same cells, but culture expanded from other patients in order to give a more accurate analysis of polymer biocompatibility and osteoinductivity on human SSCs as a whole. However, SSC availability, the need for large numbers of cells per experiment (and hence laboratory equipment/ cost/ space issues), as well as limited availability of polymers and time, meant that the use of a single culture expanded cell type appeared the best compromise. Furthermore, these experiments were performed using cells that had only been passaged on a single occasion, and hence closely represented the original *in vivo* cells. Due to the availability of fresh SSCs, many research centres have to use cells that have been passaged on numerous occasions, or use immortalised cell lines, meaning that any conclusions drawn from the behavior of these cell types in relation to scaffolds etc are even more subject to deviation from the *in vivo* situation.

8.2.4 Molecular analysis

In order to assess differentiation of cells along the osteoblastic (desired) route, a number of modalities were used, including biochemical assays for the assessment of alkaline phosphatase activity, histological and imunostaining techniques for bone markers such

as type-1 collagen and BSP. A widely accepted method used for the characterisation of cells is molecular analysis via techniques such as PCR. Multiple attempts were made to obtain results using this technique, but unfortunately technical hurdles meant that a complete data set was not obtainable for any of the experiments. The main source of error was the extraction of RNA from the cells. The chemicals required to lyse the cells also significantly dissolved the scaffolds, leading to an unacceptable level of contamination in the samples. Attempts to remove the cells from the scaffolds via trypsinisation, prior to RNA extraction was also attempted, but contamination remained and there was significant loss of cell number during the process, making any results inaccurate. On discussion with other members of the group involved in polymer/ SSC composites, this appears to be an ongoing problem with no satisfactory solution yet reached.

8.2.5 Mechanical testing

A widely accepted method for mechanically testing the impacted scaffolds was used in order to compare their shear strengths to that of milled allograft. This test was chosen as the main method of failure of allograft during IBG is in shear. It is also easy to perform, and critically it is both standardised and replicable, allowing an accurate comparison between materials. The test however does have certain limitations:

i) It was a static test, whereas in the clinical situation the impacted graft is under a continuously changing dynamic force as occurs during the gait cycle, undergoing wide variations in both compression and shear.

ii) The tests were performed after only 1 week in vitro incubation in isotonic solution. This is therefore at best a model for the scaffolds behavior during the only very early stages of the post-operative period.

iii) The tests were performed on impacted discs, shapes that are not used in the clinical situation. Some studies have impacted graft into prosthetic, cadaveric and animal femora in an attempt to address this problem, but whilst modelling the clinical situation more closely, this introduces many more variables, including impaction technique, thickness of graft and individual behaviour of femora. The reproducibility and standardization of the chosen technique meant that it was a more accurate way of testing

the true characteristics of the graft itself, as proven by the narrow error bars in the majority of the acquired data.

Clearly this part of the study was limited, but with further work and funding, these issues can be addressed. The ovine femoral condyle defect study did show ongoing biocompatibility and osteointegrative potential of the graft after an extended (3 month) incubation period, and there is a planned ovine hemiarthroplasty IBG study. This will address both long term *in vivo* potential of the graft, as well as exposing it to similar dynamic forces experienced in clinical use.

8.2.6 Time points

This issue was alluded to in the above section. Both mechanical and cellular *in vitro* testing was performed up to a maximum of two weeks incubation, which is clearly only comparable to the immediate post-operative time in the clinical situation. For cellular studies in particular, there are significant difficulties extending any *in vitro* studies consistently past this time point. Initial study protocol included a one month time point, but due to the difficult techniques required for the cell scaffold combination, and especially the impaction procedure, there was a high risk of contamination during these preparation processes. Despite multiple modifications to experimental design, as well as stringent aseptic technique, the infection rate was too high to make a one month incubation period a routine time point for all experiments. The purpose of the synthetic graft is to provide a long term replacement to bone graft and thus longer time point analysis is essential prior to any clinical translation. The planned *in vivo* hemiarthroplasty model will thus require analysis at multiple time points, ideally at least up to a year post implantation. It is also a more appropriate method of assessing the grafts ongoing mechanical potential, as in the *in vivo* scenario the bioresorption (and hence loss of mechanical integrity) of the graft, should ideally be balanced by *de novo* bone formation and host bone osseointegration (processes not modelled by the *in vitro* tests).

No basic science work can ever replicate the clinical situation with 100% accuracy, but with carefully planned models important aspects of experimental materials can be assessed. Care should be taken when interpreting *in vitro* data and hence when drawing conclusions, but in order to translate work from bench to clinic (without the use of

excessive animal experimentation), these are the best methods available. Limited resources, time, and the need to avoid stagnation at any stage of the developmental process mean that some assumptions and limited experimentation is required, further exposing the basic science work to shortfalls. However, many of the above described weaknesses can be addressed by the planned ovine hemiarthroplasty study and this will hence give a more accurate insight into the grafts long term *in vivo* potential.

8.3 Global Conclusion

The presented work details a Medical Research Council funded study (G802397) entitled 'Overcoming the Limitations of Allograft in Impaction Bone Grafting for Revision Arthroplasty'. The global objective was to test an array of polymers and polymer composites both *in vitro* and *in vivo* in order to produce an osteogenic alternative to allograft for use in IBG. This could have potential clinical benefits in terms of providing a consistent quality of graft, at a reasonable price, without the problems of limited availabilty and risks of disease transmission (Tomford *et al.* 1981a;Delloye *et al.* 2007).

Initial pilot studies allowed the development of reproducable cellular seeding protocols and validation of cellular analysis techniques. Throughout a subsequent series of *in vitro* studies, testing mechanical shear strength of impacted, milled, polymer discs, cohesiveness of impacted discs, cellular biocompatability studies, and biochemical as well as immunological measures of osteoinductivity, a high molecular weight porous version of $P_{DL}LA$ was identified as a promising candidate. Throughout the experiments an emphasis was placed on the need to identify a robust and functional candidate, rather than the optimal candidate in every respect, in order to ensure progress towards the stated end point (Evans *et al.* 2011).

Subsequent small animal (murine) *in vivo* experiments went on to show polymer biocompatibility and osteogenicity when combined with human SSCs, and a composite version of the polymer with 10 % HA further enhanced these qualities. This HA composite $P_{DL}LA$ polymer was hence selected for testing via an up-scaled ovine femoral condyle defect model.

This final study highlighted two important issues:

1. The scaffold appeared to work well on its own, without the addition of SSCs.

The focus of this thesis had been the incorporation of a *tissue engineered* scaffold for use as an allograft replacement in impaction bone grafting. The question thus must be asked as to whether the addition of a biological (cellular component) to the scaffold is really necessary if the scaffold works well independently? Certainly from a clinical perspective, a bioactive 'off the shelf' scaffold, which could be used in a single stage procedure, would be more desirable both from a patient and surgical perspective, reducing surgical time, number of procedures necessary, and hence reducing other potential complications such as infection or anaesthetic risks. The option of the addition of growth factors without detrimental effects during the supercritical CO_2 foaming process, and the option to further optimise HA availability by altering the concentration as well as the form (eg nano HA), further makes this an attractive way to proceed. However, other issues (including the very expensive FDA approval required for human trials) would also be encountered, which might limit this approach to the realm of 'big pharma' only (Law 2006).

2. There were significant differences between the way sheep and human SSCs reacted to the scaffold, as well as to the same culture conditions.

This issue highlights important problems surrounding this particular *in vivo* model, and indeed animal experimentation as a whole. Care should be taken when interpreting data from *in vivo* work for a number of reasons: Firstly, and as discussed in Sections 7.1 and 7.6, there are a multitude of limitations to models in terms of how animal models truly reflect the clinical situation. Small animal models are clearly limited when assessing bone regeneration in terms of loading, and size of any critical defect that is created. Furthermore, large animal models such as the one used in the later studies, are not necessarily adequately loaded, or the surrounding bone stock / quality into which any implant is embedded is not similar to the likely human clinical scenario (eg osteoporotic or relatively avascular bone) (Smith *et al.* 2011). Thus consideration of study design is of paramount importance when drawing any conclusions, or making any extrapolations from collected data. Secondly, certain aspects of animal experimentation are simply out of the control of the investigator. Humans and animals are clearly genetically different,

and there is no way to ensure that, even given an experiment were conditions exactly match the clinical scenario for which they are intended, the animal cells will respond in the same way as humans (Zannettino *et al.* 2010). This is widely acknowledged and has led to certain treatments translated to human use being far less efficacious than expected. A number of ethical issues surround 'straight to human' trials, but given the encouraging *in vitro* results, and relatively disappointing ovine *in vivo* data, in this instance this might be considered a viable option. As stated in Section 1.8, SSC seeded allograft has already been implanted into a small cohort of humans with femoral head avascular necrosis (Tilley *et al.* 2007) with limited success. This is thus one potential human model where tissue engineered scaffolds could be trialled for bone regenerative potential as well as biocompatibility, prior to use in a loaded situation such as IBG.

8.4 Future perspectives

The outcomes of these studies provide exciting advances in tissue engineering strategies for the replacement of lost bone stock. Further large animal scaled up *in vivo* investigations are planned, and will potentially bring this technology a stage further towards its full realisation. As is often the case, analysis of the ovine femoral defect specimens has raised further questions and opened new avenues for exploration prior to any clinical trials, but continued assessment and modification is of paramount importance if progress is to be made.

Nano hydroxyapatite preparations in combination with the porous polymer offer an exciting prospect, increasing the surface area of the HA available for its osteoinductive effects on the surrounding SSC populations, but maintaining the full biodegradability potential of the scaffold. Pilot studies are beginning to realize the potential of this product (Wang *et al.* 2007a). Rather than discreet HA particles embedded within a polymer structure, the nano particle HA offers the potential of a porous polymer matrix with the HA distributed evenly throughout it. Some preliminary work combining supercritically foamed polymers with nano HA has already been performed, with encouraging initial results in terms of enhanced cellular compatibility and osteoinductive potential. The addition of growth factors (eg BMP 2, VEGF etc) to the constructs is also a possibility, and is especially important when considering

neovascularisition of grafts, and hence increasing the survival of cells at a distance from any host nutritional supply (Kanczler *et al.* 2007;Kanczler *et al.* 2010;Reichert *et al.* 2012). This however has added complications when attempting to clinically translate products for human use (they would require additional FDA approval prior to clinical use, which is an extremely costly and difficult process).

Despite the production of any successful product, problems would still exist regarding the scale-up for commercial use. The collaboration team for this project (University of Nottingham), have concurrently investigated techniques to scale up the supercritical foaming process. Two techniques, involving either a multiple small chambered device, or a device with fewer but larger chambers, have been trialed with encouraging (as yet unpublished) results. Further work is required to analyse the polymers behavior compared to the original set.

Further clinical hurdles also need to be addressed prior to any successful translation, such as cell culture techniques acceptable for human use, operative timing, ethical considerations, finance and safety trials (Hollister and Murphy 2011;Mason and Manzotti 2010;*Smith et al*. 2011). This highlights the importance of a diverse approach to the problem, involving multiple specialties not only including cell biologists, chemists, engineers and clinicians, but also potentially commercial interest, governments, epidemiologists, ethical committees and most importantly acceptant patients. Only through close collaboration, careful planning and a combined approach will the complex step from bench to clinic be achievable.

Much progress has been made over the last decade in stem cell technology, and a steady stream of clinical applications and trials have followed on these advances. To date, there remains a paucity of randomised controlled trials to demonstrate the efficacy of many of these tissue engineered / stem cell approaches. However, it is difficult for any of these strategies to be brought into routine clinical use in the absence of large scale trials. Nonetheless, the continuing basic science breakthroughs and expanding bank of successful clinical evidence for these novel techniques has afforded the opportunity to push the boundaries of tissue engineering strategies in clinical practice, where other treatment modalities have failed. It is hoped that the work described in this thesis will further add to this bank of evidence, and the publications in clinical orthopaedic journals will highlight the potential, and stimulate interest in those who could

potentially benefit from the technology available. It is also hoped that the work highlighting barriers to clinical translation can already be utilized by others working in similar areas, to ensure successful implementation of their products, or highlight a need for similar research in a specific area prior to clinical trials.

It is likely the coming decade will herald the start of a new chapter in skeletal stem cell based regenerative therapies in orthopaedic surgery, that will help to address the currently unmet levels of an increasingly ageing population.

References

AARDEN,E.M., BURGER,E.H., and NIJWEIDE,P.J. (1994). Function of osteocytes in bone. *J Cell Biochem.* 55: 287-299.

AARVOLD,A., SMITH,J.O., TAYTON,E.R., JONES,A.M., DAWSON,J.I., LANHAM,S., BRISCOE,A., DUNLOP,D.G., and OREFFO,R.O. (2013). A tissue engineering strategy for the treatment of avascular necrosis of the femoral head. *Surgeon.*

AGRAWAL,C.M. and ATHANASIOU,K.A. (1997). Technique to control pH in vicinity of biodegrading PLA-PGA implants. *J. Biomed. Mater. Res.* 38: 105-114.

AGRAWAL,C.M. and RAY,R.B. (2001). Biodegradable polymeric scaffolds for musculoskeletal tissue engineering. *J. Biomed. Mater. Res.* 55: 141-150.

AHLMANN,E., PATZAKIS,M., ROIDIS,N., SHEPHERD,L., and HOLTOM,P. (2002). Comparison of anterior and posterior iliac crest bone grafts in terms of harvest-site morbidity and functional outcomes. *J. Bone Joint Surg. Am.* 84-A: 716-720.

ALSOUSOU,J., THOMPSON,M., HULLEY,P., NOBLE,A., and WILLETT,K. (2009). The biology of platelet-rich plasma and its application in trauma and orthopaedic surgery: a review of the literature. *J. Bone Joint Surg. Br.* 91: 987-996.

AMO,Y., MASUZAWA,M., HAMADA,Y., and KATSUOKA,K. (2004). Observations on angiopoietin 2 in patients with angiosarcoma. *Br. J. Dermatol.* 150: 1028-1029.

AMSTUTZ,H.C., CAMPBELL,P.B., KOSSOVSKY,N., and CLARKE,I.C. (1992). Mechanism and Clinical Significance of Wear Debris-Induced Osteolysis. *Clin Orthop Relat Res.* 276: 7-18.

ANSELMETTI,G,C., MANCA,A, KANIKA,K, MURPHY,K, EMINEFENDIC,H, MASALA,S, REGGE,D. (2009). Temperature measurement during polymerization of bone cement in percutaneous vertebroplasty: an in vivo study in humans. *Cardiovasc Intervent Radiol.* 32:491-8.

ARTHRITIS RESEARCH UK (2014). Who gets arthritis? Available from http://www.arthritisresearchuk.org/arthritis-information/conditions/arthritis/who-gets-it.aspx. Last accessed 2/2/14.

ASPENBERG,P. and VIRCHENKO,O. (2004). Platelet concentrate injection improves Achilles tendon repair in rats. *Acta Orthop. Scand.* 75: 93-99.

ATHANASIOU,K.A., NIEDERAUER,G.G., and AGRAWAL,C.M. (1996). Sterilization, toxicity, biocompatibility and clinical applications of polylactic acid/polyglycolic acid copolymers. *Biomaterials* 17: 93-102.

AULAKH,T.S., JAYASEKERA,N., KUIPER,J.H., and RICHARDSON,J.B. (2009). Long-term clinical outcomes following the use of synthetic hydroxyapatite and bone graft in impaction in revision hip arthroplasty. *Biomaterials* 30: 1732-1738.

BAUER,T.W. and MUSCHLER,G.F. (2000). Bone graft materials. An overview of the basic science. *Clin. Orthop. Relat Res.* 10-27.

BENDINELLI,P., MATTEUCCI,E., DOGLIOTTI,G., CORSI,M.M., BANFI,G., MARONI,P., AND DESIDERIO,M.A. (2010). Molecular basis of anti-inflammatory action of platelet-rich plasma on human chondrocytes: Mechanisms of NF-κB inhibition via HGF. *Journal of cellular physiology*, *225*(3), 757-766.

BENOIT,D.S., DURNEY,A.R., and ANSETH,K.S. (2006). Manipulations in hydrogel degradation behavior enhance osteoblast function and mineralized tissue formation. *Tissue Eng* 12: 1663-1673.

BERGMANN,G., SIRAKY,J., ROHLMANN,A., and KOELBEL,R. (1984). A comparison of hip joint forces in sheep, dog and man. *J Biomech.* 17: 907-921.

BERGSMA,E.J., ROZEMA,F.R., BOS,R.R., and DE BRUIJN,W.C. (1993). Foreign body reactions to resorbable poly(L-lactide) bone plates and screws used for the fixation of unstable zygomatic fractures. *J. Oral Maxillofac. Surg.* 51: 666-670.

BERNER,A., REICHERT,J.C., WOODRUFF,M.A., SAIFZADEH,S., MORRIS,A.J., EPARI,D.R., NERLICH,M., SCHUETZ,M.A., and HUTMACHER,D.W. (2013). Autologous vs. allogenic mesenchymal progenitor cells for the reconstruction of critical sized segmental tibial bone defects in aged sheep. *Acta Biomater.* 9: 7874-7884.

BESWICK,A. and BLOM,A.W. (2011). Bone graft substitutes in hip revision surgery: A comprehensive overview. *Injury*. 42(Supp 2): S40-46.

BIELECKI,T., GAZDZIK,T.S., and SZCZEPANSKI,T. (2008). Benefit of percutaneous injection of autologous platelet-leukocyte-rich gel in patients with delayed union and nonunion. *Eur. Surg. Res.* 40: 289-296.

BLACK,L.L., GAYNOR,J., GAHRING,D., ADAMS,C., ARON,D., HARMAN,S., GINGERICH,D.A., and HARMAN,R. (2007). Effect of adipose-derived mesenchymal stem and regenerative cells on lameness in dogs with chronic osteoarthritis of the coxofemoral joints: a randomized, double-blinded, multicenter, controlled trial. *Vet. Ther.* 8: 272-284.

BLOM,A.W., GRIMM,B., MILES,A.W., CUNNINGHAM,J.L., and LEARMONTH,I.D. (2002). Subsidence in impaction grafting: the effect of adding a ceramic bone graft extender to bone. *Proc. Inst. Mech. Eng H.* 216: 265-270.

BLOM,A.W., WYLDE,V., LIVESEY,C., WHITEHOUSE,M.R., EASTAUGH-WARING,S., BANNISTER,G.C., and LEARMONTH,I.D. (2009). Impaction bone grafting of the acetabulum at hip revision using a mix of bone chips and a biphasic porous ceramic bone graft substitute. *Acta Orthop.* 80: 150-154.

BOBYN,J.D., POGGIE,R.A., KRYGIER,J.J., LEWALLEN,D.G., HANSSEN,A.D., LEWIS,R.J., UNGER,A.S., O'KEEFE,T.J., CHRISTIE,M.J., NASSER,S., WOOD,J.E., STULBERG,S.D., and TANZER,M. (2004). Clinical validation of a structural porous tantalum biomaterial for adult reconstruction. *J Bone Joint Surg. Am.* 86-A Suppl 2: 123-129.

BOBYN,J.D., STACKPOOL,G.J., HACKING,S.A., TANZER,M., and KRYGIER,J.J. (1999). Characteristics of bone ingrowth and interface mechanics of a new porous tantalum biomaterial. *J. Bone Joint Surg. Br.* 81: 907-914.

BOLLAND,B.J., KANCZLER,J.M., DUNLOP,D.G., and OREFFO,R.O. (2008a). Development of in vivo muCT evaluation of neovascularisation in tissue engineered bone constructs. *Bone* 43: 195-202.

BOLLAND,B.J., KANCZLER,J.M., GINTY,P.J., HOWDLE,S.M., SHAKESHEFF,K.M., DUNLOP,D.G., and OREFFO,R.O. (2008b). The application of human bone marrow stromal cells and poly(dl-lactic acid) as a biological bone graft extender in impaction bone grafting. *Biomaterials* 29: 3221-3227.

BOLLAND,B.J., NEW,A.M., MADABHUSHI,S.P., OREFFO,R.O., and DUNLOP,D.G. (2007). Vibration-assisted bone-graft compaction in impaction bone grafting of the femur. *J. Bone Joint Surg. Br.* 89: 686-692.

BOLLAND,B.J., PARTRIDGE,K., TILLEY,S., NEW,A.M., DUNLOP,D.G., and OREFFO,R.O. (2006). Biological and mechanical enhancement of impacted allograft seeded with human bone marrow stromal cells: potential clinical role in impaction bone grafting. *Regen. Med.* 1: 457-467.

BOSTMAN,O., HIRVENSALO,E., MAKINEN,J., and ROKKANEN,P. (1990). Foreign-body reactions to fracture fixation implants of biodegradable synthetic polymers. *J. Bone Joint Surg. Br.* 72: 592-596.

BOSTMAN,O., HIRVENSALO,E., PARTIO,E., TORMALA,P., and ROKKANEN,P. (1992a). Resorbable rods and screws of polyglycolide in stabilizing malleolar fractures. A clinical study of 600 patients. *Unfallchirurg* 95: 109-112.

BOSTMAN,O., PARTIO,E., HIRVENSALO,E., and ROKKANEN,P. (1992b). Foreign-body reactions to polyglycolide screws. Observations in 24/216 malleolar fracture cases. *Acta Orthop. Scand.* 63: 173-176.

BOSTMAN,O.M. and PIHLAJAMAKI,H.K. (2000). Adverse tissue reactions to bioabsorbable fixation devices. *Clin. Orthop. Relat Res.* 216-227.

BRENNAN,S.A., BRABAZON,D., and O'BYRNE,J.M. (2011). Effect of vibration on the shear strength of impacted bone graft in revision hip surgery. *J. Bone Joint Surg. Br.* 93: 755-759.

BREWSTER,N.T., GILLESPIE,W.J., HOWIE,C.R., MADABHUSHI,S.P., USMANI,A.S., and FAIRBAIRN,D.R. (1999). Mechanical considerations in impaction bone grafting. *J. Bone Joint Surg. Br.* 81: 118-124.

BROOK,I.M. and HATTON,P.V. (1998). Glass-ionomers: bioactive implant materials. *Biomaterials* 19: 565-571.

BRUDER,S.P., KRAUS,K.H., GOLDBERG,V.M., and KADIYALA,S. (1998). The effect of implants loaded with autologous mesenchymal stem cells on the healing of canine segmental bone defects. *J. Bone Joint Surg. Am.* 80: 985-996.

BUCHOLZ,R.W., CARLTON,A., and HOLMES,R. (1989). Interporous hydroxyapatite as a bone graft substitute in tibial plateau fractures. *Clin. Orthop. Relat Res.* 53-62.

BULLENS,P.H., SCHREUDER,H.W., MALEFIJT,M.C., VERDONSCHOT,N., and BUMA,P. (2009). The presence of periosteum is essential for the healing of large diaphyseal segmental bone defects reconstructed with trabecular metal: A study in the femur of goats. *J. Biomed. Mater. Res. B Appl. Biomater.* 92B: 24-31.

BURCHARDT,H. (1983). The biology of bone graft repair. *Clin. Orthop. Relat Res.* 28-42.

BURKUS,J.K., GORNET,M.F., DICKMAN,C.A., and ZDEBLICK,T.A. (2002). Anterior lumbar interbody fusion using rhBMP-2 with tapered interbody cages. *J Spinal Disord. Tech.* 15: 337-349.

CALORI,G.M., TAGLIABUE,L., GALA,L., D'IMPORZANO,M., PERETTI,G., and ALBISETTI,W. (2008). Application of rhBMP-7 and platelet-rich plasma in the treatment of long bone non-unions: a prospective randomised clinical study on 120 patients. *Injury* 39: 1391-1402.

CAMMISA,F.P., JR., LOWERY,G., GARFIN,S.R., GEISLER,F.H., KLARA,P.M., MCGUIRE,R.A., SASSARD,W.R., STUBBS,H., and BLOCK,J.E. (2004). Two-year fusion rate equivalency between Grafton DBM gel and autograft in posterolateral spine fusion: a prospective controlled trial employing a side-by-side comparison in the same patient. *Spine* 29: 660-666.

CECCHI,F., MANNONI,A., MOLINO-LOVA,R., CEPPATELLI,S., BENVENUTI,E., BANDINELLI,S., LAURETANI,F., MACCHI,C., and FERRUCCI,L. (2008). Epidemiology of hip and knee pain in a community based sample of Italian persons aged 65 and older. *Osteoarthritis. Cartilage* 16: 1039-1046.

CENTENO,C.J., KISIDAY,J., FREEMAN,M., and SCHULTZ,J.R. (2006). Partial regeneration of the human hip via autologous bone marrow nucleated cell transfer: A case study. *Pain Physician* 9: 253-256.

CHANG,Z., MEYER,K., RAPRAEGER,A.C., and FRIEDL,A. (2000). Differential ability of heparan sulfate proteoglycans to assemble the fibroblast growth factor receptor complex in situ. *FASEB J.* 14: 137-144.

CHAPMAN,M.W., BUCHOLZ,R., and CORNELL,C. (1997). Treatment of acute fractures with a collagen-calcium phosphate graft material. A randomized clinical trial. *J. Bone Joint Surg. Am.* 79: 495-502.

CHARNLEY,J. (1970). Total hip replacement by low-friction arthroplasty. *Clin. Orthop. Relat Res.* 72: 7-21.

CHU,C.R., SZCZODRY,M., and BRUNO,S. (2010). Animal models for cartilage regeneration and repair. *Tissue Eng Part B Rev.* 16: 105-115.

CLAESSON-WELSH,L. (2008). VEGF-B taken to our hearts: specific effect of VEGF-B in myocardial ischemia. *Arterioscler. Thromb. Vasc. Biol.* 28: 1575-1576.

COLTON,C.K. (1995). Implantable biohybrid artificial organs. *Cell Transplant.* 4: 415-436.

CONRAD,E.U., GRETCH,D.R., OBERMEYER,K.R., MOOGK,M.S., SAYERS,M., WILSON,J.J., and STRONG,D.M. (1995). Transmission of the hepatitis-C virus by tissue transplantation. *J. Bone Joint Surg. Am.* 77: 214-224.

CORNELL,C.N. (1999). Osteoconductive materials and their role as substitutes for autogenous bone grafts. *Orthop. Clin. North Am.* 30: 591-598.

COSTAIN,D.J. and CRAWFORD,R.W. (2009). Fresh-frozen vs. irradiated allograft bone in orthopaedic reconstructive surgery. *Injury* 40: 1260-1264.

COUGHLIN,M.J., GRIMES,J.S., and KENNEDY,M.P. (2006). Coralline hydroxyapatite bone graft substitute in hindfoot surgery. *Foot Ankle Int.* 27: 19-22.

CRAIG R.F. (1993). *Soil mechanics* (5th edition) London: Chapman and Hall.

CREMER,C. and CREMER,T. (1978). Considerations on a laser-scanning-microscope with high resolution and depth of field. *Microsc. Acta* 81: 31-44.

CUKIERMAN,E., PANKOV,R., and YAMADA,K.M. (2002). Cell interactions with three-dimensional matrices. *Curr. Opin. Cell Biol.* 14: 633-639.

CUOMO,A.V., VIRK,M., PETRIGLIANO,F., MORGAN,E.F., and LIEBERMAN,J.R. (2009). Mesenchymal stem cell concentration and bone repair: potential pitfalls from bench to bedside. *J. Bone Joint Surg. Am.* 91: 1073-1083.

DAVIDSON,J.A. (1993). Characteristics of metal and ceramic total hip bearing surfaces and their effect on long-term ultra high molecular weight polyethylene wear. *Clin. Orthop. Relat Res.* 361-378.

DAVIES,O.R., LEWIS,A.L., WHITAKER,M.J., TAI,H., SHAKESHEFF,K.M., and HOWDLE,S.M. (2008). Applications of supercritical CO2 in the fabrication of polymer systems for drug delivery and tissue engineering. *Adv. Drug Deliv. Rev.* 60: 373-387.

DAWSON,J.I., KANCZLER,J.M., YANG,X.B., ATTARD,G.S., and OREFFO,R.O. (2011). Clay gels for the delivery of regenerative microenvironments. *Adv. Mater.* 23: 3304-3308.

DAWSON,J.I. and OREFFO,R.O. (2013). Clay: New Opportunities for Tissue Regeneration and Biomaterial Design. *Adv. Mater.* 25: 4069-4086.

DELLOYE,C., CORNU,O., DRUEZ,V., and BARBIER,O. (2007). Bone allografts: What they can offer and what they cannot. *J. Bone Joint Surg. Br.* 89: 574-579.

DIEPPE,P.A., SATHAPATAYAVONGS,B., JONES,H.E., BACON,P.A., and RING,E.F. (1980). Intra-articular steroids in osteoarthritis. *Rheumatol. Rehabil.* 19: 212-217.

DIGIROLAMO,C.M., STOKES,D., COLTER,D., PHINNEY,D.G., CLASS,R., and PROCKOP,D.J. (1999). Propagation and senescence of human marrow stromal cells in culture: a simple colony-forming assay identifies samples with the greatest potential to propagate and differentiate. *Br. J. Haematol.* 107: 275-281.

DIMOS,J.T., RODOLFA,K.T., NIAKAN,K.K., WEISENTHAL,L.M., MITSUMOTO,H., CHUNG,W., CROFT,G.F., SAPHIER,G., LEIBEL,R., GOLAND,R., WICHTERLE,H., HENDERSON,C.E., and EGGAN,K. (2008). Induced pluripotent stem cells generated from patients with ALS can be differentiated into motor neurons. *Science* 321: 1218-1221.

DOBSON,J. (1952). Pioneers of osteogeny: Clopton Havers. *J Bone Joint Surg. Br.* 34-B: 702-707.

DUNLOP,D.G., BREWSTER,N.T., MADABHUSHI,S.P., USMANI,A.S., PANKAJ,P., and HOWIE,C.R. (2003). Techniques to improve the shear strength of impacted bone graft: the effect of particle size and washing of the graft. *J. Bone Joint Surg. Am.* 85-A: 639-646.

DUNNING,D. (2002). Basic mammalian bone anatomy and healing. *Vet. Clin. North Am. Exot. Anim Pract.* 5: 115-128.

EGGLI,P.S., MULLER,W., and SCHENK,R.K. (1988). Porous hydroxyapatite and tricalcium phosphate cylinders with two different pore size ranges implanted in the cancellous bone of rabbits. A comparative histomorphometric and histologic study of bony ingrowth and implant substitution. *Clin. Orthop. Relat Res.* 232: 127-138.

EMMS,N.W., BUCKLEY,S.C., STOCKLEY,I., HAMER,A.J., and KERRY,R.M. (2009). Mid-to long-term results of irradiated allograft in acetabular reconstruction: a follow-up report. *J. Bone Joint Surg. Br.* 91: 1419-1423.

EPPLEY,B.L., WOODELL,J.E., and HIGGINS,J. (2004). Platelet quantification and growth factor analysis from platelet-rich plasma: implications for wound healing. *Plast. Reconstr. Surg.* 114: 1502-1508.

EVANS,C.H. (2011). Barriers to the clinical translation of orthopedic tissue engineering. *Tissue Eng Part B Rev.* 17: 437-441.

FAJARDO,M., and DI CESARE,P.E. (2005). Disease-modifying therapies for osteoarthritis. *Drugs & aging 22*, 141-161.

FENG,B., JINKANG,Z., ZHEN,W., JIANXI,L., JIANG,C., JIAN,L., GUOLIN,M., and XIN,D. (2011). The effect of pore size on tissue ingrowth and neovascularization in porous bioceramics of controlled architecture in vivo. *Biomed. Mater.* 6: 015007.

FERNANDEZ-FAIREN,M., SALA,P., DUFOO,M., JR., BALLESTER,J., MURCIA,A., and MERZTHAL,L. (2008). Anterior cervical fusion with tantalum implant: a prospective randomized controlled study. *Spine* 33: 465-472.

FIALKOV,J.A., HOLY,C.E., SHOICHET,M.S., and DAVIES,J.E. (2003). In vivo bone engineering in a rabbit femur. *J Craniofac. Surg.* 14: 324-332.

FIELD,J.R., MCGEE,M., STANLEY,R., RUTHENBECK,G., PAPADIMITRAKIS,T., ZANNETTINO,A., GRONTHOS,S., and ITESCU,S. (2011). The efficacy of allogeneic mesenchymal precursor cells for the repair of an ovine tibial segmental defect. *Vet. Comp Orthop. Traumatol.* 24: 113-121.

FORTIER,L.A., POTTER,H.G., RICKEY,E.J., SCHNABEL,L.V., FOO,L.F., CHONG,L.R., STOKOL,T., CHEETHAM,J., and NIXON,A.J. (2010). Concentrated bone marrow aspirate improves full-thickness cartilage repair compared with microfracture in the equine model. *J. Bone Joint Surg. Am.* 92: 1927-1937.

FOSTER,T.E., PUSKAS,B.L., MANDELBAUM,B.R., GERHARDT,M.B., and RODEO,S.A. (2009). Platelet-rich plasma: from basic science to clinical applications. *Am. J. Sports Med.* 37: 2259-2272.

FRANZ-ODENDAAL,T.A., HALL,B.K., and WITTEN,P.E. (2006). Buried alive: how osteoblasts become osteocytes. *Dev. Dyn.* 235: 176-190.

FREI,H., MITCHELL,P., MASRI,B.A., DUNCAN,C.P., and OXLAND,T.R. (2004). Allograft impaction and cement penetration after revision hip replacement. A histomorphometric analysis in the cadaver femur. *J. Bone Joint Surg. Br.* 86: 771-776.

FROST,H.M. (1962). Human osteoid seams. *J. Clin. Endocrinol. Metab* 22: 631-640.

FROST,H.M.(1987). Bone "mass" and the "mechanostat": A proposal. *Anat. Rec.* 219: 1–9.

FRIEDENSTEIN,A.J., DERIGLASOVA,U.F., KULAGINA,N.N., PANASUK,A.F., RUDAKOWA,S.F., LURIA,E.A., and RUADKOW,I.A. (1974). Precursors for fibroblasts in different populations of hematopoietic cells as detected by the in vitro colony assay method. *Exp. Hematol.* 2: 83-92.

FRIEDENSTEIN,A.J., GORSKAJA,J.F., and KULAGINA,N.N. (1976). Fibroblast precursors in normal and irradiated mouse hematopoietic organs. *Exp. Hematol.* 4: 267-274.

FRIEDENSTEIN,A.J., PETRAKOVA,K.V., KUROLESOVA,A.I., and FROLOVA,G.P. (1968). Heterotopic of bone marrow. Analysis of precursor cells for osteogenic and hematopoietic tissues. *Transplantation* 6: 230-247.

FRIEDENSTEIN,A.J., PIATETZKY-SHAPIRO,I.I., and PETRAKOVA,K.V. (1966). Osteogenesis in transplants of bone marrow cells. *J. Embryol. Exp. Morphol.* 16: 381-390.

GANGJI,V. and HAUZEUR,J.P. (2005). Treatment of osteonecrosis of the femoral head with implantation of autologous bone-marrow cells. Surgical technique. *J. Bone Joint Surg. Am.* 87 Suppl 1: 106-112.

GANTENBEIN-RITTER,B., SPRECHER,C.M., CHAN,S., ILLIEN-JUNGER,S., and GRAD,S. (2011). Confocal imaging protocols for live/dead staining in three-dimensional carriers. *Methods Mol. Biol.* 740: 127-140.

GERBER,H.P. and FERRARA,N. (2003). The role of VEGF in normal and neoplastic hematopoiesis. *J. Mol. Med. (Berl)* 81: 20-31.

GERBER,H.P., VU,T.H., RYAN,A.M., KOWALSKI,J., WERB,Z., and FERRARA,N. (1999). VEGF couples hypertrophic cartilage remodeling, ossification and angiogenesis during endochondral bone formation. *Nat. Med.* 5: 623-628.

GIANNOUDIS,P.V., DINOPOULOS,H., and TSIRIDIS,E. (2005). Bone substitutes: an update. *Injury* 36 Suppl 3: S20-S27.

GIANNOUDIS,P.V., EINHORN,T.A., and MARSH,D. (2007). Fracture healing: the diamond concept. *Injury* 38 (Suppl 4): S3-S6.

GIE,G.A., LINDER,L., LING,R.S., SIMON,J.P., SLOOFF,T.J., and TIMPERLEY,A.J. (1993a). Contained morselized allograft in revision total hip arthroplasty. Surgical technique. *Orthop. Clin. North Am.* 24: 717-725.

GIE,G.A., LINDER,L., LING,R.S., SIMON,J.P., SLOOFF,T.J., and TIMPERLEY,A.J. (1993b). Impacted cancellous allografts and cement for revision total hip arthroplasty. *J. Bone Joint Surg. Br.* 75: 14-21.

GROSS,U., BRANDES,J., STRUNZ,V., BAB,I., and SELA,J. (1981). The ultrastructure of the interface between a glass ceramic and bone. *J. Biomed. Mater. Res.* 15: 291-305.

HALEEM,A.M., EL SINGERGY,A.A., SABRY,D., ATTA,H.M., RASHED,L.A., CHU,C.R., EL SHEWY,L.T., AZZAM,A., and ABDEL AZIZ,M.T. (2010). The clinical use of human culture-expanded autologous bone marrow mesenchymal stem cells transplanted on platelet-rich fibrin glue in the treatment of articular cartilage defects. A pilot study and preliminary results. *Cartilage* 1: 253-261.

HALLIDAY,B.R., ENGLISH,H.W., TIMPERLEY,A.J., GIE,G.A., and LING,R.S. (2003). Femoral impaction grafting with cement in revision total hip replacement. Evolution of the technique and results. *J. Bone Joint Surg. Br.* 85: 809-817.

HARTMANN,E.K., HEINTEL,T., MORRISON,R.H., and WECKBACH,A. (2010). Influence of platelet-rich plasma on the anterior fusion in spinal injuries: a qualitative and quantitative analysis using computer tomography. *Arch. Orthop. Trauma Surg.* 130: 909-914.

HARWOOD,P.J. and GIANNOUDIS,P.V. (2005). Application of bone morphogenetic proteins in orthopaedic practice: their efficacy and side effects. *Expert. Opin. Drug Saf* 4: 75-89.

HAUER,A.D., HABETS,K.L., VAN WANROOIJ,E.J., DE,V.P., KRUEGER,J., REISFELD,R.A., VAN BERKEL,T.J., and KUIPER,J. (2009). Vaccination against TIE2 reduces atherosclerosis. *Atherosclerosis* 204: 365-371.

HE,P., SAHOO,S., NG,K.S., CHEN,K., TOH,S.L., and GOH,J.C. (2013). Enhanced osteoinductivity and osteoconductivity through hydroxyapatite coating of silk-based tissue-engineered ligament scaffold. *J. Biomed. Mater. Res. A* 101: 555-566.

HERNIGOU,P., POIGNARD,A., BEAUJEAN,F., and ROUARD,H. (2005a). Percutaneous autologous bone-marrow grafting for nonunions. Influence of the number and concentration of progenitor cells. *J. Bone Joint Surg. Am.* 87: 1430-1437.

HERNIGOU,P., POIGNARD,A., MANICOM,O., MATHIEU,G., and ROUARD,H. (2005b). The use of percutaneous autologous bone marrow transplantation in nonunion and avascular necrosis of bone. *J. Bone Joint Surg. Br.* 87: 896-902.

HERNIGOU,P., POIGNARD,A., ZILBER,S., and ROUARD,H. (2009). Cell therapy of hip osteonecrosis with autologous bone marrow grafting. *Indian J. Orthop.* 43: 40-45.

HIBI,H., YAMADA,Y., UEDA,M., and ENDO,Y. (2006). Alveolar cleft osteoplasty using tissue-engineered osteogenic material. *Int. J. Oral Maxillofac. Surg.* 35: 551-555.

HING,K.A., REVELL,P.A., SMITH,N., and BUCKLAND,T. (2006). Effect of silicon level on rate, quality and progression of bone healing within silicate-substituted porous hydroxyapatite scaffolds. *Biomaterials* 27: 5014-5026.

HO,S.T. and HUTMACHER,D.W. (2006). A comparison of micro CT with other techniques used in the characterization of scaffolds. *Biomaterials* 27: 1362-1376.

HOEBEN,A., LANDUYT,B., HIGHLEY,M.S., WILDIERS,H., VAN OOSTEROM,A.T., and DE BRUIJN,E.A. (2004). Vascular endothelial growth factor and angiogenesis. *Pharmacol. Rev.* 56: 549-580.

HOLLISTER,S.J. and MURPHY,W.L. (2011). Scaffold translation: barriers between concept and clinic. *Tissue Eng Part B Rev.* 17: 459-474.

HOLMES,R.E., BUCHOLZ,R.W., and MOONEY,V. (1986). Porous hydroxyapatite as a bone-graft substitute in metaphyseal defects. A histometric study. *J. Bone Joint Surg. Am.* 68: 904-911.

HOLMES,R.E., BUCHOLZ,R.W., and MOONEY,V. (1987). Porous hydroxyapatite as a bone graft substitute in diaphyseal defects: a histometric study. *J. Orthop. Res.* 5: 114-121.

HORAN,F.T. (2011). The bone and joint decade 2000 to 2010. *J. Bone Joint Surg. Br.* 93: 143-144.

HOU,Q., GRIJPMA,D.W., and FEIJEN,J. (2003). Preparation of interconnected highly porous polymeric structures by a replication and freeze-drying process. *J. Biomed. Mater. Res. B Appl. Biomater.* 67: 732-740.

HUBBELL,J.A. (2003). Materials as morphogenetic guides in tissue engineering. *Curr. Opin. Biotechnol.* 14: 551-558.

HUTMACHER,D.W. (2000). Scaffolds in tissue engineering bone and cartilage. *Biomaterials* 21: 2529-2543.

HUTMACHER,D.W., SCHANTZ,J.T., LAM,C.X., TAN,K.C., and LIM,T.C. (2007). State of the art and future directions of scaffold-based bone engineering from a biomaterials perspective. *J. Tissue Eng Regen. Med.* 1: 245-260.

HYDE,J.A., CHINN,J.A., and PHILLIPS,R.E., JR. (1999). Polymer heart valves. *J. Heart Valve Dis.* 8: 331-339.

ISHIYAMA,M., TOMINAGA,H., SHIGA,M., SASAMOTO,K., OHKURA,Y., and UENO,K. (1996). A combined assay of cell viability and in vitro cytotoxicity with a highly water-soluble tetrazolium salt, neutral red and crystal violet. *Biol. Pharm. Bull.* 19: 1518-1520.

JELTSCH,M., KAIPAINEN,A., JOUKOV,V., MENG,X., LAKSO,M., RAUVALA,H., SWARTZ,M., FUKUMURA,D., JAIN,R.K., and ALITALO,K. (1997). Hyperplasia of lymphatic vessels in VEGF-C transgenic mice. *Science* 276: 1423-1425.

JENIS,L.G. and BANCO,R.J. (2010). Efficacy of silicate-substituted calcium phosphate ceramic in posterolateral instrumented lumbar fusion. *Spine* 35: E1058-E1063.

JOHNSON,E.E., URIST,M.R., and FINERMAN,G.A. (1992). Resistant nonunions and partial or complete segmental defects of long bones. Treatment with implants of a composite of human bone morphogenetic protein (BMP) and autolyzed, antigen-extracted, allogeneic (AAA) bone. *Clin. Orthop. Relat Res.* 229-237.

JONCK,L.M. and GROBBELAAR,C.J. (1990). Ionos bone cement (glass-ionomer): an experimental and clinical evaluation in joint replacement. *Clin. Mater.* 6: 323-359.

JONCK,L.M. and GROBBELAAR,C.J. (1992). A glass ionomer for reconstructive surgery. Ionogran--an ionomeric micro implant. A biological evaluation. *Clin. Mater.* 9: 85-103.

JONES,A, NEW,A.M., BOLLAND,B.J., OREFFO,R.O. and DUNLOP,D.G. (2010). From roadside to revision hip surgery: the role of vibration impaction in acetabular impaction bone grafting. *J.Bone Joint Surg.Br.* 92-B (Supp III): 398-399.

JONES,A.M.H, FOONG,T.S., NEW,A.M., BOLLAND,B.J., POUND,J.C., DUNLOP,D.G. and OREFFO,R.O. (2009). The Effect of Skeletal Stem Cells, Hydroxyapatite Coated Stem Cells and Collagen Coated Allograft on the Biomechanical Properties of Impacted Bone Graft. Tissue and Cell Engineering Society Annual Conference. 08/07/2009, Glasgow.

KANCZLER,J.M., BARRY,J., GINTY,P., HOWDLE,S.M., SHAKESHEFF,K.M., and OREFFO,R.O. (2007). Supercritical carbon dioxide generated vascular endothelial growth factor encapsulated poly(DL-lactic acid) scaffolds induce angiogenesis in vitro. *Biochem. Biophys. Res. Commun.* 352: 135-141.

KANCZLER,J.M., GINTY,P.J., WHITE,L., CLARKE,N.M., HOWDLE,S.M., SHAKESHEFF,K.M., and OREFFO,R.O. (2010). The effect of the delivery of vascular endothelial growth factor and bone morphogenic protein-2 to osteoprogenitor cell populations on bone formation. *Biomaterials* 31: 1242-1250.

KANITKAR,M., TAILOR,H.D., and KHAN,W.S. (2011). The use of growth factors and mesenchymal stem cells in orthopaedics. *Open. Orthop. J* 5 (Suppl 2): 271-275.

KARAGEORGIOU,V. and KAPLAN,D. (2005). Porosity of 3D biomaterial scaffolds and osteogenesis. *Biomaterials* 26: 5474-5491.

KHAN,F., TARE,R.S., KANCZLER,J.M., OREFFO,R.O., and BRADLEY,M. (2010). Strategies for cell manipulation and skeletal tissue engineering using high-throughput polymer blend formulation and microarray techniques. *Biomaterials* 31: 2216-2228.

KHOUW,I.M., VAN WACHEM,P.B., DE LEIJ,L.F., and VAN LUYN,M.J. (1998). Inhibition of the tissue reaction to a biodegradable biomaterial by monoclonal antibodies to IFN-gamma. *J. Biomed. Mater. Res.* 41: 202-210.

KIKUCHI,A. and OKANO,T. (2005). Nanostructured designs of biomedical materials: applications of cell sheet engineering to functional regenerative tissues and organs. *J. Control Release* 101: 69-84.

KINNUNEN,I., AITASALO,K., POLLONEN,M., and VARPULA,M. (2000). Reconstruction of orbital floor fractures using bioactive glass. *J. Craniomaxillofac. Surg.* 28: 229-234.

KITOH,H., KITAKOJI,T., TSUCHIYA,H., KATOH,M., and ISHIGURO,N. (2007). Distraction osteogenesis of the lower extremity in patients with achondroplasia/hypochondroplasia treated with transplantation of culture-expanded bone marrow cells and platelet-rich plasma. *J. Pediatr. Orthop.* 27: 629-634.

KOBAYASHI,H. and LIN,P.C. (2005). Angiopoietin/Tie2 signaling, tumor angiogenesis and inflammatory diseases. *Front Biosci.* 10: 666-674.

KODACH,L.L., WIERCINSKA,E., DE MIRANDA,N.F., BLEUMING,S.A., MUSLER,A.R., PEPPELENBOSCH,M.P., DEKKER,E., VAN DEN BRINK,G.R., VAN NOESEL,C.J., MORREAU,H., HOMMES,D.W., TEN,D.P., OFFERHAUS,G.J., and HARDWICK,J.C. (2008). The bone morphogenetic protein pathway is inactivated in the majority of sporadic colorectal cancers. *Gastroenterology* 134: 1332-1341.

KON,E., MURAGLIA,A., CORSI,A., BIANCO,P., MARCACCI,M., MARTIN,I., BOYDE,A., RUSPANTINI,I., CHISTOLINI,P., ROCCA,M., GIARDINO,R., CANCEDDA,R., and QUARTO,R. (2000). Autologous bone marrow stromal cells loaded onto porous hydroxyapatite ceramic accelerate bone repair in critical-size defects of sheep long bones. *J. Biomed. Mater. Res.* 49: 328-337.

KORDA,M., BLUNN,G., GOODSHIP,A., and HUA,J. (2008). Use of mesenchymal stem cells to enhance bone formation around revision hip replacements. *J. Orthop. Res.* 26: 880-885.

KORDA,M., BLUNN,G., PHIPPS,K., RUST,P., DI,S.L., COATHUP,M., GOODSHIP,A., and HUA,J. (2006). Can mesenchymal stem cells survive under normal impaction force in revision total hip replacements? *Tissue Eng* 12: 625-630.

KOVACH,N.L., LIN,N., YEDNOCK,T., HARLAN,J.M., and BROUDY,V.C. (1995). Stem cell factor modulates avidity of alpha 4 beta 1 and alpha 5 beta 1 integrins expressed on hematopoietic cell lines. *Blood* 85: 159-167.

KRUYT,M., DE,B.J., ROUWKEMA,J., VAN,B.C., ONER,C., VERBOUT,A., and DHERT,W. (2008). Analysis of the dynamics of bone formation, effect of cell seeding density, and potential of allogeneic cells in cell-based bone tissue engineering in goats. *Tissue Eng Part A* 14: 1081-1088.

KUHNE,J.H., BARTL,R., FRISCH,B., HAMMER,C., JANSSON,V., and ZIMMER,M. (1994). Bone formation in coralline hydroxyapatite. Effects of pore size studied in rabbits. *Acta Orthop. Scand.* 65: 246-252.

LACHIEWICZ,P.F., BOLOGNESI,M.P., HENDERSON,R.A., SOILEAU,E.S., and VAIL,T.P. (2011). Can Tantalum Cones Provide Fixation in Complex Revision Knee Arthroplasty? *Clin. Orthop. Relat Res.*

LAJTHA,L.G. (1979). Stem cell concepts. *Nouv. Rev. Fr. Hematol.* 21: 59-65.

LANGER,R. (1983). Implantable controlled release systems. *Pharmacol. Ther.* 21: 35-51.

LANGER,R. and VACANTI,J.P. (1993). Tissue engineering. *Science* 260: 920-926.

LANGTON,D.J., JAMESON,S.S., JOYCE,T.J., HALLAB,N.J., NATU,S., and NARGOL,A.V. (2010). Early failure of metal-on-metal bearings in hip resurfacing and large-diameter total hip replacement: A consequence of excess wear. *J. Bone Joint Surg. Br.* 92: 38-46.

LANGTON,D.J., JOYCE,T.J., JAMESON,S.S., LORD,J., VAN,O.M., HOLLAND,J.P., NARGOL,A.V., and DE SMET,K.A. (2011). Adverse reaction to metal debris following hip resurfacing: the influence of component type, orientation and volumetric wear. *J. Bone Joint Surg. Br.* 93: 164-171.

LAW,J. (2006). *Big Pharma: how the world's biggest drug companies market illness* (1st edition). London. Robinson Publishing.

LEE,C.H., COOK,J.L., MENDELSON,A., MOIOLI,E.K., YAO,H., and MAO,J.J. (2010). Regeneration of the articular surface of the rabbit synovial joint by cell homing: a proof of concept study. *Lancet* 376: 440-448.

LEVINE,B.R., SPORER,S., POGGIE,R.A., DELLA VALLE,C.J., and JACOBS,J.J. (2006). Experimental and clinical performance of porous tantalum in orthopedic surgery. *Biomaterials* 27: 4671-4681.

LI,C., KOTHA,S., HUANG,C.H., MASON,J., YAKIMICKI,D., and HAWKINS,M. (2003). Finite element thermal analysis of bone cement for joint replacements. *J. Biomech. Eng* 125: 315-322.

LIAO,C.J., CHEN,C.F., CHEN,J.H., CHIANG,S.F., LIN,Y.J., and CHANG,K.Y. (2002). Fabrication of porous biodegradable polymer scaffolds using a solvent merging/particulate leaching method. *J. Biomed. Mater. Res.* 59: 676-681.

LIN,L., CHOW,K.L., and LENG,Y. (2009). Study of hydroxyapatite osteoinductivity with an osteogenic differentiation of mesenchymal stem cells. *J. Biomed. Mater. Res. A* 89: 326-335.

LINDER,L. (2000). Cancellous impaction grafting in the human femur: histological and radiographic observations in 6 autopsy femurs and 8 biopsies. *Acta Orthop. Scand.* 71: 543-552.

LING,R.S., TIMPERLEY,A.J., and LINDER,L. (1993). Histology of cancellous impaction grafting in the femur. A case report. *J. Bone Joint Surg. Br.* 75: 693-696.

LIU,X., CAO,L., JIANG,Y., ZENG,B., and ZHANG,C. (2011). [Repair of radial segmental bone defects by combined angiopoietin 1 gene transfected bone marrow mesenchymal stem cells and platelet-rich plasma tissue engineered bone in rabbits]. *Zhongguo Xiu. Fu Chong. Jian. Wai Ke. Za Zhi.* 25: 1115-1119.

LIU,Y., CHEN,F., LIU,W., CUI,L., SHANG,Q., XIA,W., WANG,J., CUI,Y., YANG,G., LIU,D., WU,J., XU,R., BUONOCORE,S.D., and CAO,Y. (2002). Repairing large porcine full-thickness defects of articular cartilage using autologous chondrocyte-engineered cartilage. *Tissue Eng* 8: 709-721.

LO,W., BIRCH,N,, FROHN,M,, BLUNN,G,, GOODSHIP,A. (2007) Orthogem TriPore HA: a new resorbable bone graft substitute – proof of biological concept in a long term sheep femoral condyle model. Poster Presentation at 8th EFFORT Congress, Florence, 11-15 May 2007.

LOWERY,G.L., KULKARNI,S., and PENNISI,A.E. (1999). Use of autologous growth factors in lumbar spinal fusion. *Bone* 25: 47S-50S.

LUCARELLI,E., FINI,M., BECCHERONI,A., GIAVARESI,G., DI,B.C., ALDINI,N.N., GUZZARDELLA,G., MARTINI,L., CENACCHI,A., DI,M.N., SANGIORGI,L., FORNASARI,P.M., MERCURI,M., GIARDINO,R., and DONATI,D. (2005). Stromal stem cells and platelet-rich plasma improve bone allograft integration. *Clin. Orthop. Relat Res.* 62-68.

MACCHIARINI,P., JUNGEBLUTH,P., GO,T., ASNAGHI,M.A., REES,L.E., COGAN,T.A., DODSON,A., MARTORELL,J., BELLINI,S., PARNIGOTTO,P.P., DICKINSON,S.C., HOLLANDER,A.P., MANTERO,S., CONCONI,M.T., and BIRCHALL,M.A. (2008). Clinical transplantation of a tissue-engineered airway. *Lancet* 372: 2023-2030.

MARCACCI,M., KON,E., MOUKHACHEV,V., LAVROUKOV,A., KUTEPOV,S., QUARTO,R., MASTROGIACOMO,M., and CANCEDDA,R. (2007). Stem cells associated with macroporous bioceramics for long bone repair: 6- to 7-year outcome of a pilot clinical study. *Tissue Eng* 13: 947-955.

MARIEB,E.N. and HOEHN,K. (2010). *Human Anatomy and Physiology* (8th edition), San Francisco, Benjamin Cummings.

MARINO,J.T. and ZIRAN,B.H. (2010). Use of solid and cancellous autologous bone graft for fractures and nonunions. *Orthop. Clin. North Am.* 41: 15-26.

MAROIS,Y., SIGOT-LUIZARD,M.F., and GUIDOIN,R. (1999). Endothelial cell behavior on vascular prosthetic grafts: effect of polymer chemistry, surface structure, and surface treatment. *ASAIO J.* 45: 272-280.

MARTIN,G.J., JR., BODEN,S.D., TITUS,L., and SCARBOROUGH,N.L. (1999). New formulations of demineralized bone matrix as a more effective graft alternative in experimental posterolateral lumbar spine arthrodesis. *Spine* 24: 637-645.

MASON,C. and MANZOTTI,E. (2010). Regenerative medicine cell therapies: numbers of units manufactured and patients treated between 1988 and 2010. *Regen. Med.* 5: 307-313.

MCMURRAY,R.J., GADEGAARD,N., TSIMBOURI,P.M., BURGESS,K.V., MCNAMARA,L.E., TARE,R., MURAWSKI,K., KINGHAM,E., OREFFO,R.O., and DALBY,M.J. (2011). Nanoscale surfaces for the long-term maintenance of mesenchymal stem cell phenotype and multipotency. *Nat. Mater.* 10: 637-644.

MCNAMARA,I., DESHPANDE,S., and PORTEOUS,M. (2010). Impaction grafting of the acetabulum with a mixture of frozen, ground irradiated bone graft and porous synthetic bone substitute (Apapore 60). *J. Bone Joint Surg. Br.* 92: 617-623.

MIAO,D. and SCUTT,A. (2002). Histochemical localization of alkaline phosphatase activity in decalcified bone and cartilage. *J. Histochem. Cytochem.* 50: 333-340.

MILANO,F., VAN BAAL,J.W., BUTTAR,N.S., RYGIEL,A.M., DE,K.F., DEMARS,C.J., ROSMOLEN,W.D., BERGMAN,J.J., VAN,M.J., WANG,K.K., PEPPELENBOSCH,M.P., and

KRISHNADATH,K.K. (2007). Bone morphogenetic protein 4 expressed in esophagitis induces a columnar phenotype in esophageal squamous cells. *Gastroenterology* 132: 2412-2421.

MILLERET,V., SIMONA,B., NEUENSCHWANDER,P., and HALL,H. (2011). Tuning electrospinning parameters for production of 3D-fiber-fleeces with increased porosity for soft tissue engineering applications. *Eur. Cell Mater.* 21: 286-303.

MIOT,S., WOODFIELD,T., DANIELS,A.U., SUETTERLIN,R., PETERSCHMITT,I., HEBERER,M., VAN BLITTERSWIJK,C.A., RIESLE,J., and MARTIN,I. (2005). Effects of scaffold composition and architecture on human nasal chondrocyte redifferentiation and cartilaginous matrix deposition. *Biomaterials* 26: 2479-2489.

MISHRA,A. and PAVELKO,T. (2006). Treatment of chronic elbow tendinosis with buffered platelet-rich plasma. *Am. J. Sports Med.* 34: 1774-1778.

MISTRY,S., KUNDU,D., DATTA,S., and BASU,D. (2011). Comparison of bioactive glass coated and hydroxyapatite coated titanium dental implants in the human jaw bone. *Aust. Dent. J.* 56: 68-75.

MITCHELL,M.E., GIZA,E., and SULLIVAN,M.R. (2009). Cartilage transplantation techniques for talar cartilage lesions. *J Am. Acad. Orthop. Surg.* 17: 407-414.

MJOBERG,B. (1986). Loosening of the cemented hip prosthesis. The importance of heat injury. *Acta Orthop. Scand. Suppl* 221: 1-40.

MORISHITA,T., HONOKI,K., OHGUSHI,H., KOTOBUKI,N., MATSUSHIMA,A., and TAKAKURA,Y. (2006). Tissue engineering approach to the treatment of bone tumors: three cases of cultured bone grafts derived from patients' mesenchymal stem cells. *Artif. Organs* 30: 115-118.

MOSMANN,T. (1983). Rapid colorimetric assay for cellular growth and survival: application to proliferation and cytotoxicity assays. *J. Immunol. Methods* 65: 55-63.

MURAGLIA,A., CANCEDDA,R., and QUARTO,R. (2000). Clonal mesenchymal progenitors from human bone marrow differentiate in vitro according to a hierarchical model. *J. Cell Sci.* 113 (Pt 7): 1161-1166.

MURPHY,W.L., DENNIS,R.G., KILENY,J.L., and MOONEY,D.J. (2002). Salt fusion: an approach to improve pore interconnectivity within tissue engineering scaffolds. *Tissue Eng* 8: 43-52.

MUSCHLER,G.F., NEGAMI,S., HYODO,A., GAISSER,D., EASLEY,K., and KAMBIC,H. (1996). Evaluation of collagen ceramic composite graft materials in a spinal fusion model. *Clin. Orthop. Relat Res.* 328: 250-260.

MUSCHLER,G.F., RAUT,V.P., PATTERSON,T.E., WENKE,J.C., and HOLLINGER,J.O. (2010). The design and use of animal models for translational research in bone tissue engineering and regenerative medicine. *Tissue Eng Part B Rev.* 16: 123-145.

NADEAU,M., SEGUIN,C., THEODOROPOULOS,J.S., and HARVEY,E.J. (2007). Short term clinical outcome of a porous tantalum implant for the treatment of advanced osteonecrosis of the femoral head. *Mcgill. J. Med.* 10: 4-10.

NAM,Y.S. and PARK,T.G. (1999). Porous biodegradable polymeric scaffolds prepared by thermally induced phase separation. *J. Biomed. Mater. Res.* 47: 8-17.

NAM,Y.S., YOON,J.J., and PARK,T.G. (2000). A novel fabrication method of macroporous biodegradable polymer scaffolds using gas foaming salt as a porogen additive. *J. Biomed. Mater. Res.* 53: 1-7.

NATIONAL JOINT REGISTRY FOR ENGLAND AND WALES (2013). 10th Annual Report. Available from http://www.njrcentre.org.uk. Last accessed 23/10/2013.

NEUMANN,B.S., SANSOM,K.G. (1971). The rheological properties of dispersions of laponite a synthetic hectorite-like clay, in electrolyte solutions. *Clay minerals* 9:231.

NEVE,A., CORRADO,A., and CANTATORE,F.P. (2011). Osteoblast physiology in normal and pathological conditions. *Cell Tissue Res.* 343: 289-302.

NEWMAN,E., TURNER,A.S., and WARK,J.D. (1995). The potential of sheep for the study of osteopenia: current status and comparison with other animal models. *Bone* 16: 277S-284S.

O'BRIEN,F.J., HARLEY,B.A., YANNAS,I.V., and GIBSON,L.J. (2005). The effect of pore size on cell adhesion in collagen-GAG scaffolds. *Biomaterials* 26: 433-441.

OAKES,D.A. and CABANELA,M.E. (2006). Impaction bone grafting for revision hip arthroplasty: biology and clinical applications. *J. Am. Acad. Orthop. Surg.* 14: 620-628.

OAKLEY,J. and KUIPER,J.H. (2006). Factors affecting the cohesion of impaction bone graft. *J. Bone Joint Surg. Br.* 88: 828-831.

OHGUSHI,H., KOTOBUKI,N., FUNAOKA,H., MACHIDA,H., HIROSE,M., TANAKA,Y., and TAKAKURA,Y. (2005). Tissue engineered ceramic artificial joint--ex vivo osteogenic differentiation of patient mesenchymal cells on total ankle joints for treatment of osteoarthritis. *Biomaterials* 26: 4654-4661.

OISHI,C.S., WALKER,R.H., and COLWELL,C.W., JR. (1994). The femoral component in total hip arthroplasty. Six to eight-year follow-up of one hundred consecutive patients after use of a third-generation cementing technique. *J. Bone Joint Surg. Am.* 76: 1130-1136.

OLLIER,L., (1867). *Traité expérimental et clinique de la régénération des os et de la production artificielle du tissu osseux,* Paris, Victor Masson et fils.

OLLIER,L., (1891). *Traité des résections et des opérations conservatrices qu'on peut pratiquer sur le système osseux,* Paris, G. Masson.

PALUMBO,C., PALAZZINI,S., and MAROTTI,G. (1990). Morphological study of intercellular junctions during osteocyte differentiation. *Bone* 11: 401-406.

PELTOLA,M., KINNUNEN,I., and AITASALO,K. (2008). Reconstruction of orbital wall defects with bioactive glass plates. *J. Oral Maxillofac. Surg.* 66: 639-646.

PILLAI,C.K. and SHARMA,C.P. (2010). Review paper: absorbable polymeric surgical sutures: chemistry, production, properties, biodegradability, and performance. *J. Biomater. Appl.* 25: 291-366.

PROCKOP,D.J. (1997). Marrow stromal cells as stem cells for nonhematopoietic tissues. *Science* 276: 71-74.

PUPPI,D., PIRAS,A.M., DETTA,N., DINUCCI,D., and CHIELLINI,F. (2010). Poly(lactic-co-glycolic acid) electrospun fibrous meshes for the controlled release of retinoic acid. *Acta Biomater.* 6: 1258-1268.

QUARTO,R., MASTROGIACOMO,M., CANCEDDA,R., KUTEPOV,S.M., MUKHACHEV,V., LAVROUKOV,A., KON,E., and MARCACCI,M. (2001). Repair of large bone defects with the use of autologous bone marrow stromal cells. *N. Engl. J. Med.* 344: 385-386.

RAJARATNAM,S.S., JACK,C., TAVAKKOLIZADEH,A., GEORGE,M.D., FLETCHER,R.J., HANKINS,M., and SHEPPERD,J.A. (2008). Long-term results of a hydroxyapatite-coated femoral component in total hip replacement: a 15- to 21-year follow-up study. *J. Bone Joint Surg. Br.* 90: 27-30.

REDDI,A.H. (2005). BMPs: from bone morphogenetic proteins to body morphogenetic proteins. *Cytokine Growth Factor Rev.* 16: 249-250.

REDDI,A.H. and HUGGINS,C. (1972). Biochemical sequences in the transformation of normal fibroblasts in adolescent rats. *Proc. Natl. Acad. Sci. U. S. A* 69: 1601-1605.

REICHERT,J.C., CIPITRIA,A., EPARI,D.R., SAIFZADEH,S., KRISHNAKANTH,P., BERNER,A., WOODRUFF,M.A., SCHELL,H., MEHTA,M., SCHUETZ,M.A., DUDA,G.N., and HUTMACHER,D.W. (2012). A tissue engineering solution for segmental defect regeneration in load-bearing long bones. *Sci. Transl. Med.* 4: 141ra93.

REICHERT,J.C., EPARI,D.R., WULLSCHLEGER,M.E., SAIFZADEH,S., STECK,R., LIENAU,J., SOMMERVILLE,S., DICKINSON,I.C., SCHUTZ,M.A., DUDA,G.N., and HUTMACHER,D.W. (2010). Establishment of a preclinical ovine model for tibial segmental bone defect repair by applying bone tissue engineering strategies. *Tissue Eng Part B Rev.* 16: 93-104.

REISSIS, Y, GARCIA, E, HUA, J, and BLUNN, G. (2011) The effect of heat generated by bone cement on the viability of human mesenchymal stem cells. British orthopaedic research society. 27/06/2011. Cambridge.

REZWAN,K., CHEN,Q.Z., BLAKER,J.J., and BOCCACCINI,A.R. (2006). Biodegradable and bioactive porous polymer/inorganic composite scaffolds for bone tissue engineering. *Biomaterials* 27: 3413-3431.

RICE,M.A. and ANSETH,K.S. (2004). Encapsulating chondrocytes in copolymer gels: bimodal degradation kinetics influence cell phenotype and extracellular matrix development. *J. Biomed. Mater. Res. A* 70: 560-568.

RIPAMONTI,U. (1996). Osteoinduction in porous hydroxyapatite implanted in heterotopic sites of different animal models. *Biomaterials* 17: 31-35.

ROZENDAAL,R.M., KOES,B.W., VAN OSCH,G.J., UITTERLINDEN,E.J., GARLING,E.H., WILLEMSEN,S.P., GINAI,A.Z., VERHAAR,J.A., WEINANS,H., and BIERMA-

ZEINSTRA,S.M. (2008). Effect of glucosamine sulfate on hip osteoarthritis: a randomized trial. *Ann. Intern. Med.* 148: 268-277.

RUBIN,P.A., POPHAM,J.K., BILYK,J.R., and SHORE,J.W. (1994). Comparison of fibrovascular ingrowth into hydroxyapatite and porous polyethylene orbital implants. *Ophthal. Plast. Reconstr. Surg.* 10: 96-103.

SAMALI,A. and COTTER,T.G. (1996). Heat shock proteins increase resistance to apoptosis. *Exp. Cell Res.* 223: 163-170.

SCHREURS,B.W., BOLDER,S.B., GARDENIERS,J.W., VERDONSCHOT,N., SLOOFF,T.J., and VETH,R.P. (2004). Acetabular revision with impacted morsellised cancellous bone grafting and a cemented cup. A 15- to 20-year follow-up. *J. Bone Joint Surg. Br.* 86: 492-497.

SCHREURS,B.W., KEURENTJES,J.C., GARDENIERS,J.W., VERDONSCHOT,N., SLOOFF,T.J., and VETH,R.P. (2009). Acetabular revision with impacted morsellised cancellous bone grafting and a cemented acetabular component: a 20- to 25-year follow-up. *J. Bone Joint Surg. Br.* 91: 1148-1153.

SCULCO,T.P. (1998). The acetabular component: an elliptical monoblock alternative. *Orthopedics* 21: 973-974.

SEEBACH,C., SCHULTHEISS,J., WILHELM,K., FRANK,J., and HENRICH,D. (2010). Comparison of six bone-graft substitutes regarding to cell seeding efficiency, metabolism and growth behaviour of human mesenchymal stem cells (MSC) in vitro. *Injury* 41: 731-738.

SEED, H. B. (1979). Soil liquefaction and cyclic mobility evaluation for level ground during earthquakes. *J. Geotech. Eng. Div.* 105: 201-255.

SHIKINAMI,Y., MATSUSUE,Y., and NAKAMURA,T. (2005). The complete process of bioresorption and bone replacement using devices made of forged composites of raw hydroxyapatite particles/poly l-lactide (F-u-HA/PLLA). *Biomaterials* 26: 5542-5551.

SHIRAZI-ADL,A., DAMMAK,M., and PAIEMENT,G. (1993). Experimental determination of friction characteristics at the trabecular bone/porous-coated metal interface in cementless implants. *J. Biomed. Mater. Res.* 27: 167-175.

SINGER,N.G. and CAPLAN,A.I. (2011). Mesenchymal stem cells: mechanisms of inflammation. *Annu. Rev. Pathol.* 6: 457-478.

SLOOFF,T.J., HUISKES,R., VAN,H.J., and LEMMENS,A.J. (1984). Bone grafting in total hip replacement for acetabular protrusion. *Acta Orthop. Scand.* 55: 593-596.

SMITH,J.O., AARVOLD,A., TAYTON,E.R., DUNLOP,D.G., and OREFFO,R.O. (2011). Skeletal tissue regeneration: current approaches, challenges, and novel reconstructive strategies for an aging population. *Tissue Eng Part B Rev.* 17: 307-320.

SPENCE,A. (1991). *Basic Human Anatomy* (3rd Edition), San Francisco, Benjamin Cummings.

SPITZER,R.S., PERKA,C., LINDENHAYN,K., and ZIPPEL,H. (2002). Matrix engineering for osteogenic differentiation of rabbit periosteal cells using alpha-tricalcium phosphate particles in a three-dimensional fibrin culture. *J. Biomed. Mater. Res.* 59: 690-696.

STAMBOUGH,J.L., CLOUSE,E.K., and STAMBOUGH,J.B. (2010). Instrumented one and two level posterolateral fusions with recombinant human bone morphogenetic protein-2 and allograft: a computed tomography study. *Spine* 35: 124-129.

STOLZING,A., COLLEY,H. and SCUTT,A. (2011). Effect of age and diabetes on the response of mesenchymal progenitor cells to fibrin matrices. *International journal of biomaterials* Article ID 378034, 9 pages, 2011. doi:10.1155/2011/378034.

STUCHIN,S.A. (2008). Anatomic diameter femoral heads in total hip arthroplasty: a preliminary report. *J. Bone Joint Surg. Am.* 90 (Suppl 3): 52-56.

TAI,H., MATHER,M.L., HOWARD,D., WANG,W., WHITE,L.J., CROWE,J.A., MORGAN,S.P., CHANDRA,A., WILLIAMS,D.J., HOWDLE,S.M., and SHAKESHEFF,K.M. (2007). Control of pore size and structure of tissue engineering scaffolds produced by supercritical fluid processing. *Eur. Cell Mater.* 14: 64-77.

TAKUWA,Y., OHSE,C., WANG,E.A., WOZNEY,J.M., and YAMASHITA,K. (1991). Bone morphogenetic protein-2 stimulates alkaline phosphatase activity and collagen synthesis in cultured osteoblastic cells, MC3T3-E1. *Biochem. Biophys. Res. Commun.* 174: 96-101.

TARE,R.S., BABISTER,J.C., KANCZLER,J., and OREFFO,R.O. (2008). Skeletal stem cells: phenotype, biology and environmental niches informing tissue regeneration. *Mol. Cell Endocrinol.* 288: 11-21.

TARE,R.S., KHAN,F., TOURNIAIRE,G., MORGAN,S.M., BRADLEY,M., and OREFFO,R.O. (2009). A microarray approach to the identification of polyurethanes for the isolation of human skeletal progenitor cells and augmentation of skeletal cell growth. *Biomaterials* 30: 1045-1055.

TAYLOR,G.I., MILLER,G.D., and HAM,F.J. (1975). The free vascularized bone graft. A clinical extension of microvascular techniques. *Plast. Reconstr. Surg.* 55: 533-544.

TAYLOR,M.S., DANIELS,A.U., ANDRIANO,K.P., and HELLER,J. (1994). Six bioabsorbable polymers: in vitro acute toxicity of accumulated degradation products. *J. Appl. Biomater.* 5: 151-157.

TAYTON,E., FAHMY,S., PURCELL,M., AARVOLD,A., SMITH,J.O., KALRA,S., BRISCOE,A., LANHAM,S., HOWDLE,S., SHAKESHEFF,K., DUNLOP,D.G., and OREFFO,R.O. (2012a). An analysis of polymer type and chain length for use as a biological composite graft extender in impaction bone grafting: a mechanical and biocompatibility study. *J. Biomed. Mater. Res. A* 100: 3211-3219.

TAYTON,E., PURCELL,M., AARVOLD,A., SMITH,J.O., KALRA,S., BRISCOE,A., SHAKESHEFF,K., HOWDLE,S.M., DUNLOP,D.G., and OREFFO,R.O. (2012b). Supercritical CO2 fluid-foaming of polymers to increase porosity: a method to improve the mechanical and biocompatibility characteristics for use as a potential alternative to allografts in impaction bone grafting? *Acta Biomater.* 8: 1918-1927.

TAYTON,E.R., SMITH,J.O., AARVOLD,A., KALRA,S., DUNLOP,D.G., and OREFFO,R.O. (2012c). Translational hurdles for tissue engineering: an in vitro analysis of commonly used local anaesthetics on skeletal stem cell survival. *J. Bone Joint Surg. Br.* 94: 848-855.

THURSTON,G. (2003). Role of Angiopoietins and Tie receptor tyrosine kinases in angiogenesis and lymphangiogenesis. *Cell Tissue Res.* 314: 61-68.

TILLEY,S., BOLLAND,B.J., PARTRIDGE,K., NEW,A.M., LATHAM,J.M., DUNLOP,D.G., and OREFFO,R.O. (2006). Taking tissue-engineering principles into theater: augmentation of impacted allograft with human bone marrow stromal cells. *Regen. Med.* 1: 685-692.

TILLMAN,J., ULLM,A., and MADIHALLY,S.V. (2006). Three-dimensional cell colonization in a sulfate rich environment. *Biomaterials* 27: 5618-5626.

TOMFORD,W.W., SCHACHAR,N.S., FULLER,T.C., HENRY,W.B., and MANKIN,H.J. (1981a). Immunogenicity of frozen osteoarticular allografts. *Transplant. Proc.* 13: 888-890.

TOMFORD,W.W., STARKWEATHER,R.J., and GOLDMAN,M.H. (1981b). A study of the clinical incidence of infection in the use of banked allograft bone. *J. Bone Joint Surg. Am.* 63: 244-248.

TOTH,K., MECS,L., and KELLERMANN,P. (2010). Early experience with the Depuy Proxima short stem in total hip arthroplasty. *Acta Orthop. Belg.* 76: 613-618.

UEDA,M., YAMADA,Y., OZAWA,R., and OKAZAKI,Y. (2005). Clinical case reports of injectable tissue-engineered bone for alveolar augmentation with simultaneous implant placement. *Int. J. Periodontics. Restorative. Dent.* 25: 129-137.

UK BLOOD TRANSFUSION & TISSUE TRANSPLANTATION SERVICES (2010). Guidelines for the Blood Transfusion Services in the UK. Http://www.transfusionguidelines. org.uk/index.aspx?Publication=RB&Section=25&pageid=8073. Last accessed 01/11/2013.

URIST,M.R. (1965). Bone: formation by autoinduction. *Science* 150: 893-899.

URIST,M.R. and STRATES,B.S. (1971). Bone morphogenetic protein. *J. Dent. Res.* 50: 1392-1406.

VACANTI,C.A., BONASSAR,L.J., VACANTI,M.P., and SHUFFLEBARGER,J. (2001). Replacement of an avulsed phalanx with tissue-engineered bone. *N. Engl. J. Med.* 344: 1511-1514.

VADALA,G., DI,M.A., TIRINDELLI,M.C., DENARO,L., and DENARO,V. (2008). Use of autologous bone marrow cells concentrate enriched with platelet-rich fibrin on corticocancellous bone allograft for posterolateral multilevel cervical fusion. *J. Tissue Eng Regen. Med.* 2: 515-520.

VAN HAAREN,E.H., SMIT,T.H., PHIPPS,K., WUISMAN,P.I., BLUNN,G., and HEYLIGERS,I.C. (2005). Tricalcium-phosphate and hydroxyapatite bone-graft extender for use in impaction grafting revision surgery. An in vitro study on human femora. *J. Bone Joint Surg. Br.* 87: 267-271.

VAN KLEUNEN,J.P., LEE,G.C., LEMENTOWSKI,P.W., NELSON,C.L., and GARINO,J.P. (2009). Acetabular revisions using trabecular metal cups and augments. *J. Arthroplasty* 24: 64-68.

VANDEVONDELE,S., VOROS,J., and HUBBELL,J.A. (2003). RGD-grafted poly-L-lysine-graft-(polyethylene glycol) copolymers block non-specific protein adsorption while promoting cell adhesion. *Biotechnol. Bioeng.* 82: 784-790.

VILLARS,F., BORDENAVE,L., BAREILLE,R., and AMEDEE,J. (2000). Effect of human endothelial cells on human bone marrow stromal cell phenotype: role of VEGF? *J. Cell Biochem.* 79: 672-685.

WAKITANI,S., NAWATA,M., TENSHO,K., OKABE,T., MACHIDA,H., and OHGUSHI,H. (2007). Repair of articular cartilage defects in the patello-femoral joint with autologous bone marrow mesenchymal cell transplantation: three case reports involving nine defects in five knees. *J Tissue Eng Regen. Med.* 1: 74-79.

WANG,H., LI,Y., ZUO,Y., LI,J., MA,S., and CHENG,L. (2007a). Biocompatibility and osteogenesis of biomimetic nano-hydroxyapatite/polyamide composite scaffolds for bone tissue engineering. *Biomaterials* 28: 3338-3348.

WANG,J.C., ALANAY,A., MARK,D., KANIM,L.E., CAMPBELL,P.A., DAWSON,E.G., and LIEBERMAN,J.R. (2007b). A comparison of commercially available demineralized bone matrix for spinal fusion. *Eur. Spine J.* 16: 1233-1240.

Wang,X. and Ni, Q. (2003). Determination of cortical bone porosity and pore size distribution using a low field pulsed NMR approach. *J. ortho res. 21*: 312-319

WARNKE,P.H., SPRINGER,I.N., WILTFANG,J., ACIL,Y., EUFINGER,H., WEHMOLLER,M., RUSSO,P.A., BOLTE,H., SHERRY,E., BEHRENS,E., and TERHEYDEN,H. (2004). Growth and transplantation of a custom vascularised bone graft in a man. *Lancet* 364: 766-770.

WARNKE,P.H., WILTFANG,J., SPRINGER,I., ACIL,Y., BOLTE,H., KOSMAHL,M., RUSSO,P.A., SHERRY,E., LUTZEN,U., WOLFART,S., and TERHEYDEN,H. (2006). Man as living bioreactor: fate of an exogenously prepared customized tissue-engineered mandible. *Biomaterials* 27: 3163-3167.

WHANG,K., HEALY,K.E., ELENZ,D.R., NAM,E.K., TSAI,D.C., THOMAS,C.H., NUBER,G.W., GLORIEUX,F.H., TRAVERS,R., and SPRAGUE,S.M. (1999). Engineering bone regeneration with bioabsorbable scaffolds with novel microarchitecture. *Tissue Eng* 5: 35-51.

WHEELER,D.L., JENIS,L.G., KOVACH,M.E., MARINI,J., and TURNER,A.S. (2007). Efficacy of silicated calcium phosphate graft in posterolateral lumbar fusion in sheep. *Spine J.* 7: 308-317.

WHITE,T. and FOLKENS,P. (2005). *The Human Bone Manual* (1st Edition), London, Elsevier Academic Press.

WOLFF, J. (1986). *The law of bone remodelling* (Translation of German 1892 version), Berlin, Springer.

WOODARD,J.R., HILLDORE,A.J., LAN,S.K., PARK,C.J., MORGAN,A.W., EURELL,J.A., CLARK,S.G., WHEELER,M.B., JAMISON,R.D., and WAGONER JOHNSON,A.J. (2007). The mechanical properties and osteoconductivity of hydroxyapatite bone scaffolds with multi-scale porosity. *Biomaterials* 28: 45-54.

WOODFIELD,T.B., MIOT,S., MARTIN,I., VAN BLITTERSWIJK,C.A., and RIESLE,J. (2006). The regulation of expanded human nasal chondrocyte re-differentiation capacity by substrate composition and gas plasma surface modification. *Biomaterials* 27: 1043-1053.

YOU,M.H., KWAK,M.K., KIM,D.H., KIM,K., LEVCHENKO,A., KIM,D.Y., and SUH,K.Y. (2010). Synergistically enhanced osteogenic differentiation of human mesenchymal stem cells by culture on nanostructured surfaces with induction media. *Biomacromolecules.* 11: 1856-1862.

ZAIDI,M., PAZIANAS,M., SHANKAR,V.S., BAX,B.E., BAX,C.M., BEVIS,P.J., STEVENS,C., HUANG,C.L., BLAKE,D.R. and MOONGA,B.S. (1993). Osteoclast function and its control. *Exp. Physiol* 78: 721-739.

ZANNETTINO,A.C., PATON,S., ITESCU,S., and GRONTHOS,S. (2010). Comparative assessment of the osteoconductive properties of different biomaterials in vivo seeded with human or ovine mesenchymal stem/stromal cells. *Tissue Eng Part A* 16: 3579-3587.

ZERWEKH,J.E., KOUROSH,S., SCHEINBERG,R., KITANO,T., EDWARDS,M.L., SHIN,D., and SELBY,D.K. (1992). Fibrillar collagen-biphasic calcium phosphate composite as a bone graft substitute for spinal fusion. *J. Orthop. Res.* 10: 562-572.

ZHU,Y.H., CHIU,K.Y., and TANG,W.M. (2001). Review Article: Polyethylene wear and osteolysis in total hip arthroplasty. *J. Orthop. Surg. (Hong. Kong.)* 9: 91-99.

Appendix

Appendix 1

Pilot study: designing experimental protocol.

Allograft and porous poly (DL-lactic-co-glycolic) acid) (PLGA) were seeded with SSCs from a 70 year old male patient (M70) undergoing THR. A seeding concentration of $5x10^4$ cells / ml was used, followed by 28 days incubation in osteogenic media. Both samples were analysed for evidence of SSC growth and survival via fluoromicroscopy (Cell Tracker Green/ Ethidium Homodimer (live /dead) and DAPI nuclear stains), and biochemical analysis (ALP and DNA assays). After the incubation period live / dead stain showed no growth of cells on the impacted allograft (Figure 1).

Figure 1: Micrographs (x10) showing A) Live/ dead stain and B) DAPI stain of allograft + SSC (M70), 28 days post incubation at an initial seeding density of $5x10^4$ cells / ml. Images display background uptake of stains only. (Scale bar 100 µm)

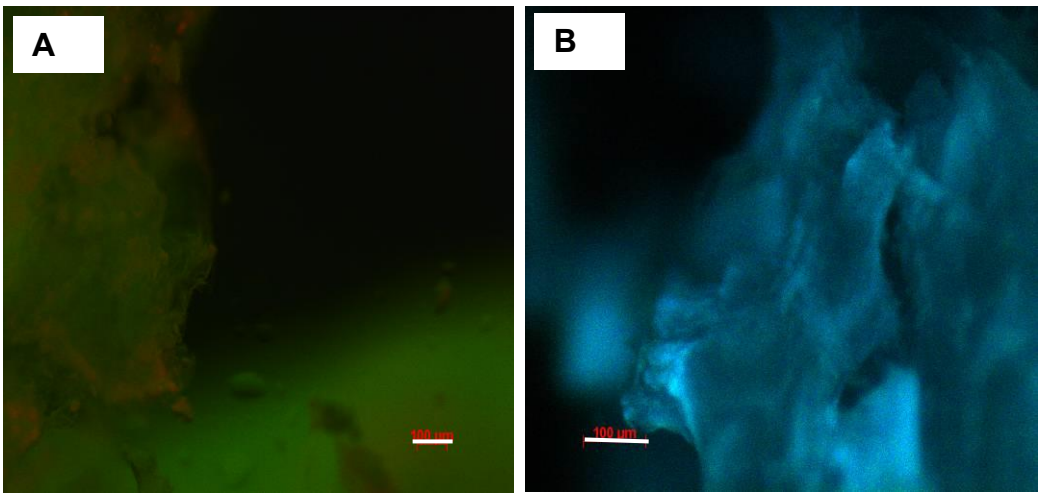

In addition there were only a negligible number of cells surviving on the PLGA scaffold (Figure 2).

Figure 2: Reconstructed 3D image stack obtained via confocal microscopy, showing live / dead stain of PLGA + SSCs, 28 days post incubation with an initial seeding concentration of $5x10^4$ cells / ml. (Scale bar 50 µm)

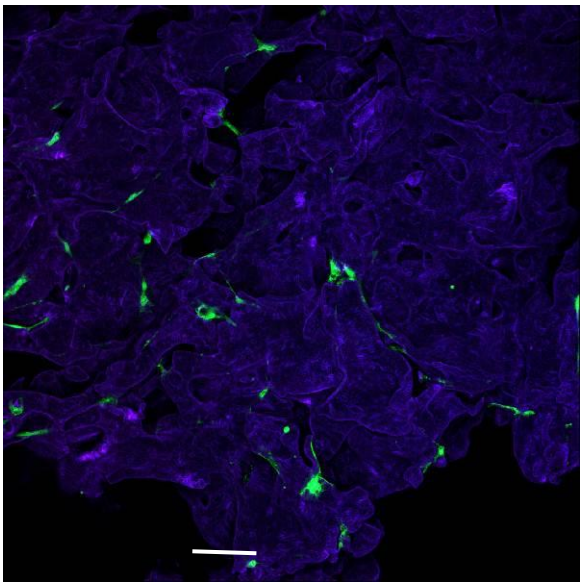

Biochemical assays (DNA/ ALP) were used as quantitative measures of cell number, as well as a measure of osteoblastic differentiation of the cells growing on the allograft (Figure 3 +4).

Figure 3: Graph showing ALP activity of allograft + SSCs (M70) vs controls (allograft alone) after 28 days incubation in osteogenic media (n=3 ± SD).

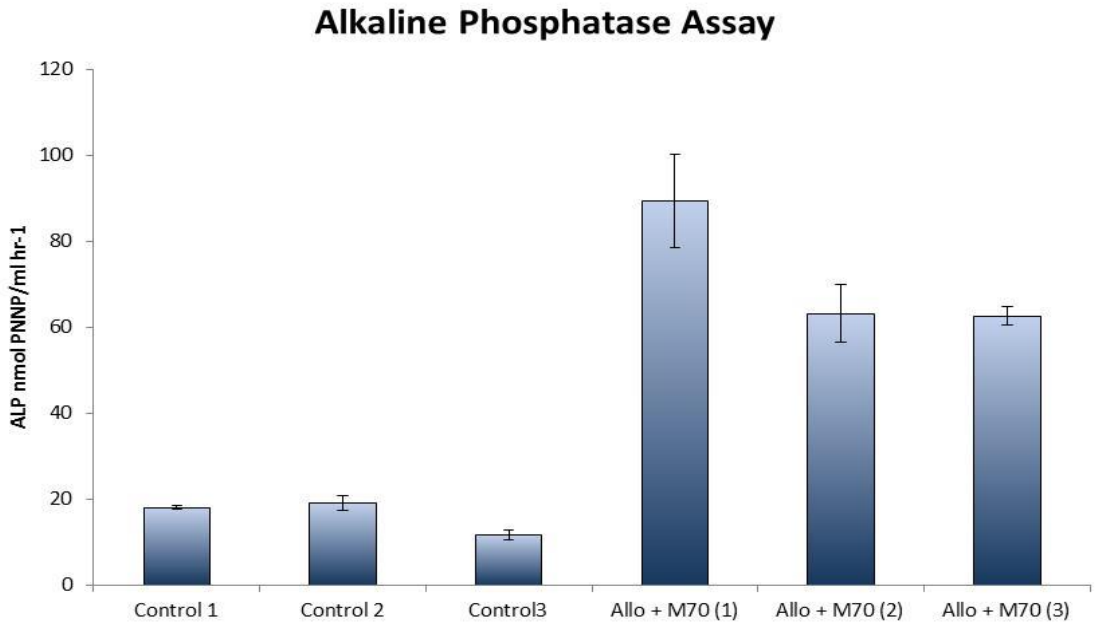

Figure 4: Graph showing DNA content of allograft + SSCs (M70) vs controls (allograft alone) after 28 days incubation in osteogenic media (n=3 ± SD).

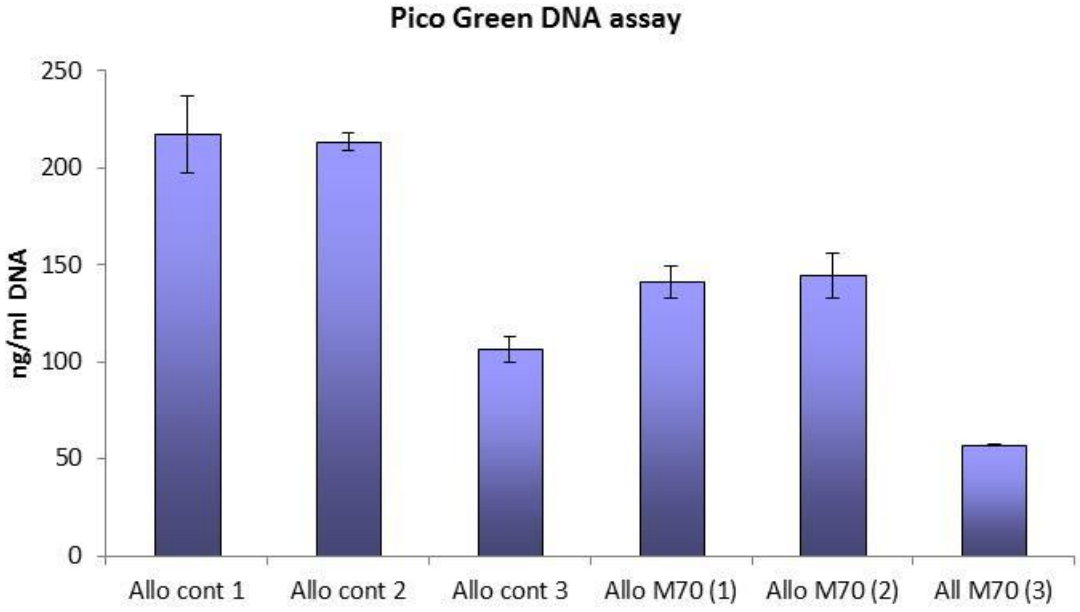

Figure 3 shows that the allograft seeded with cells (M70), in contrast to the live / dead stain (which showed no cell survival) (Figure 1A), there was positive ALP activity compared to the control samples. However, the DNA assay (Figure 4) shows the control samples to have a higher DNA content than those seeded with cells. It is therefore difficult to interpret any findings from these sets of data, and raises important questions as to seeding densities of cells, and accuracy of tests to assess their growth and survival.

The same assays were used to analyse the PLGA (s.c.f.) + cells (M70) (Figure 5+ 6). The assays were more consistent with the findings from the live / dead stain. There was negligible ALP activity (negative figures on the graph due to the standard curve gradient), and negligible DNA content. There were very few cells present, and the assays were not sensitive enough to show a difference from the controls.

Figure 5: Graph showing ALP activity of PLGA + SSC (M70) vs control (PLGA alone) after impaction and 3/52 incubation (n=3 ± SD).

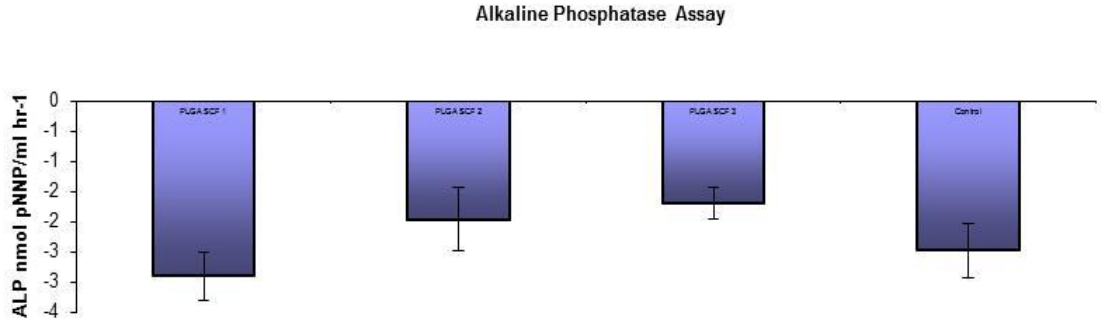

Figure 6: Graph showing DNA content of PLGA + M70 vs control (PLGA alone) after impaction and 3/52 incubation (n=3 ± SD).

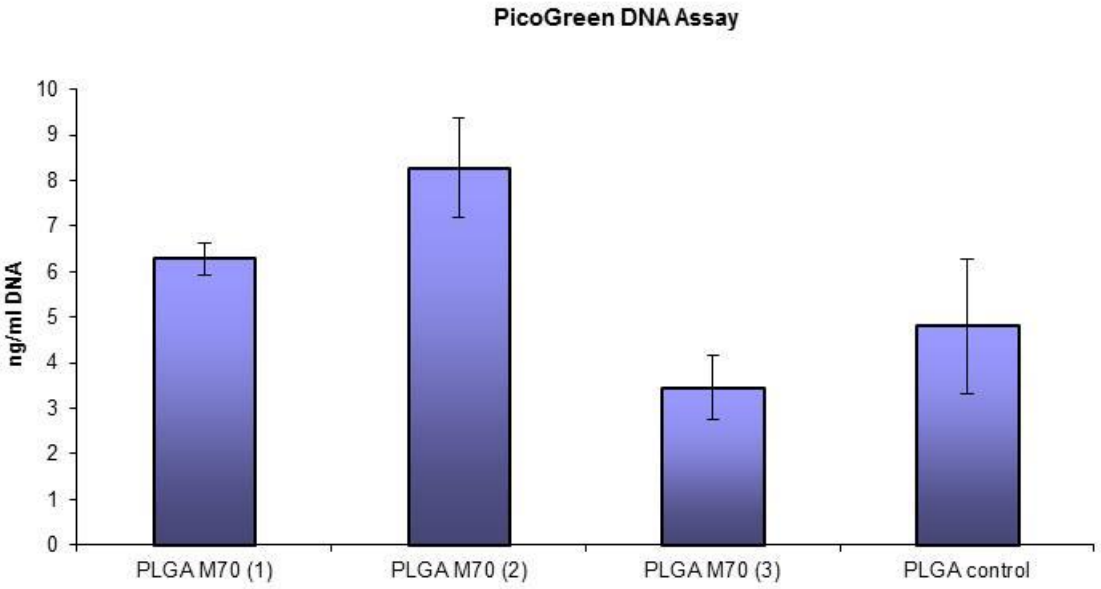

The findings of these experiments demonstrate a need to modify and optimise the experimental protocols in order to gain successful growth of SSCs on both allograft and synthetic scaffolds in these circumstances. In addition, investigation is required as to the accuracy of experimental assays when used in these particular circumstances.

Appendix 2

Detailed Results from Chapter 3, "Accuracy of Assays to be used with allograft" section.

Table 1: ALP assay results for 1 ml allograft seeded with increasing concentrations of SSC's after 1 week incubation. Each seeding concentration was repeated x6, and each sample was tested in triplicate.

Sample	ALP Conc (1) nmol pNNP/ml hr-1	ALP Conc (2) nmol pNNP/ml hr-1	ALP Conc (3) nmol pNNP/ml hr-1	Mean Conc w Time ALP nmol pNNP/ml hr-1	STDEV
CONTROL (1)	141.85	141.85	146.93	143.54	2.93
CONTROL (2)	146.50	141.01		143.76	3.89
CONTROL (3)	182.87	188.37	182.45	184.56	3.30
CONTROL (4)	181.60	176.95	184.14	180.89	3.65
CONTROL (5)	189.21	174.83	199.78	187.94	12.52
CONTROL (6)	198.09	185.83	197.67	193.86	6.96
5X10^3 (1)	162.99	156.65	161.73	160.46	3.36
5X10^3 (2)	164.69	167.22	162.99	164.97	2.13
5X10^3 (3)	168.49	162.15	168.49	166.38	3.66
5X10^3 (4)	192.59	209.93	189.21	197.24	11.12
5X10^3 (5)	185.41	182.45	181.18	183.01	2.17
5X10^3 (6)	186.67	149.46	179.06	171.73	19.66
5X10^4 (1)	256.44	236.57	242.49	245.17	10.20
5X10^4 (2)	233.19	228.11	218.81	226.70	7.29
5X10^4 (3)	193.86	185.83	185.41	188.37	4.77
5X10^4 (4)	277.58	243.76	246.29	255.88	18.84
5X10^4 (5)	235.30	217.54	205.28	219.37	15.09
5X10^4 (6)	192.59	189.21	199.78	193.86	5.40
5X10^5 (1)	226.84	190.48	194.71	204.01	19.89
5X10^5 (2)	217.12	210.78	207.82	211.90	4.75
5X10^5 (3)	228.53	217.96	202.74	216.41	12.97
5X10^5 (4)	226.42	179.91	178.22	194.85	27.36
5X10^5 (5)	274.62	193.02	193.44	220.36	46.99
5X10^5 (6)	209.08	182.02	190.48	193.86	13.84

Table 2: One-Way ANOVA comparing mean ALP assay results for 1 ml allograft seeded with increasing concentrations of SSC's after 1 week incubation.

	Sum of Squares	df	Mean Square	F	Sig.
Between Groups	10754.00	3	3584.67	9.21	<0.005
Within Groups	7780.68	20	389.03		
Total	18534.69	23			

Table 3: Post hoc Bonferroni analysis comparing mean ALP assay results for 1 ml allograft seeded with increasing concentrations of SSC's after 1 week incubation.

(I) group	(J) group	Mean Difference (I-J)	Std. Error	Sig.	95% Confidence Interval	
					Lower Bound	Upper Bound
Control	5X10^3	-1.54	11.39	1.00	-34.87	31.79
	5X10^4	-49.13*	11.39	<0.005	-82.46	-15.80
	5X10^5	-34.47*	11.39	0.04	-67.81	-1.14
5X10^3	Control	1.54	11.39	1.00	-31.79	34.87
	5X10^4	-47.59*	11.39	<0.005	-80.93	-14.26
	5X10^5	-32.93	11.39	0.05	-66.27	0.40
5X10^4	Control	49.13*	11.39	<0.005	15.80	82.46
	5X10^3	47.59*	11.39	<0.005	14.26	80.93
	5X10^5	14.66	11.39	1.00	-18.67	47.99
5X10^5	Control	34.47*	11.39	0.04	1.14	67.81
	5X10^3	32.93	11.39	0.05	-0.40	66.27
	5X10^4	-14.66	11.39	1.00	-47.99	18.67

*. The mean difference is significant at the 0.05 level.

Table 4: DNA assay results for 1 ml allograft seeded with increasing concentrations of SSC's after 1 weeks incubation. Each seeding concentration was repeated x6, and each sample was tested in triplicate.

Sample	Conc DNA (1) ng/ml	Conc DNA (2) ng/ml	Conc DNA (3) ng/ml	Mean DNA Concentration ng/ml	STDEV
CONTROL 1	438.78	458.49	483.74	920.67	45.08
CONTROL 2	495.11	469.07	477.41	961.06	26.60
CONTROL 3	511.66	491.08	454.17	971.28	58.26
CONTROL 4	504.39	518.71	531.02	1036.08	26.65
CONTROL 5	619.30	629.08	613.97	1241.57	15.33
CONTROL 6	564.76	612.46	561.38	1159.07	57.14
5X10^3,1	481.87	482.59	457.91	948.25	28.09
5X10^3,2	514.97	487.34	580.45	1055.17	95.63
5X10^3,3	613.69	650.24	642.61	1271.02	38.56
5X10^3,4	724.56	737.44	751.18	1475.46	26.63
5X10^3,5	635.77	597.79	582.03	1210.39	55.26
5X10^3,6	909.69	878.75	1066.83	1903.51	201.70
5X10^4,1	454.17	512.24	484.39	967.20	58.08
5X10^4,2	753.70	686.50	688.23	1418.95	76.62
5X10^4,3	522.96	591.45	580.01	1129.62	73.39
5X10^4,4	691.75	663.84	692.76	1365.56	32.83
5X10^4,5	1090.50	1114.67	1106.18	2207.57	24.53
5X10^4,6	513.89	530.80	455.04	999.82	79.54
5X10^5,1	599.51	677.36	604.55	1254.28	87.13
5X10^5,2	706.07	612.32	642.61	1307.33	95.69
5X10^5,3	647.00	634.77	638.36	1280.09	12.57
5X10^5,4	797.88	776.80	875.30	1633.31	103.73
5X10^5,5	953.22	1273.25	962.86	2126.22	364.10
5X10^5,6	589.94	587.06	583.83	1173.89	6.12

Table 5: One-Way ANOVA comparing mean DNA assay results for 1 ml allograft seeded with increasing concentrations of SSC's after 1 week incubation.

	Sum of Squares	df	Mean Square	F	Sig.
Between Groups	551812.05	3	183937.35	1.54	0.23
Within Groups	2378307.97	20	118915.39		
Total	2930120.03	23			

Table 6: Post hoc Bonferroni analysis comparing mean DNA assay results for 1 ml allograft seeded with increasing concentrations of SSC's after 1 week incubation.

(I) group	(J) group	Mean Difference (I-J)	Std. Error	Sig.	95% Confidence Interval	
					Lower Bound	Upper Bound
1.00	2.00	-262.35	199.09	1.00	-845.12	320.43
	3.00	-299.83	199.09	0.89	-882.60	282.94
	4.00	-414.23	199.09	0.30	-997.00	168.54
2.00	1.00	262.35	199.09	1.00	-320.43	845.12
	3.00	-37.49	199.09	1.00	-620.26	545.29
	4.00	-151.89	199.09	1.00	-734.66	430.89
3.00	1.00	299.83	199.09	0.89	-282.94	882.60
	2.00	37.49	199.09	1.00	-545.29	620.26
	4.00	-114.40	199.09	1.00	-697.17	468.37
4.00	1.00	414.23	199.09	0.30	-168.54	997.00
	2.00	151.89	199.09	1.00	-430.89	734.66
	3.00	114.40	199.09	1.00	-468.37	697.17

Table 7: Optical density of substrate from each sample after 1hr incubation in WST-1.

	1	2	3	4	5	6
Control allograft alone	0.16	0.17	0.16	0.15	0.16	0.17
$5x10^3$ cells	0.16	0.16	0.16	0.16	0.16	0.17
$5x10^4$ cells	0.20	0.22	0.18	0.21	0.18	0.22
$5x10^5$ cells	0.50	0.43	0.48	0.44	0.38	0.41

Table 8: Optical density of substrate from each sample after 4hr incubation in WST-1.

	1	2	3	4	5	6
Control allograft alone	0.21	0.21	0.19	0.18	0.19	0.19
$5x10^3$ cells	0.21	0.21	0.18	0.18	0.18	0.18
$5x10^4$ cells	0.31	0.34	0.26	0.30	0.24	0.33
$5x10^5$ cells	0.86	0.70	0.75	0.67	0.62	0.66

Table 9: One-Way ANOVA comparing mean WST-1 assay results at 2 hours for 1 ml allograft seeded with increasing concentrations of SSC's after 1 week incubation.

	Sum of Squares	df	Mean Square	F	Sig.
Between Groups	.32	3	.11	175.15	<.005
Within Groups	.01	20	.00		
Total	.33	23			

Table 10: Post hoc Bonferroni analysis comparing mean WST-1 assay results at 2 hours for 1 ml allograft seeded with increasing concentrations of SSC's after 1 week incubation.

(I) Cell Concentration	(J) Cell Concentration	Mean Difference (I-J)	Std. Error	Sig.	95% Confidence Interval	
					Lower Bound	Upper Bound
0	5000	0.00	0.01	1.00	-0.04	0.04
	50000	-0.04	0.01	0.09	-0.08	0.00
	500000	-0.28*	0.01	<0.005	-0.32	-0.23
5000	0	0.00	0.01	1.00	-0.04	0.04
	50000	-0.04	0.01	0.10	-0.08	0.00
	500000	-0.28*	0.01	<0.005	-0.32	-0.23
50000	0	0.04	0.01	0.09	0.00	0.08
	5000	0.04	0.01	0.10	0.00	0.08
	500000	-0.24*	0.01	<0.005	-0.28	-0.20
500000	0	0.28*	0.01	<0.005	0.23	0.32
	5000	0.28*	0.01	<0.005	0.23	0.32
	50000	0.24*	0.01	<0.005	0.20	0.28

*. The mean difference is significant at the 0.05 level.

Table 11: One-Way ANOVA comparing mean WST-1 assay results at 4 hours for 1 ml allograft seeded with increasing concentrations of SSC's after 1 week incubation.

	Sum of Squares	df	Mean Square	F	Sig.
Between Groups	1.09	3	.36	154.21	<0.005
Within Groups	.05	20	.00		
Total	1.14	23			

Table 12: Post hoc Bonferroni analysis comparing mean WST-1 assay results at 4 hours for 1 ml allograft seeded with increasing concentrations of SSC's after 1 week incubation.

(I) Cell Concentration	(J) Cell Concentration	Mean Difference (I-J)	Std. Error	Sig.	95% Confidence Interval	
					Lower Bound	Upper Bound
0	5000	0.00	0.03	1.00	-0.08	0.09
	50000	-0.10*	0.03	0.01	-0.18	-0.02
	500000	-0.51*	0.03	<0.005	-0.60	-0.43
5000	0	0.00	0.03	1.00	-0.09	0.08
	50000	-0.11*	0.03	0.01	-0.19	-0.02
	500000	-0.52*	0.03	<0.005	-0.60	-0.44
50000	0	0.10*	0.03	0.01	0.02	0.18
	5000	0.11*	0.03	0.01	0.02	0.19
	500000	-0.41*	0.03	<0.005	-0.49	-0.33
500000	0	0.51*	0.03	<0.005	0.43	0.60
	5000	0.52*	0.03	<0.005	0.44	0.60
	50000	0.41*	0.03	<0.005	0.33	0.49

*. The mean difference is significant at the 0.05 level.

Appendix 3

Table 1: Displaying the post hoc analysis results of the one way ANOVA test comparing the mean ALP activities (n=3) of the cell populations growing on each of the polymers.

Bonferroni's Multiple Comparison Test	*Mean Diff.*	*t*	*P value*	*95% CI of diff*
PLA vs PLA HA	-225.50	5.86	P < 0.01	-359.4 to -91.64
PLA vs PLGA	161.40	4.19	P < 0.05	27.50 to 295.30
PLA vs PLGA HA	145.00	3.77	P < 0.05	11.10 to 278.90
PLA HA vs PLGA	386.90	10.05	P < 0.001	253.0 to 520.80
PLA HA vs PLGA HA	370.50	9.63	P < 0.001	236.6 to 504.40
PLGA vs PLGA HA	-16.39	0.43	P > 0.05	-150.3 to 117.50

Appendix 4

Anaesthetic protocol for sheep

Pre-medication

Rompun 2% (Xylazine) – 0.1 mg/kg

Bayer Health Care

Strawberry Hill

Newbury

Berkshire

RG14 1JA

Induction

Ketaset (Ketamine) – 2mg/kg

Fort Dodge Animal Health Ltd

Southampton

SO30 4QH

Hypnovel (Midazolam) – 2.5mg flat rate

Roche Products Ltd

Welwyn Garden City

Hertfordshire

AL7 3AY

Maintenance

Isoflurane (IsoFlo) – approx 2% inhaled in pure oxygen

Abbott Laboratories Ltd.

Abbott House

Vanwall Road

Maidenhead

Berkshire

SL6 4XE 292

Peri- and post-operative protocol for sheep

Analgesic

Durogesic 75mcg/hr (Fentanyl) – 2 patches, 12 hrs before and 60hrs after surgery

Janssen-Cilag

50-100 Holmers Farm Way

High Wycombe

Bucks

HP12 4EG

Vetergesic (Buprenorphine) – 0.6mg approximately 72hrs after second application of fentanyl patches

Alstoe Animal Health

Pera Innovation Park

Nottingham Road

Melton Mowbray

LE13 0PB

Antibiotic Cover

Betamox LA (Amoxicillin) 150mg/ml – 15mg/kg given preoperatively

NorbrookLaboratories (GB) Limited

The Green

Great Corby

Carlisle

CA4 8LR

Ceporex (Cefalexin) – at 5ml/animal for four days

Schering-Plough Animal Health

Division of Schering-Plough Ltd

Welwyn Garden City

AL7 1TW 293

Euthanasia

Pentobarbital solution 20% – 0.7mg/kg (approx 40mg per sheep)

Pharmasol Ltd.

North Way

Andover

Hampshire SP10 5AZ

Appendix 5

J Biomed Mater Res A. 2013 Aug 21. doi: 10.1002/jbm.a.34926. [Epub ahead of print]

A comparision of polymer and polymer-hydroxyapatite composite tissue engineered scaffolds for use in bone regeneration. An in vitro and in vivo study.

Tayton E, Purcell M, Aarvold A, Smith JO, Briscoe A, Kanczler JM, Shakesheff KM, Howdle SM, Dunlop DG, Oreffo RO.

Source

Bone and Joint Research Group, Centre for Human Development, Stem Cells and Regeneration, Human Development and Health, University of Southampton Medical School, Southampton, SO16 6YD, UK.

Abstract

Previous in vitro work demonstrated porous PLA and PLGA both had the mechanical strength and sustained the excellent skeletal stem cell (SSC) growth required of an osteogenic bonegraft substitute, for use in impaction bone grafting. The purpose of this investigation was to assess the effects of the addition of hydroxyapatite (HA) to the scaffolds prior to clinical translation. PLA, PLA+10% HA, PLGA and PLGA+10% HA were milled and impacted into discs before undergoing a standardised shear test. Cellular compatibility analysis followed 14 days incubation with human skeletal stems cells (SSC). The best two performing polymers were taken forward for in vivo analysis. SSC seeded polymer discs were implanted subcutaneously in mice. All polymers had superior mechanical shear strength compared to allograft ($P<0.01$). Excellent SSC survival was demonstrated on all polymers, but the PLA polymers showed enhanced osteoblastic activity (ALP assay $P<0.01$) and collagen-1 formation. In vivo analysis was performed on PLA and PLA+10% HA. MicroCT analysis revealed increased bone formation on the PLA HA ($P<0.01$), and excellent neo-vessel formation in both samples. Histology confirmed evidence of de novo bone formation. PLA HA showed both enhanced osteoinductive and osteogenic capacity. This polymer composite has been selected for scaled-up experimentation prior to clinical translation.

KEYWORDS:

Bone regeneration, Progenitor cell, Scaffold, polymer, skeletal stem cell

PMID:
24038868
[PubMed - as supplied by publisher]

J Child Orthop. 2012 Aug;6(4):339-46. doi: 10.1007/s11832-012-0419-x. Epub 2012 Jul 7.

The role of osteoblast cells in the pathogenesis of unicameral bone cysts.

Aarvold A, Smith JO, Tayton ER, Edwards CJ, Fowler DJ, Gent ED, Oreffo RO.

Source

Bone and Joint Research Group, Centre for Human Development, Stem Cells and Regeneration, Institute of Developmental Sciences, University of Southampton School of Medicine, Tremona Road, Southampton, SO16 6YD UK ; Department of Paediatric Orthopaedics, University Hospital Southampton, Tremona Road, Southampton, SO16 6YD UK.

Abstract

PURPOSE:

The pathogenesis of unicameral bone cysts (UBCs) remains largely unknown. Osteoclasts have been implicated, but the role of osteoblastic cells has, to date, not been explored. This study investigated the pathophysiology of UBCs by examining the interactions between the cyst fluid and human bone marrow stromal cells (hBMSCs) and the effect of the fluid on osteogenesis.

METHODS:

Fluid was aspirated from two UBCs and analysed for protein, electrolyte and cytokine levels. Graded concentrations of the fluid were used as culture media for hBMSCs to determine the effects of the fluid on hBMSC proliferation and osteogenic differentiation. The fibrocellular lining was analysed histologically and by electron microscopy.

RESULTS:

Alkaline phosphatase (ALP) staining of hBMSCs that were cultured in cyst fluid demonstrated increased cell proliferation and osteogenic differentiation compared to basal media controls. Biochemical analysis of these hBMSCs compared to basal controls confirmed a marked increase in DNA content (as a marker of proliferation) and ALP activity (as a marker of osteogenic differentiation) which was highly significant ($p < 0.001$). Osteoclasts were demonstrated in abundance in the cyst lining. The cyst fluid cytokine profile revealed levels of the pro-osteoclast cytokines IL-6, MIP-1α and MCP-1 that were 19×, 31× and 35× greater than those in reference serum.

CONCLUSIONS:

Cyst fluid promoted osteoblastic growth and differentiation. Despite appearing paradoxical that the cyst fluid promoted osteogenesis, osteoblastic cells are required for osteoclastogenesis through RANKL signalling. Three key cytokines in this pathway (IL-6, MIP-1α, MCP-1) were highly elevated in cyst fluid. These findings may hold the key to the pathogenesis of UBCs, with implications for treatment methods.

KEYWORDS:

Cytokine, Osteoblast cell, Osteoclast, RANK ligand, Unicameral bone cyst

PMID:
23904902
[PubMed]
PMCID:
PMC3425701

J Bone Joint Surg Am. 2013 Apr 17;95(8):736-43. doi: 10.2106/JBJS.L.00164.

Effects of setting bone cement on tissue-engineered bone graft: a potential barrier to clinical translation?

Tayton ER, Smith JO, Evans N, Dickinson A, Aarvold A, Kalra S, Purcell M, Howdle S, Dunlop DG, Oreffo RO.

Source

Bone and Joint Research Group, Human Development and Health, University of Southampton Medical School, Tremona Road, Southampton UK. edwardtayton@hotmail.com

Abstract

BACKGROUND:

Strategies to improve mechanical strength, neovascularization, and the regenerative capacity of allograft include both the addition of skeletal stem cells and the investigation of novel biomaterials to reduce and ultimately obviate the need for allograft altogether. Use of bone cement is a common method of stabilizing implants in conjunction with impacted allograft. Curing cement, however, can reach temperatures in excess of 70°C, which is potentially harmful to skeletal stem cells. The aim of this study was to investigate the effects of setting bone cement on the survival of human adult skeletal stem cells within tissue-engineered allograft and a novel allograft substitute.

METHODS:

Milled allograft and a polymer graft substitute were seeded with skeletal stem cells, impacted into a graduated chamber, and exposed to curing bone cement. Sections were removed at 5-mm increments from the allograft-cement interface. A quantitative WST-1 assay was performed on each section as a measure of remaining cell viability. A second stage of the experiment involved assessment of methods to potentially enhance cell survival, including pretreating the allograft or polymer by either cooling to 5°C or coating with 1% Laponite, or both.

RESULTS:

There was a significant drop in cellular activity in the sections taken from within 0.5 cm of the cement interface in both the allograft and the polymer ($p < 0.05$), although there was still measurable cellular activity. Pretreatment methods did not significantly improve cell survival in any group.

CONCLUSIONS:

While the addition of bone cement reduced cellular viability of tissue-engineered constructs, this reduction occurred only in close proximity to the cement and measurable numbers of skeletal stem cells were observed, confirming the potential for cell population recovery.
PMID:
23595073
[PubMed - indexed for MEDLINE]

J Biomed Mater Res A. 2013 Dec;101(12):3431-7. doi: 10.1002/jbm.a.34646. Epub 2013 Apr 9.

The effect of porosity of a biphasic ceramic scaffold on human skeletal stem cell growth and differentiation in vivo.

Aarvold A, Smith JO, Tayton ER, Lanham SA, Chaudhuri JB, Turner IG, Oreffo RO.

Source

Bone and Joint Research Group, Centre for Human Development, Stem Cell and Regeneration, Institute of Developmental Sciences, University of Southampton, Tremona Road, Southampton SO16 6YD, United Kingdom.

Abstract

Skeletal stem cell (SSC) growth on a novel porous HA/TCP scaffold has been investigated in vivo. The effect of porosity on osteogenic differentiation was assessed by comparing two groups of scaffolds with differing porosity but controlled pore size. Histology, microCT, scanning electron microscopy, and biochemical analysis were used to assess SSC proliferation and differentiation. The 45 pores per inch (ppi) scaffold demonstrated a greater increase in density than the 30 ppi scaffold following in vivo culture, and a reduction in dimensions of the pores and channels of the higher porosity scaffold was observed, indicating generation of new tissue within the pores. All scaffolds supported SSC proliferation but the higher scaffold porosity augmented osteogenic differentiation. ALP specific activity was enhanced on the 45 ppi scaffold compared to the 30 ppi scaffold. These studies demonstrate the importance of porosity in scaffold design and impact therein for tissue engineering application. © 2013 Wiley Periodicals, Inc. J Biomed Mater Res Part A: 101A: 3431-3437, 2013.

KEYWORDS:

osteogenic differentiation, porosity, proliferation, scaffold, skeletal stem cell

PMID:
23568640
[PubMed - in process]

Surgeon. 2013 Dec;11(6):319-25. doi: 10.1016/j.surge.2013.02.008. Epub 2013 Mar 27.

A tissue engineering strategy for the treatment of avascular necrosis of the femoral head.

Aarvold A, Smith JO, Tayton ER, Jones AM, Dawson JI, Lanham S, Briscoe A, Dunlop DG, Oreffo RO.

Source

Bone and Joint Research Group, Centre for Human Development, Stem Cells and Regeneration, University of Southampton, Institute of Developmental Sciences, Tremona Road, Southampton SO16 6YD, UK. Electronic address: alexaarvold@doctors.org.uk.

Abstract

BACKGROUND & PURPOSE:

Skeletal stem cells (SSCs) and impaction bone grafting (IBG) can be combined to produce a mechanically stable living bone composite. This novel strategy has been translated to the treatment of avascular necrosis of the femoral head. Surgical technique, clinical follow-up and retrieval analysis data of this translational case series is presented.

METHODS:

SSCs and milled allograft were impacted into necrotic bone in five femoral heads of four patients. Cell viability was confirmed by parallel in vitro culture of the cell-graft constructs. Patient follow-up was by serial clinical and radiological examination. Tissue engineered bone was retrieved from two retrieved femoral heads and was analysed by histology, microcomputed tomography (μCT) and mechanical testing.

RESULTS:

Three patients remain asymptomatic at 22- to 44-month follow-up. One patient (both hips) required total hip replacement due to widespread residual necrosis. Retrieved tissue engineered bone demonstrated a mature trabecular micro-architecture histologically and on μCT. Bone density and axial compression strength were comparable to trabecular bone.

CONCLUSIONS:

Clinical follow-up shows this to be an effective new treatment for focal early stage avascular necrosis of the femoral head. Unique retrieval analysis of clinically translated tissue engineered bone has demonstrated regeneration of tissue that is both structurally and functionally analogous to normal trabecular bone.

KEYWORDS:

Avascular necrosis, Femoral head, Impaction bone grafting, Skeletal stem cells, Translation
PMID:
23540814
[PubMed - in process]

J Tissue Eng Regen Med. 2012 Oct 5. doi: 10.1002/term.1577. [Epub ahead of print]

From bench to clinic and back: skeletal stem cells and impaction bone grafting for regeneration of bone defects.

Aarvold A, Smith JO, Tayton ER, Jones AM, Dawson JI, Lanham S, Briscoe A, Dunlop DG, Oreffo RO.

Source

Bone and Joint Research Group, Centre for Human Development, Stem Cells and Regeneration, Human Development and Health, Institute of Developmental Sciences, University of Southampton, Southampton, SO16 6YD, UK.

Abstract

Tissue engineering offers enormous potential for bone regeneration. Despite extensive in vitro and in vivo work, few strategies translate into clinical practice. This paper describes the combination of skeletal stem cells (SSCs) and impaction bone grafting (IBG) for the treatment of patients with bone defects associated with avascular necrosis of the femoral head. SSCs and milled allograft were impacted into necrotic bone in the femoral heads of four patients. Three patients remained asymptomatic at 22-44 month follow-up, but one patient has required total hip replacement (both hips). This has allowed retrieval of the femoral heads, which were analysed structurally and functionally by μCT, histology and mechanical testing. A central channel of impacted bone was found in the femoral heads, which displayed a mature trabecular micro-architecture. The impacted bone was denser than the surrounding trabecular bone, as strong in compression and with histological micro-architecture comparable to that of trabecular bone. Analysis of the retrieved femoral head samples has demonstrated that this tissue-engineering strategy regenerates bone that is both structurally and functionally analogous to normal trabecular bone. SSCs, together with IBG, have proved an effective treatment for avascular necrosis of the femoral head and offer significant potential for the broader spectrum of bone defects. Copyright © 2012 John Wiley & Sons, Ltd.

PMID:
23038218
[PubMed - as supplied by publisher]

J Biomed Mater Res A. 2012 Dec;100(12):3211-9. doi: 10.1002/jbm.a.34264. Epub 2012 Jun 15.

An analysis of polymer type and chain length for use as a biological composite graft extender in impaction bone grafting: a mechanical and biocompatibility study.

Tayton E, Fahmy S, Purcell M, Aarvold A, Smith JO, Kalra S, Briscoe A, Lanham S, Howdle S, Shakesheff K, Dunlop DG, Oreffo RO.

Source

Bone and Joint Research Group, University of Southampton, SO16 6YD, United Kingdom.

Abstract

Impaction bone grafting (IBG) with human allograft remains the preferred approach for replacement of lost bone stock during revision hip surgery. Associated problems include cost, disease transmission, and stem subsidence. Synthetic grafts are therefore appealing, and ideally display similar mechanical characteristics as allograft, but with enhanced ability to form de novo bone. High and low molecular weight forms of three different polymers [poly(DL-lactide) (P(DL) LA), poly(DL-lactide-co-glycolide) (P(DL) LGA), and poly(ε-caprolactone) (PCL)] were milled, impacted into discs, and then examined in a shear testing rig, in comparison to allograft. In addition, skeletal stem cells (SSCs) were combined with each of the milled polymers, followed by impaction and examination for cell viability and number, via fluorostaining and biochemical assays. The shear strengths of high/low mwt P(DL) LA, and high/low mwt P(DL) LGA were significantly higher than allograft ($p < 0.01$). High/low mwt PCL had significantly lower shear strengths ($p < 0.01$). WST-1 assay and fluorstaining indicated significantly increased cell viability on high mwt P(DL) LA and high mwt P(DL) LGA over allograft ($p < 0.05$). Mechanical and biochemical analysis indicated improved properties of high mwt P(DL) LA and high mwt P(DL) LGA over allograft. This study indicates the potential of these polymers for use as substitute human allograft, creating a living composition with SSC for application in IBG.

PMID:
22707404
[PubMed - indexed for MEDLINE]

J Tissue Eng Regen Med. 2012 Jun 4. doi: 10.1002/term.1525. [Epub ahead of print]

Tantalum trabecular metal - addition of human skeletal cells to enhance bone implant interface strength and clinical application.

Smith JO, Sengers BG, Aarvold A, Tayton ER, Dunlop DG, Oreffo RO.

Source

Bone and Joint Research Group, Centre for Human Development, Stem Cells and Regeneration, Human Development and Health, Institute of Developmental Sciences, University Hospital Southampton, UK.

Abstract

The osteo-regenerative properties of allograft have recently been enhanced by addition of autogenous human bone marrow stromal cells (HBMSCs). Limitations in the use of allograft have prompted the investigation of tantalum trabecular metal (TTM) as a potential alternative. TTM is already in widespread orthopaedic use, although in applications where there is poor initial stability, or when TTM is used in conjunction with bone grafting, initial implant loading may need to be limited. The aim of this study was to evaluate the osteo-regenerative potential of TTM with HBMSCs, in direct comparison to human allograft and autograft. HBMSCs were cultured on blocks of TTM, allograft or autograft in basal and osteogenic media. Molecular profiling, confocal and scanning electron microscopy (SEM) and biochemical assays were used to characterize cell adherence, proliferation and phenotype. Mechanical testing was used to define the tensile characteristics of the constructs. HBMSCs displayed adherence and proliferation throughout TTM, evidenced by immunocytochemistry and SEM, with significant cellular ingrowth and matrix production through TTM. In contrast to cells cultured with allograft, cell proliferation assays showed significantly higher activity with TTM ($p < 0.001$), although molecular profiling confirmed no significant difference in expression of osteogenic genes. In contrast to acellular constructs, mechanical testing of cell-TTM constructs showed enhanced tensile characteristics, which compared favourably to cell-allograft constructs. These studies demonstrated the ability of TTM to support HBMSC growth and osteogenic differentiation comparable to allograft. Thus, TTM represents an alternative to allograft for osteo-regenerative strategies, extending its clinical applications as a substitute for allograft.

PMID:
22674820
[PubMed - as supplied by publisher]

J Bone Joint Surg Br. 2012 Jun;94(6):848-55. doi: 10.1302/0301-620X.94B6.28479.

Translational hurdles for tissue engineering: an in vitro analysis of commonly used local anaesthetics on skeletal stem cell survival.

Tayton ER, Smith JO, Aarvold A, Kalra S, Dunlop DG, Oreffo RO.

Source

University of Southampton School of Medicine, Southampton General Hospital, Tremona Road, Southampton SO16 6YD, UK. edwardtayton@hotmail.com

Abstract

When transferring tissue regenerative strategies involving skeletal stem cells to human application, consideration needs to be given to factors that may affect the function of the cells that are transferred. Local anaesthetics are frequently used during surgical procedures, either administered directly into the operative site or infiltrated subcutaneously around the wound. The aim of this study was to investigate the effects of commonly used local anaesthetics on the morphology, function and survival of human adult skeletal stem cells. Cells from three patients who were undergoing elective hip replacement were harvested and incubated for two hours with 1% lidocaine, 0.5% levobupivacaine or 0.5% bupivacaine hydrochloride solutions. Viability was quantified using WST-1 and DNA assays. Viability and morphology were further characterised using CellTracker Green/Ethidium Homodimer-1 immunocytochemistry and function was assessed by an alkaline phosphatase assay. An additional group was cultured for a further seven days to allow potential recovery of the cells after removal of the local anaesthetic. A statistically significant and dose dependent reduction in cell viability and number was observed in the cell cultures exposed to all three local anaesthetics at concentrations of 25% and 50%, and this was maintained even following culture for a further seven days. This study indicates that certain local anaesthetic agents in widespread clinical use are deleterious to skeletal progenitor cells when studied in vitro; this might have relevance in clinical applications.

PMID:
22628604
[PubMed - indexed for MEDLINE]

Acta Biomater. 2012 May;8(5):1918-27. doi: 10.1016/j.actbio.2012.01.024. Epub 2012 Jan 24.

Supercritical CO2 fluid-foaming of polymers to increase porosity: a method to improve the mechanical and biocompatibility characteristics for use as a potential alternative to allografts in impaction bone grafting?

Tayton E, Purcell M, Aarvold A, Smith JO, Kalra S, Briscoe A, Shakesheff K, Howdle SM, Dunlop DG, Oreffo RO.

Source

Human Development and Health, University of Southampton Medical School, Southampton, UK. e.r.tayton@soton.ac.uk

Abstract

Disease transmission, availability and cost of allografts have resulted in significant efforts to find an alternative for use in impaction bone grafting (IBG). Recent studies identified two polymers with both structural strength and biocompatibility characteristics as potential replacements. The aim of this study was to assess whether increasing the polymer porosity further enhanced the mechanical and cellular compatibility characteristics for use as an osteogenic biomaterial alternative to allografts in IBG. Solid and porous poly(DL-lactide) (P(DL)LA) and poly(DL-lactide-co-glycolide) (P(DL)LGA) scaffolds were produced via melt processing and supercritical CO(2) foaming, and the differences characterized using scanning electron microscopy (SEM). Mechanical testing included milling and impaction, with comparisons made using a shear testing rig as well as a novel agitation test for cohesion. Cellular compatibility tests for cell number, viability, and osteogenic differentiation using WST-1 assays, fluorostaining, and ALP assays were determined following 14 day culture with skeletal stem cells. SEM showed excellent porosity throughout both of the supercritical-foam-produced polymer scaffolds, with pores between 50 and 200 μm. Shear testing showed that the porous polymers exceeded the shear strength of allograft controls ($P<0.001$). Agitation testing showed greater cohesion between the particles of the porous polymers ($P<0.05$). Cellular studies showed increased cell number, viability, and osteogenic differentiation on the porous polymers compared to solid block polymers ($P<0.05$). The use of supercritical CO(2) to generate porous polymeric biodegradable scaffolds significantly improves the cellular compatibility and cohesion observed compared to non-porous counterparts, without substantial loss of mechanical shear strength. These improved characteristics are critical for clinical translation as a potential osteogenic composite for use in IBG.

PMID:
22307029
[PubMed - indexed for MEDLINE]

Regen Med. 2011 Jul;6(4):461-7. doi: 10.2217/rme.11.33.

Taking tissue engineering principles into theatre: retrieval analysis from a clinically translated case.

Aarvold A, Smith JO, Tayton ER, Tilley S, Dawson JI, Lanham SA, Briscoe A, Dunlop DG, Oreffo RO.

Source

Bone & Joint Research Group, Institute of Developmental Sciences Building, University of Southampton School of Medicine, Southampton General Hospital, Tremona Road, Southampton, SO16 6YD, UK.

Abstract

AIM:

Tissue engineering has enormous potential for the regeneration of bone defects. Approximately 4 years ago we reported on a 62 year old patient who underwent treatment of a benign cyst in the proximal femur by impaction bone grafting supplemented with autologous bone marrow. The cyst and symptoms subsequently recurred and this patient has now required a total hip replacement. This has provided a rare opportunity for ex vivo analysis of clinically applied tissue engineered bone.

MATERIALS & METHODS:

The femoral head was retrieved at surgery and the structural and functional characteristics of the tissue engineered bone were analyzed by micro-computed tomography, histology and mechanical testing.

RESULTS:

The impacted bone demonstrated a trabecular structure that contained islands of nonincorporated graft. The graft was denser than the patient's trabecular bone with comparable strength. The cyst material had penetrated along the channel of bone and an increased number of osteoclasts were observed.

DISCUSSION:

This study has provided detailed ex vivo analysis of retrieved human tissue engineered bone and possible reasons for the observed construct failure are discussed in this article. The impacted bone displayed some evidence of remodeled trabecular structure, although the bone marrow aspirate that was initially combined with the allograft contained a relatively low concentration of osteoprogenitor cells. Cellular augmentation was insufficient to overcome the osteoclastic process associated with renewed cyst formation. Concentration or culture expansion of osteoprogenitor cells from aspirated bone marrow is recommended for biological augmentation of bone graft.

PMID:

21749204

[PubMed - indexed for MEDLINE]

Tissue Eng Part B Rev. 2011 Oct;17(5):307-20. doi: 10.1089/ten.TEB.2011.0143. Epub 2011 Jun 30.

Skeletal tissue regeneration: current approaches, challenges, and novel reconstructive strategies for an aging population.

Smith JO, Aarvold A, Tayton ER, Dunlop DG, Oreffo RO.

Source

Bone and Joint Research Group, Centre for Human Development, Stem Cells and Regeneration, Human Development and Health, Institute of Developmental Sciences, Southampton, United Kingdom.

Abstract

Loss of skeletal tissue as a consequence of trauma, injury, or disease is a significant cause of morbidity with often wide-ranging socioeconomic impacts. Current approaches to replace or restore significant quantities of lost bone come with substantial limitations and inherent disadvantages that may in themselves cause further disability. In addition, the spontaneous repair capacity of articular cartilage is limited; thus, investigation into new cartilage replacement and regeneration techniques are warranted. Along with the challenges of an increasingly aging demographic, changing clinical scenarios and rising functional expectations provide the imperative for new, more reliable skeletal regeneration strategies. The science of tissue engineering has expanded dramatically in recent years, notably in orthopedic applications, and it is clear that new approaches for de novo skeletal tissue formation offer exciting opportunities to improve the quality of life for many, particularly in the face of increasing patient expectations. However, significant scientific, financial, industrial, and regulatory challenges should be overcome before the successful development of an emergent tissue engineering strategy can be realized. We outline current practice for replacement of lost skeletal tissue and the innovative approaches in tissue regeneration that have so far been translated to clinical use, along with a discussion of the significant hurdles that are presented in the process of translating research strategies to the clinic.

PMID:
21615329
[PubMed - indexed for MEDLINE]

Inflammation and Regeneration 2012; 32 (3): 072-089

Skeletal Regeneration: application of nanotopography and biomaterials for skeletal stem cell based bone repair

Dawson JI, Kingham E, Evans NR, Tayton E, Oreffo ROC.

Source

1. Bone & Joint Research Group, Institute of Developmental Sciences Building, University of Southampton School of Medicine, Southampton General Hospital, Tremona Road, Southampton, SO16 6YD, UK. 2. Stem Cell Unit, Department of Anatomy, College of Medicine, King Saud University, Riyadh, Saudi Arabia.

Abstract

The application of selected skeletal progenitor cells and appropriate biomimetic microenvironments and nanotopographical surfaces offer the potential for innovative approaches to bone disease treatment and bone regeneration. Skeletal stem cells, commonly referred to as mesenchymal stem cells or human bone marrow stromal stem cells are multipotent progenitor cells with the ability to generate the stromal lineages of bone, cartilage, muscle, tendon, ligament and fat. This review will examine i) the application of innovative nanotopography surfaces that provide cues for human stem cell differentiation in the absence of chemical cues, ii) unique biomimetic microenvironments for skeletal tissue repair as well as iii) data from translational studies from the laboratory through to the clinic demonstrating the potential of skeletal cell based repair using impaction bone grafting as an exemplar. The development of protocols, tools and above all multidisciplinary approaches that integrate biomimetic materials, nanotopography, angiogenic, cell and clinical techniques for skeletal tissue regeneration for *de novo* tissue formation offers an opportunity to improve the quality of life of many.